Development and evaluation of rapid methods for diagnosis of prosthetic joint infection

Alexander John Trotter

Submitted in partial fulfilment of the requirements of the degree of Doctor of Philosophy

University of East Anglia, Norwich, UK

Faculty of Medicine and Health Sciences

June 2021

Abstract

Prosthetic joint infection (PJI) is a devastating complication of total joint replacement resulting in severe pain, functional impairment and high mortality. While a small minority of joint replacements become infected, accurate diagnosis and appropriate management are essential to restore function and prevent excess morbidity. The gold standard for diagnosis, microbial culture, is slow and insensitive, hence other tests (e.g. inflammatory markers) are often used to get a more accurate diagnostic. The inability to differentiate between low-grade infections and aseptic loosening leads to some patients undergoing numerous investigations and unnecessary two-stage revisions, with higher cost and patient morbidity.

Rapid lateral flow tests have the potential for early rule-out/in of infection, directing further diagnostics and appropriate patient management. We tested a commercially available calprotectin lateral flow assay on 69 synovial fluid samples from patients undergoing joint revision at Norfolk and Norwich University Hospital (NNUH). The test sensitivity and specificity against the International Consensus Meeting (ICM) criteria for infection were 75% and 75.56%, respectively. Adjusting results following a clinical review of patient outcomes, the sensitivity improved to 94.74% and specificity was 78%. The low specificity was due to false positive results caused by metallosis or severe osteolysis. The assay showed a high negative predictive value of 96.50% compared to clinical review which would make this a good rule-out test for PJI.

Clinical metagenomics (CMg) has the potential to provide faster and more comprehensive results than culture, capable of detecting any pathogen (bacteria, viruses and fungi) within hours in a single test. The main challenge in achieving rapid turnaround CMg has been the high ratio of human:pathogen DNA present in clinical samples, resulting in slow and expensive sequencing tests. We developed and optimised a rapid CMg pipeline for the diagnosis of PJI that overcomes these challenges. The pipeline includes: a simple and highly efficient differential-lysis-based host DNA depletion step, automated DNA extraction, rapid library preparation, low-input nanopore sequencing and real-time identification of microorganisms using Epi2Me (Oxford Nanopore). The pipeline was optimised using excess sonication fluid samples from suspected PJI patients at the NNUH. The optimised pipeline was then evaluated in a study using MicroDTTect whole prosthesis sampling from 42 revision patients. The developed CMg test had a turnaround time of six hours for the identification of bacterial pathogens with 88.89% specificity and 60% sensitivity compared to routine culture. Sensitivity increased to 92% after investigation into discordant samples as many of the pathogens missed by metagenomics were likely to be culture contaminants. The performance was also better when compared to culture of the MicroDTTect fluid; 73.33% sensitivity and 85.19% specificity.

One of the major challenges in diagnosing PJI is determining whether detection of skin commensal bacteria (which can cause PJI) is indicative of infection or contamination of the sample by skin flora during sampling. We set out to identify novel biomarkers of biofilm formation, which if detected in an organism, would indicate that it had recently been in a biofilm and had originated from the PJI and not from the skin. Staphylococcal strains were transformed using electroporation and plasmids specifically designed for Transposon-Insertion Sequencing (TIS) to develop a *Staphylococcus caprae* library of ~250,000 insertion mutants. This library could be used for gene function profiling to discover new biomarkers of biofilm formation, which could eventually be translated into novel diagnostic tests.

In conclusion, we investigated three important areas in PJI: detecting host biomarkers, utilising CMg for the rapid identification of pathogens and antimicrobial resistance (AMR) and biofilm biomarker discovery through TIS. We think these three approaches could be combined into a single test in the future, sequencing bacterial biofilm and host mRNA biomarkers and identifying bacteria and AMR. This test would rapidly and accurately detect PJI in patients, improving patient management, reducing hospital costs and reducing both patient morbidity and mortality.

Table of Contents

List of Figures

List of Tables

Acknowledgements

Firstly, I would like to thank my supervisory team, Prof. Justin O'Grady, Prof. John Wain and Iain McNamara for their guidance and support. I would also like to thank Orthopaedic Research UK for funding my PhD studentship.

I am especially grateful to Prof. Justin O'Grady for the opportunity to learn so much and do so many cool things. We've come so far together and I cannot overstate how much I've valued your teaching and friendship on this journey. For giving me this platform, for supporting me through lockdown, for keeping me during your career transition and so much more, thank you.

To my mentor, Dr. Gemma Kay. Thank you for tolerating and teaching me through years of struggle. For the endless time invested, the help writing the thesis, and support inside and outside of the lab. Everyone who has been part of the O'Grady group has been lucky to have your support. I could not ask for a better mentor and a friend.

I am grateful to Prof. John Wain and Dr. Emma Manners for taking me on to such a challenging project while at a time when I was unable to progress with the core aim of my project. Thank you for the opportunity and the support that you have given to me over the years. Special thanks also go to Claire Hill and Dr. Mark Webber for their assistance with this section of the thesis.

Thank you to Iain McNamara for enthusiastically facilitating sample collection for this research. To work so closely with clinical colleagues on prospectively collected samples was a real pleasure. Thank you to Kasia Schmidt, Celia Whitehouse, the NNUH Microbiology laboratory and the NRP Biorepository for your constant support in sample and metadata collection.

I would also like to thank Lyfstone AS, especially Dr. Jarle Mikalsen and Stein Lian, for the exciting opportunity to perform the first external study using their assay and their support and friendship. You made me feel very welcome in our time together at conferences.

My thanks go out to everyone in the O'Grady group and the wider MMRL group who have made such a fun environment to work and wind down over the years. It has been a huge pleasure to work alongside you. I also want to thank Dr. Andrew Page and the whole COG-UK team at Norwich for their more recent support in this crazy year.

To all my family and friends, thank you for being you. For supporting me through some rough and spooky times. For giving me a place to escape to and keep sane. Your support has been invaluable over the years and I am very lucky to have you all.

To my darling wife, Libby. I cannot find the words to describe how much you have done for me over these years. Without your support I could not have completed this PhD and gotten to where I am now. Thank you so much for your unwavering support and encouragement to see me through this, always.

To Norman John and Bramwell Nurse, who always believed in me.

Chapter 1 – Introduction

1.1 Total Joint Replacement

Artificial joint replacements are becoming increasingly common as the population's average age continues to rise with advances in modern medicine and improved living standards (Singh et al., 2019). In the U.S. in 2010, 719,000 knee and 332,000 hip replacements were performed and it is predicted this will increase to as many as 3,480,000 and 572,000 knee and hip replacements, respectively, by the year 2030 (Kurtz et al., 2007). The majority of total joint arthroplasties (TJA) are a complete success, granting the patient pain free movement and support. Across England, Wales and Northern Ireland, a reported 160,000 knee and hip replacements are performed each year (NJR 17th Annual Report 2020).

Of these replacements, ~80% are able to last for 25 years without any issue (NIHR). However, ~20% are known to have a range of issues which can include aseptic bone loosening from the artificial implant surface, a bone fracture near the implant, a mechanical break of the prosthetic itself, gradual wearing down of the prosthesis and infection (Tande and Patel, 2014).

Studies show that the incidence of arthroplasty failure by infection is rising. In the USA the occurrence of infection driven joint failure rose between 2001 and 2009 from 1.99% to 2.18% for hip replacements and 2.05% to 2.18% for knee replacements (Kurtz et al., 2012). Similarly, the Nordic Arthroplasty Register Association reported that the proportion of prosthetics that failed in the first five years after implantation rose from 0.46% in 1995-99 to 0.71% in 2005-09 (Dale et al., 2012). While the incidence of PJI is currently low, ranging from 1-2% in primary procedures, the UK national joint registry has reported that the number of joint revision surgeries for infected arthroplasties has increased from 140 in 2003 to over 1,200 in 2019 (NJR 17th Annual Report 2020).

All prosthetic joint failures require surgical intervention to repair or replace the implant, contributing to the economic burden that is associated with all arthroplasty revisions. Although prosthetic joint infection (PJI) is a comparatively rare complication following TJA, the associated impact is significant. PJI is notoriously difficult to manage, requiring multiple interventions and

prolonged courses of antibiotics with long periods of immobility, psychological stress, and repeated hospital stays (Palmer et al., 2020). Beyond patient mortality and morbidity, the healthcare associated cost of infected joint revision is estimated at £50,000 per patient in the UK (Ahmed and Haddad, 2019). In the USA, the direct cost of treating a PJI has been estimated to cost $100,000 per patient (Bozic and Ries, 2005; Kurtz et al., 2012), with the overall cost of lifetime treatment for a 65-year-old estimated to cost $390,806 (Parisi et al., 2017). Increasing case numbers will result in an increasing economic burden to healthcare systems, with annual PJI-related hospital costs in the USA predicted to rise to $1.85 billion by 2030 unless patient diagnostics and management improves (Premkumar et al., 2021).

Due to the necessity for debridement (removal of dead, damaged or infected tissue), cleaning, specific antibiotics, and potentially multiple surgeries in the case of a two-stage revision (where prosthesis removal and reimplantation are performed as separate surgical interventions) (Vanhegan et al., 2012), a PJI driven revision surgery with joint retention can cost three times more than the original implantation (Peel et al., 2013). Furthermore, revision surgeries involving replacement of the infected prosthesis can cost 3.4 to 6 times as much as primary surgery if they are single or two-stage revisions respectively (Klouche et al., 2010).

Infected arthroplasties are also associated with a five-fold increase in mortality compared with aseptic implant failure during the first year after implantation (Zmistowski et al., 2013). In addition, there is a considerably higher chance (17.7-27.5%) of developing repeat infections after being treated for PJI, and this is often due to the increased infection risk of exposure associated with additional surgeries (Alamanda and Springer, 2019, 2018). Furthermore, late and/or inadequate antimicrobial treatment brings the risk of failure to eradicate the original infection and the selection of antimicrobial resistant pathogens (Siljander et al., 2018).

1.2 Implant Associated Infection

PJI commonly manifests as pain localised to the joint area, swelling, erythema, fever and drainage from a sinus tract from the skin surface to the joint (Duff et al., 1996; Trisha N. Peel et al., 2012; P.

Sendi et al., 2011a). While most of these symptoms are suggestive of a PJI, the development of the sinus tract, a dead space opening in the surgical wound often containing pus, is considered a definitive indicator alone (Osmon et al., 2013; Oussedik et al., 2012; Parvizi et al., 2011b).

PJIs can be separated into three categories depending on the time at which the infection manifests. Early onset PJI develops in the first three months following surgery, often when the surgical site has become contaminated during the procedure. Delayed onset PJI occurs three-to-12-months after arthroplasty, also commonly caused by intraoperative contamination but with an organism which takes longer to establish an infection, such as non-aureus staphylococci (NAS) (Zimmerli et al., 2004). Finally, late onset PJI typically occurs at least a year after the arthroplasty procedure often as a result of a haematogenous infection which has translocated to the implant sit (Tande and Patel, 2014).

Most PJIs are defined as early or delayed onset infections that are seeded during surgery through either direct-contact or aerosolised contamination of the prosthesis or surrounding tissue. The frequency at which contamination causes infection is attributed to how easily bacteria can colonize a prosthetic joint surface. Southwood *et al.* used a rabbit model to demonstrate how as few as $1x10^2$ *Staphylococcus aureus* cells can establish infection in a hip replacement, while an inoculation of $1x10^4$ cells was required in the no prosthesis control (Southwood et al., 1985).

As well as direct contamination, the superficial surgical wound can become infected following the surgery, allowing the pathogen to contiguously infect the joint through adjacent tissue that does not fully heal around the surgical site (Tande and Patel, 2014). Another cause of PJI is from haematogenous seeding. In this instance a pathogen from an alternative site in the body moves, through the blood stream, to establish infection at the prosthetic joint. The occurrence of haematogenous seeding is relatively low, as Uçkay *et al.* demonstrated in one study where only 6% (5/81) of bacteraemia patients with a prosthetic joint developed PJI (Uçkay et al., 2009). However, depending on the pathogen, haematogenous infection can be high risk. *S. aureus* is the causative organism in 30-40% of bacteraemia associated PJIs (Murdoch et al., 2001; Parham Sendi et al., 2011) making it a highly significant organism when found in during microbiological testing.

1.3 Aetiology

Gram-positive cocci are the most commonly identified causes of PJI worldwide (Table 1.1). This is driven largely by infection with *S. aureus* and NAS, which contribute to >50% of PJIs. Aerobic Gram-negative bacilli are the next most commonly reported organism (9% across all time periods) while streptococci and enterococci together account for ~10% of cases (8% and 3% respectively). The proportions of PJIs caused by *S. aureus* and NAS species were reported to be relatively equal when aggregated across multuiple large, worldwide studies by Tande and Patel (2014). Aerobic Gram-negative bacilli are involved in 10% of cases of knee and hip PJI. This has implications for the perioperative antimicrobial management of these patients.

Table 1.1 Common causes of PJI worldwide

Reported Cause	% of patients with PJI in aggregated studies					
	Hip and Knee		Hip[3]	Knee[4]	Shoulder[5]	Elbow[6]
	All time periods[1]	Early infection[2]				
Staphylococcus aureus	27	38	13	23	18	42
Non-aureus *Staphylococcus*	27	22	30	23	41	41
Aerobic Gram-negative bacilli	9	24	7	5	10	7
Streptococcus species	8	4	6	6	4	4
Enterococcus species	3	10	2	2	3	0
Anaerobic bacteria:	4	3	9	5		
Propionibacterium acnes					24	1
Other anaerobes					3	0
Culture-negative PJI	14	10	7	11	15	5
Polymicrobial infections	15	31	14	12	16	3

Results compiled from 14 large, worldwide, studies by Tande and Patel (2014). [1]Data aggregated from 2,435 patients across 14 studies; [2]Data aggregated from 637 patients across eight studies; [3]Data aggregated from 1,979 hips and 1,427 knees at the Mayo Clinic, Rochester, USA; [4]Data aggregated from 199 patients across eight studies; [5]Data aggregated from 110 patients across five studies.

A report of organisms isolated from orthopaedic tissues processed by three hospitals across the county of Norfolk; Norfolk and Norwich University Hospital (NNUH) in Norwich, Queen Elizabeth Hospital (QEH) in Kings Lynn and James Paget University Hospital (JPUH) at Great Yarmouth, by Dr. Panagiotis Papastergiou (consultant microbiologist at QEH, unpublished data), identified the most common causes of PJI in this region of the UK (Table 1.2). Of the 1,222 samples tested the most commonly isolated organism was *S. aureus*, in 22.09% of samples. The remainder of the top five causative organisms were: any individual NAS (18.25%), Bacillus sp. (3.85%), Diptheroids (3.60%) and polymicrobial infection of mixed NAS (2.62%). These numbers are similar to the global picture, with PJI reported to be caused by staphylococcal species in greater than 50% of cases and *Bacillus* spp. the next most commonly identified organism (Tande and Patel, 2014) (Table 1.1). All of these bacteria are known to form biofilms (Cerca et al., 2005; Singhal et

al., 2011; Vlamakis et al., 2013) and as inorganic surfaces such as a prosthesis are prone to biofilm attachment (Cappelli et al., 2007) the biofilm mechanism of infection is clinically important to PJI.

Table 1.2 Common causes of PJI in Norfolk, UK

Reported cause	**% of patients with PJI**
S. aureus	22.09
Non-aureus *Staphylococcus*	18.25
Bacillus spp.	3.85
Diptheroids	3.6
polymicrobial infection of mixed Non-aureus *Staphylococcus*	2.62

Results compiled 1,222 samples collected from 284 patients between 1/1/2014 and 3/12/2016 from three regional hospitals in Norfolk, UK.

S. aureus and aerobic Gram-negative bacilli together make up >60% of early-onset infections. The increased virulence of these organisms likely leads to the onset of symptoms within the first several months, resulting in earlier diagnosis of infection. NAS species are less likely to be found in early-onset PJI than *S. aureus*, however, NAS remain important pathogens in this setting. *Staphylococcus epidermidis* is the most commonly identified NAS (Harris et al., 2010) and is a high-risk organism for PJI due to its potency for biofilm formation on abiotic materials (Fey and Olson, 2010). Other NAS often found to be the cause of PJI include *Staphylococcus simulans* (Razonable et al., 2001), *Staphylococcus caprae* (Allignet et al., 1999) and *Staphylococcus lugdunensis* (Sampathkumar et al., 2000). Clinically, NAS infections are challenging to diagnose as the majority are found as part of the human skin flora, and as such are common contaminants of samples taken from a non-infected joint (Aslam et al., 2010; Berbari et al., 1998; Peel et al., 2011; Pulido et al., 2008). The difficulty in determining whether a NAS is causative of infection or not makes diagnosis of the patient much more difficult.

Across the Norfolk hospitals, a wide variety of streptococcal species were isolated from orthopaedic tissues, 5.88% of the patients over the 3-year study had a streptococcal isolate (each streptococcus group was recorded separately hence streptococcal infections were not reported as one of the five top causes). Group A (Meehan et al., 2003), group B (P. Sendi et al., 2011b), group

C (Park et al., 2012) and group G (Pons et al., 1997) streptococci are well known to cause PJI. Enterococcal infections cause between 10-15% of early onset PJI (Cobo et al., 2011; T. N. Peel et al., 2012; Tande and Patel, 2014) and are one of the most commonly found isolates in polymicrobial infections, along with *S. aureus* and aerobic gram-negative bacilli (Marculescu and Cantey, 2008; Trisha N. Peel et al., 2012). These polymicrobial infections are far more common in early-onset PJI than late-onset infections at 35% and 20% of total infections respectively (Bengtson and Knutson, 1991; Berbari et al., 1998; Cobo et al., 2011; T. N. Peel et al., 2012), with 56% of all polymicrobial infections occurring within the first 90 days from surgical operation (Marculescu and Cantey, 2008).

1.4 Epidemiology

Many studies show an association between obesity (BMI >35) and increased risk of PJI (Malinzak et al., 2009; Namba et al., 2013, 2012; Pulido et al., 2008). This increased risk is potentially due to the prolonged duration of surgical intervention (Liabaud et al., 2013) or other co-morbidities associated with obesity. Type 2 Diabetes Mellitus (diabetes) is also associated with a heightened risk of PJI development (Cazanave et al., 2013; Kurd et al., 2010; Malinzak et al., 2009; Namba et al., 2013). The risk of infection may also be associated with impaired leukocyte function negatively impacting wound healing and thereby facilitating superficial surgical site infections (Tande and Patel, 2014). Alternatively, the risk could be due to hyperglycaemic events during surgery. Mraovic *et al.* reported that hyperglycaemia was associated with a higher risk of infection during TJAs, irrespective of if the patient suffered from diabetes (Mraovic et al., 2011). This observation suggests that elevated blood glucose levels could be supporting biofilm formation by providing a more nutrient rich environment.

Autoimmune conditions such as Rheumatoid Arthritis (RA) pose a major risk for infection, with PJI development reported to occur in 3.7% of RA patients with a prosthetic joint (Bongartz et al., 2008). All conditions that require immunosuppressant treatments are believed to increase the risk of PJI (Berbari et al., 2010). However, it is challenging to dissect the relative importance of the primary morbidity from its comorbidities and the impact of the therapy used, as anti-inflammatory

drugs, typically inhibiting tumour necrosis factor alpha (TNF-α) and/or interleukin-6 (IL-6), will increase the risk of surgical site infection. Both the British society for Rheumatology and the American college of Rheumatology recommend cessation of anti TNF-α drug treatments around TJA or TJR surgery (Ding et al., 2010; Saag et al., 2008). Likewise, allogenic blood transfusion is implicated with increased risk of surgical site infections. This is likely due to the co-transfused immunomodulatory agents as autologous transfusions are not reported to carry the same risk (Innerhofer et al., 2005; Rosencher et al., 2003).

Infection is more common following revision surgery than primary implantation (Berbari et al., 1998; Poss et al., 1984; Singh et al., 2012), likely due to prolonged surgical intervention and the risk of recurrent infection from an inaccurately diagnosed or improperly treated pathogen at the time of revision. Prolonged surgery increases the risk of developing a deep surgical site infection, with the risk increasing per 15-minute increment by 9% (Namba et al., 2013). Metal-on-metal (MoM) prostheses are often reported as more readily infected compared with metal to plastic joints (Poss et al., 1984). Current infection of distant body sites, such as urinary or respiratory tract infections, during surgical intervention are also associated with an increased risk of infection due to the risk of transient bacteraemia, although this is very rare (Kurd et al., 2010; Pulido et al., 2008). Given the complications with surgically acquired PJI it is essential for appropriate antimicrobial prophylaxis during perioperative care, meticulous surgical techniques and infection control practices to be in place.

1.5 Culture negative PJI

Culture negative infections are cases where a patient exhibits key symptoms of PJI, such as the presence of sinus tract, purulence surrounding the prosthesis, or inflammation of periprosthetic tissue samples consistent with infection, however, routine microbiological culture reports no causative organisms present. The incidence of culture negative PJI ranges from 5-35% of patients depending on the study (Biring et al., 2009; Mahmud et al., 2012). Culture negative PJI is more commonly found in delayed or late onset infections with only 15% of culture negative PJI being attributed to early onset infections (Malekzadeh et al., 2010). Pathogens responsible for delayed

onset infections are typically more challenging to culture than those causing early onset infections. Organisms causing acute infections are more likely to proliferate rapidly than those causing slower, chronic infections. Many chronic PJI are caused by fastidious microbes forming a biofilm, under significantly different conditions than would be found in a rich growth medium during routine culture (Bjarnsholt et al., 2013). Prior antimicrobial therapy has also been shown to reduce the sensitivity of periprosthetic tissue culture (Trampuz et al., 2006), hence is not recommended in the weeks leading up until sampling before surgical intervention if it is safe to do so. Culture of periprosthetic tissue (PPT) samples can fail if the organisms have died during transit or due to exposure of prophylactic antibiotics administered during surgical intervention (Berbari et al., 2007). Inadequate or inappropriately applied culture techniques may miss uncommon pathogens such as fungi or mycobacteria which may not grow on routine aerobic and anaerobic media. It is also possible that some of these cases are truly aseptic but misclassified as PJI based on current classification schemes.

1.6 Biofilms

A biofilm is an assembly of bacterial cells that is irreversibly associated (not removed by gentle rinsing) with a surface that are enclosed in a matrix of primarily polysaccharide material. Extracellular materials such as mineral crystals, corrosion particles and blood components, depending on the environment in which the biofilm has developed, may also be found within the matrix. Biofilm-associated organisms also differ from planktonic (freely suspended) growing organisms of the same species with respect to the genes that are transcribed. Biofilms may form on a wide variety of surfaces, including living tissues, indwelling medical devices (such as a prosthetic joint), water system piping or natural aquatic systems (Donlan, 2002).

A biofilm mediated infection is initiated when bacterial cells adhere to a host or foreign-body surface from the air or an adjacent tissue. The biofilm is formed as cells aggregate and become encased in an extracellular matrix (ECM) composed of teichoic acids, proteins, polysaccharides, extracellular DNA (eDNA) and host ECM/plasma (Izano et al., 2008; Rohde et al., 2005; Sadovskaya et al., 2005). As bacteria form biofilms they produce protein adhesins, a collection of

cell wall associated proteins that facilitate attachment to host cells or foreign-body surfaces (Chavakis et al., 2005; Foster et al., 2014; Izano et al., 2008; Patti et al., 1994). Bacteria also make use of non-proteinaceous adhesins such as polysaccharide adhesins, for example, polysaccharide intercellular adhesin (PIA) which is crucial in *S. aureus* pathogenesis (Lin et al., 2015), and highly charged teichoic and lipoteichoic acid cell wall polymers (Becker et al., 2014). The ECM constructed around bacterial cells is comprised of a mixture of polysaccharides, proteins and eDNA which forms an external barrier providing the sessile bacteria with physical protection from the host immune system and antimicrobial agents (Donlan and Costerton, 2002).

The lifecycle of a biofilm can be divided into five stages: Initial reversible attachment (1), irreversible attachment (2), proliferation (3), maturation (4) and dispersion (5) (Monroe, 2007). Initially, bacterial cells settle on a biotic or abiotic surface, securing themselves through adhesin mediated attachment. Following attachment, the cells replicate into tight aggregates bound by intercellular adhesins in multiple layers of cells. After adhesion, the cell layers become more structurally defined as the biofilm undergoes maturation. As the biofilm matures, fluid channels form through the layers to facilitate the passing of required nutrients and oxygen down to the deeper cell layers. Once fully matured, a biofilm can release cell aggregates through budding, disseminating bacterial cells from the localized environment into the surrounding tissue, seeding infections at alternative host sites (Costerton et al., 1999) (Figure 1.1).

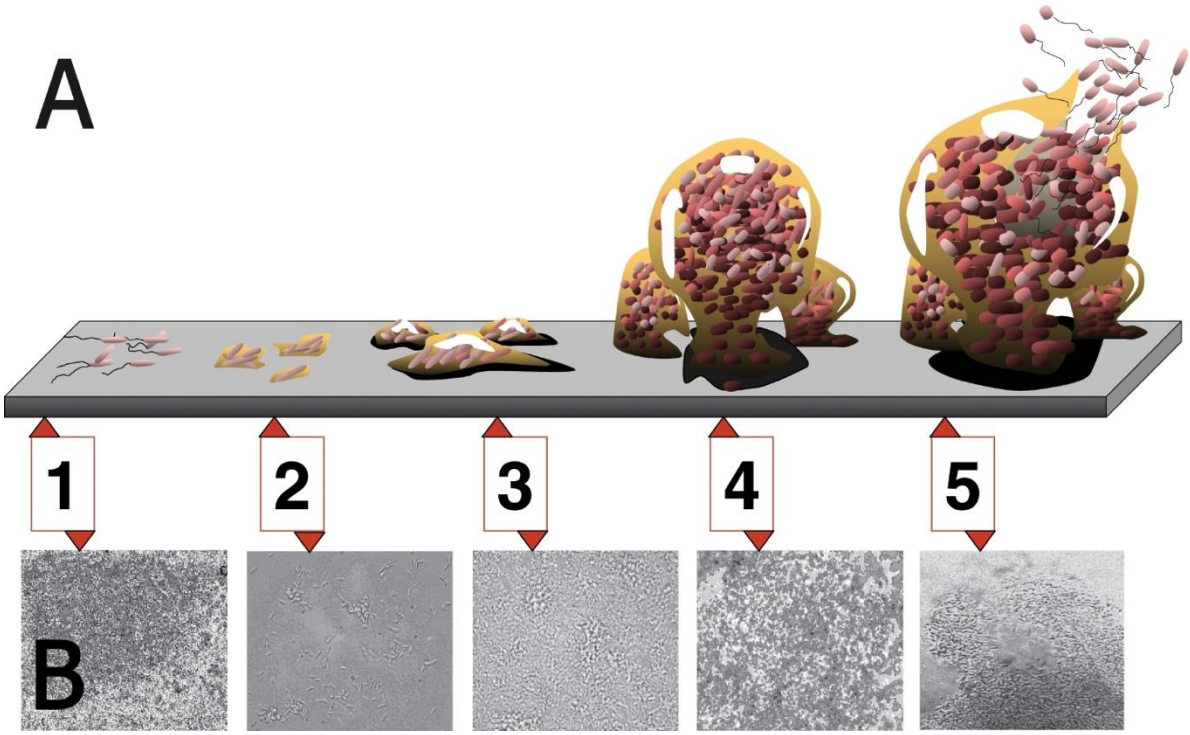

Figure 1.1 Biofilm life cycle. Graphical representation of the stages of biofilm development (A) paired with photomicrographs of a developing *P. aeruginosa* biofilm (B) (Monroe, 2007). 1 - Initial attachment of planktonic cells to an abiotic surface through adhesin mediated attachment; 2 - Aggregation of bacterial cells in monolayer with the production of biofilm ECM; 3 - Formation of multi-layered microcolony encased in ECM; 4 - Matured biofilm encasing bacterial cells protected from environmental stresses in polysaccharide mushroom shape; 5 - Dispersion of bacterial cells into the environment through budding of the biofilm structure.

An organism's ability to attach to abiotic surfaces such as plastics increases the risk of a PJI developing. Initial reversible attachment is mediated by the protein AtlE which hydrolyses host cell wall peptidoglycans, promoting host cell autolysis. The release of cell components then provides usable material, such as eDNA, for biofilm ECM assembly. eDNA availability is known to be essential for the propagation of biofilms as the use of DNase I has been demonstrated to prevent cell attachment and degrade existing biofilms in both *S. aureus* and *S. epidermidis* models (Izano et al., 2008; Qin et al., 2007). AtlE is also known to mediate pathogenesis through host cell internalisation of biofilm-causing organisms (Foster et al., 2014), allowing cells to avoid host immune responses until a biofilm can be established. Once available, bacteria utilise microbial surface components recognising adhesive matrix molecules (MSCRAMMs) to mediate adherence to ECM components (Mazmanian et al., 1999; Schneewind et al., 1993; Vazquez et al., 2011). MSCRAMMs such as clumping factor A and fibrinogen binding protein bind to host molecules

such as fibrinogen, fibronectin and collagen to assemble the biofilm ECM structure (Foster et al., 2014; Kang et al., 2013). *S. aureus* can produce a 240 kDa surface protein known as Bap which mediates cell attachment to abiotic surfaces such as polystyrene (Cucarella et al., 2001). Homologous proteins have also been identified in other organisms, for example, NAS species produce Bhp (Tormo et al., 2005).

Cell wall teichoic acids maintain biofilm integrity by covalently linking to peptidoglycan in neighbouring cell walls, while lipoteichoic acids link to adjacent cytoplasmic cell membranes via a membrane spanning lipid anchor (Becker et al., 2014). Teichoic and lipoteichoic acids also contribute to the bacterial cell wall's negative charge. Studies have shown that mutations in cell wall proteins which reduce the overall negative charge, such as DltA (Gross et al., 2001) and TagO (Holland et al., 2011), show less biofilm activity than wild-type cells.

After a prosthetic joint has been implanted it becomes covered in host ECM and plasma proteins such as fibrinogen, fibronectin and collagen (Becker et al., 2014). These host factors serve as receptors for bacteria that express their respective cell surface adhesins, thereby making the prosthesis susceptible to biofilm attachment and subsequent infection.

1.7 Aseptic loosening

Causative organisms from biofilm-related infections can be challenging to identify in a diagnostic laboratory as the cells are specialised to live in a sessile, nutrient low-state, rather than planktonically in the nutrient-rich media environment typical of routine culture. There is some evidence to suggest that genuine culture negative PJIs can be misdiagnosed as aseptic loosening (AL), the most common cause of TJA failure (Parvizi et al., 2011a).

AL occurs when the host rejects a prosthesis through an immune response in the absence of infection (Abu-Amer, 2005). Over time, wear debris forms at prosthetic joint articulations and modular interfaces of implants (Goldring et al., 1993). The majority of wear debris particles are smaller than 5 μm in size, incoherently shaped and are phagocytosed by host macrophages, triggering an immune response (Gelb et al., 1994; Sabokbar et al., 2003). In-vitro studies have

shown that smaller wear particles are responsible for a greater immune response. Polymethylmethacrylate (PMMA) and polyethylene particles smaller than 20 μm in diameter result in significantly more inflammatory cytokine release than larger particles (Abbas et al., 2003; Shanbhag et al., 1994). Once wear particles are detected by macrophages, the immune response begins with local encapsulation of the prosthesis as macrophages, fibroblasts, giant cells, neutrophils and lymphocytes form a granuloma (Clohisy et al., 2004; Goldring, 2002). This collection of granular cells releases proteases and inflammatory cytokines, such as RANKL, which trigger the osteolysis process on periprosthetic bone tissue, loosening the implant from the host site (Khosla, 2001).

The mechanism of AL, osteolysis, is mediated by phagocytes as they induce the release of cytokines which promote the differentiation of osteoclasts from monocytes and macrophages (Perry et al., 1995; Purdue et al., 2007; Shanbhag et al., 1995). Upon encountering a foreign body, such as prosthetic wear particles, host immune cells release pro-inflammatory cytokines such as TNF-α, IL-6, receptor activator of NF-κB ligand (RANKL), Prostaglandin E_2, Interleukin 1 alpha and Interleukin 1 beta (IL-1β) (Lam et al., 2002; Mundy, 1991; Schwarz et al., 2000). Healthy bone remodelling through resorption and formation is maintained in flux by autoregulation of RANKL binding to receptor activator of NF-κB (RANK), the receptor activator of nuclear factor κB (NF-κB); with competitive inhibition of RANK by osteoprotegerin (OPG) (Lacey et al., 1998). This balance is upset during the inflammatory response with net bone tissue loss from upregulated osteoclast activity to induce the NF-κB cascade (Abu-Amer, 2005; Lam et al., 2002). RANK binding by RANKL activates IκB kinases to phosphorylate IκB, dislocating it from NF- κB allowing the nuclear factor to translocate into the nucleus and bind to DNA, affecting gene expression (Abu-Amer, 2005). Studies in RANK/RANKL deficient animals have shown that less osteolysis occurs in reaction to PMMA particle introduction than in wild type animals (Lam et al., 2002; Schwarz et al., 2000). Likewise, TNF-α deficient animal models also show less bone loss in response to wear particles (Gallo et al., 2002; Schwarz et al., 2000).

The inflammatory response to wear particles upregulates osteoclast proliferation above osteoblast activity resulting in a net loss of bone tissue from the prosthesis site, outweighing osteoblast mediated bone formation and causing loosening (Abu-Amer, 2005; Lam et al., 2002). An immune

response to wear particles will not irreversibly trigger aseptic loosening, however, prolonged osteolysis where the granuloma is maintained over time will result in irreversible aseptic loosening (Shanbhag et al., 2000). This inflammatory response is not unique to AL as it is also the natural response to infection. As such PJI/AL cannot be diagnosed based on joint loosening alone, a full diagnostic workup is required to accurately ascertain the true clinical condition.

1.8 Diagnosis

Despite the burden of PJI on healthcare systems, there is no single diagnostic test that can confirm or exclude PJI (Shahi and Parvizi, 2016). Microbiological culture could be considered the 'gold standard' but it is far from perfect as it has poor sensitivity for PJI samples (pathogens originating from biofilms tend not to grow well in nutrient-rich media). Hence, multiple inflammatory marker tests are used alongside culture in an attempt to confirm or exclude infection. Variation in the tests used and the interpretation of the results makes PJI very difficult to accurately diagnose. The Musculoskeletal Infection Society (MSIS) have attempted to address this issue by releasing guidelines in 2011 which were modified in 2013 (Parvizi et al., 2014b). The MSIS guidelines inform the diagnosis of PJI based on either (a) the confirmation of a major criterion for PJI i.e. the presence of a sinus tract communicating with the joint site or multiple cultured samples displaying phenotypically identical organisms or (b) the combination of multiple minor criteria, such as inflammatory biomarkers, histopathological evidence, or a single positive culture. In 2018, the International Consensus Meeting (ICM) published a revised algorithmic approach, slightly modifying the older MSIS guidelines, to include new diagnostic tests, apply different weights to synovial and serum diagnostic markers and to separate peri- and pre-operative diagnostics (Parvizi et al., 2018) (Figure 1.2).

Major criteria (at least one of the following)	Decision
Two positive cultures of the same organism	Infected
Sinus tract with evidence of communication to the joint or visualization of the prosthesis	

		Minor Criteria	Score	Decision
Preoperative Diagnosis	Serum	Elevated CRP *or* D-Dimer	2	≥6 Infected
		Elevated ESR	1	
	Synovial	Elevated synovial *WBC count or LE*	3	**2-5 Possibly Infected [a]**
		Positive alpha-defensin	3	
		Elevated synovial PMN (%)	2	0-1 Not Infected
		Elevated synovial CRP	1	

	Inconclusive pre-op score *or* dry tap [a]	Score	Decision
Intraoperative Diagnosis	Preoperative score	-	≥6 Infected
	Positive histology	3	**4-5 Inconclusive [b]**
	Positive purulence	3	
	Single positive culture	2	≤3 Not Infected

Figure 1.2 ICM criteria for the diagnosis of PJI. Scoring based system for the diagnosis of PJI published from the 2018 ICM (Parvizi et al., 2018). CRP – C-reactive protein, ESR – erythrocyte sedimentation rate; WBC – white blood cell, LE – leukocyte esterase; PMN – polymorphonuclear neutrophils. [a]If preoperative minor criteria are inclusive; definition to be fulfilled with intraoperative criteria. [b]Consider molecular diagnostics if decision is still inconclusive.

Microbiological culture is considered the gold-standard approach for diagnosing PJI, with two or more positive cultures of the same organism one of only two indications considered a major criterion sufficient for classifying a joint as infected, without the need for supporting evidence. Typically, culture is performed on multiple samples of periprosthetic tissue and synovial fluid, with five or greater samples recommended (Parvizi et al., 2018). In the UK, three to five samples are recommended to be taken during surgery, with antibiotic treatment stopped two weeks prior to surgery if possible (UK SMI B 44). Culture for suspected PJI samples is traditionally performed on both aerobic and anaerobic blood agar as well as in cooked meat broth, which has shown significantly higher sensitivity for fastidious organisms (83%) compared with anaerobic broth (57%) or on solid media (39%) (Hughes et al., 2011).

Routine culture has a low sensitivity rate of 65% for the identification of causative bacteria in PJI, this is often due to the presence of fastidious organisms or where patients have received antimicrobial treatment resulting in a negative culture result (Atkins et al., 1998; Bejon et al., 2010). Attempts have been made to improve the sensitivity of culture in recent years with the application of sonication, the use of low-frequency ultrasound waves to dislodge biofilm-encased bacteria from a prosthesis or peri-prosthetic tissue (Trampuz et al., 2003). Kempthorne *et al.* reported improved detection of pathogens from patients with suspected aseptic loosening using sonication, finding potential pathogens from 15% of patients who had been reported as culture negative (Kempthorne et al., 2015). The application of sonication and other, chemical-based methods for the removal of biofilms will be explored further in Chapter 3 (Pathogen Sequencing). Even with improvements offered by sonication, culture remains problematic due to its slow turnaround times, low sensitivity and potential for contamination by commensal organisms. The challenge of differentiating commensal contaminants from causative organisms will be explored in Chapter 2 (Pathogen Biomarkers). Until culture can be further improved or replaced with a stand-alone diagnostic test, it will remain necessary to use additional diagnostic indicators to diagnose PJI.

1.9 Molecular Diagnostics

While not included within the MSIS/ICM guidelines, polymerase chain reaction (PCR) based methods have been investigated for potential use in PJI diagnostics. Compared to routine culture, PCR is more rapid and less affected by antimicrobial treatment strategies (Järvinen et al., 2009; Melendez et al., 2010; Scerbo et al., 2016). PCR, which targets known DNA sequences and amplifies a fragment of a specific gene or non-coding region, is the most common molecular technique applied to PJI. Originally, PCR methodology used end-point detection for the presence or absence of the target product or ‘amplicon’. However, advances in PCR have led to the use of real-time PCR methods wherein amplicons are detected in real-time using fluorescent probes with the added advantage of generating quantitative results i.e. qPCR (Hartley and Harris, 2014).

PCR methods can be separated into two categories, specific or broad-range. Specific PCR can be used to detect a single bacterial species or group of closely related species, typically in real-time. Specific PCR assays can be developed for any known organisms and are highly sensitive and specific and have a rapid turnaround time (hours). The drawback of such an approach is that only known, or expected, organisms can be identified, potentially missing atypical causes of infection within a sample. Broad-range PCR by comparison allows detection of any bacteria present in the sample, typically by targeting the variable regions of the 16s rRNA gene, a highly conserved region of the genome that is panbacterial. However, further testing is required to identify the sequence of the amplified product and hence the pathogen present – this can take hours to days (Hartley and Harris, 2014).

An ideal PCR based diagnostic test would combine multiple specific PCR assays into a multiplexed test for the identification of all probable pathogens in a sample type. Achermann *et al.* applied one such commercial multiplex PCR approach, SeptiFast, to sonicated implant samples for the diagnosis of PJI. SeptiFast is a real-time multiplex PCR test for use with whole blood samples, which targets the 19 most frequent bacterial and 6 most common fungal pathogens associated with bloodstream infections with a five-hour run time (Korber et al., 2017). While the test is designed for the bloodstream infection, when applied to PJI it was shown to have higher overall sensitivity of pathogen detection than culture using sonication fluid (78% and 62% respectively) (Achermann et al., 2010). This study highlighted the advantage of PCR over culture for the detection of organisms which have been exposed to antimicrobial therapy. Sensitivity for organism detection in patients who had received prior antibiotic treatment was 100% by PCR against 42% by culture. Eight false-negative PCR results were attributed to organisms not included in the multiplex PCR panel (*P. acnes* n=7, Corynebacterium n=1), however PCR was 100% sensitive for organisms included in the panel (Achermann et al., 2010). While improved sensitivity with patients who have received antimicrobial treatment is an advantage of PCR-based diagnostics, the risk of missing less-common organisms is always present when running a selective PCR panel.

Commercial multiplex PCR kits are also available specifically for implant and tissue infection diagnostics. The Unyvero® Implant and Tissue Infection cartridge system developed by Curetis is one example. The assay utilises an automated lysis step followed by multiplex PCRs combined

with amplicon detection by array hybridization for identification of a panel of the most prevalent pathogens and their resistance genes within five hours from liquid or solid periprosthetic samples. The first version of the system, i60 ITI, covers 80 diagnostic targets clinically relevant to the diagnosis of PJI. An improved assay, the ITI G2, was later developed to cover an extended panel of 102 diagnostic targets, comprising 85 relevant pathogens including several fungi and 17 antibiotic resistance markers (Lafeuille et al., 2021). A recent study by Suren *et al.* demonstrated that the Curetis® Unyvero ITI G2 multiplex PCR assay was more sensitive and more specific than culture on joint fluid samples (Suren et al., 2020). In a study of 26 patients, 15 infected and 11 aseptic, PCR sensitivity was 80% compared to 67% by routine culture and was 100% specific compared to 91% using culture. Older studies report significantly lower sensitivity by the Unyvero i60 ITI assay - Morgenstern *et al.* reported 60% sensitivity by PCR compared to 52% by routine culture (Morgenstern et al., 2018), while Malandain *et al.* reported in a study of 484 samples that less than half of either monomicrobial or polymicrobial infections were detected by PCR compared to culture (47.4% and 48% respectively) (Malandain et al., 2018). A more recent study by Suren *et al.* reports higher sensitivities, perhaps due to improvements in the multiplex assay with the G2 kit used, which includes more pathogen targets. However, only 8% of samples missed with PCR by Malandain *et al.* were not included in the panel, which would not account for the total difference in performance observed between the two studies. Broader more inclusive target organism panels are required to improve sensitivity and for targeted molecular tests to replace culture for the diagnosis of PJI. Hence culture is still required for the detection of atypical organisms and comprehensive antimicrobial susceptibility testing, although some AMR gene targets have been incorporated into PCR panels.

1.10 Treatment of PJI

Due to the protective barrier of the ECM, and efflux pump action exporting antimicrobials from the biofilm environment, antimicrobial treatment alone is not sufficient for PJI and surgical intervention is required to remove biofilm material from the prosthesis and surrounding area (Olivares et al., 2019; Taha et al., 2018). Surgical management depends on the classification of the

PJI along with empirical antibiotics or targeted antimicrobial therapy guided by microbiological tests (Izakovicova et al., 2019; Tande and Patel, 2014). Surgical intervention is performed in up to three stages with either retention of the prosthesis, exchange or explanation followed by reimplantation at a later date depending on the condition of the patient (Izakovicova et al., 2019; Li et al., 2018) (Figure 1.3).

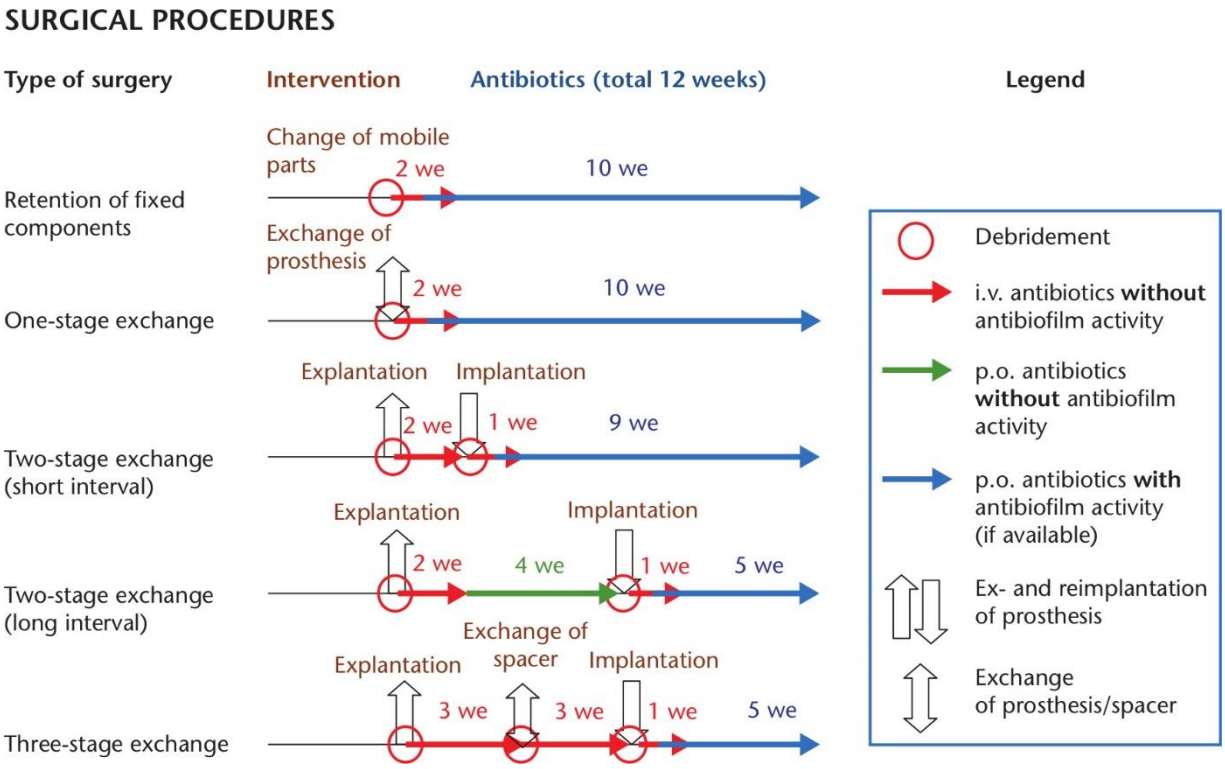

Figure 1.3 Overview of surgical procedures for PJI. Surgical intervention strategies for the treatment of PJI highlighting timeframe of joint debridement, prosthesis replacement and switching from intravenous to oral antimicrobial therapy. i.v. – intravenous; p.o – oral. (Izakovicova et al., 2019).

In early-onset PJI, a Debridement, Antibiotics and Implant Retention (DAIR) procedure is preferred. This is a surgical intervention where there is extensive debridement of all necrotic, synovial and sinus tract tissues, combined with irrigation using copious volumes of sterile saline solution followed by the replacement of mobile or easily exchanged parts (Grammatopoulos et al., 2017). The less invasive, arthroscopic DAIR is not recommended as the outcome is typically poorer than open surgical revision as adequate debridement and exchange of mobile prosthetic elements are far more challenging arthroscopically (Liu et al., 2013; Tsang et al., 2017; Zaruta et

al., 2018). Local antibiotic treatments are applied to the joint area during revision surgery. Antibiotic-loaded PMMA beads may be used, however, as beads can become colonised with new biofilms after the local antibiotic concentration has decreased, additional surgery is required for their removal. Bio-absorbable carriers such as gentamycin loaded sponges or calcium sulphate beads are recommended as a less invasive alternative (Izakovicova et al., 2019).

In later-onset cases where symptoms have persisted for a longer duration (>3 months), a complete removal of the prosthesis is often necessary as a mature biofilm is likely present. The gold standard for a full prosthesis revision is a two-stage revision surgery with a two-week interval between removal of the infected prosthesis and implantation of the new joint (Matthews et al., 2009). However, current literature suggests that reinfection rates may be similar between one- and two-stage revisions (Beswick et al., 2012).

If a two-stage exchange is required, then there is typically an interval of two to four weeks to allow for thorough antimicrobial action against the causative agent of PJI, but in cases of difficult to treat organisms this period can be extended up to six weeks (Zimmerli et al., 2004). During the prosthesis-free interval between surgeries, antibiotic-loaded PMMA spacers are used for local antimicrobial therapy while also providing some degree of mobility and dead-space management. Additional debridement and replacement of the spacer can be used in cases where signs of infection persist despite both local and systemic antimicrobial therapy in a three-stage exchange, most commonly used in cases of fungal PJI (Izakovicova et al., 2019). As two-stage surgeries are associated with higher morbidity, prolonged hospitalisation, worse outcome and greater healthcare cost, two-stage revisions should not be used unless the patient has significantly compromised bone and soft tissue, previous failed surgeries or a difficult to treat organism causing infection (Klouche et al., 2010; Matthews et al., 2009).

In general, antimicrobial therapy begins with empirical broad-spectrum treatment after an initial reduction in bacterial load through surgical debridement. The standard local antimicrobial therapy employed for PJI if the causative organism is known to be susceptible, or if the organisms is unknown, is a combination of gentamicin and clindamycin (loaded into PMMA/bone cement) additionally to systemic antimicrobial treatment of ampicillin/sulbactam or amoxicillin/clavulanic

acid (Izakovicova et al., 2019). Switching to targeted therapy is recommended as soon as the causative agent is known (along with susceptibilities) to ensure effective treatment is administered (Table 1.3), highlighting the need for more rapid diagnostic techniques.

Table 1.3 Recommended antimicrobial treatment for PJI

Micro-organism	**Antibiotic**
***Staphylococcus* spp.**	
- Oxacillin/methicillin-susceptible	Flucloxacillin† for 2 weeks, followed by (according to suceptibility) Rifampin + - Levofloxacin‡ or - Cotrimoxazole‡ or - Doxycyclin‡ or - Fusidic acid‡
- Oxacillin/methicillin-resistant	Daptomycin† or Vancomycin† for 2 weeks, followed by an oral Rifampin‡ combination as above
- Rifampin-resistant*	Intravenous treatment according susceptibility for 2 weeks (as above), followed by long-term suppression for ≥ 1 year
***Streptococcus* spp.**	Penicillin G† or Ceftriaxon† for 2-3 weeks, followed by Amoxicillin‡ or Levofloxacin‡
***Enterococcus* spp.**	
- Penicillin-susceptible	Ampicillin† + Gentamicin† for 2-3 weeks followed by Amoxicillin‡
- Penicillin-resistant	Vancomycin† or Daptomycin† + Gentamicin† for 2-4 weeks followed by Linezolid‡ (maximum 4 weeks)
- Vancomycin-resistant* (VRE)	Individual; removal of the implant or lifelong suppression necessary
Gram-negative	
- Enterobacteriaceae (*E. coli, Klebsiella, Enterobacter* etc.)	Ciprofloxacin‡
- Non-fermenters (*P. aeruginosa, Acinetobacter* spp.)	Piperacillin†/Tazobactam† or Meropenem† or Ceftazidim† + Tobramycin† (or Gentamicin†) for 2-3 weeks followed by Ciprofloxacin‡
- Ciprofloxacin-resistant*	Depending on susceptibility: Meropenem†, Colistin† and/or Fosfomycin† followed by oral supression
Anaerobes	
- Gram-positive (*Cutibacterium, Peptostreptococcus, Finegoldia magna*)	Penicillin G† or Ceftriaxon† for 2 weeks, followed by: Rifampin+ - Levofloxacin‡ or - Amoxicillin‡
- Gram-negatvie (*Bacteroides, Fusobacterium*)	Ampicillin†/Sulbactam† for 2 weeks, followed by Metronidazol‡
***Candida* spp.**	
- Fluconazole-susceptible*	Caspofungin† or Anidulafungin† for 1-2 weeks, followed by: Fluconazole‡ (suppression for ≥ 1 year)
- Fluconazole-resistant*	Individual; removal of the implant or long-term suppression
Culture-negative	Ampicillin†/Sulbactam† for 2 weeks, followed by: Rifampin‡ + Levofloxacin‡

Table adapted from Izakovicova *et al.* (Izakovicova et al., 2019). *Difficult to treat, †Intravenously, ‡per os.

While surgical treatment is typically preferred, long term antibiotic suppression with implant retention may be considered for elderly patients with morbid contraindications for surgical intervention. However, the causative organisms' susceptibilities must be known, and the patient must show no radiological signs of implant loosening (Li et al., 2020).

1.11 Study aims

Successful management of PJI requires treatment of the underlying infection whilst preserving/restoring joint function. Effective diagnosis and treatment of PJI relies on an algorithmic, patient-adapted approach and interdisciplinary collaboration (infectious disease specialists, internal medicine specialists, orthopaedic surgeons etc.) (Li et al., 2018). Rapid, accurate diagnostic tests are essential for choosing the correct surgical intervention and antimicrobial therapy for a positive treatment outcome. Microbiological culture, the current gold standard for the diagnosis of PJI, is slow and insensitive, hence new diagnostic technology is required to improve the management of PJI. The overall aim of this project was to investigate novel molecular methods for the rapid and accurate diagnosis of PJI.

The objectives were to (explained in detail in their respective chapters):

- Evaluate a new rapid point-of-care test, Lyfstone Calprotectin, for the diagnosis of PJI from synovial fluid samples (Chapter 2).
- Develop a metagenomic sequencing pipeline for rapid pathogen identification directly from whole prosthesis sampling using nanopore sequencing (Chapter 3).
- Use Transposon Directed Insertion Site Sequencing (TraDIS) to identify potential novel biomarkers of biofilm formation in non-aureus staphylococci to distinguish between PJI and skin contamination (Chapter 4).

Chapter 2 – Host biomarkers of infection

2.1 – Introduction

Pathogen biomarkers are not the only target for diagnostics, infection can also be diagnosed using host biomarkers. The MSIS/ICM criteria (Parvizi et al., 2018, 2014b) already include multiple tests that measure inflammatory biomarkers for the diagnosis of PJI (Chapter 1.8). However, these tests are not specific only to infection (Monastero and Pentyala, 2017) and can be expensive or unavailable to some clinicians (Trotter et al., 2020). An ideal host biomarker test for PJI would be rapid, inexpensive and simple to perform on synovial fluid. This chapter details the evaluation of a new commercial rapid point-of-care (POC) test which measures calprotectin in synovial fluid (lyfstone.com). We assessed this test using a collection of clinical synovial fluid samples stored in the NRP Biorepository. This work was published in Bone & Joint Research in 2020 (Appendix 1).

2.1.1 Inflammatory biomarkers

Inflammation is a non-specific host-mediated reaction to induce the removal of damaged cells. These cells may be physically damaged by trauma, chemical irritants, biological toxins or invaded by pathogens. The inflammatory response to these conditions forms a signalling cascade to recruit the host immune system to remove both these damaged cells as well as the causative agents (Ferrero-Miliani et al., 2007).

The immune response is comprised of two arms, innate and adaptive immunity (Medzhitov, 2007). The innate immune response is instigated by pattern recognition receptors (PRRs) which have broad specificities for many conserved features of pathogens (Janeway, 1989). The adaptive immune response reacts to antigen receptors that are each specific to a pathogen. These receptors are expressed individually on lymphocytes to develop immunological memory (Schatz et al., 1992).

The innate immune system acts as a first line of defence against bacterial infection. Mucosal epithelia provide a physical barrier to infection, as well as secreting antimicrobial peptides. If a pathogen passes this barrier, then the innate immune response will attempt to detect its presence by

pathogen-associated molecular patterns (PAMPs), which can be recognised by pathogen recognition receptors (PRRs) (Medzhitov, 2007). While many classes of PRRs exist, the most characterised are Toll-like receptors (TLRs). TLRs are a family of transmembrane proteins found on both mucosal epithelia and phagocytes which recognise a variety of bacterial products, such as the lipopolysaccharides and lipoteichoic acids presented in gram-positive and gram-negative cell walls respectively (Morgenstern et al., 2018; Vijay, 2018). Activated TLRs trigger macrophages to secrete pro-inflammatory cytokines such as tumour-necrosis factors (TNFs), interleukin-1β (IL-1β) and IL-6 which begin the complement cascade, signalling for both local and systemic inflammatory responses (Dunkelberger and Song, 2010). These cytokines trigger vasodilation to allow more leukocyte recruitment to the site of infection, coagulation to prevent microorganism dissemination around the body and secretion of collectins and pentraxins, such as C-reactive protein (CRP), which bind to foreign material to highlight it for phagocytosis (Dunkelberger and Song, 2010; Kishore and Reid, 2007). Serum CRP has classically been used for the diagnosis of PJI in combination with erythrocyte sedimentation rate (ESR) (Alijanipour et al., 2013).

The transcription factor NF-κβ exponentially upregulates the inflammatory response during infection (Kawai and Akira, 2007). When RANK is activated by RANKL, a TNF, NF-κβ upregulates production of proinflammatory cytokines such as TNFα, as well as IL1 and IL6 (Ghosh et al., 1998). NF-κβ acts as a regulator of bone remodelling, with RANK and its decoy receptor osteoprotegerin driving osteoblast and osteoclast activity (Boyce et al., 2015). But when RANK activation heavily outweighs osteoprotegerin attenuation due to increased TNF presence from the detection of a pathogen it drives the complement cascade in a positive feedback loop (Beutler, 2009).

As well as stimulating the innate immune response, this cytokine release promotes the lymphocyte activity of the adaptive immune response. By contrast to the wide array of PRRs involved in the innate immune response, the adaptive immune response is mediated by only two types of receptor, B-cell and T-cell antigen receptors (Medzhitov, 2007). Microbial antigens are carried to these lymphocytes in the lymph nodes and spleen by antigen-presenting cells and recognised by specific B and T-cells. The recognition of non-host material triggers either cytokine release and

inflammation mediated by B and T-helper cells or targeted cell death by cytotoxic T cells (Medzhitov, 2007).

While these cytokines can be detected and measured as a biomarker to quantify the immune response, and therefore predict infection, they are not specific for infection (Monastero and Pentyala, 2017). As previously mentioned, inflammation is also a reaction to physical and chemical damage. However, the immune response can occasionally react to host markers under specific conditions such as incomplete removal of lysed host cells (Marshak-Rothstein, 2006; Matzinger, 2002). As such, inflammatory biomarkers can be more difficult to use for diagnosis of infection in patients who suffer from autoimmune diseases such as RA (Plate et al., 2018) and wear damage/metallosis (Bonanzinga et al., 2017).

2.1.2 Current host biomarkers for PJI

Inflammation of a joint observed through erythema or pain are early indications of suspected PJI. While severe inflammation can be visually diagnosed if a joint contains pus or a sinus tract, biomarkers of inflammatory cytokines are also used as diagnostic tools (Parvizi et al., 2018, 2014b).

CRP is a pentraxin released by macrophages which is elevated in the blood during infection as part of the innate immune response (Pepys and Hirschfield, 2003). CRP attaches to foreign or apoptotic cells to prime them for phagocytosis through the complement system (Dunkelberger and Song, 2010). Levels of serum CRP are commonly measured in conjunction with ESR. ESR measures the rate at which blood clots, a process which is upregulated under inflammatory conditions as clotting proteins such as fibrinogen are secreted to prevent bacterial dissemination (Kishore and Reid, 2007). Reports have shown a sensitivity of 91% and specificity of 72% for ESR and a sensitivity of 94% and specificity of 74% for CRP (Parvizi et al., 2013, 2012; Shahi et al., 2015). ESR and CRP are well-known biomarkers of systemic responses to inflammation and are typically used as a first line of diagnostic evaluation for suspected PJI (Gabay and Kushner, 1999). However, these markers are elevated with any type of inflammation and infection, compromising their specificity for diagnosis of PJI. Reports also suggest that PJI with some slow-growing organisms (such as

NAS and *C. acnes*) may not result in may not result in elevation of CRP and ESR in the serum, raising a concern regarding the sensitivity of the tests in some settings (Becker et al., 2014; Le et al., 2018; Pérez-Prieto et al., 2017; Shahi and Parvizi, 2016). Early-onset PJI in particular is challenging to diagnose with inflammatory markers as they are usually elevated in the early post-operative period. ESR can be elevated for up to six weeks after surgery, and CRP by up to two weeks post-surgery, which would generate false-positive results (Parvizi and Della Valle, 2010). Therefore, the use of CRP and ESR for diagnosis of PJI is only meaningful when combined with other MSIS/ICM diagnostic criteria.

Leukocyte esterase (LE), an enzyme produced by leukocytes, can be measured to detect increased levels of white blood cells and is traditionally used to detect urinary tract infections (UTI) (Chernow et al., 1984). LE has more recently been included in the MSIS/ICM criteria and has shown very high sensitivity and specificity for diagnosing PJI, 87% and 96% respectively in a 28-study meta-analysis (Chernow et al., 1984). While the test is cheap and easy to use, the presence of blood can potentially interfere with the colourimetric changes of the test strip making the test unsuitable for some synovial fluid samples (Goswami et al., 2018). More recently, rapid point-of-care (POC) tests are being developed for biomarker assays.

2.1.3 Rapid diagnostic POC tests

Rapid diagnostic tests that can be used at POC have become popular in recent years as they provide rapid results without requiring complex analytical instruments and skilled operators (Kim et al., 2019). Simple lateral flow tests such as FebriDx®, which measures CRP and myxovirus resistance protein A levels specific to bacterial and viral infections respectively (Self et al., 2017), show promise for supporting early treatment plans in respiratory tract infections. This style of test is also beginning to be considered for use in the diagnosis of PJI. Due to the rapid emergence of new PJI biomarkers in recent years, the ICM criteria were revised in 2018 to include the previously mentioned LE, as well as serum d-dimer and synovial alpha defensin (Parvizi et al., 2018).

D-dimer, like ESR, measures fibrin mediated coagulation in response to infection. However, a metanalysis of eight studies using D-dimer for the diagnosis of PJI reported a lower pooled

sensitivity (82%) and similar pooled specificity (70%) compared to what has previously been reported with ESR (Lu et al., 2020).

Alpha defensins are a group of antimicrobial peptides released from neutrophils during infection to destroy invading pathogens (Bonanzinga et al., 2019). A systematic review including 11 studies reported synovial alpha defensin to have very high accuracy for the diagnosis of PJI, with an enzyme-linked immunosorbent assay (ELISA) reporting 100% sensitivity and 96% specificity (Wyatt et al., 2016). An alpha defensin rapid POC test is also available (Figure 2.1) showing 85% sensitivity and 90% specificity for the diagnosis of PJI across 11 studies (Marson et al., 2018). While the POC test is not as accurate as the laboratory-based assay, the test has been included into the ICM criteria for PJI diagnosis (Parvizi et al., 2018). However, the application of these POC biomarker tests are currently limited with none of these three used widely in the UK due to either availability or cost (Trotter et al., 2020).

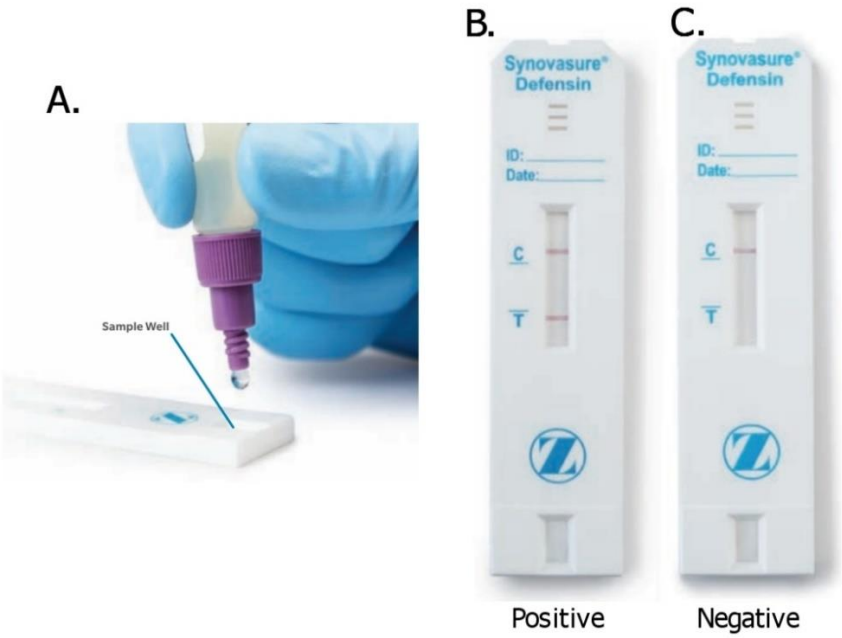

Figure 2.1. Synovasure® Alpha Defensin lateral flow test. A, Addition of prepared synovial fluid sample to the sample well of the lateral flow test. B, Positive test result denoted by visible control and test line. C, Negative test result denoted by visible control line with no visible test line (adapted from www. https://www.zimmerbiomet.com/).

2.1.4 Calprotectin as a PJI biomarker

A potential addition to the list of PJI biomarkers is synovial fluid calprotectin. Calprotectin is a complex of antimicrobial peptides released from neutrophils during inflammation and is abundant

in the innate immune response as it makes up 60% of all soluble proteins contained in neutrophils (Stríz and Trebichavský, 2004). Faecal calprotectin levels are currently used to screen for inflammatory bowel disease and the biomarker has also been shown to be capable of detecting relapse RA (Abildtrup et al., 2015; van Rheenen et al., 2010). Recently, synovial fluid calprotectin has been investigated as a potential biomarker for the diagnosis of PJI. Using an off label faecal calprotectin test, Wouthuyzen-Bakker *et al.* demonstrated that the test had high potential for ruling out PJI from synovial fluid with a negative predictive value (NPV) of 94.4% (Wouthuyzen-Bakker et al., 2018). This finding was supported by Salari *et al.* who, using an ELISA based calprotectin test reported high sensitivity and specificity for PJI diagnosis, 100% and 95% respectively (Salari et al., 2020).

Biofilm mediated infections, especially by NAS, can cause very low levels of inflammation, making them harder to detect by the immune system and therefore harder to diagnose with current host biomarkers (Becker et al., 2014; Rewa et al., 2012; Zimmerli et al., 2004). As calprotectin is the most abundant neutrophil protein marker, low grade inflammation should be more readily detectable compared to less abundant host markers, thereby increasing test sensitivity.
A Norwegian company, Lyfstone AS, have developed a lateral-flow device that measures synovial fluid calprotectin for the diagnosis of PJI. The manufacturer reported that the test had a high NPV suggesting it could be a powerful tool for cheap, early, rule out of PJI to enhance both diagnosis and treatment plans (lyfstone.com). We collaborated with the company to perform the first external study of this promising test.

2.1.5 Study Objectives

Here we tested a collection of retrospective synovial fluid samples from patients undergoing revision surgery, stored at the NRP Biorepository. Using the Lyfstone Calprotectin rapid POC test and compared the results to the ICM defined gold standard to determine the sensitivity, specificity, positive predictive value (PPV), NPV and accuracy of the test.

2.2 – Methods

2.2.1 Patient Recruitment

2.2.1.1 Sample collection

73 synovial fluid samples that had been collected by the Biorepository at the University of East Anglia (UEA; Norwich, UK) between February 2016 and January 2019 were retrospectively tested with the Lyfstone Calprotectin lateral flow test (lyfstone.com). Samples were taken from a consecutive series of patients during total hip and total knee arthroplasty performed at the Norfolk and Norwich University Hospital (NNUH; Norwich, UK). Samples were only stored by the biorepository if patient consent was obtained at the time of surgery and sufficient sample remained following routine clinical evaluations.

2.2.1.2 Exclusion criteria

Samples were only included for this study if there was sufficient remaining volume (≥100 µl) and results for microbiological culture, frozen-section histology, and serum CRP were available. Subsequently, four samples were removed from the analysis due to incomplete or erroneous patient data (two samples had no preoperative notes and two were collected from a patient who had two separate surgeries, although the samples were labelled with the same date). A final total of 69 samples were analysed in the dataset (37 male, 32 female; mean age 74.3 years (45 to 89); mean body mass index (BMI) 29.8 kg/m^2 (19.7 to 42.4)); 52 were taken from hip revision surgery and 17 during knee revision.

2.2.2 Diagnostic Criteria

2.2.2.1 International consensus meeting criteria for infection.

Cases were classified as either infected or aseptic using the latest definition of prosthetic hip and knee infection from the 2018 ICM, hereafter referred to as ‘ICM’ criteria (Table 2.1). A case was deemed as infected if the patient presented either with one or more major criterion (two or more

cultures of the same organism or the presence of a sinus tract) or met three or more minor criteria (elevated serum CRP levels, purulence, one positive microbiological culture, and/ or positive histological analysis of periprosthetic tissue for inflammation). Other minor criteria from the 2018 ICM criteria were not included as many of those tests are not used as standard in the UK or routinely at NNUH. Clinical information was not made available to index test performers prior to testing.

Table 2.1 Scoring based definition for prosthetic joint infection from the 2018 International Consensus Meeting criteria.

Major Criteria (one or more of the following)	Decision
Two positive cultures of the same organism	Infected
Sinus tract with evidence of communication to the joint or visualization of the prosthesis	

Minor Criteria	Score	Decision
Elevated serum [1]CRP (≥10 mg/L) *or* D-Dimer (D-Dimer unavailable)	2	≥6 Infected
Positive histology	3	
Positive purulence	3	
Single positive culture	2	
Elevated serum [2]ESR (unavailable)	1	
Elevated synovial [3]WBC count *or* [4]LE (unavailable)	3	<6 Aseptic
Positive alpha-defensin (unavailable)	3	
Elevated synovial [5]PMN (%) (unavailable)	2	
Elevated synovial CRP (unavailable)	1	

[1]CRP – C-reactive Protein, [2]ESR – Erythrocyte Sedimentation Rate, [3]WBC - White Blood Cell, [4]LE - Leucocyte Esterase, [5]PMN Polymorphonuclear Neutrophil

2.2.2.2 Routine microbiological culture.

Microbiological culture was performed by the NNUH Microbiology department from tissue and fluid specimens (it was recommended that three to five tissue/fluid samples were sent for testing) for 48 hours on blood agar and chocolate agar, five days on fastidious anaerobe agar, and five days in cooked meat broth before 48-hour subculture on chocolate agar, sabouraud agar, fastidious

anaerobe agar and in fastidious antimicrobial neutralization bottles, all according to the UK Standards for Microbiology Investigations B 44 (UK SMI B 44).

2.2.2.3 Frozen section histology.

Histology was performed by frozen section microscopy by the NNUH Histopathology department according to UKAS ISO 8405 (UKAS 8405). In brief, PPT samples were frozen and prepared in paraffin wax blocks then sectioned for analysis by microscopy for signs of inflammation.

2.2.2.4 Serum CRP.

Serum CRP was performed by the NNUH Biochemistry department according to UKAS ISO 10295 (UKAS 10295). In brief, blood samples were collected in Li Heparin tubes and measured for CRP content using an Abbott Architect c8000.

2.2.3 Clinical Review

In cases where the calprotectin result was discordant with the ICM based diagnosis of infection, further investigation was performed by Iain McNamara (Consultant Orthopaedic Surgeon) and his team (Majeed Shakokani, Alexander Durst). The team were blind to the calprotectin result and asked to review medical records, surgical notes, and radiographs. As this was a retrospective examination, records from the treating team were reviewed to ascertain the clinical decisions made at the time. For example, a patient who had met the criteria for infection with ICM by two positive microbiology samples may not have been treated for if those bacteria had been thought to be contaminants (following multidisciplinary team discussion with the microbiologist at the time). The longer-term clinical outcome of the patient was also reviewed using one-year follow-up notes to determine if the clinical decision had been justified. These results were classified as ICM with Clinical Review (ICM-CR).

Aseptic loosening was graded according to the Paprosky classification (Paprosky et al., 1994).

Blood contamination of synovial fluid samples was categorised by eye into three categories: no blood, low blood and high blood. Samples that appeared clear or white in colour were assigned to no blood. Samples that appeared orange, pink or light red were classified as low blood. Samples with clear contamination from blood appearing dark red were designated as high blood.

Relevant conditions were defined as written in the patient notes and searched on the NHS internal reporting system. Conditions within the patient set defined as relevant were rheumatoid arthritis, type 2 diabetes mellitus, chronic lymphoid leukaemia, polymyalgia rheumatica, ankylosing spondylitis and ulcerative colitis.

2.2.4 Lyfstone Calprotectin Test

The Lyfstone calprotectin test was carried out according to the manufacturer's kit instructions (Lyfstone AS). Synovial fluid samples (20 µl) were diluted in a premixed dilution buffer (2 ml – 101 × dilution) and added to the test cassette (80 µl). Gold-conjugated antibody complexes bind calprotectin and travel along the membrane within the cassette then further bind to immobilized calprotectin-specific antibodies to form a visible test line. Any remaining gold-conjugated antibody not bound to calprotectin is immobilized on a control line. After a 15-minute inclubation at room temperature, the cassettes were photoimaged, and the calprotectin levels calculated by the Lyfstone smartphone application (Lyfstone AS) (Figure 2.2). The colour intensity of the test line was proportional to the concentration of calprotectin in the sample. A calprotectin result of ≤14 mg/L was considered negative according to the cutoff set by the Lyfstone smartphone application at the time of testing. Moderate (14 mg/L to 50 mg/L) and severe (>50 mg/L) risk of infection categories were grouped together as test positive (LYFCLP005 Lateral Flow Test Kit Instructions For Use. Lyfstone AS.).

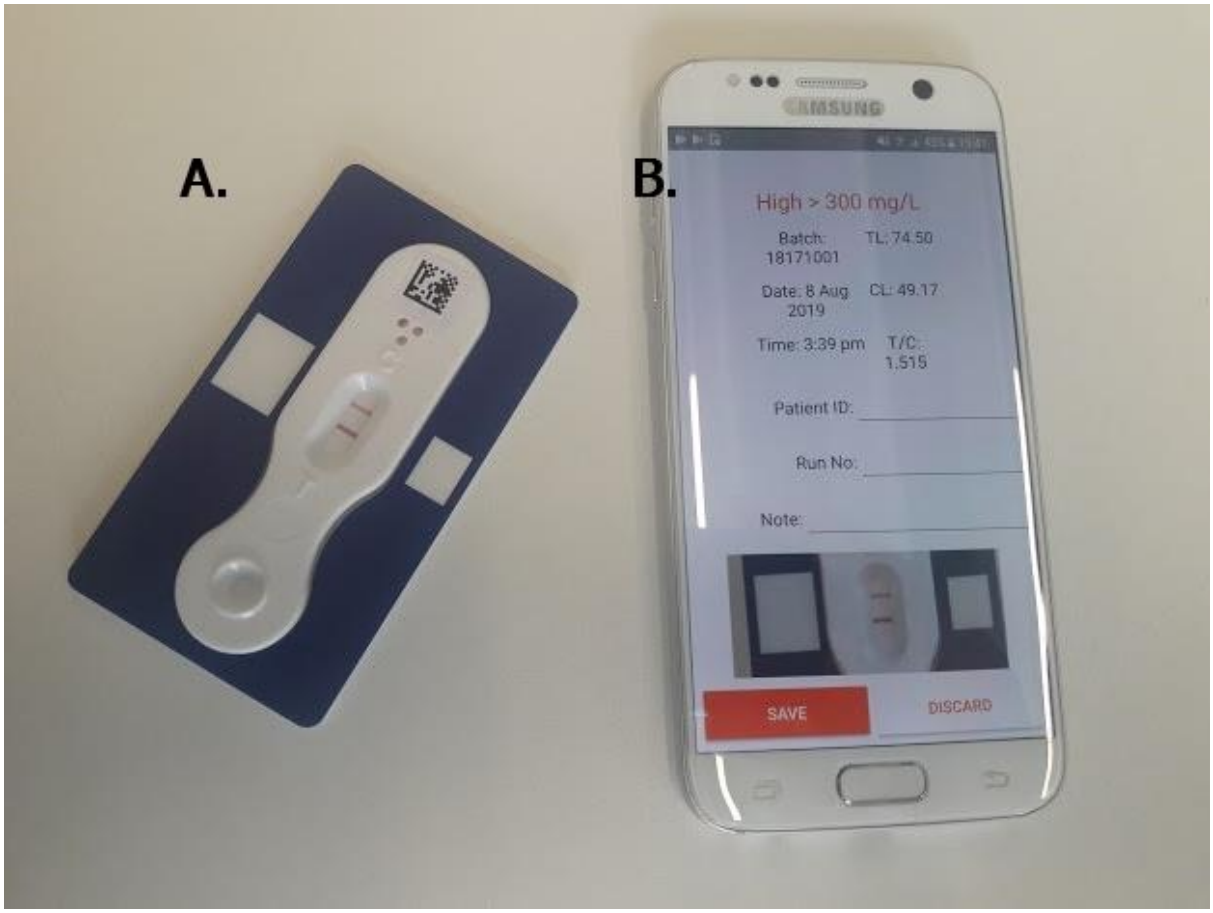

Figure 2.2. Lyfstone Calprotectin lateral flow test. A. Lyfstone Calprotectin test, B. Lyfstone application report (Lyfstone AS, Tromsø, Norway)

2.2.5 Statistical analysis

All statistical calculations were performed using MedCalc Statistical Software version 19.1 (*MedCalc Statistical Software version 19.1*, n.d.). Statistical significance was set at $p < 0.05$.

2.3 – Results

2.3.1 Lyfstone test performance compared to ICM

In total, 24 cases were classed as infected (15 hips, nine knees) and 45 cases classified as aseptic (37 hips, eight knees) according to ICM criteria. Of the infected cases, 21 were found to be positive by routine microbiology alone (two or more cultures were positive for the same organism). Two of the remaining cases were found to be positive by histology, elevated serum CRP, and one positive culture (*Collinsella aerofaciens* and 'Diphtheroids') and the remaining infected case was positive by a combination of histology, CRP, and purulence (Table 2.2). In this infected group there were 18 true positive and six false negative results according to calprotectin. The reported organisms in these false negative cases were *Cutibacterium acnes* (n = 3), *Bacteroides fragilis* (n = 1), *Staphylococcus epidermidis* (n = 1), and a polymicrobial infection of *Pseudomonas aeruginosa* with *Corynebacterium tuberculostearicum* (n = 1). The remaining 45 cases were aseptic according to ICM criteria, and of these 45 cases, 34 were true negatives and 11 were false positives by calprotectin. Of the 11 false positive cases, one case was positive for inflammation by histology and elevated CRP and one case was CRP positive without significant histology. The remaining nine false positive samples were negative for any ICM criteria tested.

Table 2.2 Available ICM criteria and calprotectin test results.

Sample number	Hip or knee	Histology *	Culture†	CRP ‡	Sinus tract§	Purulence ¶	ICM**	Calprotectin ††
1	K	negative	negative	13	N	N	negative	negative
2	H	negative	negative	40	N	N	negative	negative
3	H	negative	negative	N/A	N	N	negative	negative
4	H	negative	negative	2	N	N	negative	positive
5	H	positive	negative	47	Y	Y	positive	positive
6	H	negative	negative	2	N	N	negative	negative
7	H	negative	negative	6	N	N	negative	negative
8	K	negative	negative	< 1	N	N	negative	negative
9	H	negative	negative	7	N	N	negative	negative
10	H	negative	negative	2	N	N	negative	negative
11	H	negative	negative	7	N	N	negative	positive
12	H	negative	negative	21	N	N	negative	negative
13	H	positive	negative	35	Y	Y	positive	positive
14	H	negative	negative	< 1	N	N	negative	positive
15	K	N/A	positive	69	Y	N	positive	positive
16	H	negative	negative	1	N	N	negative	positive
17	H	negative	negative	4	N	N	negative	negative
18	H	N/A	positive	87	N	Y	positive	negative
19	H	N/A	positive	101	N	Y	positive	positive
20	H	negative	negative	1	N	N	negative	negative
21	K	N/A	positive	5	N	N	positive	negative
22	H	N/A	positive	25	N	N	positive	positive
23	H	negative	negative	10	N	N	negative	negative
24	H	negative	negative	5	N	N	negative	negative
25	K	positive	positive	286	N	Y	positive	positive
26	H	N/A	positive	44	Y	N	positive	positive
27	H	negative	negative	17	N	N	negative	positive
28	H	negative	negative	1	N	N	negative	positive
29	K	negative	negative	19	N	N	negative	negative
30	H	positive	positive	61	N	Y	positive	positive
31	K	negative	negative	N/A	N	N	negative	negative
32	H	negative	negative	< 1	N	N	negative	negative
33	H	negative	negative	6	N	N	negative	negative
34	K	positive	positive	91	N	N	positive	positive
35	H	negative	negative	5	N	N	negative	positive
36	H	negative	negative	8	N	N	negative	positive
37	H	positive	positive	114	N	Y	positive	positive

Continued on next page.

Table 2.2 Continued. Available ICM criteria and calprotectin test results.

Sample number	Hip or knee	Histology *	Culture†	CRP ‡	Sinus tract§	Purulence ¶	ICM**	Calprotectin ††
38	K	negative	negative	< 1	N	N	negative	negative
39	H	negative	negative	3	N	N	negative	negative
40	H	negative	negative	1	N	N	negative	negative
41	K	negative	negative	29	N	N	negative	negative
42	H	N/A	positive	18	N	N	positive	positive
43	H	negative	negative	1	N	N	negative	negative
44	H	negative	negative	4	N	N	negative	negative
45	H	negative	negative	2	N	N	negative	negative
46	K	N/A	positive	219	N	N	positive	positive
47	H	negative	negative	< 1	N	N	negative	negative
48	H	negative	positive	< 1	N	N	positive	negative
49	H	negative	negative	3	N	N	negative	negative
50	K	negative	positive	4	N	N	positive	negative
51	H	positive	negative	36	N	Y	positive	positive
52	H	negative	negative	2	N	N	negative	negative
53	H	negative	negative	< 1	N	N	negative	positive
54	K	negative	negative	2	N	N	negative	negative
55	K	N/A	positive	31	N	N	positive	positive
56	H	negative	positive	30	N	N	positive	negative
57	K	negative	positive	1	N	N	positive	negative
58	H	negative	negative	< 1	N	N	negative	negative
59	H	N/A	positive	49	N	Y	positive	positive
60	K	N/A	positive	67	N	Y	positive	positive
61	H	negative	negative	3	N	N	negative	negative
62	H	N/A	positive	284	Y	Y	positive	positive
63	H	negative	negative	15	N	N	negative	negative
64	H	negative	negative	4	N	N	negative	negative
65	H	negative	negative	3	N	N	negative	positive
66	K	negative	negative	6	N	N	negative	negative
67	H	positive	negative	15	N	N	negative	positive
68	H	positive	negative	3	N	N	negative	negative
69	H	N/A	positive	51	Y	N	positive	positive

Available ICM criteria results reported for samples tested with Lyfstone Calprotectin. Cells shaded green contain test negative results; cells shaded red contain test positive results; *Positive/negative for signs of inflammation by frozen section microscopy; †Positive/negative for two or more cultures of the same organism from periprosthetic tissue and fluid samples; ‡Positive when serum CRP level ≥10 mg/l; §Y represents the presence of sinus tract; ¶Y represents visible wound purulence; **Positive/negative according to scoring in Methods table 3.1; ††Positive when ≥14 mg/l synovial calprotectin measured by Lyfstone calprotectin test (Lyfstone AS, Tromsø, Norway); ICM, International Consensus Meeting 2018 criteria; N/A, not available.

The overall sensitivity and specificity of the lyfstone calprotectin test for the diagnosis of PJI compared to the available ICM criteria (2.2.2.1) were 75.00% (18/24) and 75.56% (34/45), respectively. The PPV was 62.07% (18/29), the NPV was 85.00% (34/40), and the accuracy was 75.36% (52/69) (Table 2.3). The area under the receiver operating characteristic (ROC) curve (AUC) was 0.78 (95% CI 0.66 to 0.87) (Figure 2.3).

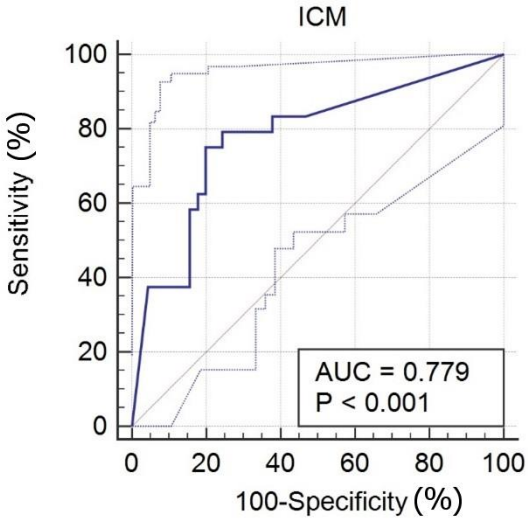

Figure 2.3. ROC AUC of the Lyfstone calprotectin test against ICM criteria for infection. True positivity rate (sensitivity) plotted against false positivity rate (100-specificity) using MedCalc. Bold line represents data, dashed lines represent 95% confidence intervals.

In the hip revision surgery group (n = 52) the test had a sensitivity of 80.00% (12/15) and specificity of 70.27% (26/37). The PPV and NPV were 52.17% (12/23) and 89.66% (26/29), respectively, overall test accuracy was 73.08% (38/52). All 11 false positive results in the study were from hip revision samples. In the knee revision surgery group (n = 17) the test was 66.67% sensitive (6/9) and 100.00% specific (8/8). With no false positive results from knee revision, the PPV was 100.00% (6/6) but the NPV was 72.73% (8/11) (Table 2.3). Overall test accuracy was higher from knee revisions than in the hip revision group at 82.35% (14/17).

Table 2.3 Performance of Lyfstone Calprotectin test against ICM criteria

Lyfstone test	All samples (n = 69)	Hips (n = 52)	Knees (n = 17)
Sensitivity, % **(95% CI)**	75.00 (18/24) (53.29 to 90.23)	80.00 (12/15) (51.91 to 95.67)	66.67 (6/9) (29.93 to 92.51)
Specificity, % **(95% CI)**	75.56 (34/45) (60.46 to 87.12)	70.27 (26/37) (53.02 to 84.13)	100.00 (8/8) (63.06 to 100.00)
PPV, % **(95% CI)**	62.07 (18/29) (48.23 to 74.19)	52.17 (12/23) (38.48 to 65.55)	100.00 (6/6) (100.00 to 100.00)
NPV, % **(95% CI)**	85.00 (34/40) (73.54 to 92.04)	89.66 (26/29) (75.51 to 96.06)	72.73 (8/11) (51.42 to 87.04)
Accuracy, % **(95% CI)**	75.36 (52/69) (63.51 to 84.95)	73.08 (38/52) (58.98 to 84.43)	82.35 (14/17) (56.57 to 96.20)

2.3.2 Lyfstone test performance compared to ICM-CR

A clinical review was performed for patients associated with discordant results between Lyfstone Calprotectin and ICM to better define the clinical outcome (ICM-CR). Overall, the test accuracy compared to ICM-CR was 82.61% (57/69). Sensitivity and specificity were 94.74% (18/19) and 78.00% (39/50), respectively, with a PPV of 62.07% (18/29) and NPV of 97.50% (39/40) (Table 2.4). The AUC against ICM-CR was 0.91(95% CI 0.81 to 0.96) (Figure 2.4). The clinical review (ICM-CR) increased the sensitivity of the Lyfstone test from 75.00% (18/24) to 94.74% (18/19).

Table 2.4 Performance of Lyfstone Calprotectin test against clinical review outcome (ICM-CR)

Lyfstone test	All samples (n = 69)	Hips (n = 52)	Knees (n = 17)
Sensitivity, %	94.74 (18/19)	92.31 (12/13)	100.00 (6/6)
(95% CI)	(73.97 to 99.87)	(63.97 to 99.81)	(54.07 to 100.00)
Specificity, %	78.00 (39/50)	71.79 (28/39)	100.00 (11/11)
(95% CI)	(64.04 to 88.47)	(55.13 to 85.00)	(71.51 to 100.00)
PPV, %	62.07 (18/29)	52.17 (12/23)	100.00 (6/6)
(95% CI)	(49.00 to 73.60)	(39.23 to 64.83)	(100.00 to 100.00)
NPV, %	97.50 (39/40)	96.55 (28/29)	100.00 (11/11)
(95% CI)	(85.20 to 99.62)	(80.83 to 99.47)	(100.00 to 100.00)
Accuracy, %	82.61 (57/69)	76.92 (40/52)	100.00 (17/17)
(95% CI)	(71.59 to 90.68)	(63.16 to 87.47)	(80.49 to 100.00)

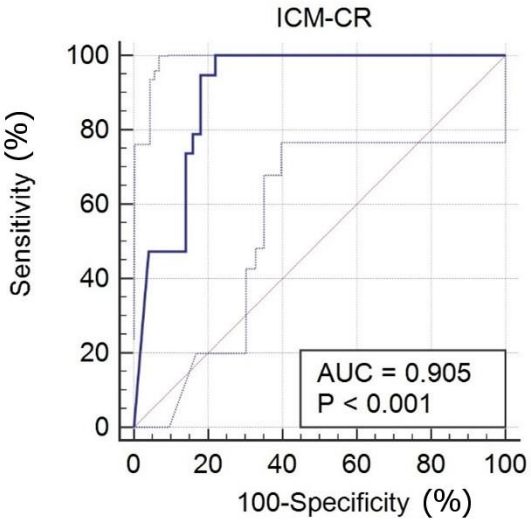

Figure 2.4. ROC AUC of Lyfstone calprotectin test against ICM-CR classification for infection. True positivity rate (sensitivity) plotted against false positivity rate (100-specificity) using MedCalc. Bold line represents data, dashed lines represent 95% confidence intervals.

Results which remained discordant by Lyfstone Calprotectin again ICM-CR were investigated to resolve possible false positives by metallosis/severe osteolysis. In the hip revision group, radiograph and medical record review identified five patients had metal-on-metal implants with evidence of an adverse reaction to metal debris. Additionally, two patients showed severe metal

staining of tissue caused by wear of the acetabular component following wear of the polyethylene liner. The remaining false positive cases (n=4) had aseptic loosening listed as the initial indication for operation. Review of preoperative radiographs and operation notes reported pre- and intraoperative evidence of osteolysis in three out of these four cases, to either the proximal femur or acetabulum (Table 2.5).

Table 2.5 Paprosky femoral and acetabular classification of patients diagnosed with aseptic loosening and with high calprotectin levels reported.

Sample number	Femur	Acetabulum
4	IIIB	I
27	I	IIIA
28	II	IIB

One-year follow-up of the final unresolved case (patient 35) revealed that they were still experiencing pain in their joint and their CRP level had risen from 5 mg/l to 19 mg/l. This indicated a possible chronic infection and the patient remains under investigation by the treating team. A total of 53 patients remained once both metallosis and severe osteolysis cases had been removed from the dataset. This resulted in improved specificity, PPV, and the overall accuracy of the test against both ICM and ICM-CR (Table 2.6). The three false negative results within the hip subset were all ICM positive by culture alone (two or more cultures of the same organism). Patient 18 was culture positive for *B. fragilis*, which was isolated from all cultured tissue samples, also reporting a high CRP and noted joint purulence. The Calprotectin result was 13.36 mg/l, which falls just below the threshold value for a positive result (≥14 mg/l) (Appendix table for supplementary CLP data). Sample 48 was culture-positive for *C. acnes* but both histology and CRP were negative. The calprotectin test was negative with 0.0 mg/L reported. The initial indication for operation for this case was aseptic loosening and a single-stage revision had been performed. The *C. acnes* culture report was considered contamination and the patient was not treated for infection. One-year follow-up of the patient showed no signs of infection, therefore the calprotectin result agreed with the clinical findings. Sample 56 was a similar case of a revision for aseptic loosening yielding

significant culture results (*P. aeruginosa* and *C. tuberculostearicum*) with no detectable synovial fluid calprotectin. The patient underwent a single-stage revision and upon two-month follow-up showed no sign of infection, indicating another true negative calprotectin result.

Table 2.6 Performance of calprotectin test on tested synovial fluid samples, excluding metallosis and severe osteolysis cases.

Lyfstone* test	**Gold standard**	
	ICM (n = 53)†	**ICM-CR‡**
Sensitivity, % (95% CI)	71.43 (47.82 to 88.72)	93.75 (69.77 to 99.84)
Specificity, % (95% CI)	96.88 (83.78 to 99.92)	97.30 (85.84 to 99.93)
PPV, % (95% CI)	93.75 (68.14 to 99.06)	93.75 (68.36 to 99.05)
NPV, % (95% CI)	83.78 (72.37 to 91.06)	93.70 (84.36 to 99.59)
Accuracy, % (95% CI)	86.79 (74.66 to 94.52)	96.23 (87.02 to 99.54)

*Lyfstone AS, Tromsø, Norway; †Calprotectin result against ICM criteria (n = 53) for infection excluding all samples associated with metallosis and severe osteolysis; ‡Calprotectin result against ICM criteria (n = 53) for infection with discrepant samples investigated by clinical follow-up excluding all samples associated with metallosis and severe osteolysis.

In the knee group, three more false negative results were recorded; two cases of *C. acnes* and one case reporting *S. epidermidis*. Both the *C. acnes* cases (samples 50 and 57) were from patients displaying no preoperative indication of infection and were treated as aseptic loosening. The clinical review found no complications after patient follow-up, suggesting that both cases were aseptic and that the calprotectin results had been accurate. Sample 21 (*S. epidermidis*) was taken during the second stage of revision surgery performed one year after the initial first-stage operation. Clinical review revealed that the patient was originally treated for gross infection. At the time of the second-stage revision, the patient showed no remaining signs of infection, as such, treatment progressed to implantation of the prosthesis. Postoperative microbiology cultured *S. epidermidis* from three of six samples taken at the time of surgery. One-year follow-up reported no sign of infection, confirming the calprotectin result to be correct thus far. Overall, the Lyfstone test was 100% accurate for the diagnosis of PJI in knee samples after clinical review (n = 17; Tables 2.3 and 2.4).

Overall test accuracy against ICM-CR was higher in those patients with inflammatory past medical conditions, 89.47% (17/19, 95% CI 66.86 to 98.70) than in patients with no prior conditions, 80.00% (40/50, 95% CI 66.28 to 89.97) (Table 2.7). While it may be expected that inflammatory conditions could generate false positive test results the overlapping confidence intervals suggest that there is not significant impact on performance of the Lyfstone Calprotectin test.

The proportion of false positive results in patients with a relevant medical condition as described in the treating surgeon's notes is lower (2/10) than in patients without any relevant conditions noted (9/19). No false positives were reported from patients with either RA (n=6), chronic lymphoid leukaemia (CLL) (n=2) or ankylosing spondylitis (AS) (n=1). 11.1% of patients (1/9) with type-2 diabetes mellitus (T2DM), 33.3% (1/3) with polymyalgia rheumatica (PR) and 100% (1/1) with ulcerative colitis (UC) did record a false positive result. Patients with a record of more than one relevant condition recorded a 33.3% (1/3) false positive test rate.

Table 2.7 Accuracy of calprotectin test on patients with past medical history of inflammatory conditions against ICM-CR.

Relevant Past Medical History	**No Condition**	**Any Condition**	**Rheumatoid Arthritis**	**[1]T2DM**	**[2]CLL**	**Polymyalgia Rheumatica**	**Ankylosing spondylitis**	**Ulcerative Colitis**	**Multiple Conditions**
Accuracy, % (n/total n) (95% CI)	80.00 (40/50) (66.28 to 89.97)	89.47 (17/19) (66.86 to 98.70)	100 (6/6) (54.07 to 100)	88.89 (8/9) (51.75 to 99.72)	100.00 (2/2) (100.00 to 100.00)	66.67 (2/3) (9.43 to 99.16)	100 (1/1) (n/a)	0 (0/1) (n/a)	66.67 (2/3) (9.43 to 99.16)
Test positives, % (n/total n)	38.00 (19/50)	52.63 (10/19)	50.00 (3/6)	66.67 (6/9)	0.00 (0/2)	66.67 (2/3)	100.00 (1/1)	100.00 (1/1)	100.00 (3/3)
False positives, % (n/total n)	47.37 (9/19)	20.00 (2/10)	0.00 (0/3)	16.67 (1/6)	0.00 (0/0)	50.00 (1/2)	0.00 (0/1)	100.00 (1/1)	33.34 (1/3)

Medical conditions determined relevant as recorded in treating surgeon's notes; No Condition, no relevant past medical history recorded by the treating surgeon; Any Condition, any of the six conditions listed in the next six columns; [1]T2DM, Type 2 Diabetes Mellitus; [2]CLL, Chronic Lymphoid Leukaemia; Multiple Conditions, any combination of the conditions listed in this table; Test positives calculated as positive test results from total patients within a condition subset; False positives calculated as number of false positive test results from total positive test results from patients within a condition subset.

The instructions for use for the Synovasure lateral flow test warn that blood presence may lead to false negative results (Zimmer Biomet. Diagnostics C. Synovasure Alpha Defensin Lateral Flow Test Kit: Instructions For Use). A total of 49 samples tested with Lyfstone Calprotectin had notes taken on blood presence within the synovial fluid sample to determine if the test was suitable for use with synovial fluid samples containing blood.

14 samples were categorised as containing no blood, nine samples with low blood contamination and 26 samples containing a high level of blood (Table 2.8). Overall test accuracy against ICM was highest in the no blood group at 92.86% (13/14, 95% CI 66.13 to 99.82). Sensitivity against ICM was highest in the high blood group 84.62% (11/13 95% CI 54.55 to 98.08) over no blood and low blood, both at 66.67% (2/3 95% CI 9.43 to 99.16). However, against ICM-CR both no blood and low blood showed 100% sensitivity (2/2 in both groups) while the high blood group still contained one false negative result with a sensitivity of 91.67% (11/12 95% CI 61.52 to 99.79).

Specificity in the no blood and low blood groups was 100% against both ICM and ICM-CR as no false positive results were recorded in either of these groups. Six false positive results were recorded in the high blood group resulting in a specificity of 53.85% (7/13, 95% CI 25.13 to 80.78) against ICM and 57.14% (8/14, 95% CI 28.86 to 82.34) against ICM-CR.

Samples from the hip group were more likely to fall into the high blood group with 62.86% of hip samples (22/35) being classified as high blood (8 no blood, 5 low blood), whereas samples from the knee group were more evenly spread between the three categories (6 no blood, 4 low blood, 4 high blood) (Table 2.8).

Table 2.8 Performance of calprotectin test under varying blood presence within the synovial fluid sample.

Lyfstone* test	**Level of Blood in Sample/Gold Standard**					
	No Blood		**Low Blood**		**High Blood**	
	ICM	**ICM-CR**	**ICM**	**ICM-CR**	**ICM**	**ICM-CR**
Sensitivity, %	66.67 (2/3)	100.00 (2/2)	66.67 (2/3)	100.00 (2/2)	84.62 (11/13)	91.67 (11/12)
(95% CI)	(9.43 to 99.16)	(100.00 to 100.00)	(9.43 to 99.16)	(100.00 to 100.00)	(54.55 to 98.08)	(61.52 to 99.79)
Specificity, %	100.00 (11/11)	100.00 (12/12)	100 (6/6)	100.00 (7/7)	53.85 (7/13)	57.14 (8/14)
(95% CI)	(71.51 to 100.00)	(100.00 to 100.00)	(54.07 to 100.00)	(100.00 to 100.00)	(25.13 to 80.78)	(28.86 to 82.34)
PPV, %	100.00 (2/2)	100.00 (2/2)	100 (2/2)	100.00 (2/2)	64.71 (11/17)	64.71 (11/17)
(95% CI)	(100.00 to 100.00)	(100.00 to 100.00)	(100.00 to 100.00)	(100.00 to 100.00)	(49.37 to 77.51)	(49.44 to 77.46)
NPV, %	91.67 (11/12)	100.00 (12/12)	85.71 (6/7)	100.00 (7/7)	77.78 (7/9)	88.89 (8/9)
(95% CI)	(68.95 to 98.20)	(100.00 to 100.00)	(54.77 to 96.75)	(100.00 to 100.00)	(47.06 to 93.24)	(53.71 to 98.22)
Accuracy, %	92.86 (13/14)	100.00 (14/14)	88.89 (8/9)	100.00 (9/9)	69.23 (18/26)	73.08 (19/26)
(95% CI)	(66.13 to 99.82)	(100.00 to 100.00)	(51.75 to 99.72)	(100.00 to 100.00)	(48.21 to 85.67)	(52.21 to 88.43)

*Lyfstone AS, Tromsø, Norway; ICM, International Consensus Meeting 2018 criteria; ICM-CR, International Consensus Meeting 2018 criteria with clinical review; No Blood, no visible blood contamination in the synovial fluid sample; Low Blood, some blood contamination visible with sample colour ranging from orange to light red; High Blood, sample heaving contaminated by blood presence with a dark red colour.

2.4 – Discussion

PJI is a serious complication of arthroplasty with significant associated patient morbidity and a substantial economic burden of treatment (Barrack et al., 2007; Berend et al., 2013). Microbiological culture techniques are slow and insensitive (Boyle et al., 2018; Parvizi et al., 2014a) and although new diagnostic tests are being developed, none of the current methods are capable of reliably diagnosing PJI (Fernández-Sampedro et al., 2017; Parvizi et al., 2018).

Rapid biomarker-based tests have the potential to assist clinicians in making a preoperative diagnosis. Early differentiation of PJI from aseptic loosening may reduce the number of unnecessary two-stage revisions performed on patients with a presumptive diagnosis of low-grade infection.

The Synovasure test (Zimmer Biomet, Warsaw, Indiana, USA), measuring α-defensin, functions very similarly to the Lyfstone calprotectin test. Studies using the lateral flow version of the Synovasure test had a mean sensitivity of 85% and a mean specificity of 90% (Marson et al., 2018). The recent studies using calprotectin either by ELISA method or an off-label lateral flow assay for measuring faecal calprotectin have shown similar diagnostic performance. Wouthuyzen-Bakker *et al.* demonstrated a sensitivity of 89% and a specificity of 90% in a pilot study (Wouthuyzen-Bakker et al., 2017) and 86.7% and 91.6% in a follow-on study using the lateral flow assay (Wouthuyzen-Bakker et al., 2018). The more recent study by Salari *et al.* (2020) reported a sensitivity of 100% and a specificity of 95% utilizing an ELISA-based calprotectin test.

In our hands, the Lyfstone Calprotectin lateral flow test demonstrated a sensitivity of 75.00% and a specificity of 75.56% using similar gold standard diagnostic criteria. Our study is of a comparable size (69 samples compared to 61 (Wouthuyzen-Bakker et al., 2017), 52, (Wouthuyzen-Bakker et al., 2018) and 76 (Salari et al., 2020)) and featured a similar prevalence of infected samples to these three studies (35% compared to 31% (Wouthuyzen-Bakker et al., 2017), 29%, (Wouthuyzen-Bakker et al., 2018) and 37% (Salari et al., 2020)), however the sensitivity and specificity of the lateral flow assay is lower than previous calprotectin-based studies have shown. Similar differences

in performance have previously been reported between the Synovasure α-defensin lateral flow test and the α-defensin ELISA method (Suen et al., 2018).

A recent study using Lyfstone Calprotectin has been published by the Cleveland Clinic, Ohio (Warren et al., 2021). This study compared synovial fluid calprotectin using cutoffs of both ≥14 mg/L (as used in our study) and ≥50 mg/L to MSIS criteria for infection, using samples from 123 TKA patients (53 infected, 70 aseptic). They report very high sensitivity and specificity of 98.1% and 95.7%, respectively, using a ≥50 mg/L cutoff, with a lower specificity of 87.1% at ≥14 mg/L but no change in sensitivity. If we were to apply a ≥50 mg/L cutoff for calprotectin to our dataset the specificity would improve from 76% to 86% against ICM criteria with a decrease in sensitivity from 75% to 63%. This cutoff would not be appropriate for our dataset as 6/18 infections detected by calprotectin at ≥14 mg/L would have been missed. The higher performance of the Cleveland Clinic study is likely because their samples were only taken from knee revisions which we saw to perform better with the assay than hip samples in our study.

The sensitivity and specificity after clinical review (93.75% and 97.30% respectively) are consistent with other calprotectin studies. Differences in inclusion criteria, sample collection, and microbiology techniques applied may explain other differences in performance observed. Observed test accuracy was different for hip and knee revisions. False positive results were only observed in hip revisions, likely affected by the absence of metal-on-metal reactions in the knee revision group. While the test accuracy for knee revisions compared to ICM-CR was 100%, the sample size is small (17 revisions, eight positive for infection) and the 95% confidence intervals are too wide (sensitivity CI 54.07% to 100.00%; specificity CI 71.51% to 100.00%) to draw conclusions with high confidence. As such, more data are required to confirm these findings.

The clinical review of discordant cases revealed that the low specificity of the calprotectin lateral flow test was associated with metallosis (7/11 false positive cases). The removal of these samples increased the specificity from 75.56% to 83.78%. The use of inflammation biomarker-based diagnostic tests is reported to be unreliable in patients with metal-on-metal implants as these can cause gross inflammation generating false positive results (Bonanzinga et al., 2017; Drummond et al., 2015). Severe osteolysis can also cause false positive results for the same reason and removing

patients with severe osteolysis (n = 3) from the analysis further increased specificity to 96.88%, which is more in line with the previously published calprotectin studies (Salari et al., 2020; Wouthuyzen-Bakker et al., 2018, 2017) (Salari *et al.* excluded patients with metal-on-metal implants).

Clinical review also revealed that five out of six false negative results were from samples wherein the organisms detected by culture could be considered contaminants. Three of these six false negative samples were positive for *C. acnes* by culture. This organism is commonly considered a laboratory contaminant and not typically a cause of PJI when isolated from hip or knee tissues (Both et al., 2018; Levy et al., 2008; Patel et al., 2009). Only one false negative case was considered a genuine infection by clinical review (case 18), in which the calprotectin result was close to the positive cut-off value (13.36 mg/l, <1 mg/l below the positive cut-off). Future optimization of the test could set a lower threshold value for infection which would have classified this case as positive. This readjustment could lead to more false positive results; however, it may improve test performance in detecting low-grade infections. If the test is to be used as a rapid rule-out test for PJI then a more sensitive, less specific, test would be more useful.

No individual inflammatory condition showed high false positive rates from inflammation unrelated to infection, outside of those with very small sample sizes (1-3 patients) which have very wide 95% confidence intervals. RA would be one of the more likely conditions to cause false positive results as the inflammation is localised to the joints (Scott et al., 2010), and as such is normally excluded from studies and not recommended for use with these tests (Bingham et al., 2014). However, there were no false positive results from patients with RA (three true positive, three true negative). RA and T2DM were the most common inflammatory conditions within our sample set, with 14 of the 19 patients displaying one or more of these conditions (six RA, nine T2DM, one patient with both). Only one false positive result was found from these patients. If the test is suitable for patients with these conditions it would be a significant advantage, as these patients typically cannot be offered such tests.

The false positive rate was lower in patients with a relevant condition than with no condition reported at 20.00% and 47.37% respectively. As inflammatory conditions should increase the level

of calprotectin found in synovial fluid as a result of an increase in neutrophil activity (Chavakis et al., 2009; Ley et al., 2007) it would be expected that these patients would be more likely to trigger false positive results. The clinical review shows that both false positive cases associated with a relevant inflammatory condition were metallosis patients, explaining why the recorded calprotectin level was high showing the high calprotectin level was not caused by the inflammatory condition. The remaining five metallosis false positives were in the no condition group, along with the three gross osteolysis and one remaining unresolved case. The higher false positive rate is likely an artefact of all gross osteolysis patients belonging to the no condition group, while metallosis incidence is similar between no condition and condition present (5/50 and 2/19, respectively).

There was no great trend towards false negative results in any blood category (no blood = 1, low blood = 1, high blood =2) against ICM in our results. Although the sample size is small, the false negative results are evenly split across the blood level groups. While the theory of blood presence diluting accessible calprotectin for testing suggest that any false negatives would be part of the high blood category, we see a false negative result in both the low blood and no blood groups. However, the one remaining false negative following clinical review (sample 18) is part of the high blood contamination group. This may be significant as the reported calprotectin level was very close to the positive threshold and as such may have tested as true positive in the absence of blood. There is insufficient evidence that blood presence in the samples has affected test performance as sensitivity against ICM-CR in the high blood group is still high at 91.67%.

The specificity within the high blood group was low against ICM and ICM-CR as all false positives were in the high blood category. As all false positives within the study were from hip patients the high blood level may just be a coincidence and not be related to low specificity; hip samples may just be more likely to contain high levels of blood (62.86% of hip samples fell into the high blood category). It would be expected that hip samples would be more likely to show blood contamination than knee samples due to the joint being surrounded by deep tissue that requires puncturing for synovial fluid sample aspiration (Hansford and Stacy, 2012). While blood presence in the synovial fluid is theorised to dilute host pathogen markers beyond test detection levels there is no established reason that blood contamination would trigger false positive test results. Not all

samples with high blood presence trigger false positive results which would be expected if blood was causing false positive results.

As 35/49 samples (71.43%) with notes on blood presence contained some blood contamination, this accounts for a significant proportion of our study. As the overall test accuracy against ICM and ICM-CR was high, the test is suitable for use with blood contaminated samples, which are commonly collected.

This study was limited by the use of retrospective samples. However, by testing all eligible samples in the biorepository we did not introduce any sample selection bias. The relatively small sample size has resulted in wide 95% CIs throughout, hence larger studies are required to confirm study findings. The samples had been frozen for storage before testing and the freeze-thaw process may have resulted in leucocyte cell lysis and an increase in calprotectin. As the test is validated for use on fresh synovial fluid samples, the recommended cut-offs may not necessarily be appropriate for the samples tested in this study.

The Lyfstone calprotectin lateral flow test shows good potential for rapid diagnosis of PJI. A high NPV makes this a potentially powerful rule-out test for infection in suspected PJI cases. However, larger prospective studies, using consecutive samples from patients undergoing revision of all synovial joint arthroplasties, are required to more accurately define the test's diagnostic performance.

Chapter 3 – Pathogen Sequencing

3.1 Introduction

The rapid detection of host cell biomarkers can be used to determine if a patient has an infection. However, pathogen identification is also required to identify the cause of infection and decide an appropriate treatment plan. As previously discussed (Chapter 1.9), the gold standard for pathogen identification is microbial culture, however, molecular diagnostics (e.g. PCR based methods) can provide a more rapid approach. A new area in the field of molecular diagnostics is the application of metagenomic sequencing for the diagnosis of pathogens i.e. clinical metagenomics. This chapter details the application of clinical metagenomics (CMg) to agnostically detect pathogens directly from whole prosthesis and periprosthetic tissue samples using rapid nanopore sequencing.

3.1.1 DNA sequencing

DNA sequencing technology was originally developed in 1977 by Prof Frederick Sanger and colleagues, known as Sanger sequencing, a method by which DNA sequences are identified through chain termination by dideoxynucleotide triphosphates (ddNTPs). ddNTPs are chemical analogues of deoxyribonucleotide triphosphates (dNTPs) lacking the 3' hydroxyl group required to bind the next section of the phosphate backbone, thereby enabling chain termination Incorporating radioactive or fluorescently labelled ddNTPS for each base position enables the nucleotide pattern to be visualised providing the original DNA sequence (Heather and Chain, 2016). Sanger sequencing is still used now e.g for PCR amplicon sequencing (da Fonseca et al., 2016). Advancements in sequencing technology led to the development of next generation sequencing (NGS) (for a comprehensive history of sequencing technology refer to (Heather and Chain, 2016)). The NGS market is currently dominated by Illumina sequencing, which works based on the incorporation of dNTPs at the last position of a DNA strand during DNA synthesis in a method known as 'sequencing by synthesis'. The incorporated dNTP is detected through specific fluorophore excitation and then enzymatically removed to allow DNA synthesis to continue. Illumina sequencing provides high throughput short-read sequence data (50-600bp in length)

(Heather and Chain, 2016). The drawback of short-read sequencing is the inability to sequence long stretches of DNA. To sequence a large genome, the DNA has to be fragmented and amplified then assembled into a contiguous sequence (Mardis, 2017). This poses a challenge when sequencing a complex and repetitive genome, such as the human genome, as PCR amplification preferentially amplifies repetitive DNA and short read sequencing can fail to generate significant overlap sequences from the amplified fragments (Adewale, 2020).

In contrast to Illumina's sequencing by synthesis approach, nanopore sequencing reads are generated directly from an existing DNA sequence. dsDNA fragments are enzymatically unwound so that ssDNA can translocate through a protein pore embedded in a membrane (a nanopore). This membrane is immersed in a charged solution, as the ssDNA passes through the membrane a unique change in current is recorded for each of the four bases. The squiggle plot generated from each current change is then used to identify the sequence of the DNA strand (Ip et al., 2015; Jain et al., 2018; Tyson et al., 2018) (for a comprehensive history of nanopore sequencing refer to (Deamer et al., 2016)). ONT released its first commercial sequencer, the MinION, in 2014. While nanopore sequencing initially had poor sequency accuracy (60-70%) compared to other technologies such as Illumina (99%) (Rang et al., 2018), improvements in the flow cell pores (from R6/7 to R9 and R10) and basecalling software (from event-based basecalling to raw signal-based basecalling) has improved the raw read accuracy to >97% (nanoporetech.com/accuracy).

Nanopore sequencing is a long-read technology, typically producing average read-lengths >5kb and can generate extremely long reads (>4Mb reported). While short reads are more accurate (Amarasinghe et al., 2020), long reads facilitate mapping of resistance genes in bacterial chromosomes without the need for assemblies (Ashton et al., 2015; Leggett et al., 2020), the identification of genome rearrangements (Page and Langridge, 2019), more accurate assembly of repetitive sections of genomes (eg human genome) (Logsdon et al., 2021; Miga et al., 2020) and can be combined with short reads to generate the most accurate genome assemblies (Stewart et al., 2019). An advantage of nanopore sequencing is real-time data analysis (Eisenstein, 2012; Loman et al., 2012), key for rapid diagnostic applications.

While sequencing approaches can offer a more rapid turnaround time than culture, with some sequencing companies advertising run time options of 4-6 hours, lengthy library preparation along with the requirement for end point analysis results in considerably longer actual turnaround times. According to the manufacturer's websites, Illumina sequencers have the longest run times (4-55 hours), compared to Ion Torrent (2.5-4 hours) and PacBio (0.5-30 hours). ONT devices offer the shortest and most flexible run times as sequence reads are generated and can be analysed while the sequencer is running.

3.1.2 Diagnostic sequencing

Diagnosis of infection by sequencing can be either targeted or non-targeted. Targeted sequencing uses deep sequencing to detect known and novel variants in genomic regions or gene sets, typically selected by hybridization capture or amplicon sequencing. Non-targeted approaches (metagenomics) study all genomic information present in a primary sample (clinical, environmental, animal or food) (Thomas et al., 2012; Wooley et al., 2010). Clinical metagenomics (CMg) is the untargeted sequencing of all genetic material (DNA and/or RNA) within a patient sample, both microbial and host in origin (Ruppé et al., 2017a; Ruppé and Schrenzel, 2018).

CMg utilising nanopore sequencing can return rapid diagnostic results. With results generated in real-time analysis instead of waiting for end-point analysis, a clinical metagenomics pipeline performed on an ONT MinION compared to an Illumina MiSeq demonstrated that the MinION workflow could provide results over 14 hours earlier (6 compared to >20 hours) (Greninger et al., 2015). Schmidt *et al.* developed a diagnostic pipeline for urinary tract infections with turnaround as short as 4 hours from sample-to-result (Schmidt et al., 2017).

3.1.2.1 Targeted sequencing

Diagnostic targeted metagenomic sequencing approaches typically utilise PCR amplification of housekeeping genes to differentiate microbes in a clinical sample (Bertelli and Greub, 2013). The most common target for bacteria is the 16S rRNA gene due to highly conserved and hypervariable

regions in its sequence (Clarridge, 2004). While this was originally done by Sanger sequencing, the development of NGS allows for genus level identification of bacteria in complex communities (Gupta et al., 2019). While short read sequencing can only sequence fragments of the 16S gene, e.g. V3-V4, without assembly, long-read technologies (ONT and PacBio) can sequence the full gene (~1500 bp), providing more accurate bacterial identification (Johnson et al., 2019). Due to traditionally slow turnaround times, 16S sequencing has mainly been used in reference laboratories to identify fastidious organisms or to detect pathogens in difficult sterile site clinical samples when culture has failed to detect anything e.g. in blood for sepsis and CSF for meningitis (Mongkolrattanothai and Dien Bard, 2017). However, recent studies have demonstrated that full-length 16S rRNA gene sequencing can be performed using ONT platforms to identify pathogens within clinical samples in <1 hour (Mitsuhashi et al., 2017; Moon et al., 2017). The drawbacks to 16S sequencing are that pathogen differentiation is not reliable at the species level, universal targets are not available for viruses (although 18S sequencing is available for fungi) and 16S targets are unable to provide information on AMR (Trotter et al., 2019). We wrote a review on the topic of rapid diagnosis of infection and antimicrobial resistance published in Current Opinion in Microbiology in 2019 (google scholar citations: 27 as of 29/06/2021) (Appendix 2).

Targeted sequencing approaches that can detect whole pathogen genomes or a selection of relevant pathogens and resistance genes are being designed through amplicon sequencing panels. These panels can be organism specific such as the ARTIC network amplicon panel designed for whole genome sequencing of SARS-CoV-2, which has been used worldwide to generate over 2 million genomes (www.gisaid.org). This tiling PCR approach allows for targeted sequencing of the whole genome providing data to determine SNP differences between samples, building up phylogenetic trees of virus lineages to analyse transmission patterns and detect potentially concerning mutations during the pandemic (COVID-19 Genomics UK (COG-UK) consortium, 2020) (For a list of papers that I was involved with during my write-up time as part of COG-UK see Appendix 3). Alternatively, panels can be designed to cover multiple bacteria or viruses (Allicock et al., 2018) for diagnosis, however, a panel can only be designed based on what organisms and/or AMR gene targets are known and cannot be used to identify novel species/AMR genes (Franco-Duarte et al.,

2019). This approach can be particularly useful in diseases where high sensitivity tests are required, such as sepsis, however, these methods need to be sufficiently rapid to be clinically useful.

3.1.2.2 Clinical metagenomics

CMg is the culture-free characterisation of all genetic material in a clinical sample. As such, it can bypass some limitations of culture such as turnaround time and difficulty detecting fastidious organisms. By characterising all available genetic material, CMg is also more comprehensive than targeted methods. An example is demonstrated in a study of a patient with suspected encephalitis despite negative viral PCR and bacterial culture results. CMg, however, was able to diagnose an astrovirus infection, an uncommon encephalitis pathogen which was not included in the routine diagnostic workup (Naccache et al., 2015). However, care must be taken when interpreting metagenomics results as a detected organism may not necessarily be the cause for disease and there is a risk of reagent or laboratory contamination of the sequencing pipeline.

Another issue is that human DNA largely dominates primary clinical samples (Doughty et al., 2014). One bacterial cell contains approximately 2,000-fold less DNA (2.8 fg for *S. aureus*) (Staphylococcus aureus subsp. aureus NCTC 8325) than a human cell (6 pg) (Bäumer et al., 2018) and human cells vastly outnumber bacterial cells e.g. a typical blood sample from a sepsis patient will contain <50 CFU/ml bacteria (Stranieri et al., 2018) and 10^6 leukocytes per ml (Sharma and Marwaha, 2010) resulting in >10^8:1 human:bacterial DNA ratio in the sample. This limitation was demonstrated by Pendleton *et al.* who applied CMg for the diagnosis of two confirmed cases of bacterial pneumonia without any microbial enrichment or host depletion strategy. The vast majority of sequencing reads generated were from host cells (99%) with only three pathogen reads identified in the samples tested (two *S. aureus* and one *P. aeruginosa*) (Pendleton et al., 2017). In samples where the ratio of human to microbial DNA is very high, pathogen identification requires time consuming deep sequencing to generate sufficient genome coverage (Chiu and Miller, 2019). As this approach yields slow turnaround times greater than two days, along with incurring high costs, it would not be a suitable replacement for culture-based methods. Therefore, successful enrichment of microbial DNA or depletion of host cell DNA is essential in CMg (Couto et al., 2018).

3.1.3 CMg for pathogen identification from PJI samples

A proof-of-concept study by Ruppé *et al*. used differential cell lysis of human cells and the elimination of free DNA with the Molzym Ultra-Deep Microbiome Prep kit. They showed that utilising host cell depletion before Illumina sequencing, CMg could be used to diagnose PJI from tissue samples, with a sensitivity of 100% in monomicrobial infections (n=8) and 58.2% sensitive in polymicrobial infections (n=16, 32/55 organisms found) to species level. The authors were also able to successfully predict antibiotic susceptibility in 94.1% and 76.5% of samples, respectively (Ruppé et al., 2017b).

Culture of sonication fluid from explanted prostheses or PPT is sometimes used to improve diagnostic sensitivity through mechanical disruption of bacterial biofilms, increasing bacterial yield. Since its initial application to hip prostheses samples in 1998 (Tunney et al., 1998), multiple studies have reported improved sensitivity of sonication fluid over routine PPT culture across a range of explant locations (Piper et al., 2009; Trampuz et al., 2007). The method has been adopted either alone or in conjunction with PPT but is not commonly used in the UK. Street *et al.* applied CMg to 131 sonication fluid samples and compared to culture of the sonication fluid as well as 1-8 PPT samples per patient. Prosthesis components were placed in sterile containers with saline solution and manipulated by vortex and sonication. The sonication fluid was concentrated by centrifugation and human cells were removed from the resuspended pellet using filtration to deplete human DNA. DNA was extracted followed by sequencing on the Illumina MiSeq (Street et al., 2017). Compared to sonication fluid culture, CMg was 84% sensitive (26/31) in the derivation set at species level. They also reported a specificity of 89% (42/47). Of the cultured organisms not identified by CMg, three were found to the genus level, two were not cultured from PPT, only sonication fluid, one was reported as polymicrobial by culture but not all organisms were found by CMg leaving two remaining samples detected by both culture methods, but not CMg. Organisms not found by culture were reported in 12 samples although the authors note that some of these appeared to be contaminants - *P. acnes* in particular was a common contaminant in the study. The authors applied a pathogen enrichment method on six samples using the NEBNext microbiome

DNA enrichment kit to remove mainly non-microbial DNA. This kit utilises immunomagnetic beads for the separation and capture of human DNA by binding methylated CpG sites. While bacterial methylation patterns are sporadic and mosaic in order to characterise DNA sections, the vast majority of CpG sites in human DNA are methylated (the exception being CpG islands which are typically unmethylated) with ~15 fold more methylated sites per kb than in bacterial genomes (Feehery et al., 2013). However, despite applying this method the authors reported no significant reduction in human reads in the tested samples (98.4% with enrichment and 98.2% without). Overall, human reads accounted for 90% of reads in the vast majority of samples. Despite this, sufficient depletion was achieved to generate enough reads for pathogen identification in the study (Street et al., 2017).

Thoendel *et al.* used the MolYsis Basic5 kit on sonication fluid of 408 resected prosthesis samples. The MolYsis kit is based on differential lysis of human cells using a chaotropic buffer, followed by DNase treatment to digest the cell-free host DNA before microbial DNA extraction (Thoendel et al., 2018). Following DNA extraction, samples underwent whole genome amplification (WGA) and were sequenced on the Illumina HiSeq. Organisms reported from sonication fluid culture were also reported by CMg in 94.8% of cases (109/115), with 99 cases matching exactly to culture and 11 cases featuring additional detections not found by culture. Potential pathogens were also found in 43/98 culture negative PJI samples, 19 of which were found by other methods from these samples, 24 were unique identifications by CMg. Potential pathogens were also reported in the aseptic loosening (AL) set in 7/195 samples (3.6%). The remaining AL samples also contained substantial reads; however, these mapped poorly and were reported to look similar to the reads observed in the negative control samples. Combining host cell depletion and WGA, this study showed strong evidence that CMg could be used to diagnose PJI from sonication fluid, with identification missed in only 6/115 culture positive samples. Of these cases, two were reported as polymicrobial infections where only one of the reported organisms was identified by CMg, two samples had insufficient data to reach the positivity threshold, and the remaining two samples contained *P. aeruginosa* and were missed. Thoendel *et al.* reported that the MolYsis depletion method may be lysing *P. aeruginosa* as well as host cells resulting in the failure to identify by CMg (Thoendel et al., 2018).

This group went on to apply the same pipeline to 168 synovial fluid samples to determine if CMg could be used for preoperative diagnostics. Also using the MolYsis Basic5 kit for host cell depletion, Ivy *et al.* reported concordant results from CMg in 144/168 samples compared to synovial fluid culture (Ivy et al., 2018). Organisms were not reported by CMg in 14/67 culture positive PJI samples. Five of these organisms were identified but failed to meet either the cut-offs put in place for species-specific reads (n=3) or genome coverage (n=2). They report that adjusting the cut-offs to include these results would have resulted in a significant reduction in specificity caused by contaminant reads. A high proportion of the cultured organisms not reported by CMg were NAS species (9/14) which may have been the result of contamination and not infection. The study does however show potential for CMg to be used with synovial fluid samples as an alternative to sonication fluid which would be an advantage as synovial fluid can be sampled pre-operatively.

3.1.4 Nanopore clinical metagenomics

CMg using MinION sequencing has previously been employed for a wide range of sample types including blood (Greninger et al., 2015), urine (Schmidt et al., 2017), faeces (Leggett et al., 2020) and respiratory samples (Charalampous et al., 2019). A recent study by Noone *et al.* used nanopore sequencing to identify organisms in PPT samples from 32 PJI patients. The authors split soft tissue biopsies from 28 culture positive and four culture-negative PJI cases between conventional culture and metagenomics, no aseptic loosening cases were included. Host cell depletion was performed on samples using the Molzym ultra-deep microbiome prep kit before DNA extractions. Library preparation was carried out using the SQK-RPB004 rapid PCR barcoding kit and sequenced on either the MinION or GridION for 48 hours (Noone et al., 2021). The data was analysed using ONT software (EPI2ME). In 72% of cases CMg detected the same organism/s as culture (23/32) and additional organisms were found in 28% of cases (9/32). The authors report eight cases where cultured organisms were not found by CMg, however, in two of these cases an organism was only cultured from one PPT samples which would not be considered sufficient for a positive diagnosis by MSIS/ICM criteria. Two cases were, as commonly seen in the other PJI CMg studies,

polymicrobial infections where only one organism was identified by CMg. While sequencing was run for 48 hours for all samples, the authors report that organisms which were detected by both culture and CMg took a median time of 1 hour to detect, ranging from 1 to 18 hours. Factoring in the 6 hours of sample preparation pre-sequencing the turnaround time for these samples in a clinical setting would be a maximum of 24 hours, demonstrating the advantage of real-time analysis with nanopore sequencing. Unsurprisingly, the median time to result for the nine cases where organisms were found by sequencing but not culture was greater, at 5 hours, as there was likely less available material to sequence if the organism was not culturable. The authors report that in 16/20 cases where the sequencing result agreed with the culture report, the pathogen would have been found within 2 hours of sequencing, 8 hours total turnaround time (Noone et al., 2021).

The capability for rapid CMg with the MinION has also been demonstrated by Charalampous *et al.* who developed a CMg pipeline for the diagnosis of lower respiratory tract infections, with a turnaround time of 6 hours from sample-to-result (Charalampous et al., 2019). The authors applied a saponin based host cell depletion method to a selection of respiratory samples, mainly sputum, to remove 99.9% of host DNA (measured by qPCR). DNA extractions were sequenced on the MinION using either the Rapid Low Input by the SQK-RLI001 PCR Sequencing Kit, the SQK-RLB001 Rapid Low-Input Barcoding Kit or the SQK-RPB004 Rapid PCR Barcoding Kit also used by Noone *et al.* Sequencing data was basecalled using ONT Albacore and analysed though EPI2ME using WIMP and ARMA. The authors report a pilot study of the method applied to 40 Lower Respiratory Tract Infection (LRTI) samples yielded 91.4% sensitivity and 100% specificity against routine culture when not counting additional detections in culture positive samples by CMg. The authors optimised their DNA extraction method by introducing a sample pre-treatment step (bead-beating or an enzyme cocktail approach) for improved bacterial cell lysis in an attempt to increase the pipeline sensitivity. Notably, the amount of bacterial DNA from a *S. aureus* sample was increased four-fold by the enzymatic approach, and 21-fold by bead-beating, according to 16S qPCR. The optimised method was run on a set of 41 LRTI samples reporting an increased sensitivity of 96.6% and a lower specificity of 41.7% against routine culture when not counting additional detections in culture positive samples by CMg (Charalampous et al., 2019). Follow up testing of samples where results were discordant between CMg and culture using pathogen-specific

probe-based qPCR assays showed that CMg had a sensitivity and specificity 100% and 83.3% respectively.

This pipeline provides vastly superior data over the results reported by Pendleton *et al.* Where 1-2 pathogen reads were sequenced per sample with 99% human reads when not applying a host depletion method (Pendleton et al., 2017), Charalampous *et al.* demonstrated, using the same sequencing platform, that sufficient removal of host DNA can result in thousands of bacterial reads generated within two hours of sequencing, sufficient for both pathogen and antibiotic resistance gene identification (Charalampous et al., 2019).

3.1.5 The PJI CMg pipeline

3.1.5.1 Whole prosthesis sampling

As many implant-associated infections are caused by microorganisms embedded in biofilms attached to the device service, dislodgement of the matrix should be attempted prior to diagnosis, especially in cases of chronic low-grade infection (Clauss et al., 2010). Mechanical disruption of a biofilm through sonication, as used by Street *et al.*, is the most routinely used method in routine culture-based diagnostic work (Holinka et al., 2011; Karbysheva et al., 2019). Sonication has been reported to yield greater rates of bacterial recovery than scraping of the prosthesis surface (Berbari et al., 2007) and is further improved when combined with vortexing (Trampuz et al., 2006, 2003).

Studies have also been performed on chemical approaches to biofilm dislodgment. The metal chelating ability of ethylenediaminetetraacetic acid (EDTA) has been shown to destabilize biofilms by sequestering magnesium, zinc, calcium and iron (Banin et al., 2006). N-acetylcysteine (NAC) is an antioxidant thiol widely used to dissolve mucus in respiratory tract infections reported to prevent the production of extracellular polysaccharide matrix and remove mature biofilms (Olofsson et al., 2003). Dithiothreitol (DTT) is a reducing agent that cleaves disulphide bonds between cysteine groups. DTT acts as a protein denaturant through cleaving and preventing the formation of disulphide bridges between polysaccharides and neighbouring proteins. This action is applied in microbiology laboratories to liquify sputum samples but has also been shown to degrade

staphylococcal biofilms (Wu et al., 2011). Drago *et al.* found that NAC treatment did not significantly improve bacterial recovery from *S. aureus*, *S. epidermidis*, *E. coli* and *P. aeruginosa* biofilms compared to scraping but that DTT treatment showed slightly improved recovery even over sonication (mean 5.3 and 4.9 LogCFU/ml respectively) (Drago et al., 2012). Karbysheva *et al.* compared the chemical activity of EDTA and DTT to sonication on biofilms of the same four species tested by Dragon *et al.* and reported that sonication yielded ~1 log greater CFU/ml recovery for all species than EDTA and DTT (Karbysheva et al., 2020). The major advantage of chemical treatment over mechanical removal of biofilm material is the reduced risk of contamination, as excessive manipulation of the prostheses is not required.

3.1.5.2 Host cell depletion

In our experience, PJI samples (synovial fluid, sonicated tissue biopsy or DTT whole prosthesis wash) contain on average 10^5 human cells per ml. Studies have shown that PJI samples typically contain 10^3 CFU/ml bacterial cells (Cai et al., 2021; Street et al., 2017). Previous studies reporting successful pathogen identification from PJI samples have typically used commercial pathogen DNA enrichment kits such as MolYsis, however, these studies do not report reduction of human DNA to the level that was reported by Charalampous *et al.* using saponin based differential cell lysis (up to 99.99% removal of human DNA) (Charalampous et al., 2019).

3.1.5.3 Saponin based host cell depletion

Saponins are naturally found terpenoids on plant cell walls as surface glycosides and believed to mainly act as antimicrobial and antifungal defence molecules (Francis et al., 2002; Lorent et al., 2014). As saponins are amphipathic, they had mainly been used as soaps due to their surfactant activity. More recently saponins are becoming widely used in cosmetic and pharmaceutical settings such as in vaccine adjuvants (Lorent et al., 2014; Sun et al., 2009).

Saponins consist of a lipophilic triterpene and a hydrophilic carbohydrate chain. Monodesmosidic saponins (that contain only one hydrophilic sugar carbohydrate chain), are particularly disruptive to

biological membranes as they can increase membrane permeability and induce pore formation (Francis et al., 2002; Lorent et al., 2014). This lytic activity has been utilised in cancer research to destroy cancer cells and prevent cell proliferation (Chen et al., 2011; Waheed et al., 2012), although the therapeutic usage of saponins for cancer treatment may be limited as they also induce haemolysis due to their high affinity for cholesterols (Bissinger et al., 2014). This is, however, where saponins become a powerful tool for host cell depletion methods. Interactions between the carbohydrate chains and cholesterols or sterols in cell membranes result in increased permeability through membrane rearrangements or micelle formation (Francis et al., 2002; Sudji et al., 2015). While cholesterols and sterols are commonly found in eukaryotic cell membranes, they are very rare in prokaryotic cells. As such, they present a target for saponin to deliver differential cell lysis between human and bacterial cells.

This action has been put to use in selecting for pathogens in low titre infections such as blood stream infections (BSI). Zelenin *et al.* designed a microfluidic-based device which utilized a saponin-based lysis followed by osmotic shock to rapidly lyse human cells in blood samples to facilitate the rapid diagnosis of BSIs without the need for culture (Zelenin et al., 2015). The device was able to lyse blood cells without lysing bacterial cells, allowing for molecular testing directly from a treated sample without the need to first perform culture-based enrichment. The method was further optimised by Anscombe *et al.* who coupled the saponin based host cell lysis with DNase depletion of human DNA, bacterial isolation and whole genome amplification followed by sequencing on pathogen spiked horse blood. The authors reported recovery of 92% of spiked pathogen genomes with only 7% of reads classified as host (Anscombe et al., 2018). As previously mentioned, Charalampous *et al.* went further to apply saponin based differential cell lysis to clinical samples to provide rapid CMg results with up to 99.99% removal of human DNA (Charalampous et al., 2019).

3.1.5.4 PLC based host cell depletion

Another host depletion method was also developed in the O'Grady group using phospholipase C (PLC) in place of saponin for selective host cell lysis, for depletion of human DNA in blood

samples in cases of suspected sepsis, although the the method is applicable to all mammalian sample types (O'Grady et al., 2018). PLC is a cytolysin, another natural defence, but in this case against the human immune response secreted by bacterial species. Some cytolysins disrupt cell membranes by detergent action or by inducing pore formation as saponin does. However, other type of cytolysins, phospholipases such as PLC, act to cleave phospholipids through hydrolysis, thus dissolving the phospholipid bilayer that forms eukaryotic cell membranes (Titball, 1993).

The PLC recommended for use in this method is the *Clostridium perfringens* alpha-toxin, a major cause of foodborne illness (Scallan et al., 2011). *C. perfringens* alpha-toxin consists of two structural domains, an N-domain of nine tightly packed α-helices and a C-domain of an eight-stranded antiparallel β-sandwich binding domain for phospholipid membranes. Alpha-toxin is classed as a Zinc-metallophospholipase C as the N-domain contains three divalent zinc cations for zinc activation of hydrolytic action (Sakurai et al., 2004). The toxin is responsible for gas gangrene and myonecrosis in infected tissue, as well as haemolysis, hence the application in host cell depletion of blood samples.

3.1.5.5 Sample preparation for sequencing

Following host depletion/microbial enrichment, DNA is extracted from the remaining intact pathogen cells. The majority of pipelines use a combination of chemical and enzymatic lysis. It is important to ensure efficient lysis of hard to lyse microorganisms such as *S. aureus*, as it is a major PJI pathogen. A mechanical lysis step such as bead-beating is recommended to ensure the efficient lysis of all microbes in a sample (Shehadul Islam et al., 2017; Vandeventer et al., 2011). After cell lysis, nucleic acid purification can be performed manually using spin columns or commercial purification kits. Clinical microbiology laboratories typically use automated extraction platforms as they provide a standardised, less laborious approach. One such platform is the Roche MagNA Pure Compact, which can perform DNA extraction and purification on eight samples in 27 minutes (Kessler et al., 2001).

Once purified, the DNA has to be converted into a sequencing library suitable for the platform on which the samples will be sequenced. While the rapid turnaround time offered by nanopore

sequencing is arguably not as important for PJI diagnostics as it would be for infections which require rapid antibiotic intervention such as sepsis, the option of more cost-effective low-throughput sequencing is a big advantage over other sequencing platforms. It is unlikely that batch testing (i.e 95 samples) PJI samples would be feasible in a clinical setting to make a short-read sequencing technology pipelines cost-effective.

The library preparation kit used dependends on the sample used. In cases where starting DNA quantity is low, a PCR-based library preparation method is necessary in order to amplify starting material to a sufficient quantity to be detectable by sequencing. Previous studies report that PJI samples typically contain <1ng/µl after host depletion, which is insufficient for a non-PCR based library preparation (Noone et al., 2021; Ruppé et al., 2017b). For PJI samples the most appropriate ONT kit would be the SQK-RPB004 Rapid PCR barcoding kit, as used by Noone *et al.* This kit enables library preparation and multiplexing of up to 12 samples from low input DNA concentrations (which can work with input as low as the pg range in our experience) (Charalampous et al., 2019). This method enzymatically fragments and tags extracted DNA with specific adapters. Primers complementary to the tagmented adapters amplify the DNA in a PCR reaction. Non-PCR library preparation kits such as the SQK-RBK004 Rapid Barcoding kit offer a shorter preparation time (10 minutes) using the same steps as the low input kit. However, the minimum required input DNA is 400ng so this would not be suitable for direct sequencing of PJI samples without a prior WGA step.

3.1.5.6 Bioinformatics for clinical sequencing

Metagenomic sequencing produces a large amount of data which requires computational processing to profile the microbial community of a sample. The appropriate analysis tools need to be selected depending on the aim of the study (Quince et al., 2017). A bioinformatics pipeline will typically begin with basecalling of the say raw sequencing files (e.g. FAST5 for ONT platforms). Once this has been performed, a quality control filter can be applied to remove low-quality reads and adaptor sequences (Quince et al., 2017). The ONT platforms are controlled using a graphical user interface (GUI), MinKNOW (provided by ONT). During sequencing, the squiggle plot

measurement of the current changes across the nanopores are recorded by MinKNOW in raw FAST5 format. A live-basecalling feature is incorporated in MinKNOW to facilitate real time analysis by converting the raw data to basecalled FAST5 or FASTQ file formats. Basecalling can also be performed after sequencing for users who do not require real-time analysis using offline tools such as Albacore and Guppy, provided by ONT and more recently Bonito which has improved accuracy. The two programs run similarly, however, while Albacore only utilises a computer's central processing unit (CPU), Guppy is able to use graphics processing units (GPUs) for considerably improved speed. As such, support for Albacore has been discontinued in favour of Guppy in 2018 (Wick et al., 2019).

Following basecalling and removal of low-quality data, downstream analysis can be initiated using a wide range of available tools. In a diagnostic setting the first step for analysis is typically microorganism classification down to at least the genus level, ideally to a species level. If sequencing data is of sufficient quality, further analysis can be run to provide information on antibiotic resistance genes found that may be relevant to any identified pathogens (Charalampous et al., 2019; Leggett et al., 2020) as well as for whole genome assembly (Miller et al., 2010) and use for infection control to identify outbreaks and study epidemiology (Huang et al., 2019; Roy et al., 2019).

Tools for taxonomic classification from metagenomic data utilise a number of algorithmic approaches such as alignment of microbial reads or contigs to reference databases, mapping of marker genes, protein sequences translated from the DNA sequence and analysis of *k*-mer content (overlapping of short sequences with a length of *k*) (Breitwieser et al., 2019).

Nanopore data can be analysed using a GUI provided by ONT, EPI2ME, which consists of a desktop application for uploading basecalled reads and selecting from a range of analysis pipelines for pathogen identification and AMR gene detection along with a web interface to report results for interpretation. The FASTQ Antimicrobial Resistance pipeline combines pathogen identification using WIMP (What's In My Pot), and AMR gene identification using ARMA (Antimicrobial Resistance Mapping Application). WIMP is a real time read binning tool based on Centrifuge, a classification engine designed to enable rapid quantification of reads to sub/species level for

metagenomic classification on desktop computers (Kim et al., 2016). Using this classifier, WIMP maps *k*-mers from uploaded reads to the RefSeq database for the identification of bacteria, fungi and viruses (Charalampous et al., 2019). ARMA aligns reads using a general-purpose alignment program, Minimap2, against the CARD database to detect AMR genes (Charalampous et al., 2019).

3.1.6 Aims

The main aim of this section was to adapt previously developed host cell depletion methods and sequencing pipelines to PJI samples collected at the NNUH for pathogen identification. Both saponin and PLC based depletion methods were tested to determine the most efficient human DNA depletion method for PJI sample types (e.g. sonication fluid, synovial fluid and DTT washed whole prosthesis). A pilot study was performed using the MicroDTTect sealed bag system for DTT based removal of biofilm material from whole prosthesis samples using our adapted pipeline and compared with routine microbiological culture and with culture of the DTT fluid. This proof-of-concept study was performed to determine if CMg based accurate, same day, pathogen identification was possible for PJI samples.

3.2 – Methods

3.2.1 Sample collection

All samples were collected from NNUH under ethical approval provided by University of East Anglia, Faculty of Medicine and Health Sciences Research Ethics Committee, project reference: 2016/17 21 SE.

3.2.1.1 Sonication fluid sampling

Excess sonication fluid from clinical samples for method development was provided by Katarzyna Schmidt from the NNUH Microbiology department. Peri-prosthetic tissue samples were processed by sonication to release bacteria from the tissue sample to facilitate organism detection. Tissue specimens were placed into sterile containers with Ballotini beads and 5 mL (0.85%) saline (EO Labs, Bonnybridge, UK). Samples were mixed by vortexing at 40 Hz (2500 RPM) for 30 seconds followed by sonication in an ultrasound bath for 5 minutes at 40 kHz +/- 2 kHz and 0.22 +/- 0.04 W/cm2 power density (70% ultrasonic power). Samples were again vortexed at 40 Hz (2500 RPM) for 30 seconds to remove any residual microorganisms and to disperse them evenly in the sonication fluid before transport to UEA.

Culture negative sonication fluid was spiked with bacterial culture for use in method development. 200 µl of culture-negative sonication fluid was spiked with either 100, 1000 or 10000 cells of *S. epidermidis* (strain 15TB0821 collected from the NRP Biorepository as part of the NAS transformation work in Chapter 4) or not spiked. Spiked samples were treated for human DNA depletion by the PLC method only (3.2.2.1) before enzyme based bacterial lysis (3.2.2.2) and MagNApure DNA extraction (3.2.4). Sample DNA was then quantified by qPCR using the 16S SYBR Green protocol (3.2.5).

3.2.1.2 MicroDTTect sampling

A total of 42 prosthesis samples taken between April 2018 and February 2020 were prospectively collected for sequencing using the ONT rapid PCR barcoding kit (SQK-RPB004, Oxford Nanopore Technologies) on the MinION (Oxford Nanopore Technologies). Samples were intraoperative

specimens from a consecutive series of patients collected during total hip, total knee and partial spine arthroplasty surgery performed at NNUH. Samples were only collected if patient consent was obtained at the time of surgery. Whole prosthesis samples were processed to remove biofilm using the MicroDTTect® system (Figure 3.1) (NovaHealth Srl) according to the manufacturer's instructions. In brief, samples were placed within a sealed bag and washed for 15 minutes with 0.1% v/v of DTT before fluid was removed by syringe action into sterile collection tubes for testing.

Figure 3.1. MicroDTTect system. Closed bag system for whole prosthesis sampling (adapted from www.microdttect.com)). 1. DTT fluid pouch for chemical removal of biofilm material from prosthetic joint components; 2. Main pouch for prosthesis washing. Prosthesis is placed into bag which is then sealed. Once sealed the DTT fluid is released into the main pouch by breaking off the red tab and the bag is manipulated for 15 minutes to fully wash the prosthesis; 3. Filtered tube for extracting DTT wash fluid. Fluid is pulled by syringe action through a filter to remove pieces of tissue without exposing DTT fluid to the environment; 4. Collection tube for aseptic collection and transport of DTT fluid; 5. Visualisation of placement of prosthesis into the MicroDTTect bag. Bag is sealed along the blue line once prosthesis is inside.

Once disconnected from the MicroDTTect bag, the Sample tubes containing DTT fluid were centrifuged for 10 minutes at 3,220 g. Supernatant was removed using a syringe from the red port on the tube lid, avoiding the pellet. The pellet was then resuspended in DTT fluid remaining at the bottom of the tube using a syringe in the blue port, then removed and an equal volume transferred to two 1.5 ml Eppendorf microcentrifuge tubes. Samples were then centrifuged for 5 minutes at 12,000 g, the DTT fluid supernatant was removed, and each pellet was resuspended in 600 µl PBS. 1 ml was inoculated into blood culture bottles for culture and the remaining sample was stored at 4^{o}C until host cell depletion processing. Results were compared with routine culture results reported by the NNUH Microbiology department (Figure 3.2). Microbiological culture was performed as previously described (2.2.2.2).

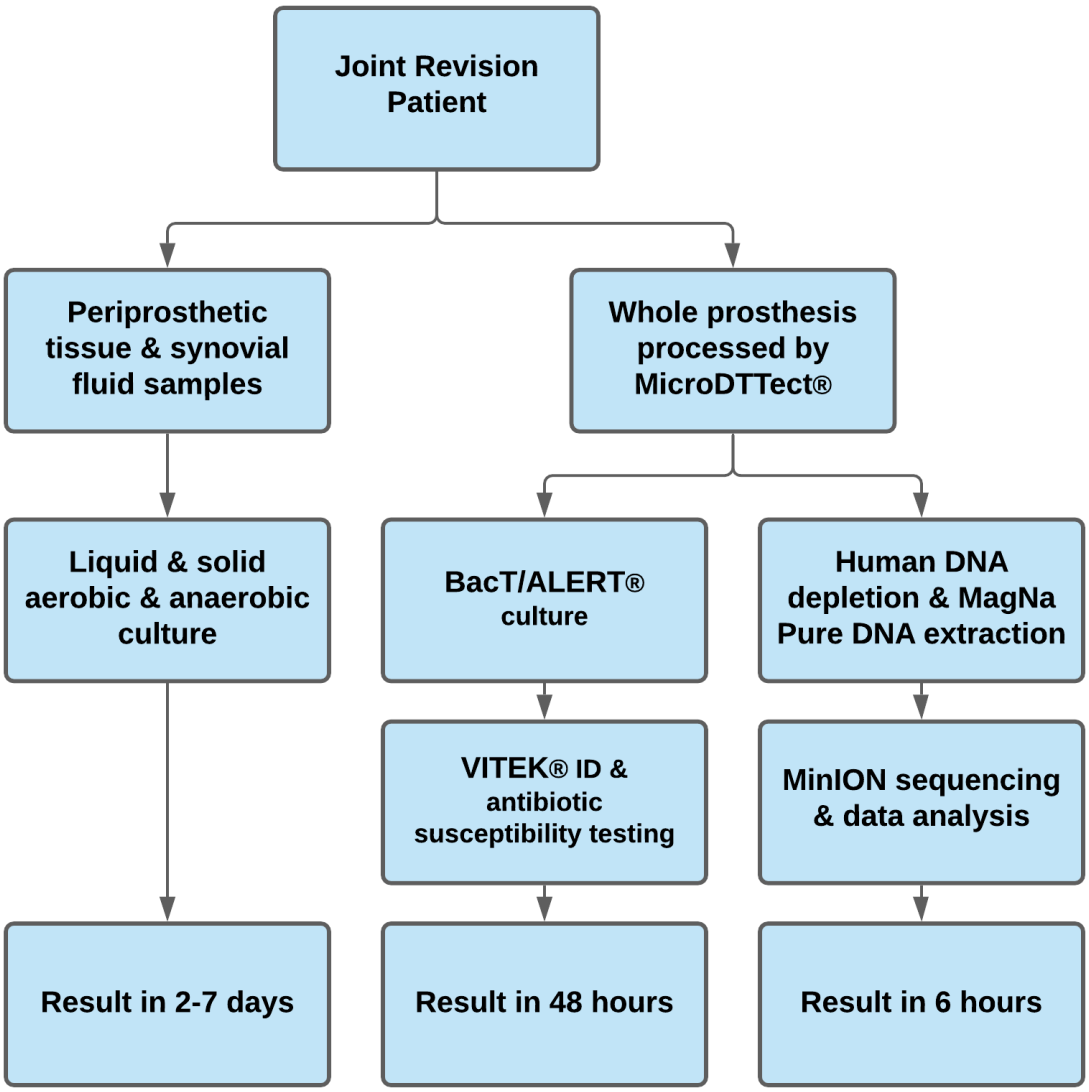

Figure 3.2. MicroDTTect study protocol. Flowchart of sample handling from patients enrolled in MicroDTTect study. Routine culture (left) and DTT fluid culture (central) performed by NHS staff at the NNUH Microbiology laboratory; Metagenomic sequencing (right) performed at UEA.

3.2.2 Host cell depletion

For each sample treated for selective host cell depletion, samples were aliquoted into 2x 200ul in two 1.5 ml Eppendorf tubes. One aliquot was used for depletion and the other reserved as a no-depletion control. This control was set aside until the bacterial cell lysis step before DNA extraction.

3.2.2.1 PLC method for host cell depletion

20 µl of 4% PLC (4 mg PLC in 100 µl water) (extracted from *Clostridium perfringens*, Sigma-Aldrich) was added to each 200 µl sample for depletion, mixed by pipetting and incubated for 15 minutes at 37ºC, 1,000 RPM on a ThermoMixer (Eppendorf). The sample was then centrifuged at 10,000 g for 5 minutes and the supernatant carefully discarded ensuring to not disturb the pellet. The sample was resuspended in 200 µl PBS by pipetting before adding 200 µl HL-SAN buffer (5M NaCl and 100 mM $MgCl_2$ in water) and 10 µl HL-SAN DNase (ArcticZymes AS) followed by a 15-minute incubation at 37ºC, 1,000 RPM. Following incubation, 1 ml of PBS was added to the sample, mixed by pipetting, then centrifuged at 8,000 g for 5 minutes. Ensuring to not disturb the pellet, the supernatant was carefully discarded. The pellet was washed once more by resuspending in 1.5 ml PBS, centrifuging for 5 minutes at 8,000 g and carefully discarding the supernatant again. The remaining pellet was used for DNA extraction.

3.2.2.2 Saponin method for host cell depletion

50 µl of PBS was added to each 200 µl of sample. 100 µl of 5% Saponin (Tokyo Chemical Industry) v/v in PBS was added to the sample (to a final concentration of 1.43%), mixed by pipetting and incubated at room temperature for 10 minutes, mixing by pipetting every 2 minutes. After incubation, 350 µl of nuclease free water was added, mixed by pipetting and left for 30 seconds. Then 12 µl of 5M NaCl was added and vortexed for 2 seconds to mix. The sample was centrifuged at 10,000 g for 5 minutes and the supernatant carefully discarded, ensuring to not disturb the pellet. The pellet was resuspended in 100 µl PBS by pipetting. 100 µl HL-SAN buffer (5.5M NaCl, 100 mM $MgCl_2$) and 10 µl HL-SAN DNase (ArcticZymes AS) was added to each sample, mixed by pipetting and incubated for 15 minutes at 37ºC, 1,000 RPM on a ThermoMixer (Eppendorf). After incubation, 800 µl PBS was added, and the sample was centrifuged for 5 minutes at 8,000 g. The supernatant was carefully discarded, ensuring to not disturb the pellet, and the pellet was washed once more by resuspending in 1 ml PBS, centrifuging for 5 minutes at 8,000 g and carefully discarding the supernatant again. The remaining pellet was used for DNA extraction.

3.2.3 Bacterial cell lysis

Following PLC or saponin treatment for the selective lysis of host cells, bacterial cells were lysed by either an enzyme cocktail or bead beating along with no-depletion controls.

3.2.3.1 Enzyme based bacterial cell lysis

The cell pellet following the final wash step after HL-SAN DNase treatment was re-suspended in 350 µl bacterial lysis buffer (BLB, Roche) and added to a MagNA Pure sample tube (Roche). Non-depleted positive controls were made up to 350 µl total volume with BLB and reintroduced into the pipeline at this stage. 5 µl RNase A and 20 µl MetaPolyzyme (Sigma-Aldrich) were added to each tube and incubated for 15 minutes at 37ºC, 800 RPM. After incubation, 20 µl of proteinase K (Sigma-Aldrich) was added to each tube and incubated for 10 minutes at 65ºC. Samples were then processed on the MagNA Pure for DNA extraction.

3.2.3.2 Bead beating bacterial cell lysis

The cell pellet following the final wash step after HL-SAN DNase treatment was resuspended in 600 µl bacterial lysis buffer (BLB, Roche). Non-depleted positive controls were also topped up to 600 µl volume with BLB and reintroduced into the pipeline at this stage. Samples were transferred to bead-beating tubes (Lysing matrix E, MP Bio) and lysed for 5 minutes at 50 oscillations per second (Qiagen TissueLyser LT) then centrifuged for 1 minute at 20,000 g. 150 µl of supernatant was taken twice, up to a final volume of 300 µl (avoiding pipetting beads from the tube) and added to a MagNA Pure sample tube (Roche). 20 µl of proteinase K (Qiagen) was added to each tube and incubated for 5 minutes at 65ºC, 800 RPM. Samples were then processed on the MagNA Pure for DNA extraction in.

3.2.4 DNA extraction

DNA extraction was performed after either the enzymatic lysis or bead beating step with the MagNA Pure Compact NA Isolation Kit I (Roche) on a MagNA Pure Compact (Roche) using the protocol bacterial_V3_2 protocol according to the manufacturer's instructions.

3.2.5 qPCR

DNA extractions were checked by qPCR to quantify the level of host cell depletion, mitochondrial DNA depletion and determine the amount of bacterial DNA that had been inadvertently lost during PLC and/or saponin treatment. Extracted non-depleted controls were used to determine the starting amount of host and bacterial DNA in the original sample. All qPCR experiments were run with a water negative control where 5 µl of molecular grade water was added to one reaction in place of the 5 µl of template DNA. All qPCRs were performed using the LightCycler® 480 system (Roche). Concentrations for the probe-based assay are listed in table 3.1 with primers listed in table 3.2.

Table 3.1 Reaction mix for Probe based qPCR

Component	**Volume added**	**Final concentration**
2x LightCycler 480 Probes Master (Roche)	10 µl	1x
Forward Primer (10 µM)	0.5 µl	0.25 µM
Reverse Primer (10 µM)	0.5 µl	0.25 µM
Probe (10 µM)	0.4 µl	0.2 µM
PCR-grade H_2O	3.6 µl	-
Template DNA	5 µl	-

The conditions for a probe-based qPCR assay were an initial denaturation of 5 minutes at 95ºC followed by 45 cycles of: 95ºC for 30 seconds, 55ºC for 30 seconds, 72ºC for 30 seconds. The final extension period was 5 minutes at 72ºC.

Table 3.2 SYBR Green primer sets

Target organism	Target gene	Forward primer (5'-3')	Reverse primer (5'-3')	Reference
Universal Bacterial	16s rRNA gene V3-V4 fragment (including Illumina adapter)	TCGTCGGCAGCG TCAGATGTGTAT AAGAGACAGCCT ACGGGNGGCWG CAG	GTCTCGTGGGCTCG GAGATGTGTATAA GAGACAGGACTAC HVGGGTATCTAAT CC	(Klindworth et al., 2013)
Human Mitochondria	tRNA-Leu (UUR)	CACCCAAGAACA GGGTTTGT	TGGCCATGGGTAT GTTGTTA	(Ayala-Torres et al., 2000)

Conditions for the SYBR green based assay used listed in table 3.3, primers listed in table 3.4.

Table 3.3 Reaction mix for SYBR Green based qPCR

Component	Volume added	Final concentration
2x LightCycler SYBR Green Master (Roche)	10 µl	1x
Forward Primer (10 µM)	1 µl	0.5 µM
Reverse Primer (10 µM)	1 µl	0.5 µM
PCR-grade H_2O	3 µl	-
Template DNA	5 µl	-

The run conditions for a SYBR Green based qPCR assay were an initial denaturation of 5 minutes at 95ºC followed by 45 cycles of: 95ºC for 30 seconds, 55ºC for 30 seconds, 72ºC for 30 seconds. The final extension period was 5 minutes at 72ºC. Melt curve analysis was performed by heating to 95ºC for 5 seconds, followed by 65ºC for 1 minute. Temperature was then increased from 65ºC back to 95ºC at a rate of 0.03ºC/s. Fluorescence was measured at a rate of 5 acquisitions/ºC.

Table 3.4 Probe based primer sets

Organism	Gene target	Forward primer (5'-3')	Reverse primer (5'-3')	Probe (5'-3')	Reference
Human	RNA polymerase A	TGAAGCCGTGCGGAAGG	ACAAGAGAGCCAAGTGTCG	[6FAM]TACCACGTCATCTCCTTTGATGGCTCCTAT[BHQ1]	Designed in house
Universal Bacterial	16s rRNA gene V3-V4 fragment	CCTACGGGDGGCWGCA	GGACTACHVGGGTMTCTAATC	[6FAM]CAGCAGCCGCGGTA[BHQ1]	(Liu et al., 2012)
Escherichia coli	*cyaA*	CGATAATCGCCAGATGGC	CCTAAGTTGCAGGAGATGG	[6FAM]TAGAGCGCCTTCGGTGTCGGT[BHQ1]	Designed in house
Staphylococcus aureus	*eap*	ACTGTAACTTTGGCACTGG	GCAGATACCTCATTACCTGC	[6FAM]ATCGCAACGACTGGCGCTA[BHQ1]	Designed in house
Pseudomonas aeruginosa	*oprL*	AGCCTTCCTGGTCCCCTTAC	CCTAATGAACCCCAGTGTATAAGTTTG	[6FAM]TGAACTGACGGTCGCCAACGGTT[BHQ1]	(Fukumoto et al., 2015)
Streptococcus pneumoniae	*ply*	GCTTATGGGCGCCAAGTCTA	CAAAGCTTCAAAAGCAGCCTCTA	[6FAM]CTCAAGTTGGAAACCACGAGTAAGAGTGATGAA[BHQ1]	(Fukumoto et al., 2015)

3.2.6 DNA quantification

DNA quantification was performed using the high sensitivity dsDNA assay kit (Thermo Fisher) on the Qubit 3.0 Fluorometer (Thermo Fisher). In brief, High sensitivity Qubit working solution was made up in a ratio of 199 µl Quant-iT dsDNA HS buffer and 1 µl of Qubit dsDNA HS Reagent (Thermo Fisher). Samples were prepared by adding 2 µl of eluted DNA to 198 µl of working solution in Qubit Assay Tubes (Thermo Fisher), mixed by vortexing, and incubated in the dark for 2 minutes. Calibration standards were made by adding 10 µl of HS Standard 1 or 10 µl of HS Standard 2 to 190 µl of working solution in Qubit Assay Tubes. The two standards were then

mixed by vortexing and incubated in the dark for 2 minutes. Standards and samples were then read on the Qubit 3.0 fluorometer (Thermo Fisher) using the dsDNA high sensitivity program.

DNA fragment size and quality analysis was performed using the TapeStation 2200 (Agilent Technologies) automated electrophoresis platform with genomic screen tape (Agilent Technologies) according to manufacturer's instructions. In brief, 1 µl of DNA was added to 10 µl of sample buffer (Agilent Technologies), briefly vortexed and placed in the TapeStation. Samples were run with the Agilent genomic DNA ladder provided with the sample buffer and gels were visualised by the TapeStation analysis software (Agilent Technologies).

3.2.7 Nanopore sequencing

Sequencing libraries were prepared using the Rapid PCR Barcoding Kit (SQK-RPB004) (Oxford Nanopore Technologies) with modifications as detailed below.

To purify the input DNA, a 1.2X AMPure bead wash was performed on 30 µl of extracted DNA from the MagNA Pure (3.2.4). In a 1.5 ml Eppendorf DNA LoBind tube, 36 µl of AMPure XP beads were mixed with 30 µl of extracted DNA by pipetting and incubated at room temperature on a Hula mixer (rotating mixer) for 5 minutes. After mixing, the sample was pulse centrifuged and pelleted on a magnetic rack. While on the magnetic rack the supernatant was removed and the beads washed twice with 500 µl of 70% ethanol for 30 s. Residual ethanol was pipetted off and the pellet was left to dry on the magnetic rack for up to 10 minutes, before the pellet starts to crack. The tube was removed from the magnetic rack and the pellet resuspended in 18 µl of nuclease-free water and incubated for 5 minutes at room temperature on the Hula mixer, then returned to the magnetic rack for 2 minutes. The beads were re-pelleted on the magnet and 17 µl was eluted into a clean 1.5 ml Eppednorf DNA LoBind tube.

Eluted DNA (2µl) was quantified using the Qubit high sensitivity dsDNA assay (3.2.6).

In a 0.2ml flat capped PCR tube, 7.5 µl of extracted/washed DNA was mixed with 2.5 µl FRM by gently flicking the tube, and pulse centrifuged. The tube was incubated in a thermal cycler at 30^{o}C for 1 minute and then at 80^{o}C for 1 minute, then held at 4^{o}C.

Barcodes were added to the tagmented DNA through the following PCR reaction (Table 3.5):

Table 3.5 Reaction mix for low input barcoding PCR:

Component	Volume added	Final concentration
2x LongAmp Taq Polymerase (NEB)	50 µl	1x
Rapid barcode primer (RPB 1-12A)	2 µl	
Water	38 µl	-
Tagmented DNA	10 µl	-

Run conditions for the PCR were an initial denaturation at 95ºC for 3 minutes, followed by 25 cycles of: 95ºC for 15 seconds, 56ºC for 15 seconds, 65ºC for 4 minutes. The final extension period was 6 minutes at 65ºC.

Eluted DNA was quantified by Qubit (3.2.6) and samples were pooled in equal concentrations (where possible. Very low concentration samples, presumed to be aseptic, were not used as a benchmark for normalisation).

Pooled PCR products were transferred to a 1.5 ml Eppendorf DNA LoBind tube for a 0.6X AMPure XP bead wash. When multiplexing, samples were pooled to similar concentrations with a final concentration of 50-150 fmoles. 0.6X volume of AMPure XP beads were added to the pooled DNA (e.g. 100ul pooled DNA with 60ul beads), mixed by pipetting and incubated at room temperature on a Hula mixer (rotating mixer) for 5 minutes. After mixing, the sample was pulse centrifuged and pelleted on a magnetic rack. While on the magnetic rack the supernatant was removed and the beads washed twice with 500 µl 70% ethanol. Residual ethanol was pipetted off and the pellet was left to dry on the magnetic rack for up to 10 minutes, before the pellet starts to crack. The tube was removed from the magnetic rack and the pellet resuspended in 14 µl of 10 mM Tris-HCl pH 8.0 with 50 mM NaCl and incubated at room temperature for 5 minutes, on a Hula Mixer (rotation speed 15, timer 10; reciprocal tilting turning angle 45°, timer 5; vibration turning angle 5°, timer 5), then returned to the magnetic rack for 2 minutes. The beads were re-pelleted on the magnet and 13 µl was eluted into a clean 1.5 ml Eppendorf DNA LoBind tube.

Eluted DNA (2 µl) was quantified by Qubit, 1 µl was used for fragment size analysis on the Tapestation.

1 µl of rapid sequencing adapter (RAP) was added to the pool of barcoded DNA, mixed by pipetting and incubated at room temperature for 5 minutes. The sequencing library was stored on ice until ready to load.

A MinION (FLO-MIN106) flow cell was loaded onto a MinION Mk1B and run through dry quality control by the MinKNOW program (Oxford Nanopore Technologies). Flow cells were only used if the quality control score showed 800 or more active pores.

From the SQK-RPB004 kit, Sequencing Buffer (SQB), Loading Beads (LB), Flush Tether (FLT) and a Flush Buffer (FB) tube were thawed at room temperature. Once thawed, 30 µl of FLT was added to a tube of FB and mixed by vortexing to make the priming mix.

The priming port of the flow cell was opened and a p1000 pipette set to 200 µl inserted into the priming port. 20-30 µl of fluid was drawn up using the dial rather than the plunger of the pipette to avoid bubbles. 800 µl of the priming mix was loaded into the priming port again using the dial to avoid the introduction of bubbles into the flow cell and left for 5 minutes.

The library was prepared for loading by the following mix:

- 34 µl SQB
- 25.5 µl L), mixed immediately before use to resuspend the beads
- 4.5 µl nuclease-free water
- 11 µl DNA library

After the 5 minute incubation for priming the flow cell, the SpotON sample port cover was lifted. The final 200 µl of the priming mix was then added again into the priming port, avoiding the introduction of bubbles. Prior to loading the library, it was mixed by gentle pipetting to resuspend the beads and added drop by drop into the SpotON sample port. After loading, the SpotON sample port and priming port were closed and the MinION Mk1B lid closed.

Sequencing was run using the MinKNOW software provided by ONT to operate the MinION device for 24 hours and basecalling was performed using either Albacore or Guppy.

3.2.8 Bioinformatics

3.2.8.1 Basecalling

Offline basecalling was performed using two programs, Albacore and Guppy. Albacore was used for initial experiments assessing the performance of the PLC and saponin assays on sonication fluid and synovial fluid samples. Guppy was used for samples in the MicroDTTect study due to the discontinuation of Albacore.

Albacore basecalling was run using the following command: "C:/Program Files/OxfordNanopore/ont-albacore/read_fast5_basecaller.exe" -f FLO-MIN106 -k SQK-RPB004 --barcoding -o fastq --input (input folder location) -s (output folder location) -r -t 4

Guppy basecalling was run using the following command: guppy_basecaller --input_path (input folder location) --recursive --save_path (output folder location) --flowcell FLO-MIN106 --SQK-RPB004

3.2.8.2 Microbial classification

The output format for downstream analysis was FASTQ reads. For all samples tested, both the first 2 hours of reads and all 12 hours of reads were analysed separately. FASTQ files generated by basecalling were uploaded to a cloud-based data analysis platform, EPI2ME (Oxford Nanopore Technologies), and run through the species identification pipeline, What's In My Pot (WIMP). WIMP is a *k*-mer based read binning tool that uses Centrifuge (Deshpande et al., 2019) to assign reads to different species from a reference database using a minimum basecalling q score of 7. Classified bacterial reads were determined as significant to call pathogen identification if both of the following parameters were met:

For analysis of the first 2 hours of reads:

- Species level classified reads totalled 200 or greater

- Species level classified reads were proportionally 30% or greater of the total classified microbial reads

For analysis of all 12 hours of reads:

- Species level classified reads totalled 500 or greater
- Species level classified reads were proportionally 30% or greater of the total classified microbial reads

3.3 – Results

3.3.1 PLC host depletion efficiency of sonication fluid samples

Culture negative sonication fluid samples were spiked with *S. epidermidis* and processed with the PLC method (3.2.2.1) to determine if the method, previously used for blood samples, would be suitable for PJI samples in our study. The DNA extractions were tested by qPCR with a human specific probe to quantify the removal of human DNA and with a SYBR green assay using 16S universal bacterial primers to confirm that bacterial DNA had not been lost during the depletion process (Table 3.4).

qPCR showed that human DNA was depleted by ~15 C_T (range 14.78 – 15.28 C_T, Table 4.6), a 32,768-fold removal equating to ~10,000-fold less DNA or a 99.99% reduction in host cell DNA present in the extraction (Figure 3.3). Bacterial DNA was detected using the 16S qPCR assay in all three spiked samples treated for host cell depletion (Table 3.7). The no depletion control was spiked with 100 *S. epidermidis* cells, hence a successful depletion in the *S. epidermidis* 100 cell inoculation sample with no inadvertent loss of bacterial DNA would be expected to result in ΔC_T 0 between sample and control. The 1,000-cell and 10,000-cell inoculations would be expected to show a ΔC_T 3.3 and ΔC_T 6.6 compared to the control, respectively. The 100-cell inoculation depleted sample showed a 4-fold gain in bacteria over the no depleted control, the 1,000-cell inoculation showed a 27-fold gain, and the 10,000-cell inoculation showed a 97-fold gain. The difference between the no depletion control and 100 cell inoculation is likely due to the quantity of human DNA in the no depletion control affecting the PCR efficiency, as the no depletion control amplification curve appeared inhibited (Figure 3.4.A2).

Table 3.6 PLC based depletion of host cell DNA from sonication fluid of a culture negative clinical sample.

Sample	Human DNA assay (C_T)	Human DNA depletion (ΔC_T)*
No depletion sample positive control	23.09	0
S. epidermidis 100 cell inoculation	37.87	14.78 (28,133-fold depletion)
S. epidermidis 1,000 cell inoculation	37.90	14.81 (28,724-fold depletion)
S. epidermidis 10,000 cell inoculation	38.37	15.28 (39,786-fold depletion)
qPCR water negative control	-	-

*Depletion measured as ΔC_T between the no depletion control and the depleted sample.

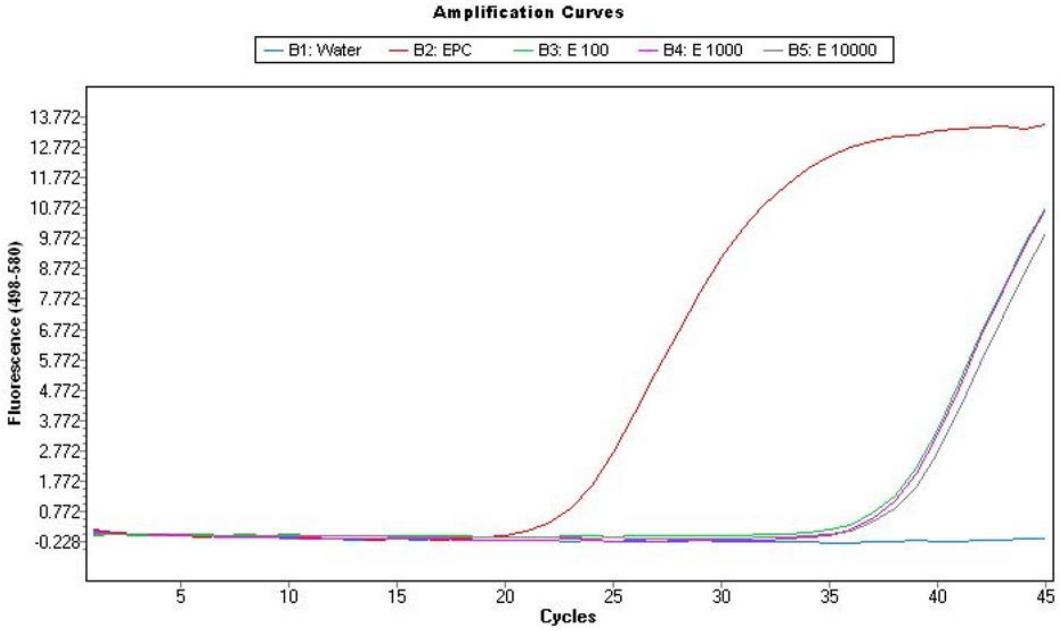

Figure 3.3. PLC based depletion of host cell DNA from sonication fluid of a culture negative clinical sample. qPCR amplification curves of specific human probe assay on DNA extractions from culture-negative sonication fluid spiked with *S. epidermidis* cells. B1 – Negative control; B2 – No depletion positive control of sample spiked with 100 bacterial cells; B3 – Depleted sample spiked with 100 bacterial cells; B4 – Depleted sample spiked with 1,000 bacterial cells; B5 – Depleted sample spiked with 10,000 bacterial cells.

Table 3.7 qPCR of bacterial presence by universal 16S primers after host cell depletion on spiked sonication fluid of a culture negative clinical sample.

Sample	16S assay (C_T)	Bacterial gain (ΔC_T)
No depletion sample positive control - 100 cell inoculation	37.25	-
100 cell inoculation	35.26	-1.99 (4-fold gain)
1,000 cell inoculation	32.47	-4.78 (27-fold gain)
10,000 cell inoculation	30.65	-6.6 (97-fold gain)
S. epidermidis DNA positive control	12.83	-
qPCR water negative control	35.06	-

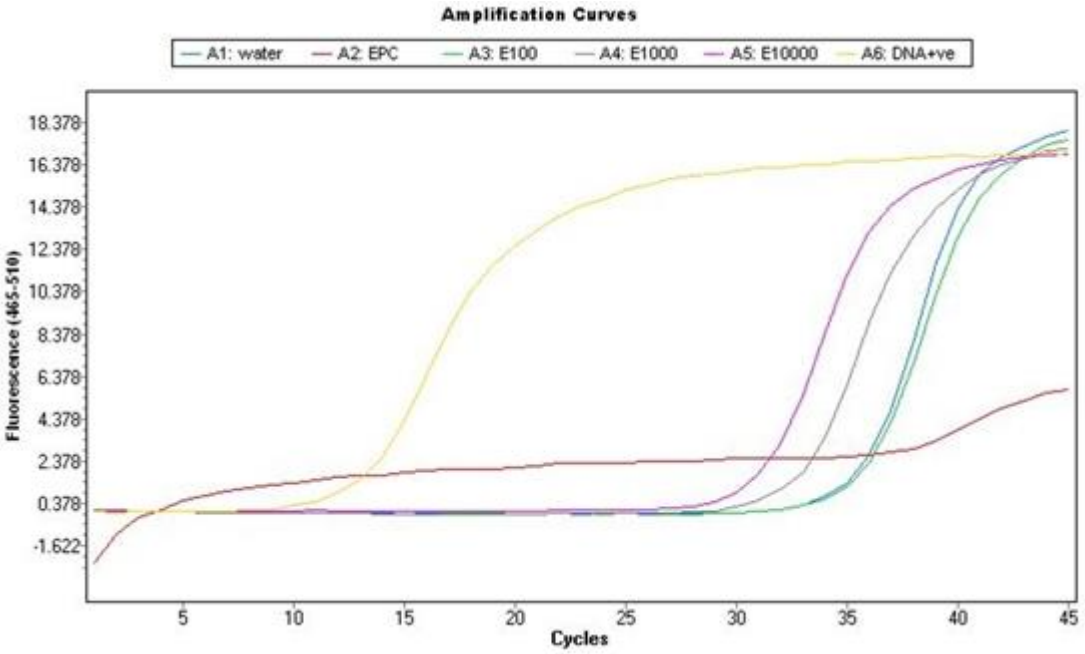

Figure 3.4. Bacterial presence by 16S qPCR after host cell depletion on spiked sonication fluid. qPCR amplification curves of 16S SYBR green assay on DNA extractions from culture-negative sonication fluid spiked with *S. epidermidis* cells. A1 – water negative control of PCR; A2 – no depletion positive control of sample spiked with 100 bacterial cells; A3 – depleted sample spiked with 100 bacterial cells; A4 – depleted sample spiked with 1,000 bacterial cells; A5 – depleted sample spiked with 10,000 bacterial cells; A6 – DNA positive control of direct DNA extraction from culture of spiked organism.

The negative control curve generated a lower C_T than the two samples spiked with 100 cells, however the melt curve analysis showed the target amplicon melt peak between 74°C and 76°C for

the 100-cell depleted sample and an inhibited melt peak for the no-depletion control (Figure 3.5). These could be easily differentiated from the primer dimer melt peaks at 70°C and 74°C.

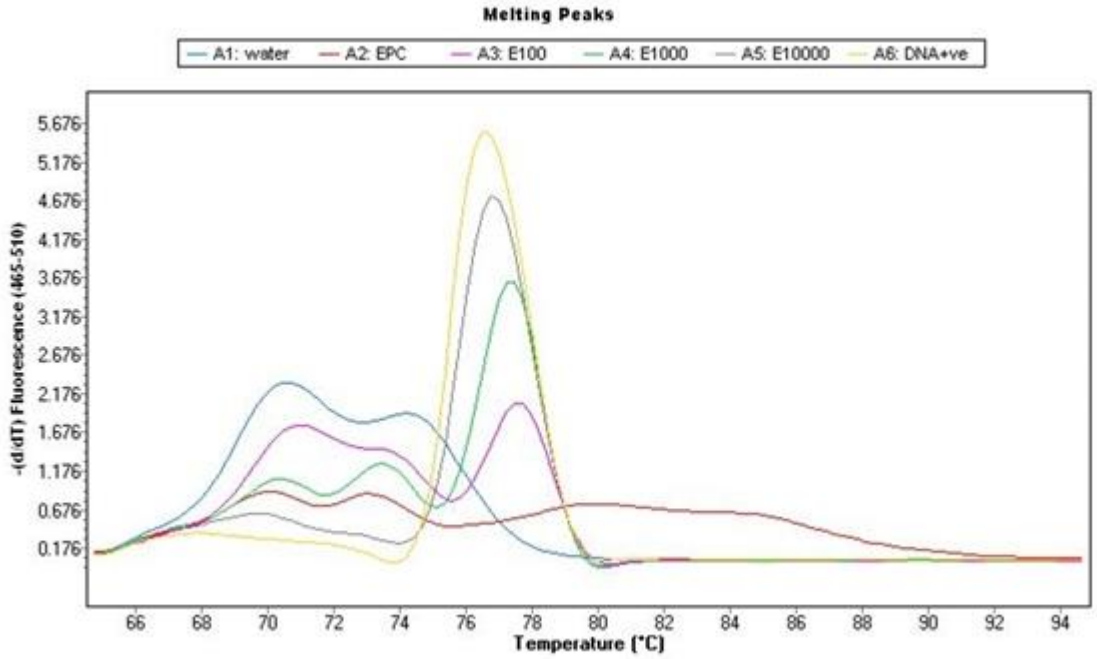

Figure 3.5. Melt curve analysis of 16S qPCR on spiked sonication fluid samples. A1 – water negative control of PCR; A2 – no depletion positive control of sample spiked with 100 bacterial cells; A3 – depleted sample spiked with 100 bacterial cells; A4 – depleted sample spiked with 1,000 bacterial cells; A5 – depleted sample spiked with 10,000 bacterial cells; A6 – DNA positive control of direct DNA extraction from culture of spiked organism.

A 10-fold increase in inoculation should result in a 10-fold gain of DNA, a ΔC_T of 3.3, compared to the control. The ΔC_T reported between inoculations in this first spiking experiment were ~1.8-2.8, lower than expected. To determine if bacterial DNA was being lost by the host cell depletion process, a standard curve for quantifying *S. epidermidis* DNA was set up for qPCR. A log series of *S. epidermidis* DNA (15TB0821) was quantified by 16S qPCR from 1 to 10^6 cells. This experiment yielded a series of C_T values with the expected ~3.3. ΔC_T between 10-fold inoculations with the major exceptions found at either end of the scale (Table 3.8). The low ΔC_T observed between 1 and 10-cell inoculations may be due to the C_T value generated by primer dimers in the assay again seen in the water negative control (35.27) putting a limit on the sensitivity of the assay. This data suggested that the 16S qPCR assay was efficient and sensitive and suitable for monitoring bacterial loss in depletion experiments. However, care must be taken when interpreting results outside the quantification range, which was accurate between 10 and 100,000 cells.

Table 3.8 16S qPCR of *S. epidermidis* inoculation standard curve

Sample Inoculation (cells)	**16S assay (C_T)**	**ΔC_T between serial dilutions**
qPCR water negative control	35.27	-
1	35.91	-
10	34.71	1.2
100	31.90	2.81
1,000	28.78	3.12
10,000	25.16	3.62
100,000	21.93	3.23
1,000,000	16.43	5.5

3.3.2 PLC host cell depletion efficiency of clinical samples

Following successful spiking experiments, we began to test clinical samples with the PLC depletion method. Three culture-positive sonication fluid samples were collected from the clinical microbiology laboratory, one positive for *E. coli* and two positive for *S. aureus*.

The most effective human depletion was observed in the *E. coli* sample with a 14.52 ΔC_T, 23,494-fold ~99.99% reduction in host cell DNA (Table 3.9). This 23,494-fold reduction is in line with the previous depletions on the culture negative samples that had been spiked with *S. epidermidis*. The *S. aureus* depletions showed less reduction in human DNA with 9.17 (*S. aureus* 1) and 10.76 (*S. aureus* 2) ΔC_T, equivalent to approx. 1,000-fold depletion (99.9%).

Table 3.9 PLC based depletion of host cell DNA from culture positive sonication fluid samples.

Sample	Human DNA assay (C_T)	ΔC_T
qPCR water negative control	-	-
S1 (*E. coli*) control	24.33	-
S1 (*E. coli*) depleted	38.85	14.52
S2 (*S. aureus*) control	24.71	-
S2 (*S. aureus*) depleted	33.88	9.17
S3 (*S. aureus*) control	23.29	-
S3 (*S. aureus*) depleted	34.05	10.76

A ΔC_T of 1 was observed between the non-depleted control and the depleted sample indicating a 2-fold loss of bacteria (50% loss) (Table 3.10). However, this is within the error range of qPCR and was not considered significant.

Table 3.10 Loss of *E. coli* qPCR signal after PLC depletion.

Sample	*E. coli* DNA assay (C_T)	ΔC_T
qPCR water negative control	39.05	-
S1 (*E. coli*) control	18.29	-
S1 (*E. coli*) depleted	19.35	1.06 (2-fold loss)

The *S. aureus* probe-based assay only detected *S. aureus* in one of the no depletion controls (sample 1, Figure 3.6, D4) at with a late C_T 38.96. *S. aureus* DNA was not detected in either of the depleted samples or the other control.

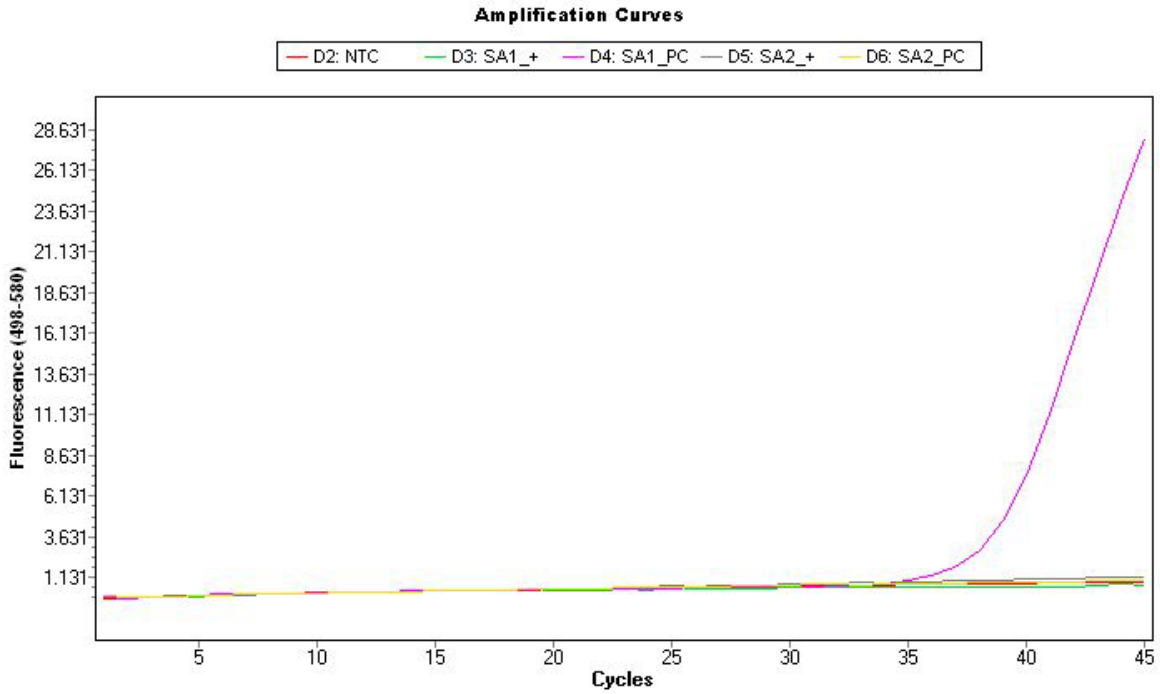

Figure 3.6. *S. aureus* probe-based PCR on S. aureus DNA extractions. D2, water negative-control; D3, *S. aureus* sample 1 after depletion; D4, *S. aureus* sample 1 no depletion control (C_T 38.96); D5, *S. aureus* sample 2 after depletion; D6, *S. aureus* sample 2 no depletion control.

The three depleted samples and their non-depleted controls were sequenced using the MinION as described in the methods (3.2.7) to see if the levels of depletion achieved were suitable for pathogen detection from sonication fluid.

E. coli was successfully identified in both of the *E. coli* samples run on the MinION with 3,072 *E. coli* reads in the no depletion control and 59,507 *E. coli* reads from the depleted sample, with 31,690 and 198 human reads in no depletion control and depleted sample respectively (Table 3.11).

The 14.52 ΔC_T depletion observed by qPCR (Table 3.9) equates to a 99.99% reduction in human DNA. This level of depletion resulted in a 10-fold difference in the proportion of bacterial reads by sequencing from ~10% to ~100% bacterial reads in the depleted sample (Figure 3.7). The increased percentage of bacterial reads meant that 20-fold more *E. coli* reads were reported following host cell depletion.

S. aureus was not detected in any of the four samples that had been culture positive for *S. aureus*, matching the qPCR results which suggested that *S. aureus* DNA was not present in three of the four samples (Figure 3.6). The sequencing results suggest that the late C_T reported in the no depletion

control of *S. aureus* sample 1 may have been a false positive result and that both sonification fluid samples may not have contained *S. aureus* despite the routine culture report.

Table 3.11 MinION sequencing reads detected in the first set of PJI clinical samples.

	Classified Reads*		
Sample	**Human**	***S. aureus***	***E. coli***
S1 (E. coli) PC[#]	31,690	0	3,072
S1 (E. coli) D[@]	198	0	59,507
S2 (*S. aureus*) PC	13,990	0	0
S2 (*S. aureus*) D	17,578	0	0
S3 (*S. aureus*) PC	72,962	0	0
S3 (*S. aureus*) D	731	0	0

*Reads classified by WIMP through EPI2ME (see 3.2.8.2) from 24 hours of MinION sequencing. [#]PC – process control with no depletion; [@]D – depleted sample processed with the PLC method

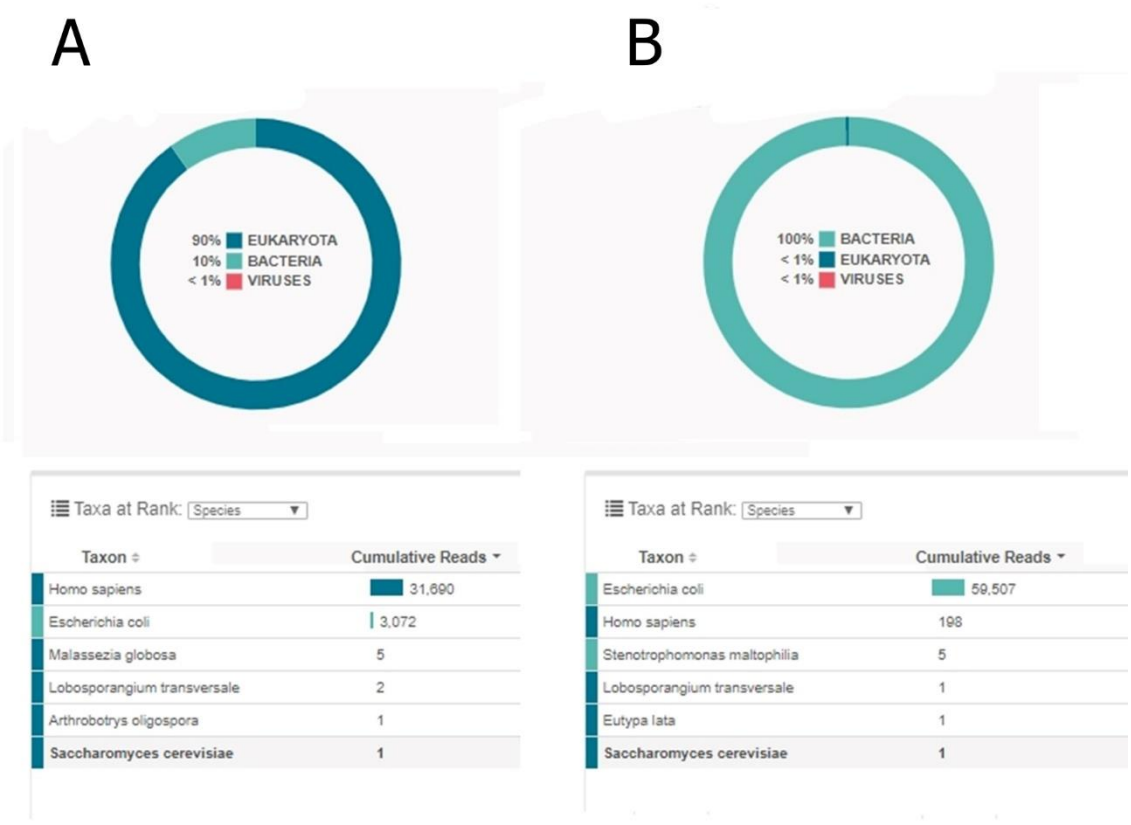

Figure 3.7. Comparison of WIMP output between a depleted sample (S1, *E. coli*) and a no-depletion control. A. S1 process control sample with no host cell depletion; B. S1 depleted with PLC method

3.3.2 Comparison of PLC and saponin depletion methods

To optimise the depletion of host cell DNA, we investigated another depletion method that had been developed in the group. This method utilises the detergent, saponin, in place of PLC. The saponin method was adjusted slightly allow both methods to be run side-by-side and compared (3.2.2.2). The methods were tested on both sonication fluid and MicroDTTect samples to compare the efficacy of host cell depletion and the loss of bacterial cells for both sample types.

Both methods were successful in depleting human DNA by a similar amount (Table 3.12). Average human DNA depletion was 9.96 C_T by PLC (range 7.54 to 11.56, average 997-fold reduction) and 10.92 C_T by saponin (range 7.69 to 13.38, average 1,932-fold reduction). The saponin method resulted in a more human DNA depletion than PLC with a later C_T in four out of five comparable samples (6120, 18TB0218, 18TB0266 and 18TB0288) by ΔC_T between 1.60 and 2.34. Depletion by the PLC method was higher by 2.34 C_T in one sample (18TB0220) and the four remaining samples were not comparable as both depletion methods reduced human DNA to undetectable levels. Two of these samples had very low human DNA prior to depletion (Samples 6036 and 6082), however, two samples contained a significant amount of starting DNA (Sample 6024, C_T 24.83; sample 18TB0273, C_T 28.19). No C_T value was generated for these samples post-depletion after 45 cycles of PCR, equivalent to 10^6-fold depletion of sample 6024 (99.9999% reduction of human DNA).

Table 3.12 Comparison of depletion using PLC or Saponin methods.

	Depletion Method					
Sample ID	**No depletion**	**PLC**		**Saponin**		**Comparison of PLC vs Saponin(ΔC_T)**
	Human DNA assay (C_T)	**Human DNA assay (C_T)**	**ΔC_T**	**Human DNA assay (C_T)**	**ΔC_T**	
6024 (SF*)	24.83	Not detected	-	Not detected	-	-
6036 (SF)	37.89	Not detected	-	Not detected	-	-
6082 (SF)	37.49	Not detected	-	Not detected	-	-
6120 (SF)	28.64	36.18	7.54 (186-fold)	38.25	9.61 (781-fold)	2.07 (Additional 4-fold loss by saponin)
18TB0218 (DTT#)	24.44	34	9.56 (755-fold)	35.6	11.16 (2,288-fold)	1.6 (Additional 3-fold loss by saponin)
18TB0220 (DTT)	25.52	35.55	10.03 (1,046-fold)	33.21	7.69 (207-fold)	2.34 (Additional 5-fold loss by PLC)
18TB0266 (DTT)	24.04	35.6	11.56 (3,019-fold)	37.42	13.38 (10,661-fold)	1.82 (Additional 4-fold loss by saponin)
18TB0288 (DTT)	22.91	34.03	11.12 (2,226-fold)	35.65	12.74 (6,841-fold)	1.62 (Additional 3-fold loss by saponin)
18TB0273 (DTT)	28.19	Not detected	-	Not detected	-	-

*Sonication fluid sample; #MicroDTTect fluid sample.

The PLC method resulted in a general gain of bacterial DNA measured by the 16S assay on average ΔC_T 1.38 (2.6-fold) lower than each sample's respective no-depletion control (range of

3.71 C_T loss to 4.76 C_T gain) (Table 3.13). A loss of bacterial DNA was only detected in three samples after PLC depletion (6024, 18TB0220 and 18TB0288) with an average ΔC_T 2.01 (4-fold).

The saponin based depletion method yielded a consistent loss in bacterial DNA by 16s qPCR in most samples with an average ΔC_T of 4.00 (16-fold loss). In four samples saponin based depletion removed almost all bacterial DNA in the sample as the depleted samples had C_Ts similar to the qPCR no-template controls. The saponin depletions showed a later C_T for bacterial 16s than PLC depletion in every sample with an average difference of 5.39 C_T (42-fold less bacterial DNA after saponin depletion) (range 2.93 to 9.64 C_T).

Table 3.13 qPCR comparison of bacterial DNA loss using PLC or Saponin depletion.

	Depletion Method					
Sample ID	**No depletion**	**PLC**		**Saponin**		**Additional loss by PLC over Saponin (ΔC_T)**
	16S assay (C_T)	**16S assay (C_T)**	**Loss or gain of bacterial DNA (ΔC_T)**	**16S assay (C_T)**	**Loss or gain of bacterial DNA (ΔC_T)**	
6024 (SF*)	18.59	22.3	3.71 (13-fold loss)	26.06	7.47 (177-fold loss)	3.76 (14-fold loss)
6036 (SF)	31.78	27.92	-3.86 (15-fold gain)	34.21	2.43 (5-fold loss)	6.29 (78-fold loss)
6082 (SF)	28.46	27.75	-0.71 (2-fold gain)	34.02	5.56 (47-fold loss)	6.27 (77-fold loss)
6120 (SF)	30.08	26.79	-3.29 (10-fold gain)	33.78	3.7 (13-fold loss)	6.99 (127-fold loss)
NC 1[@]	34.16	-	-	-	-	-
18TB0218 (DTT[#])	28.72	25.12	-3.6 (12-fold gain)	34.76	6.04 (66-fold loss)	9.64 (797-fold loss)
18TB0220 (DTT)	25.11	26.84	1.73 (3-fold loss)	30.87	5.76 (54-fold loss)	4.03 (16-fold loss)
NC 2[=]	34.7	-	-	-	-	-
18TB0266 (DTT)	31.1	28.83	-2.27 (5-fold gain)	34.09	2.99 (8-fold loss)	5.26 (38-fold loss)
18TB0288 (DTT)	30.57	31.16	0.59 (2-fold loss)	34.49	3.92 (15-fold loss)	3.33 (10-fold loss)
18TB0273 (DTT)	33.5	28.74	-4.76 (27-fold gain)	31.67	1.83 (4-fold gain)	2.93 (7.6-fold loss)
NC 3[+]	32.79	-	-	-	-	-

*Sonication fluid sample; [#]MicroDTTect fluid sample; [@]template free control for samples 6024, 6036, 6082 and 6120; [=]template free control for samples 18TB0218 and 18TB0220; [+]template free control for samples 18TB0266, 18TB0288 and 18TB0273

3.3.3 Mitochondrial DNA depletion

Investigation into the human DNA remaining after depletion revealed that the majority of sequence reads (>90%) mapped to human mitochondrial DNA (mtDNA) so we compared saponin and PLC based depletions to determine if there was a difference in their ability to remove mtDNA. A MicroDTTect sample (DTT4) was treated with both depletion methods and tested by qPCR with a specific mitochondrial DNA probe-based assay to quantify mitochondrial depletion. The no depletion control reported in a C_T of 15.72. The PLC method resulted in a 6-fold depletion of mitochondrial DNA (2.5 ΔC_T) whereas the saponin method was able to deplete 23-fold (4.5 ΔC_T) (Figure 3.8). Other MicroDTTect samples showed that ~15 C_T was typical for mitochondrial DNA in a non-depleted sample (results not shown), this equates to ~1.2 billion mitochondria present in DTT fluid wash from a prosthetic joint sample. With ~60 million mitochondria present per 200 µL sample taken for processing, efficient mtDNA depletion would be beneficial prior to sequencing samples containing low numbers of bacteria.

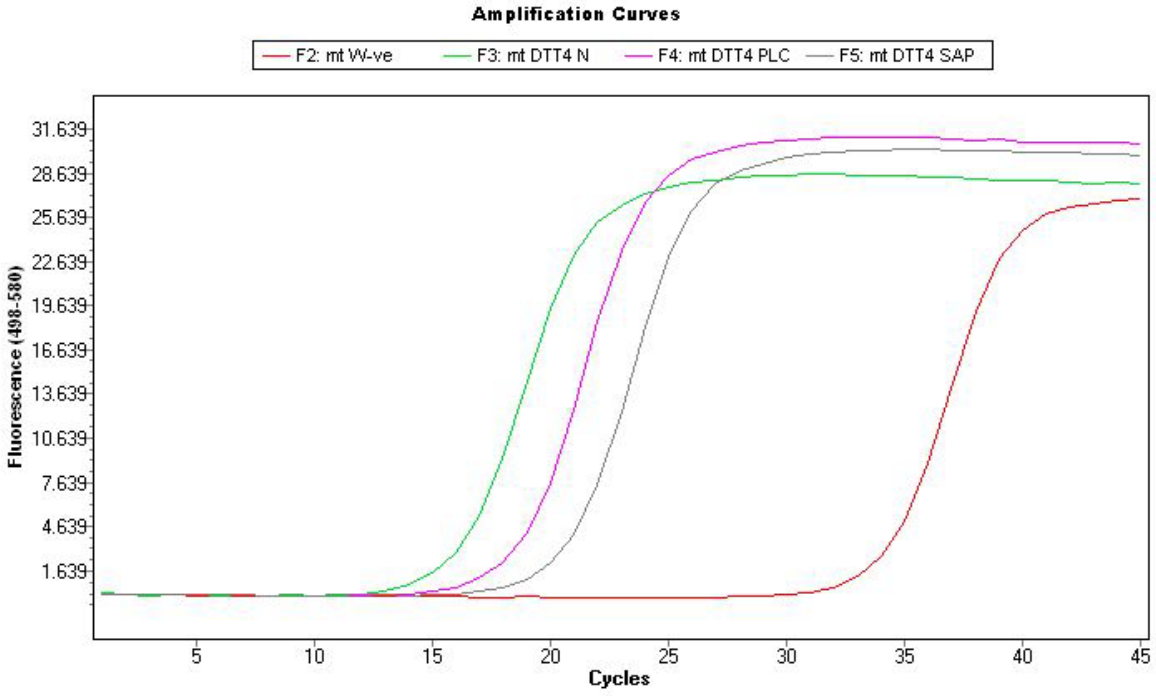

Figure 3.8. qPCR of mitochondrial DNA depletion of a MicroDTTect sample. F2 – Template-free qPCR negative control (C_T 33.74); F3 – Process control sample with no depletion performed (C_T 15.72); F4 – Sample depleted with PLC method (C_T 18.26); F5 – Sample depleted with Saponin method (C_T 20.24)

With saponin shown to have improved mtDNA depletion compared to PLC, but with significant bacterial DNA loss, an attempt was made to combine a lower concentration of saponin into the PLC method to improve the removal of mitochondria DNA, but without the loss of bacteria.

Three sets of depletion experiments were performed in an attempt to improve the reduction of mitochondrial DNA found in extractions performed on excess MicroDTTect samples processed with the PLC depletion method (3.2.2.1). All three sets were prepared for DNA extraction by bead beating (3.2.3.2). Detergents were incorporated alongside PLC in the first set of depletions. A control depletion sample without additional detergents was run alongside three other conditions: PLC with 0.025% saponin, PLC with 0.025% Triton X-100 and PLC with 0.1% Tween 20. Each detergent was added following the initial 15-minute incubation period with PLC and incubated for a further 15 minutes at 37ºC, 1,000 RPM, the control PLC depletion was incubated alongside the detergent- containing samples. All three tested detergents showed greater mitochondrial depletion combined with PLC than PLC treatment alone (Table 3.14). Saponin resulted in an additional 1.26 C_T (2.4-fold) depletion over PLC alone, but with the additional loss of 0.65 C_T (1.6-fold) bacterial DNA compared to PLC. Triton X-100 resulted in 0.98 C_T (2-fold) more mtDNA removal but with an additional 1.29 C_T (2.5-fold) loss of bacterial DNA compared to PLC. Tween 20 treatment showed 2.62 C_T (6-fold) less mitochondrial DNA, but 4.09 C_T (17-fold) additional bacterial DNA loss.

Table 3.14 Depletion of mitochondrial DNA using detergents combined with PLC

Depletion Method	Human DNA assay (C_T)	Loss of human DNA (ΔC_T)	16S assay (C_T)	Gain of bacterial DNA (ΔC_T)	Mitochondrial assay (C_T)	Loss of mitochondrial DNA (ΔC_T)
Process control	25.79	-	27.85	-	15.94	-
PLC only	34.56	8.77 (436-fold)	27.49	-0.36 (1-fold gain)	18.45	2.51 (6-fold)
PLC + Saponin	35.48	9.69 (826-fold)	28.14	-0.29 (1-fold gain)	19.71	3.77 (14-fold)
PLC + Triton X-100	35.59	9.8 (891-fold)	28.78	-0.93 (2-fold gain)	19.43	3.49 (11-fold)
PLC + Tween 20	36.79	11 (2,048-fold)	31.58	-3.73 (13-fold gain)	21.07	5.13 (35-fold)
Negative control	Not detected	-	34.56	-	36.55	-

A second set of depletions was performed incorporating alternative phospholipases along with PLC. Again, a control depletion without the incorporation of additional phospholipase from the standard PLC method was run alongside test conditions: PLC with 20 µl phospholipase A1 (PLA1) (Sigma), PLC with 20 µl phospholipase A_2 (PLA_2) (20 µl of 1 mg/ml) and PLC with 1 ml phospholipase D (PLD) (from *Streptomyces chromofuscus*, Sigma). Each additional phospholipase was added following the initial 15-minute incubation period with PLC and incubated for a further 15 minutes at 37ºC, 1,000 RPM, the control PLC depletion was incubated alongside the test samples.

The three phospholipases tested showed similar levels of *E. coli* loss with PLA1 and PLD losing an additional 0.66 C_T over PLC alone and PLA2 showing a loss of 0.17 C_T (Table 3.15). As with the detergent test, the additional phospholipases marginally improve mtDNA depletion with an additional 2.23 C_T with PLA1, 0.78 C_T with PLA2 and 0.83 C_T over PLC treatment alone.

Table 3.15 Depletion of mitochondrial DNA using phospholipase combinations.

Depletion Method	Human DNA assay (C_T)	Loss of human DNA (ΔC_T)	16s assay (C_T)	Loss of bacterial DNA (ΔC_T)	Mitochondrial assay (C_T)	Loss of mitochondrial DNA (ΔC_T)
Process control	26.29	-	24.6	-	14.49	-
PLC only	38.44	12.15 (4,544-fold)	26.7	2.1 (4-fold)	19.9	5.41 (43-fold)
PLC + PLA1	40	13.71 (13,400-fold)	27.36	2.76 (7-fold)	22.13	7.64 (199-fold)
PLC + PLA2	37.44	11.15 (2,272-fold)	26.87	2.27 (5-fold)	20.68	6.19 (73-fold)
PLC + PLD	40	13.71 (13,400-fold)	27.36	2.76 (7-fold)	20.73	6.24 (76-fold)
Negative control	Not detected	-	Not detected	-	32.06	-

.

The third set of depletions included a selection of previously successful conditions; PLC with 20 µl PLA1 (Sigma), PLC with 0.025% saponin, PLC with 0.025% Triton X-100 and PLC with 0.1% Tween 20, alongside two new combinations of depletion agents; PLC with 20 µl PLA1 (Sigma) and 0.025% saponin and a depletion cocktail (DC) PLC with 20 µl PLA1, 0.025% saponin and 0.025% Triton X-100. As before, additional reagents were added following the initial 15 minute incubation with PLC and incubated for a further 15 minutes at 37ºC, 1,000 RPM with the PLC control incubated alongside.

The two most successful methods for reducing mtDNA while preserving bacterial DNA were - PLC with saponin and PLC with PLA1 (Table 3.16). Individual detergent or phospholipase addition resulted in an additional 0.65-1.88 C_T (1.6-3.7-fold) removal of mtDNA compared to PLC only, while the combination of saponin and PLA1 depleted 6-fold more than PLC only (ΔC_T 2.69). A depletion cocktail (DC) combining five additional differential lysis agents to PLC showed the

greatest reduction in mtDNA, with 19-fold more depletion than PLC only (ΔC_T 4.25). Negligible levels of bacterial loss were observed across most of the methods of 1-1.5-fold loss (ΔC_T 0.12-0.64). However, PLC with Tween 20 showed 2.5-fold loss of *E. coli* compared to PLC only (ΔC_T 1.3). However, the modest gains in mtDNA removal, the additional cost associated with additional enzymes and the risk of bacterial loss when using saponin resulted in choosing the original PLC host depletion method moving forward.

Table 3.16 Depletion of mtDNA using phospholipase and detergent combinations.

Depletion Method	***E. coli* assay (C_T)**	***E. coli* loss (ΔC_T)**	**Mitochondrial assay (C_T)**	**Mitochondrial loss (ΔC_T)**
PLC only	30.67	2.87 (7-fold loss)	23.46	7.58 (191-fold loss)
PLC + PLA1	30.93	3.13 (9-fold loss)	25.34	9.46 (704-fold loss)
PLC + Saponin	30.03	2.23 (5-fold loss)	24.11	8.23 (300-fold loss)
PLC + Triton X-100	30.79	2.99 (8-fold loss)	25.27	9.39 (671-fold loss)
PLC + Tween 20	31.97	4.17 (18-fold loss)	25.08	9.2 (588-fold loss)
PLC + PLA1 + Sap	30.9	3.1 (9-fold loss)	26.15	10.27 (1,235-fold loss)
DC*	30.87	3.07 (8-fold loss)	27.71	11.83 (3,641-fold loss)
Negative control	Not detected	-	35.95	-

*DC – Depletion cocktail of PLC, saponin, Triton X-100 and PLA1.

3.3.4 Synovial fluid samples

When collecting whole prosthesis samples, where possible, an intraoperative synovial fluid aspiration was also collected by the clinicians. These synovial fluid samples were processed with the PLC depletion method followed by sequencing to determine if pathogens could be identified by

CMg from this sample type. In total 10 synovial fluid samples were collected alongside prostheses as part of the MicroDTTect study (3.2.1.2), five were culture positive (DTT3-SF, DTT5-SF, DTT7-SF, DTT9-SF and DTT21-SF) and five were culture negative (DTT4-SF, DTT6-SF, DTT10-SF, DTT11-SF and DTT20-SF). PLC depletion resulted in an average 3,821-fold reduction in human DNA (ΔC_T 11.90) and an average 3-fold gain of bacterial DNA (ΔC_T 1.45) (Table 3.17).

Table 3.17 qPCR results for PLC depletions of clinical synovial fluid samples.

Sample	Treatment	Human DNA assay (C_T)	Loss of human DNA (ΔC_T)	16S assay (C_T)	Gain or loss of bacterial DNA (ΔC_T)
DTT3-SF	No-depletion	28.15	-	30.71	-2.09 (4-fold gain)
	PLC	Not detected		28.62	
DTT4-SF	No-depletion	30.8	7.63 (198-fold)	33.15	-4.68 (26-fold gain)
	PLC	38.43		28.47	
DTT5-SF	No-depletion	26.26	13.74 (13,682-fold)	32.82	-2.57 (6-fold gain)
	PLC	40		30.25	
DTT6-SF	No-depletion	28.47	-	32.91	-1.4 (3-fold gain)
	PLC	Not detected		31.51	
DTT7-SF	No-depletion	23.18	-	29.86	-1.09 (2-fold gain)
	PLC	Not detected		28.77	
DTT9-SF	No-depletion	20.93	7.29 (156-fold)	27.09	-2.25 (5-fold gain)
	PLC	28.22		24.84	
DTT10-SF	No-depletion	22.02	17.58 (195,932-fold)	28.56	1.15 (2-fold loss)
	PLC	39.6		29.71	
DTT11-SF	No-depletion	28.13	9.75 (861-fold)	35.84	-0.73 (2-fold gain)
	PLC	38.88		36.57	
DTT20-SF	No-depletion	21.72	15.43 (44,146-fold)	29.86	0.85 (2-fold loss)
	PLC	37.15		29.01	
DTT21-SF	No-depletion	26.74	-	34.46	1.35 (3-fold loss)
	PLC	Not detected		33.11	

Available synovial fluid samples were initially sequenced alongside whole prosthesis wash samples from the same patients. The first sequencing run included two synovial fluid samples (DTT3-SF and DTT-SF4). Neither synovial fluid sample returned a significant result when the sequencing thresholds were applied (3.2.8.2) despite a culture-positive report for DTT3-SF (Figure 3.9). A single bacterial read was reported by WIMP from DTT4-SF, classified as *Clostridium perfringens*, an artefact of the PLC method. This sample was negative by culture, so this result was expected. DTT3-SF, however, was culture positive for *P. aeruginosa* and *C. tuberculostearicum*, neither of which were detected by CMg. The most abundant pathogen detected by sequencing was *E. coli* (84 reads), however, this was below the cut-off of >500 pathogen reads after 24hr sequencing.

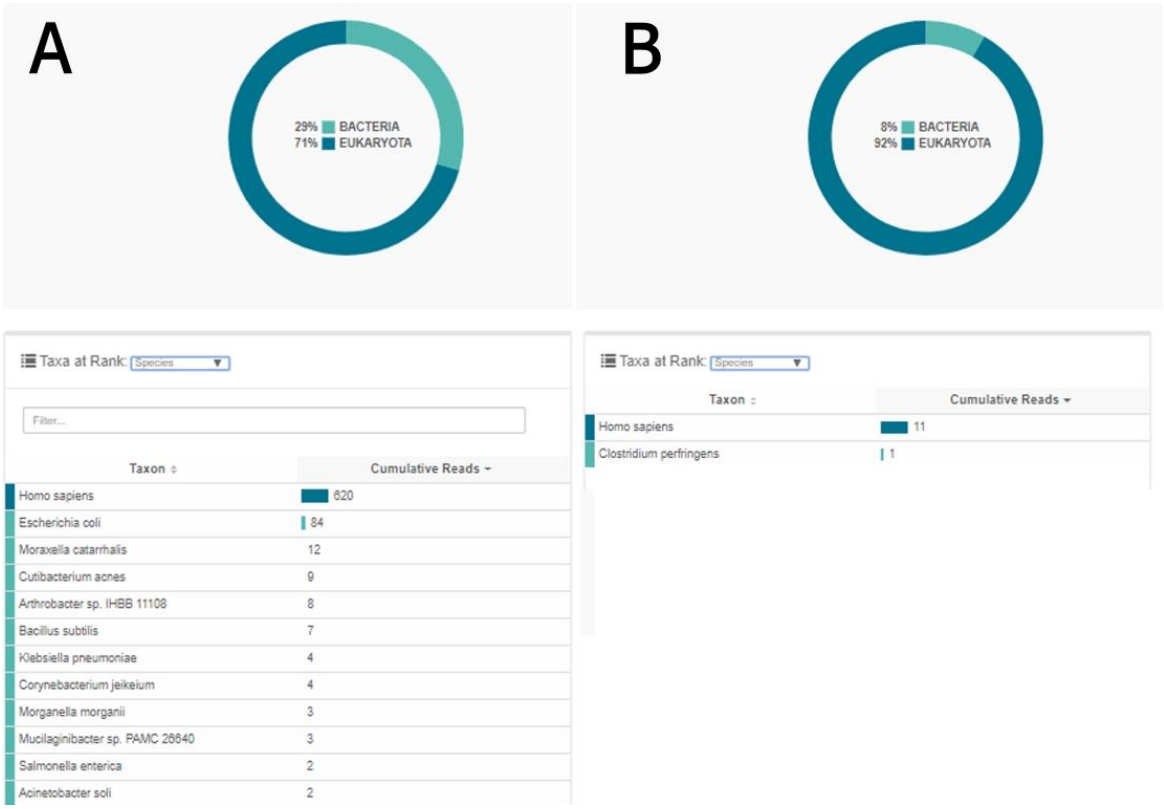

Figure 3.9 WIMP readout of sequenced synovial fluid samples. A. DTT3-SF, clinical result: *Pseudomonas aeruginosa* and *Corynebacterium tuberculostearicum*; B. DTT4-SF, clinical result: culture negative.

The next synovial fluid sample sequenced was from a joint reported to be grossly infected with *S. lugdunensis* (synovial fluid samples from MicroDTTect patient 9). The joint was visibly contaminated with pus during surgery as was the synovial fluid sample itself. 198 *S. lugdunensis* reads (below significant threshold of 500 reads in 24 hrs) were reported by WIMP from the

synovial sample compared to 28,414 from the prosthesis sample from the same patient (Figure 3.10), over 1,000-fold fewer. The synovial fluid sample generated more reads than the prosthesis sample (257,298 and 167,111 respectively), the majority of which were human (254,905), suggesting poor human depletion. This was confirmed with a human ΔC_T of only 7.29 (156-fold reduction), significantly less than the other samples (Table 3.17). The poor depletion in this sample was likely due to the excessive puss present in the sample, inhibiting the depletion process .

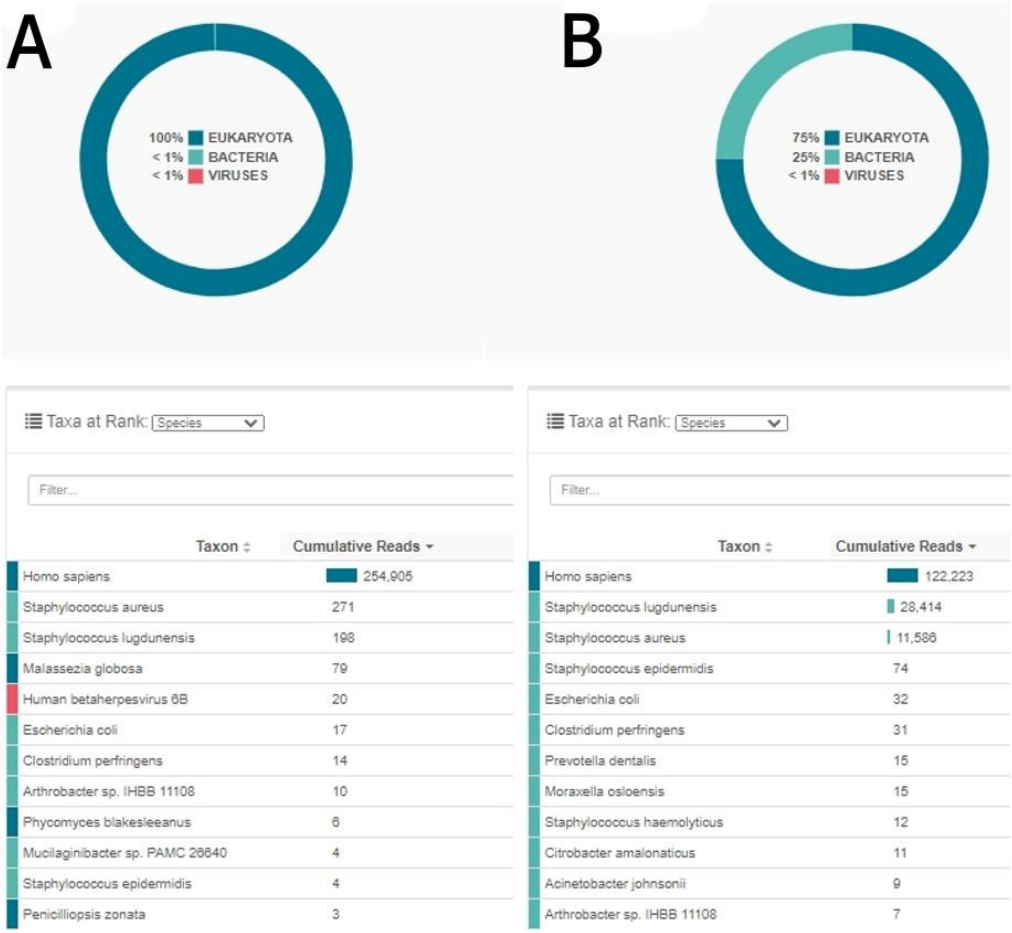

Figure 3.10 Wimp readout of sequenced synovial fluid sample DTT9-SF and corresponding whole prosthesis sample. A: DTT9-SF after 24 hours of sequencing and B: DTT9 after 24 hours of sequencing.

3.3.5 MicroDTTect study

A total of 42 prostheses were processed using MicroDTTect. The DTT fluid was analysed by both culture, using blood culture bottles, and CMg. The results were then compared to the routine culture of periprosthetic tissue and synovial fluid samples taken from the same patients. Results

presented in this section are from samples treated using the PLC depletion method with 2 hours for sequencing.

As the first CMg run (DTT 1-4) was only 50% concordant with culture, results were investigated further. DTT2 and DTT3 DNA extracts were tested by qPCR for the CMg reported pathogens and the clinical notes were reviewed. With 642 reads assigned to *S. pneumoniae* in DTT2 within the first two hours of sequencing (51.69% of the classified microbial reads), the CMg result was valid (Table 3.18). The qPCR detected *S. pneumoniae* DNA with a C_T of 29.53 and the negative control was negative (Figure 3.11). The clinical notes reported that a previously taken fluid aspirate from the prosthesis site contained pus and the patient was treated with vancomycin and operated on three days later. While no significant growth was detected by routine culture or DTT fluid, Gram-positive cocci were reported in one routine sample tested by Gram staining.

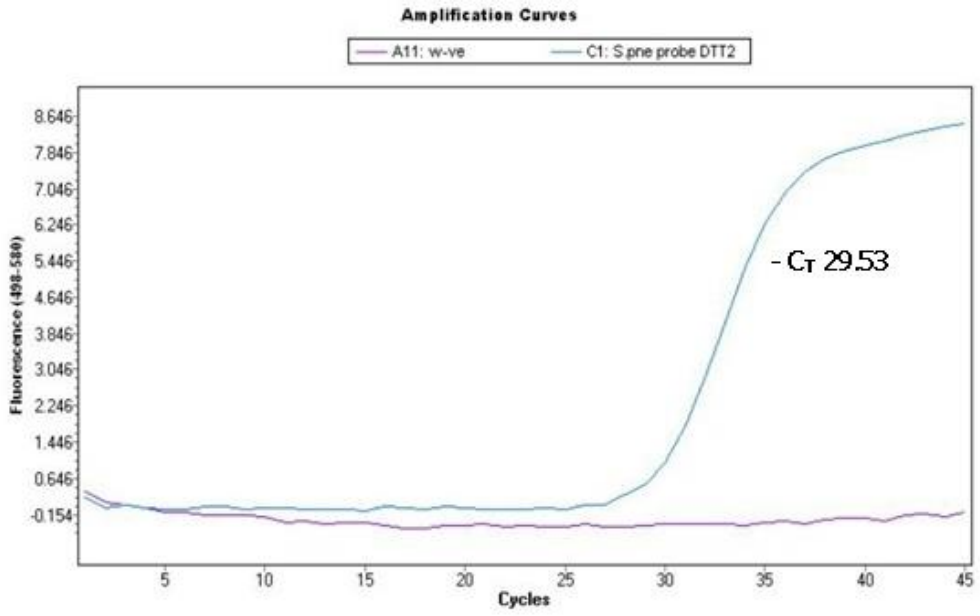

Figure 3.11. *S. pneumoniae* qPCR of DTT sample 2. A11 – water negative qPCR control; C1 – DNA extraction of depleted DTT2 fluid sample.

Sample DTT3 reported no significant reads by CMg for any organism. The top hits for bacterial reads were 112 *E. coli* and 23 *C. perfringens* at 24.56% and 5.04% of total microbial reads respectively, insufficient to pass thresholds (Table 3.18). Routine culture of seven periprosthetic tissue samples yielded two cultures of *P. aeruginosa*, two cultures of *C. tuberculostearicum* and three reports of no biological growth. *P. aeruginosa* was also cultured from the DTT fluid. qPCR

was unable to detect the presence of *P. aeruginosa* DNA in the total nucleic acid extractions of DTT3, either with or without host cell depletion (positive and negative controls gave expected results, Figure 3.12). The patient was initially diagnosed with aseptic loosening as frozen sections showed no sign of infection. This patient was also tested in the calprotectin study in Chapter 2 where the patient was calprotectin test negative (Calprotectin sample 56). Patient follow-up indicated the patient had not been infected.

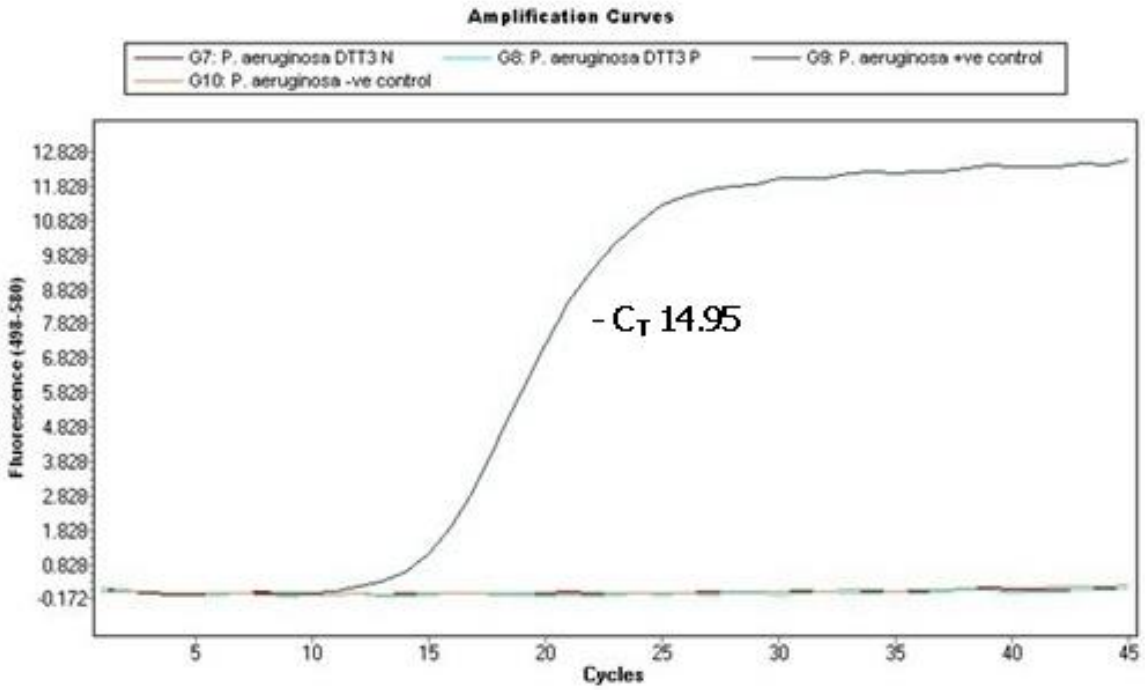

Figure 3.12. *P. aeruginosa* qPCR of DTT sample 3. G7 – DNA extraction from DTT3 no-depletion process control; G8 – DNA extraction from depleted DTT3 sample; G9 – *P. aeruginosa* positive control DNA; G10 – water negative qPCR control.

As sequencing was shown to be supported by both qPCR and clinical findings, the study was continued without alterations to the protocol for the remaining 38 samples (Table 3.18). Sequencing of these initial samples with the saponin method yielded poor results, with *S. pneumoniae* not detected (results not shown) so sequencing was only pursued for the MicroDTTect samples depleted with the PLC method.

28 of 42 samples were concordant across all three methods (routine culture, DTT culture and CMg), seven positives and 21 negatives. The most detected organism by each method was *S. epidermidis*, found four times by routine culture, six times by DTT culture and three times by CMg. 12 different organisms were isolated by routine culture. Of these, five organisms were not detected by either method used to test DTT fluid (*C. striatum, C. acnes, C. tuberculostearicum, F. magna* and Bacillus sp.). *S. haemolyticus* was only isolated from DTT fluid culture, *S. pneumoniae* and *E. coli* were only detected by CMg.

Table 3.18 Bacteria identified in the MicroDTTect study samples tested by routine culture, DTT culture and CMg

Sample ID	**Organisms reported by routine culture (>2 positive cultures)**	**Organisms cultured from DTT fluid**	**Significant species reported by CMg***		
			Species name	**Species specific reads**	**% of total microbial reads**
DTT 1					
DTT 2			*S. pneumoniae*	642	51.69
DTT 3	*P. aeruginosa, C.tuberculostearicum*	*P. aeruginosa*			
DTT 4					
DTT 5	*C. acnes*				
DTT 6					
DTT 7	*P. mirabilis*	*P. mirabilis*	*P. mirabilis*	2033	82.47
DTT 8					
DTT 9	*S. lugdunensis*	*S. lugdunensis*	*S. lugdunensis*	4770	69.20
DTT 10		*S. epidermidis*			
DTT 11					
DTT 12					
DTT 13		*S. epidermidis*			
DTT 14					
DTT 15					
DTT 16					
DTT 17		*S. warneri*	*S. warneri*	1802	71.54
DTT 18					
DTT 19	*S. anginosus*	*S. anginosus*	*S. anginosus*	31832	98.07
DTT 20					
DTT 21	*S. aureus*	*S. aureus*	*S. aureus*	5050	94.15

Continued on next page.

Table 3.18 Continued. Bacteria identified in the MicroDTTect study samples tested by routine culture, DTT culture and CMg

Sample ID	Organisms reported by routine culture (>2 positive cultures)	Organisms cultured from DTT fluid	Significant species reported by CMg*		
			Species name	Species specific reads	% of total microbial reads
DTT 22	*S. epidermidis*	*S. epidermidis*	*S. epidermidis*	1892	80.48
DTT 23	*C. striatum*, *F. magna*	*S. haemolyticus*			
DTT 24					
DTT 25	*S. epidermidis*, *C. striatum*	*S. epidermidis*	*S. epidermidis*	307	76.94
DTT 26	*S. epidermidis*	*S. epidermidis*			
DTT 27	*S. aureus*, *P. mirabilis*	*P. mirabilis*	*P. mirabilis*	1166	20.08
DTT 28			*E. coli*	3354	95.04
DTT 29					
DTT 30					
DTT 31	*S. aureus*	*S. aureus*	*S. aureus*	1431	90.23
DTT 32					
DTT 33			*E. coli*	18723	81.00
DTT 34					
DTT 35					
DTT 36	*S. epidermidis*	*S. epidermidis*	*S. epidermidis*	457	81.90
DTT 37	Bacillus sp				
DTT 38					
DTT 39					
DTT 40					
DTT 41	Group G Streptococcus sp		*S. dysgalactiae*	27760	96.35
DTT 42					

*Significant species reported by WIMP (EPI2ME) with reads greater than the cutoff value of 200 reads and greater than 30% of the total non-human classified reads counted as significant.

CMg identified all organisms detected by routine culture in 8/15 cases (Table 3.19). In two cases CMg was able to detect one but not all of the organisms reported by routine culture (Samples DTT25 and DTT27). There were 4 cases in which the organism/s reported by culture were not reported as either of the top two most abundant organisms by WIMP and no organism reached the cut-off of >200 reads in 2hrs (DTT3, DTT5, DTT23 and DTT37). In one sample (DTT26) the

cultured organism, *S. epidermidis*, was the most abundant organism reported by WIMP (40.32% after 2 sequencing) but failed to reach the cutoff for significant reads (with only 125 and 416 reads after 2 and 24 hours of sequencing, respectively). There were three cases with organisms identified by CMg that had not been isolated by either culture method: *S. pneumoniae* (DTT2) and *E. coli* (DTT28 and DTT33).

DTT fluid culture identified all organisms reported by routine culture in 8/15 cases (Table 3.19). In three cases one but not all reported organisms were found (DTT3, DTT25 and DTT27), two of which were concordant with the results reported by CMg (DTT25 and DTT27). There were four cases in which DTT fluid culture was unable to detect any organisms reported by routine culture (DTT5, DTT23, DTT37 and DTT41), three of which were concordant with CMg (DTT5, DTT23 and DTT37). In three cases DTT fluid culture reported an organism not detected by either other method, *S. epidermidis* (DTT10 and DTT13) and *S. haemolyticus* (DTT23).

Five organisms were detected by routine culture but never by either other method: *C. tuberculostearicum* (DTT3), *C. acnes* (DTT5), *C. striatum* (DTT23 and DTT25), *F. magna* (DTT23) and Bacillus sp (DTT37). There were two cases in which routine culture reported two organisms but only one organism was found by DTT culture and CMg (DTT27 *S. aureus* and *P. mirabilis* reported by routine culture, only *P. mirabilis* detected by CMg and DTT fluid culture; DTT25 *S. epidermidis* and *C. striatum* reported by routine culture, only *S. epidermidis* found by CMg and DTT fluid culture) (Table 3.19).

Table 3.19 Comparison of organisms detected using the three methods in the MicroDTTect study.

	Detected organisms		
Study No.	**Routine culture**	**DTT fluid culture**	**CMg**
2			***S. pneumoniae***
3	*P. aeruginosa, C. tuberculostearicum*	***P. aeruginosa***	
5	*C. acnes*		
7	*P. mirabilis*	***P. mirabilis***	***P. mirabilis***
9	*S. lugdunensis*	***S. lugdunensis***	***S. lugdunensis***
10		***S. epidermidis***	
13		***S. epidermidis***	
17		***S. warneri***	***S. warneri***
19	*S. anginosus*	***S. anginosus***	***S. anginosus***
21	*S. aureus*	***S. aureus***	***S. aureus***
22	*S. epidermidis*	***S. epidermidis***	***S. epidermidis***
23	*C. striatum, F. magna*	***S. haemolyticus***	
25	*S. epidermidis, C. striatum*	***S. epidermidis***	***S. epidermidis***
26	*S. epidermidis*	***S. epidermidis***	
27	*S. aureus, P. mirabilis*	***P. mirabilis***	***P. mirabilis***
28			***E. coli***
31	*S. aureus*	***S. aureus***	***S. aureus***
33			***E. coli***
36	*S. epidermidis*	***S. epidermidis***	***S. epidermidis***
37	Bacillus sp		
41	Group G Streptococcus sp		***S. dysgalactiae***

Yellow: additional organism not reported by routine culture found; Orange: one but not all organisms reported by routine culture found; Red: No organisms reported by routine culture found; Green: full concordance with routine culture result.

The overall sensitivity and specificity of CMg compared to routine culture were 53.33% (8/15, 95% CI 26.59% to 78.73%) and 85.19% (23/27, 95% CI 66.27% to 95.81%) respectively, with an accuracy of 73.81% (31/42, 95% CI 57.96% to 86.14%) (Table 3.18). Culture of the DTT fluid compared to routine culture results yielded a sensitivity and specificity of 53.33% (8/15, 95% CI

26.59% to 78.73%) and 88.89% (24/27, 95% CI 70.84% to 97.65%) respectively, with an accuracy of 76.19%% (32/42, 95% CI 60.55% to 87.95%) (Table 3.18).

Retrospectively setting a cutoff value of 125 reads and greater than 30% of the total non-human classified reads improved the sensitivity of CMg compared to routine culture to 60.00% (9/15, 95% CI 32.29% to 83.66%) without changing the specificity. Using these cutoffs, the sensitivity and specificity of CMg compared to culture of the same sample (DTT fluid culture) was 73.33% (11/15, 44.90% to 92.21%) and 85.19% (23/27, 66.27% to 95.81%), respectively. As expected, the performance of CMg was greater compared to DTT fluid than routine culture as DNA was extracted from the same sample tested.

3.4 – Discussion

3.4.1 Sequencing as a diagnostic tool

Informative and accurate PJI diagnosis is essential for choosing an appropriate and effective treatment plan. While rapid biomarker tests have a role to play in ruling in or out infection as a cause of disease, pathogen identification is required when a joint is infected to dictate treatment. At present, the role of pathogen identification and antimicrobial susceptibility testing relies on microbiological culture. However, the slow turnaround time and prevalence of culture-negative infection makes microbial culture a poor gold standard method.

We developed a clinical metagenomics pipeline capable of pathogen identification within six hours of suspected PJI sample collection. This rapid turnaround time is vastly superior to routine culture (>48 hours) and is also quicker than previously reported studies using Illumina platforms (>60 hours) (Ivy et al., 2018; Street et al., 2017; Thoendel et al., 2018). Our turnaround time is comparable with other studies using the same sequencing platform (i.e. MinION), where Noone *et al.* reported a minimum turnaround time of seven hours from sample collection to result (Noone et al., 2021).

Using this pipeline, we performed a study on prospectively collected whole prosthesis samples, treated with DTT using the MicroDTTect® closed bag system. After two hours of sequencing, we report a sensitivity of 60% and specificity of 85% compared to routine culture. While the specificity is slightly greater than that reported by Street *et al.* (80%) (2017), our sensitivity is much lower than that reported by Street *et al.* (88%) (2017) and Thoendel *et al.* (83%) (2018) on sonication fluid of whole prosthesis samples, a similar sample type to that used in our study. The sensitivities reported by these studies were calculated against in-house culture of the sonication fluid tested by CMg as opposed to corresponding PPT culture performed at the hospital in our study. We report a sensitivity of 73% compared to the culture of DTT fluid which remains lower than what has been previously reported. We know from the clinical review undertaken as part of the calprotectin study (2.3.2) that some of the organisms identified from patients included in our studies were likely contaminants. Street *et al.* noted that they did not attempt to sequence samples which were potentially contaminated (Street et al., 2017). It would be expected that a clinical

review into the patients included in the MicroDTTect study would yield a higher sensitivity than that compared to routine culture alone. However, despite the low sensitivity, CMg showed slightly higher concordance with culture in our hands compared with the other study utilising nanopore sequencing, 79% and 72% respectively (Noone et al., 2021).

3.4.2 Host cell depletion

Due to the high ratio of human to microbial DNA in clinical samples, sensitive pathogen detection by metagenomic sequencing requires efficient depletion of host DNA or enrichment of pathogen DNA (Charalampous et al., 2019). Previous work by our group has utilised either PLC or saponin, coupled with HL-SAN DNase for the depletion of host cell nucleic acid in blood (O'Grady et al., 2018) and respiratory samples (Charalampous et al., 2019).

Based on the methods described in these studies we tailored two sample preparation methods to PJI samples using PLC or saponin for differential host cell lysis. Charalampous *et al.* reported the removal of up to 99.99% of human DNA in respiratory tract samples using the saponin based depletion method, equating to a 10,000-fold enrichment of microbial DNA (Charalampous et al., 2019). We achieved between 87 and 14,362-fold of host cell depletion with both our saponin and PLC based methods, with an average depletion of 1,407-fold. This level of host depletion has not been reported in the literature for PJI samples to date. Thoendel *et al.* investigated the efficacy of the NEBNext Microbiome DNA Enrichment kit and the MolYsis Basic5 kit for the depletion of host cell DNA in sonication fluid samples spiked with *S. aureus* as only 1% of bacterial DNA was recovered without depletion (Thoendel et al., 2016). They reported ~10% depletion using the NEBNext kit, which in a study by Schmidt *et al.* was deemed insufficient for nanopore based CMg on urine samples (Schmidt et al., 2017). By contrast, the MolYsis kit showed ~80% depletion of host cell DNA, which was sufficient for Thoendel *et al.* and Ivy *et al.* to determine pathogen ID in PJI samples with the additional use of WGA (Ivy et al., 2018; Thoendel et al., 2018). WGA is a valuable tool for sequencing from low input samples, however, we achieved pathogen identification without the need for WGA from whole prosthesis samples in our study. This approach may be necessary for synovial fluid samples where there is significantly less microbial

biomass than on a whole prosthesis as demonstrated by Ivy *et al.* who successfully applied CMg to synovial fluid samples using WGA, while our approach was unsuccessful in this sample type. Another potential use for WGA may be for generating enough sequencing depth for AMR gene identification, although neither of these were thoroughly investigated as part of this work.

By comparison to commercially available kits, our methods show significantly greater ability to remove host nucleic acid from a sample, likely due to the application of HL-SAN DNase, which remains stable in the high salt buffer utilised in our methods. The high salt buffer applied in the cell free host DNA digestion step likely enhances the efficiency of DNase activity as chromatin-associated proteins become more soluble with increasing concentration of NaCl making DNA more accessible for enzyme activity (Basnet and Massague, 2019). As HL-SAN DNase remains active at high salt concentrations, it is better suited to this application than enzymes commonly used in commercial kits which are not stable in such conditions.

Bacterial retention is important when applying host cell depletion methods, especially when working with samples with low microbial load. While both depletion methods that we tested were capable of consistently removing ≥99.9% of human DNA from our samples, the PLC based method was chosen to take forward with the MicroDTTect study as it showed better retention of bacterial DNA, despite less host cell depletion. For example, *S. pnemoniae*, an easily lysed organism (Martner et al., 2008), was identified from DTT3 following PLC depletion but not after the saponin method. Any damaged bacterial cells are likely to be susceptible to saponin activity and along with lysed bacterial cells will have had their DNA degraded and removed during the HL-SAN DNase. It appears likely that bacterial cells have been damaged by sonication, which is used at higher frequencies to lyse bacteria (Joshi and Jain, 2017), and osmotic shock if not rapidly pelleted from the 0.1% DTT solution before resuspension in PBS following DTT wash (Shehadul Islam et al., 2017).

The average loss of bacterial DNA with saponin was 4 C_T, over 10-fold loss compared to the untreated samples, significantly greater than that observed with the PLC method. According to qPCR, PLC based depletions contained more bacterial DNA than their untreated counterparts,

although this is likely an artefact of the high ratio of host to microbial DNA in the samples inhibiting the 16S PCR assay in the no depletion control samples.

Comparisons between PLC and saponin depletion methods by qPCR using specific mtDNA primers showed consistently greater depletion of mitochondria with saponin. While mitochondrial cells contain a relatively small amount of DNA compared to bacterial cells (16,569 bp compared to 2,800,000 bp for the *S. aureus* genome (Chua et al., 2013)) (Taylor and Turnbull, 2005), multiple mitochondria may be present per cell. Cells that require a lot of energy to operate typically contain a greater number of mitochondria, 1000-2000 per cell (Alberts et al., 2002). A recent study by Dache *et al.* suggests that cell-free mitochondria can also be found in great numbers in blood, estimated at between 200,000 and 3.7 million organelles per millilitre of blood plasma (Al Amir Dache et al., 2020). PPT samples are therefore likely to contain large quantities of mitochondria as prostheses are typically surrounded by muscle cells and blood. This is supported by our findings of ~1.2 billion copies of mitochondrial DNA in the total DTT fluid volume of a washed prosthesis with no host-cell depletion.

Unfortunately, mtDNA removal by our host depletion approaches was less efficient than for nuclear DNA. Saponin has a high affinity for cholesterols, mitochondrial membranes contain much less cholesterol than the typical plasma membrane, suggesting saponin disruption of the membrane could be less effective (Mathers and Staples, 2015). The reason for the reduced PLC lysis of mitochondria is unknown but it may be due to the double mitochondrial membrane and the folded nature of the inner membrane reducing PLC efficacy.

Comparative qPCR results for mtDNA after treatment with PLC and saponin showed that the saponin method removed 2-10-fold more mitochondrial DNA than PLC. Incorporating a lower concentration of saponin or other detergents showed early promise for improving mitochondrial depletion with the PLC method (2-6-fold more depletion combining a detergent with PLC than PLC alone). Similar improvements were seen with the range of alternative phospholipases combined with PLC. Ideally an improved method would have been designed incorporating a cost-effective combination of PLC with a detergent, another phospholipase or a combination of both (19-fold more depletion achieved using a combination of PLC, saponin, Triton X-100 and PLA1).

All additions to the PLC method improved host cell depletion, however, incorporation of Tween 20 led to a significant loss of bacterial cells probably due to inadvertent bacterial cell lysis. Although this work showed promise, the marginal gains in host/mtDNA depletion were not considered worth the risk of lysing more bacteria and the additional cost/complexity of the method.

3.4.3 Synovial fluid samples

The impact of effective host-cell nucleic acid on CMg is significant in all samples, however, the issue is particularly relevant for samples containing low microbial load, such as synovial fluid (Salter et al., 2014). Despite the previous success of Ivy *et al.* in pathogen ID from synovial fluid samples by CMg (Ivy et al., 2018), synovial fluid CMg performed poorly in our hands.

Using our host cell depletion methods, we were able to successfully remove ~99.99% of host DNA from synovial fluid samples, however, despite this level of depletion, the number of pathogen reads did not reach the required threshold for significance in the sequenced samples.

While it is unsurprising that *P. aeruginosa* and *C. tuberculostraricum* found by routine culture were not detected from DTT3-SF, as the organisms were not identified by whole prosthesis wash sequencing from the same patient. It was expected that a known culture positive sample such as DTT9-SF would result in significant *S. lugdunensis* reads. The case for infection with this patient was clear, pus was visible within the prosthesis site during surgical intervention, all tissue samples taken for routine microbiology cultured the same organism which was also detected by DTT fluid culture and CMg. However, while *S. lugdunensis* reads were generated by CMg, the results were insufficient to meet the in-place cut-offs after either 2 or 24 hours of sequencing. The high starting level of human DNA in this sample couples with poor depletion is the likely reason why CMg failed to identify the cultured pathogen. The depleted synovial fluid sample from this patient (DTT9-SF) contained over 10-fold more human DNA than the DTT fluid sample taken as part of the same operation (DTT9) and yielded 100-fold fewer reads, highlighting the importance of efficient host-cell depletion. This result suggests that synovial fluid samples containing pus may need to be processed differently, perhaps using less starting material or diluting the sample.

Another potential solution may be to pass the sample through a filter, as performed by Street *et al.* (Street et al., 2017), prior to depletion to remove pus cells.

3.4.4 Discordant samples

Despite observing some discordance between diagnostic methods used, whole prosthesis sampling with DTT treatment does show some promise for the detection of pathogens that can be missed by routine culture. This was particularly evidenced by sample DTT17 which was reported as no growth from any routinely cultured PPT sample. *S. warneri* however, was isolated from the DTT fluid and also identified by CMg. As *S. warneri* are known to be capable of strong biofilm formation (Gajewska and Chajęcka-Wierzchowska, 2020), this case may represent a biofilm-mediated infection where PPT culture was not able to detect cells tightly adhered to the prosthesis. Results such as this were expected as both sonication and DTT based methods for biofilm removal from whole prosthesis samples have been reported to improve sensitivity over routine PPT culture (Drago et al., 2012; Evangelopoulos et al., 2013; Karbysheva et al., 2020). There is also evidence to suggest that the use of blood culture bottles over traditional PPT culture methods can improve sensitivity for diagnosis of PJI (Peel et al., 2016), which may have been a factor in additional detections in the DTT culture arm.

Sequencing missed an organism found by both culture methods in one other sample, DTT 26 containing *S. epidermidis*. *S. epidermidis* reads were detected by WIMP, representing ≥30% of the total microbial reads, however, the total number of reads fell below the initial threshold for a significant result of 200 reads after 2 hours, or 500 reads after 24 hours. Lowering the threshold to 125 reads after 2 hours improved the sensitivity to 60% against routine culture and 73% against DTT fluid culture without lowering the specificity.

A common problem associated with PPT culture is the potential for contamination, either during sampling or in the microbiology laboratory. The sealed bag system of MicroDTTect was designed to mitigate potential contamination during sample handling. Organisms reported by routine culture methods were undetected by both DTT fluid culture and CMg in four cases. The majority of organisms detected by PPT culture from these samples would be considered common

contaminants, *C. acnes* in particular is commonly found in PPT samples but typically not associated with knee and hip PJI (Tande and Patel, 2014). These organisms which are reported as missed by DTTect sampling may be false positives derived from contamination that has not affected the whole prosthesis samples. In these cases, the closed bag method may have prevented contamination, demonstrating the potential of MicroDTTect to improve culture specificity. However, contamination may still be possible within the DTT fluid culture pipeline as three DTT fluid cultures reported an organism not found by either routine culture or CMg. It is unlikely these organisms originated from the actual prosthesis as they were not detected by CMg from the same sample. All three organisms were NAS so it is likely that they were skin contaminants introduced onto the prosthesis during surgery but present in insufficient numbers to be detected by CMg. If these cases where these three organisms not found by either routine culture or CMg were treated as negative, the sensitivity of CMg compared to DTT fluid culture would be much higher (92%).

In one case, an organism was detected by both culture methods but CMg was negative (DTT3 – zero reads of *P. aeruginosa* detected by culture). qPCR was used to test whether *P. aeruginosa* was present in both the depleted and non-depleted DTT fluid samples, but was negative, suggesting the cultured *P. aeruginosa* was due to lab contamination or was misidentified. This was investigated further when a clinical review was performed on this same patient in the calprotectin study (2.3.2) which concluded that the patient was not infected. It is curious that the same organism was cultured by both methods but not found by sequencing. A contamination event at the surgical site could affect both whole-prosthesis and PPT sampling methods, however, this contamination would be present in the DTT fluid and would be expected to have been detected by either CMg, qPCR, or both. The risk of contamination poses a significant challenge to clinicians when determining infections based purely on culture. This is of particular concern when the contaminant is a known pathogen e.g. *Pseudomonas* species which account for ~20% of Gram negative PJIs (Parikh and Antony, 2016). If the clinical review performed as part of the calprotectin study was accurate then all pathogens identified by DTT fluid culture, not considered to be likely contaminants, were detected by CMg.

In our study we did not detect any polymicrobial infections by sequencing. This is potentially concerning as polymicrobial infections are considered responsible for ~15% of PJIs (Tande and

Patel, 2014). However, while four cases in our study yielded multiple organisms reported by routine culture, the majority of these organisms were common lab contaminants. The exception to this was DTT27 in which both *S. aureus* and *P. mirabilis* were cultured but only *P. mirabilis* was found by sequencing and DTT fluid culture. It is encouraging that DTT fluid and CMg were concordant, however, as *S. aureus* is the most common single cause of PJI it is difficult to rule out as contamination (Tande and Patel, 2014). It is unclear if the report is of a genuine pathogen or if PPT samples were contaminated during collection or laboratory processing.

While four cases of polymicrobial infection were reported by routine culture, no cases were reported by DTT fluid culture, suggesting that either the reported organisms were laboratory contaminants or of organisms that were infecting the surrounding tissue but not attached to the prosthesis. It is therefore important to consider the performance of CMg compared to DTT fluid culture as a gold standard, as tests were performed on the same sample. Considering the organisms found by DTT culture which are potential contaminants the performance of CMg in this study is likely higher than reported, with the major discordant results resolved by qPCR/clinical review or attributed to contamination during sequencing.

3.4.5 Data analysis

For CMg studies there is a necessity to apply thresholds/cut-offs prior to/during data analysis to maximise sensitivity while preventing false-positive results to ensure an accurate diagnostic test. Various thresholds are often applied to CMg bioinformatics pipelines to remove low-quality reads, barcode crosstalk, potential misclassification of reads as well as contamination (Kunin et al., 2008; Salter et al., 2014). Appropriate cut-offs are method dependant with the number of reads expected differing depending on the sequencing technology used and host depletion achieved. Thoendel *et al.* applied a threshold of >10,000 reads and >80% of microbial reads for a significant result (Thoendel et al., 2018) which would not have been appropriate for our work as most positive samples did not generate >10,000 species specific reads for the identified organism. Noone *et al.* applied a threshold of 10-times greater read count of bacteria common to both a sample and its respective negative control for significance on results generated by nanopore (Noone et al., 2021).

This would have generated a lot of false positive results as samples were typically generating >10-fold more reads than negative controls for multiple species. Our cut-offs were chosen by comparing sequencing results to culture for the first samples of the MicroDTTect study. A cut-off for both total number of reads as well as proportion of microbial reads, as used by Thoendel *et al.*, strikes a good balance between specificity and sensitivity and is important for accurate pathogen identification.

Changing the thresholds to increase sensitivity is an option, however, this is likely to result in more false positives, reducing specificity. Further statistical analyses are often required to pick the most appropriate thresholds. Retrospectively lowering the threshold used for total species-specific reads in this study changed sample DTT26 from a false negative to a true positive without introducing any additional false positive results. These new thresholds generated from this derivation set of samples could be used on a future validation set as performed by Street *et al.* in their study (Street et al., 2017). Derivation data sets are important for CMg studies such as these to provide appropriate cutoff values for defining the performance of a test.

During data analysis a number of organisms were seen across the majority of samples. These included *P. acnes*, *E. coli* and *C. perfringens*. *P acnes* has previously been identified as a common contaminant when performing CMg on PJI samples as demonstrated by Street *et al.* (2017). The identification of *C. perfringens* was to be expected due to the use of PLC which was harvested from *C. perfringens* and should be categorised as a known contaminant of this method. The presence of *E. coli* reads is likely to be attributed to the "kitome" (bacterial DNA found in kit reagents) as recombinant *E. coli* strains were used for producing some of the enzymes required in the library preparation. Lowering thresholds would lead to false positive results, reporting these and other organisms. Negative controls can be used to both highlight and resolve contamination (Salter et al., 2014). One sequencing run was heavily contaminated with all six samples and both negative controls positive for *E. coli* above thresholds. Contamination was roughly proportional over all samples and negative controls on the run, at ~15% of total microbial reads. Subtracting *E. coli* reads equivalent to 15% of total microbial reads per sample resulted in concordance with routine culture results for 4/6 samples. Two samples could not be resolved using this approach, reporting false positive *E. coli* results. Unfortunately, there was not sufficient material remaining

from the samples to repeat the sequencing, which would be the best approach when significant contamination is observed in the negative control/s.

Microbial classification can be challenging, especially for closely related species in a genus or genera. Most metagenomic classifiers use *k*-mer based classification due to the speed at which results can be generated (Vervier et al., 2016). The length of *k*-mers used for analysis can impact the quality of data reported. Long *k*-mers may result in lower sensitivity as exact matches may not be identified, either due to sequencing errors or differences in the sequenced data, conversely short length *k*-mers can result in multiple possible matches per *k*-mer, potentially reducing specificity (Noé and Martin, 2014). A clear example of *k*-mer misclassification was found in DTT9, where sequencing reported a significant number of *S. aureus* reads in addition to the pathogen identified by both culture methods, *S. lugdunensis*. A qPCR investigation with an *S. aureus* specific qPCR assay confirmed that *S. aureus* was not present in the sample and that the result was likely an informatics error, significant *S. aureus* reads were not present in any other sample on the sequencing run ruling out barcode crosstalk or contamination. The percentage of total microbial reads fell under threshold, so *S. aureus* was not reported as significant. More work needs to be done to improve the specificity of *k*-mer based read identification tools (Manekar and Sathe, 2018), particularly if this approach is being applied to clinical samples.

The PJI nanopore CMg study by Noone *et al.* used a cut-off of >10 fold more reads than found in the negative control to be significant, leading to potentially false reporting of misclassified organisms (Noone et al., 2021). The authors report three cases where sequencing detected additional staphylococcal species to the one detected by culture, implying that sequencing was detecting polymicrobial infections missed by routine culture. The possibility that these reads were misclassified due to similarities between the species, as seen in our study, demonstrates that caution is required when interpreting CMg data. Ideally, discordant results such as additional detections should be confirmed by other methods such as specific probe-based qPCR, and accurate thresholds should be put in place to prevent reporting of misclassified reads. This could include implementation of *k*-mer alignment score thresholds (Charalampous et al., 2019), utilising more accurate read identification tools (Ye et al., 2019) and/or using curated microbial databases (Schlaberg et al., 2017).

3.4.6 Strengths of the MicroDTTect study

One of the main strengths of this study is the host DNA depletion levels achieved in sample processing. Depletion levels here are greater than any reported for depletion of PJI samples in the literature. Noone *et al.* report that despite sufficient depletion for rapid pathogen identification, the majority of sequenced reads were classified as human, although they do not report what their average depletion was (Noone et al., 2021). While this was also true for the majority of our samples (average 75% human reads), some samples had a higher proportion of microbial reads compared to human, with 98.79% microbial reads reported in one sample.

This was a prospective study, collecting and testing samples from all patients that consented, with no known sample type selection bias. Similar studies contain disproportionately large numbers of infected cases compared to aseptic loosening and wear damage, potentially biasing the accuracy of results, and missing the opportunity to detect culture negative infections in patients classified as aseptic. Samples were not frozen, as in other studies, avoiding any positive or negative effects of freeze thaw (Gunnarsdóttir et al., 2012; Morley et al., 1983). Freezing is not recommended when using differential cell lysis-based host DNA depletion, as this can lead to bacterial cell lysis and consequent DNA loss.

The CMg pipeline was capable of rapidly identifying organisms found by routine culture, as well as detecting additional organisms not found by routine methods (such as *S. pneumoniae*). Sensitivity is low when compared to culture but increases significantly when likely contaminants and clinical review is considered (100% compared to DTT fluid culture, 85% compared to routine culture).

3.4.7 Limitations of the MicroDTTect study

The study contains relative low sample numbers. While the study recruited more patients (n=42) than reported by Noone *et al.* (n=32) (2021), the numbers fall short of the larger studies performed by Street *et al.* (97) (2017) and Thoendel *et al.* (115) (2018). A larger validation study should be

pursued, potentially with some improvements to the depletion method to remove mitochondrial DNA and the potential inclusion of whole genome amplification.

The absence of polymicrobial detections within this study is a potential limitation, driven either by suboptimal thresholds or the absence of genuine polymicrobial infections tested in the study. Future work should include known polymicrobial infections, confirmed by both routine culture and qPCR to assess if these methods are capable of detecting polymicrobial infections, as has been demonstrated for LRTIs (Charalampous et al., 2019).

Despite attempting to reduce potential routes of contamination through application of the closed bag MicroDTTect system, both culture of the DTT fluid and sequencing were shown to be susceptible to contamination. Extra care should be taken with these procedures to minimise potential contamination events and appropriate thresholds must be applied to any sequencing results utilising this pipeline.

Antimicrobial susceptibility testing was not investigated during this study as it was believed that the sequencing data was not of significant breadth or depth to accurately call AMR genes. Future work should investigate if this could be possible, particularly if whole genome amplification was included to increase breadth and depth of coverage.

3.4.8 Future work

A limit of detection study should be performed to determine the analytical sensitivity of the pipeline. This work was planned but unfortunately was not completed due to time constraints and a limit on available clinical material to test.

The depletion method could be further optimised to improve mitochondrial depletion through the combination of multiple enzymes and/or detergents. Combining host cell lysis and DNase treatment in a single step as part of a ‘one-pot’ method could improve turnaround time and make the method simpler to use.

CMg on synovial fluid samples should be reattempted as they are an ideal sample type due to the less invasive nature of sampling, if collected as an arthroscopy, potentially guiding patient

management prior to the first surgical intervention. It is likely that a WGA step before sequencing would be required to enable pathogen identification in this low bacterial load sample type. It may be advantageous to implement this step for whole prosthesis too, as it may improve sensitivity and genome coverage for AMR detection. Additional steps such as filtering or diluting may improve pathogen identification from heavily infected samples.

Future work should include a clinical review of the MicroDTTect study participants, as in the calprotectin lateral flow study, to assess the sensitivity and specificity of these sequencing-based methods compared to clinical outcome, rather than culture-based methods which we know to be fallible.

Ideally a larger study would be performed, including a more comprehensive sample workup, with synovial fluid collected from every patient, on patients with mono- and polymicrobial infections, as well as patients diagnosed with aseptic loosening and wear damage. This study could use improved depletion and WGA. Comparing sonication with DTT to assess whether chemical or mechanical biofilm loosening is most suitable for diagnostic work would also be useful. Finally, qPCR should be used to investigate all discordant results between routine methods and CMg.

Chapter 4 – Pathogen biomarkers of infection

4.1 Introduction

As previously discussed (Chapter 1.8), it can be difficult to determine whether a commensal organism is causing an infection when isolated from a PJI sample. One way to differentiate if an organism is a sample contaminant or the cause of infection is to look for evidence that the bacterial cells have come from a biofilm. Cells isolated from a biofilm are likely to have been growing on the artificial surface of the prosthesis rather than on the skin, and as such causing PJI. By looking for biomarkers of biofilm growth, skin contaminants could be ruled out and only genuine PJI causing organisms reported.

4.1.1 Phenotype by random mutagenesis

Bacterial evolution and adaptation are naturally driven by mutagenesis. Through spontaneous mutations (Drake, 1991) or exposure to mutagens, (Muller, 1927) the DNA of an organism changes, resulting in new genotypes and conferring new phenotypes. These phenotypical changes can be detrimental to the organism, with either a loss of function or lethal effect; but can also result in a gain of function or a conditional benefit (Griffiths et al., 2000).

Genetic adaptation to viability in certain conditions, such as on a host surface or gaining a defensive mutation against antimicrobials or immune cells, will increase virulence (Beceiro et al., 2013; Siryaporn et al., 2014). Screening gene function against phenotype-driven mutagenesis is an effective method for identifying novel genes and pathways which are linked to a target phenotype (Brown and Nolan, 1998; Brown and Peters, 1996).

As biofilm formation is a virulence factor for pathobiont organisms that would be commensal when found outside of a joint, but pathogenic if found within a joint (Phillips and Schultz, 2012), identifying these genes through mutagenesis studies could yield targets for differentiating a pathogen from a contaminating commensal.

Previously, mutagenesis studies have been done by the use of chemicals (Auerbach, 1973) or radiation (Kodym and Afza, 2003). More recently, genome studies have been undertaken by directly introducing transposable genetic elements into the target organism, transposon mutagenesis. This chapter describes the application of transposon mutagenesis to staphylococci strains to generate mutant libraries for mutagenesis studies.

4.1.2 Transposon mutagenesis

Targeted mutagenesis to knock-out specific genes can be used to determine their function when host bacteria are cultured under specific conditions. However, this approach requires an initial hypothesis on the function of a specific gene. An alternate approach is to generate a library of random knockout mutants by introducing transposons, a transposable element of DNA, which can randomly insert into the host genome, resulting in either a deletion or altered expression of neighbouring genes (Chao et al., 2016). Phenotypic effects of these mutations can then be screened against different selection pressures for loss of function in the affected genes.

Transposons were discovered in the 1940s as a genetic regulatory mechanism in maize (Comfort, 2001) but have also been found in both prokaryotes and eukaryotes (Hayes, 2003). Transposon mutagenesis studies in prokaryotes commonly use the *mariner* family of transposon, originally found in Drosophila (Robertson, 1993); or the Tn5 family, discovered in *E. coli* (Berg et al., 1975).

Transposons are flanked by terminal inverted repeats which are recognised by their respective transposases. These transposases then cleave at these repeats facilitating insertion of the transposon into a random target site by strand exchange (Hayes, 2003).

As transposons insert randomly, the specific target site deletions need to be identified in order to locate the knock-out on the chromosome and assign phenotype changes to the loss of a gene. Signature tagged mutagenesis was a method originally used, combining DNA hybridisation with transposon mutagenesis, to identify mutants which survived a selection pressure (Hensel et al., 1995). However, the introduction of high-throughput sequencing allowed for collections of multiple mutants to be screened under a selection pressure simultaneously at a higher throughput,

revolutionising transposon mutagenesis studies (Chao et al., 2016). By sequencing a library of thousands of knockout mutants, following selective growth or permissive growth, then comparing the genome coverage of both sets and looking for areas of missing coverage, essential genes for that selective condition can be identified by absent knockouts – this process is known as Transposon Insertion Sequencing (TIS) (Figure 4.1). For a comprehensive history of transposon insertion sequencing refer to (Cain et al., 2020).

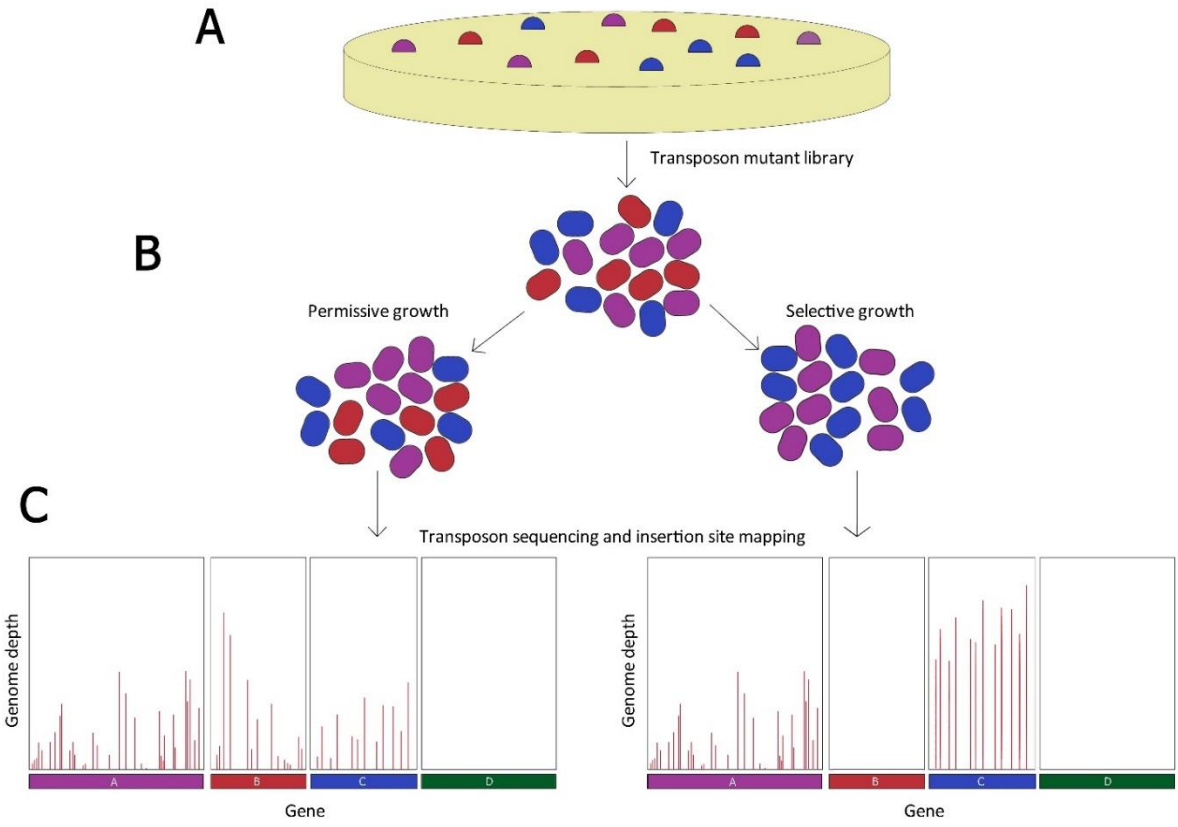

Figure 4.1 Overview of Transposon Insertion Sequencing. A. A library of transposon mutants generated by random insertion across the genome is constructed. Mutants are harvested and pooled for selection pressure studies; B. The pooled mutants are grown under the selection pressure being investigated, as well as without the selection pressure; C. DNA is extracted from any surviving mutants and sequenced. Insertion site frequency and fitness by relative abundance can be calculated for each growth condition tested; GeneA has insertions present under both growth conditions and in relatively similar abundance appearing to have no relation to the selection pressure; GeneB has insertions present under permissive growth but absent under the selection pressure, therefore the gene is essential for growth under this condition as deletion mutants did not survive; GeneC has insertions found at greater levels under biofilm conditions, so it appears to be beneficial to growth under the selective pressure used; GeneD has no insertions present in either condition because the gene was essential for growth under all conditions.

Four groups initially developed protocols for TIS to identify an essential gene list from their chosen organism. Goodman et al. developed insertion-sequencing (INSeq) to screen for genes required in a commensal gut bacterium, *Bacteroides thetaiotaomicron*, for establishment in the gut microbiota (Goodman et al., 2009). Using a *mariner* transposon, they generated a library of 35,000 unique insertion mutants identifying 325 genes essential for growth in rich media. They also characterised a vitamin B12 regulated pathway dependent on community composition where genes were essential under mono-colonisation.

Gawronski *et al.* developed high-throughput insertion tracking by deep sequencing (HITS) in a study attempting to identify *Haemophilus influenzae* virulence genes that improved survival in the lung (Gawronski et al., 2009). Using the same *Himar1 mariner* system as Goodman *et al.*, this study developed a library of 55,935 unique *H. influenzae* mutants identifying 358 essential genes under rich growth conditions. They also identified multiple genes with potential roles for survival during oxidative stress, nutrient limitation and anti-microbial interactions as potential virulence markers. They identified that these genes implicated phosphate uptake as a condition for pathogenicity. This demonstrates the potential use of transposon sequencing for identifying pathogenic bacteria from a clinical sample.

Van Opijnen *et al.* developed transposon insertion sequencing (Tn-Seq) to assess the impact of each gene on the fitness of *Streptococcus pneumoniae* (van Opijnen et al., 2009). Also using the *mariner* transposon, they reported a library containing 23,875 unique insertion sites and that 16% of the *S. pneumoniae* genome is essential for growth in rich media. Following their investigation into bacterial fitness by gene, they also applied Tn-seq to bacteria containing targeted deletions of carbohydrate metabolism genes. One target, *ccpA*, chosen due to its association with fitness and virulence, was shown to have 64 gene interactions identified by Tn-seq negative selection. This study demonstrated the potential for Tn-seq to not only analyse individual essential genes under chosen conditions, but also associated genes and regulatory networks within a bacterium.

Langridge *et al.* developed transposon directed insertion-site sequencing (TraDIS) to generate an essential gene list in *Salmonella enterica* serovar Typhi (Langridge et al., 2009). As opposed to the other three methods, TraDIS was initially developed using the bacterial Tn5 transposon. After

reporting 356 essential genes in rich media, Langridge et al. went on to identify 169 genes essential for growth in the presence of bile as a pathogenicity factor for S. Typhi. These genes could be future targets for antimicrobial therapies as well as providing a deeper understanding of the pathogen's disease cycle.

The bacterial mutant pool of 1.1 million transposon mutants contained 370,000 unique insertion sites, translating to an average of 80 insertions per gene. This high-level unique insertion density is important for the statistical classification of essential vs non-essential genes as more unique insertions provide more statistical points for essential gene calling. At an average of one insertion per 13 base pairs this library had far greater genome coverage than the other three initial approaches. A HITS *H. influenzae* library reported the next highest coverage at an insertion per 32 base pairs (Tn-seq – 1/91 bp, INSeq – 1/182 bp) (Gawronski et al., 2009; Goodman et al., 2009; Langridge et al., 2009; van Opijnen et al., 2009).

4.1.3 Bacterial transformations

Bacteria can take up new genetic elements by horizontal gene transfer in a number of ways. Natural competency was discovered in 1928 by Frederick Griffith when he noted that non-pathogenic bacteria could become pathogenic when exposed to heat-killed cells of a pathogenic strain (Griffith, 1928). Altering bacterial genomes by the introduction of DNA from lysed cells, bacterial transformation, has been used in countless studies, including characterisation of biofilm formation genes in *S. aureus* (Valle et al., 2007) and *S. epidermidis* (Conlon et al., 2004). However, the introduction of foreign DNA is not always easy. Gram-positive bacteria are more difficult to transform than Gram-negatives due to the increased complexity of the cell wall (Lin et al., 2010), and restriction modification (RM) systems which can further impede transformation by degrading incoming DNA.

RM systems, which have been found in around 90% of bacterial genomes, allow bacteria to distinguish between host chromosomal DNA and exogenous DNA (Vasu and Nagaraja, 2013). Using a methyltransferase, the RM system marks the DNA in a specific pattern. These methylated

sequences are recognized as self, while recognition sequences on DNA introduced to the cell lacking methylation are recognized as nonself and are cleaved by the restriction endonuclease (Vasu and Nagaraja, 2013). This system is presumed to have evolved as a defence mechanism against the introduction of foreign DNA during bacteriophage infection (Stern and Sorek, 2011). Depending on how efficient or specific the RM system is, introduction of DNA can be prevented from closely related species or even strains of the same species (Ando et al., 2000; Purdy et al., 2002; Wilson, 1991).

As all Staphylococci are Gram-positive, transforming NAS with a transposon to make a knock-out library is challenging. However, NAS are a crucial target for biofilm biomarkers in the context of PJI as NAS are responsible for 27% of reported PJI infections (Tande and Patel, 2014) while also being common skin commensals.

Staphylococci have previously been transformed in genetic studies by protoplast fusion, removing the cell wall before the introduction of a foreign DNA element to facilitate uptake into the cell (Götz et al., 1983, 1981). However, the use of protoplast transformation for staphylococcal studies is inefficient due to the high resistance of some NAS species, such as *S. epidermidis*, to lysostaphin, which is used to remove the cell wall (Schindler and Schuhardt, 1964).

For our study, we chose to use electroporation to generate cell competency. Electroporation is the process of subjecting cells to a high voltage electrical field which forms transient pores in the cell membrane, allowing DNA to pass into the cell (Powell et al., 1988). Electroporation has been used previously to develop a high-density transposon library in *S. aureus* consisting of over 690,000 unique insertion sites (Santiago et al., 2015). While multiple successful transposon libraries have been made in *S. aureus*, no high-density NAS transposon libraries have been reported with enough insertions per gene to get the unique insertion density required to determine any one gene as essential. A transposon library was generated using *Staphylococcus carnosus* (Krismer et al., 2012), however, this library only totalled 1,300 mutants and the study does not report the number of unique insertion sites. The genome of *S. carnosus* is around 2.6 megabases (Mb) (Müller et al., 2016) - if each mutant was generated by a unique insertion then there would only be one insertion per 2,035 bp, far below the coverage reported by the four initial TIS studies. In order to screen a

whole genome for gene function, theoretically at least one insertion would be required in each gene, however, only a subset of the pool is taken to assay in any experiment so multiple insertions per gene are required to classify a gene as essential per selective pressure tested. However, potential biomarkers have been found using poor coverage libraries; Wang *et al.* reported a *mariner* transposon library in *S. epidermidis* with similar mutant numbers (around 1,000) to the *S. carnosus* libraries. They found 12 mutants defective in biofilm formation, one of which was a mutant lacking a functional gene with previously unknown function characterised as encoding a stress response protein. Named *ygs*, this gene appears to influence biofilm development by PIA-dependent cell accumulation (Wang et al., 2011). Even with low mutant numbers they were able to identify and characterise a new biofilm biomarker.

4.1.4 Biofilm Biomarkers

While many pathways of biofilm formation are well characterized in controlled laboratory settings, such as *ica*-dependent biofilm formation (O'Gara, 2007), biofilm detection in clinical settings remains challenging (Azeredo et al., 2017). Biofilm associated infections are typically not confirmed until the device is explanted, as biofilms can produce occult/subclinical infections in which inflammatory symptoms are less pronounced than with acute infection (Donlan and Costerton, 2002). Although biofilms formed on prostheses cannot be directly sampled without surgical intervention, biofilm growth may produce unique molecules which could be detected using standard methods. Antypas *et al.* demonstrated that cellulose, found in the ECM component of biofilms, could be used as a biomarker for biofilms causing UTIs (Antypas et al., 2018). By analysing the spectral signature of cellulose from uropathogenic *E. coli*, they proposed that the detection of this biomarker could be used as a clinical test for biofilm driven UTI. Secor *et al.* reported a potential biomarker of biofilm production in *S. aureus*, aureusimine, which was being produced at elevated levels from *S. aureus* grown under biofilm conditions (Secor et al., 2012). This product could potentially be used as a biomarker for biofilm forming *S. aureus*, however, it requires further research to confirm and develop into a clinical assay.

This peptide, aureusimine, is only one biomarker from one staphylococcal species. The aim of this study was to generate full gene lists involved in biofilm formation from multiple NAS species. These biofilm biomarker lists could then be used to select targets to be included in diagnostic assays, distinguishing commensal NAS contaminants from NAS originating from biofilms and causing infection.

Generating NAS libraries with sufficient coverage to knock out every gene would make it possible to screen strains under defined biofilm promoting growth conditions and to characterise the genes involved in biofilm formation and maintenance under these conditions. These genes can then be investigated as potential biofilm biomarkers in the context of PJI. To achieve this, we developed methods using either a *Mariner* or Tn5 transposon construct for *in vivo* transposition using electroporation for transformation. This approach was applied to a collection of NAS strains stored in the NRP biorepository, consisting of environmental, commensal and clinical isolates that had previously been assessed for their biofilm forming ability under laboratory conditions.

4.2 – Methods

4.2.1 Plasmids used for electroporation

Early method development (reported in 4.3.1) for the electroporation protocol used a pT181cop608 plasmid backbone without a transposon (Addgene: Vector Database - pT181), conferring tetracycline resistance (Figure 4.2) to assess transformation efficiency of electrocompetent cell preparations.

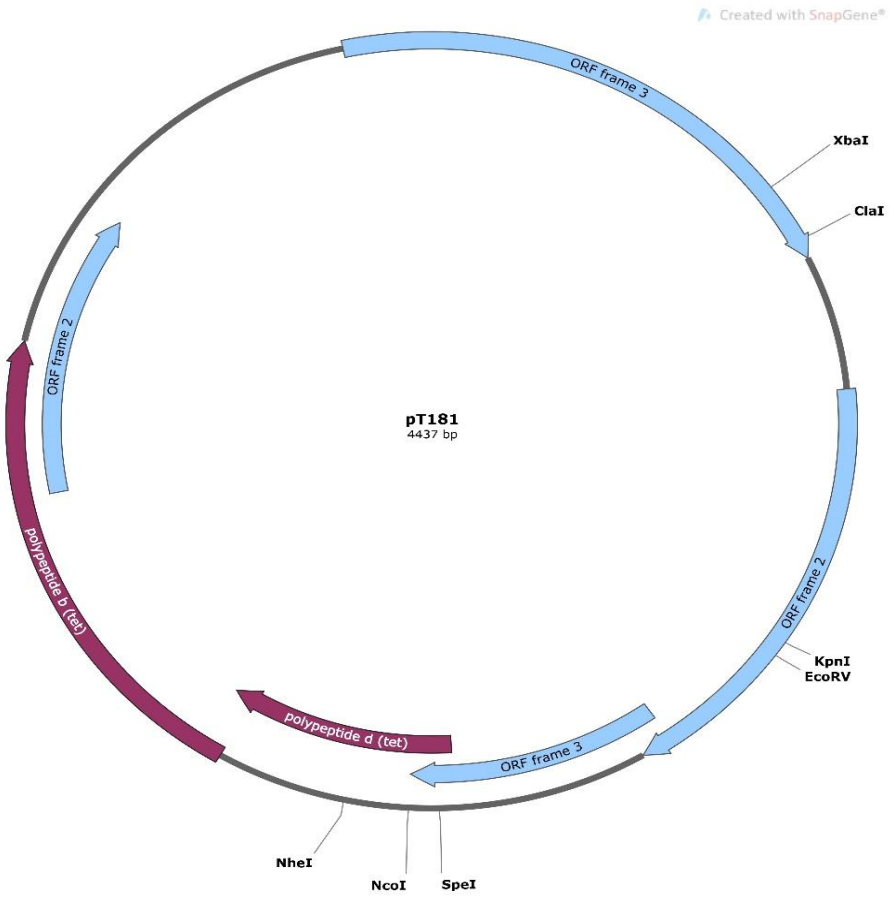

Figure 4.2. pt181cop68 plasmid backbone. Plasmid map of pt181 plasmid used for electroporation method development. This naturally occurring S. aureus plasmid encodes for tetracycline resistance through polypeptides b and d, DSM 4911 (DSMZ-German Collection of Microorganisms and Cell Cultures).

Later method development and the optimised electroporation method used pIMAY plamids containing transposons. *Mariner* or Tn5 were cloned into the multiple cloning site (MCS) using kpn1 and sma1 into pIMAY, is a temperature sensitive *E. coli*/*Staphylococcus* plasmid (Figure 4.3). Transposases were bought in as synthetic gene fragments.

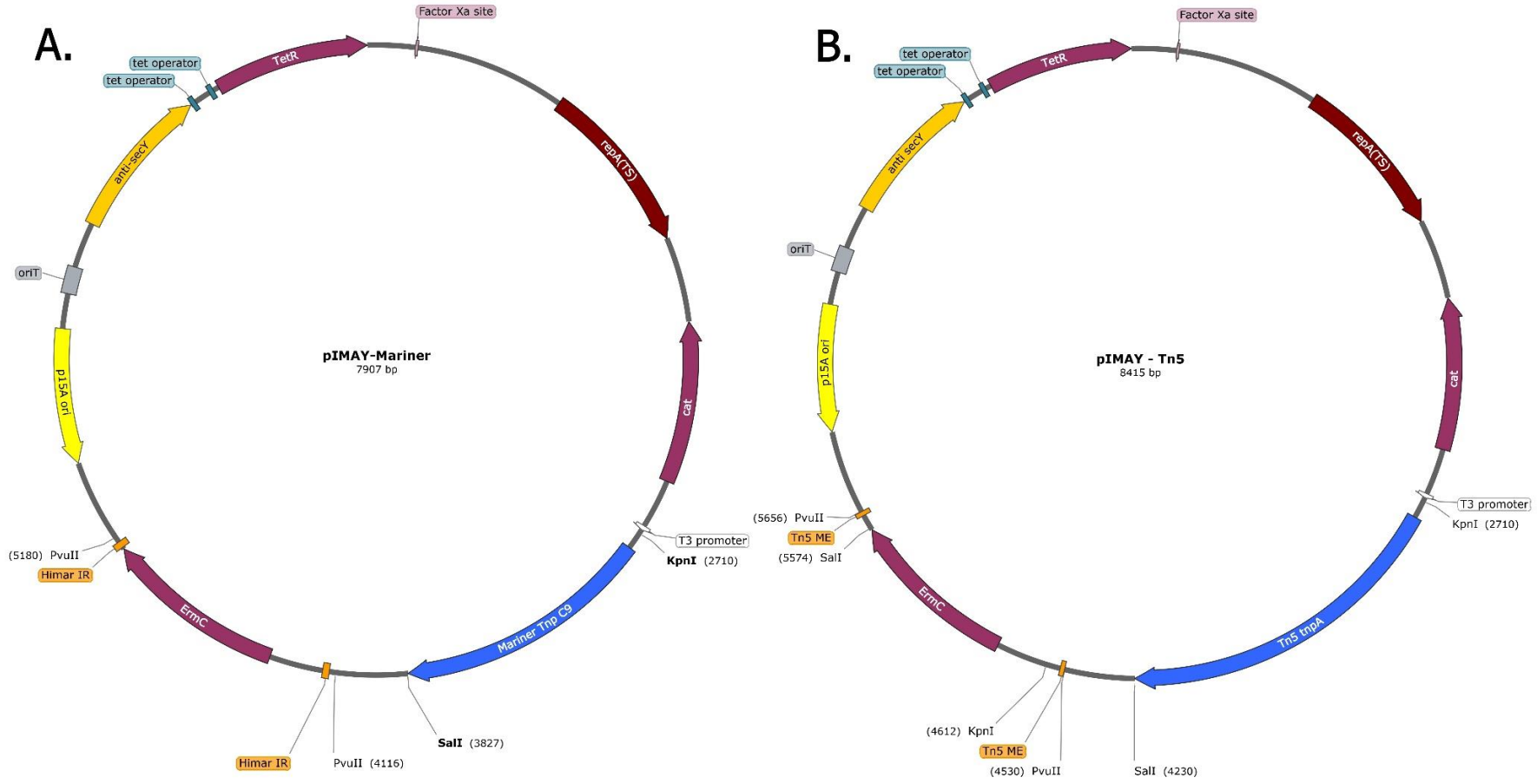

Figure 4.3 pIMAY transposon-loaded plasmids. Plasmid maps of pIMAY used for electroporation method development and transposon mutagenesis of NAS strains. A. pIMAY plasmid with *mariner* transposon, B. pIMAY plasmid with Tn5 transposon. The *E. coli*/staphylococcal plasmid contains a temperature-sensitive replication initiator (RepA) and the highly expressed cat gene (Phelp-cat) promoting chloramphenicol resistance (Monk et al., 2008). A kill-switch in the form of a tetracycline-inducible antisense secY region (anti-secY) for plasmid removal (Bae and Schneewind, 2006).

4.2.2 Optimised electroporation method

Electrocompetent cells were prepared using BHI broth as the growth medium; 10 ml of BHI was inoculated with 100 µl of overnight starter culture. The growth culture was incubated at 37ºC with shaking at 180 RPM until the culture had reached 0.5 $O.D._{600}$. The cells were then centrifuged for 5 minutes at 4,000 g and the supernatant was removed. Cells were resuspended in 10 ml of ice cold, sterile water, and then centrifuged again using the same conditions. The cell pellet was resuspended in 1 ml of ice-cold water and transferred to a microcentrifuge tube and centrifuged again. After this second wash with water, the cells were resuspended in 1 ml of ice cold 10% glycerol and washed once more. The cells were finally resuspended in ice cold 20% glycerol and aliquoted into 100 µl batches and frozen at -80ºC.

Frozen aliquots of electrocompetent cells were defrosted at room temperature for 5 minutes. Once thawed, 250 ng of either the Tn5 or Mariner pIMAY plasmid was added to each 100 µl aliquot. The cells were transferred into 1 mm gap electroporation cuvettes (ThermoFisher) and shocked at 2100 V, 100 Ohms, 25 µF (BTX Electro Cell Manipulator 360). Electroporation negative controls were performed by taking an additional aliquot of cells with plasmid but not applying the electric shock before recovery. Transformations were returned to microcentrifuge tubes and recovered in 1 ml of BHI broth at 28ºC with shaking at 180 RPM. After 4 hours the tubes were centrifuged for 1 minute at 10,000 RPM and all but 100 µl of the supernatant was discarded. The cells were resuspended and plated on Tryptic Soy Agar (TSA) (Sigma) containing 10 µg/ml erythromycin and 10 µg/ml chloramphenicol. The plates were incubated for four nights at 28ºC for NAS strains and two nights for *S. aureus*.

4.2.3 NAS transformations

Transformations were initially attempted on a set of 16 NAS strains obtained from the NRP biorepository (Set 1. Table 4.1) using the optimised electroporation method with both *mariner* and Tn5 loaded pIMAY plasmids that had been previously extracted from *S. aureus*.

Table 4.1 Set 1 of NAS strains tested with the optimised electroporation method

Strain ID	Species
15TB0712	*S. warneri*
15TB0951	*S. epidermidis*
15TB0956	*S. pasteuri*
15TB0964	*S. lugdunensis*
15TB0970	*S. lugdunensis*
15TB0993	*S. cohnii*
16TB0525	*S. xylosus*
16TB0536	*S. simulans*
16TB0553	*S. sciuri*
16TB0554	*S. vitulinus*
16TB0586	*S. caprae*
16TB0593	*S. saprophyticus*
16TB0611	*S. warneri*
16TB0615	*S. capitis*
16TB0623	*S. caprae*

Strain species designated by MALDI-TOF; all strains were electroporated with both pIMAY plasmids containing either the *mariner* or Tn5 transposons; all strains obtained from the NRP Biorepository.

Potential mutants were plated with their respective parent strains on a range of chromatic agar plates to visually compare phenotypes using mannitol salt agar, cystine lactose electrolyte deficient agar and Columbia blood agar. Cultures were incubated overnight at 37°C.

4.2.3.1 Plasmid DNA extractions

Plasmid extractions were performed to confirm the presence of the *mariner* or Tn5 plasmids within electroporated cells. Bacterial culture was grown in 10 ml BHI for 48 hours at 28°C. The dense culture was centrifuged at 4,000 g for 1 minute, the supernatant was discarded, and cells were resuspended in 250 µl P1 buffer (Qiagen). Bacteria were incubated overnight at 37°C with 25 µl of 0.5 mg/ml lysostaphin per 10 ml of original growth culture. Plasmid was purified from lysed cells using the QIAprep Spin Miniprep Kit (Qiagen) according to the manufacturer's instructions. In brief, bacteria are lysed under alkaline conditions, the lysate is then neutralised and adjusted to high-salt binding conditions on a silica membrane in a spin column. The columns are washed by high salt buffers and plasmid DNA is finally eluted in a low salt buffer. Plasmid concentrations

were measured by NanoDrop 2000 (ThermoFisher) according to manufacturer's instructions. In brief, 1 µl of sample was loaded onto the NanoDrop 2000 and analysed by the NanoDrop software (ThermoFisher). The machine was blanked with 1 µl of sterile media before each set of readings.

4.2.3.2 Plasmid PCR

Plasmid PCR was performed on extractions using MarSec or Himar (for *mariner* transposon) and ME (for Tn5 transposon) primers designed specifically for either the *mariner* transposon or the Tn5 transposon (Table 4.2). Plasmid PCR reactions were made up as described in Table 4.3.

Table 4.2 PCR primers

Primer set	Target	Forward primer (5'-3')	Reverse primer (5'-3')
MarSec	*mariner*	GGTCTCTAGACACATAGATG	GGTCTCTAGACGCGTATAAC
ME	Tn5	CTGTCTCTTATACACATCT	TGTCTCTTATACACATCT
Himar	*mariner*	CTTGCTCATAAGTAACGGTAC	GATTCGTCATGTTGGTATTCC

All primers designed in-house.

Table 4.3 Plasmid PCR conditions

Component	Final Concentration
PCR master mix (NEBNext High Fidelity 2x Master Mix)	1x
MarSec/ME Forward primers	0.25 µM
MarSec/ME Reverse primers	0.25 µM
Plasmid DNA	100 ng
Molecular grade water	Up to a total volume of 25 µl

The conditions for the run were an initial denaturation of 2 minutes seconds at 95ºC followed by 30 cycles of: 95ºC for 30 seconds, 55ºC for 30 seconds, 72ºC for 1 minute. The final extension period was 10 minutes at 72ºC.

4.2.3.3 Tapestation PCR product analysis

Plasmid presence in PCR products from potential mutant strains was confirmed by DNA gel electrophoresis using the Tapestation 2200 as previously described (3.2.6) using 2.5 µl of plasmid DNA.

4.2.3.4 Set 2 of NAS transformations

A second set of NAS strains (n=18), without innate erythromycin resistance, was investigated to potentially generate transposon transformants utilising a plasmid extracted from an earlier successful NAS transformation. Erythromycin MICs had been previously reported on the collected strains prior to this project (Table 4.4). Strains were spotted on a TSA plate containing 10 µg/ml chloramphenicol and another TSA plate containing 10 µg/ml erythromycin to check for resistance that might impede transposon mutant selection further down the line (Table 4.4).

Table 4.4 Set 2 of NAS strains set to be electroporated with the transposon plasmids extracted from *S. cohnii* strain 15TB0993.

Strain ID	**Staphylococcus strain**	**erythromycin MIC (µg/ml)**
15TB0715*	*S. simulans*	0.5
15TB0721*	*S. epidermidis*	0.25
15TB0726	*S. epidermidis*	<1
15TB0749*	*S. warneri*	0.5
15TB0765*	*S. pasteuri*	0.5
15TB0789	*S. epidermidis*	128
15TB0875*	*S. haemolyticus*	0.25
15TB0951	*S. epidermidis*	>256
15TB0994*	*S. epidermidis*	128
16TB0554*	*S. vitulinus*	4
16TB0596*	*S. saprophyticus*	64
16TB0600*	*S. epidermidis*	64
16TB0604	*S. epidermidis*	>256
16TB0606	*S. epidermidis*	>256
16TB0612*	*S. epidermidis*	32
16TB0623*	*S. caprae*	0.25
16TB0641*	*S. saprophyticus*	16
16TB0652*	*S. hominis*	8

Erythromycin minimum inhibitory concentration (MIC) data taken from our strain database; MIC experiments previously performed by Lizzie Gray; *Strains taken forward for electroporation following chloramphenicol and erythromycin susceptibility testing.

Strains which showed growth on 10 µg/ml chloramphenicol and/or had a previously reported erythromycin MIC of >256 µg/ml were excluded, and the remaining strains were prepared for electrocompetency as previously described. Strains were electroporated with the plasmids previously used, those extracted from *S. aureus* containing either the *mariner* or Tn5 transposon (*mariner* ex-*S. aureus* and Tn5 ex-*S. aureus*), as well as the two plasmids extracted from a previously successful transformation of the *S. cohnii* strain 15TB0993 (*mariner* ex-*S. cohnii* and Tn5 ex-*S. cohnii*).

Potentially successful transformants were again tested for phenotypic similarity to parent strains using the three chromatic identification agars, CLED, TSA and MSA as well as Tapestation of PCR products following plasmid extraction.

4.2.4 Transposon Library QC

The quality of successful transposition mutants was assessed through successful translocation of the transposon from the plasmid backbone into the nucleus of the transformant cells. Plasmid cells, those retaining the plasmid backbone, were removed by the application of heat. Transformants were plated on TSA containing 10 µg/ml erythromycin and chloramphenicol from glycerol stocks. The plates were incubated at 28ºC for 4 days to allow for transposition to occur. Streaks of colonies were taken from these plates and incubated in antibiotic-free BHI for 4 hours at 42ºC, preventing the replication of plasmid containing cells through the temperature-sensitive replication initiator (Figure 4.3).

Following high temperature incubation to reduce plasmid numbers, the cultures were titred through serial dilutions down to 10^{-7} and spotted on a panel of agar plates for colony counts. Titrations were spotted on TSA containing 1.25 µg/ml of anhydrous tetracycline (AHT) to select against the plasmid backbone through the anti-secY kill gene (Figure 4.3). Titrations were also spotted on TSA plates containing 1.25 µg/ml of AHT and 10 µg/ml erythromycin to select for any cell containing the transposon, and TSA plates containing 1.25 µg/ml of AHT and 10 µg/ml chloramphenicol to select for cells still containing the plasmid backbone. Comparative colony counts between the selection pressures were used to calculate the parent, mutant and plasmid cell populations to determine the success of transposition.

4.2.5 Transposon Library Confirmation

For each successful transformant from NAS set 2, four colonies were taken from the TSA plates supplemented with 1.25 µg/ml AHT and 10 µg/ml erythromycin and each used to inoculate a 2 ml

overnight culture of BHI at 28ºC with shaking at 180 RPM. A single colony of each parent strain was taken from the 1.25 µg/ml AHT plate for a transposon-negative control, starter cultures were prepared in parallel with the mutants in the same way.

4.2.5.1 gDNA extractions

Cultured cells were harvested for gDNA extractions using the ThermoFisher GeneJET Genomic DNA Purification Kit, according to the manufacturer's instructions for Gram-positive bacteria. In brief, 2 ml overnight cultures were harvested by centrifugation at 5,000 g, resuspended in 180 µl of digestion solution (ThermoFisher) at 56ºC for 30 mins, lysed with 200 µl of lysis solution (ThermoFisher), 5 ul of 0.5 mg/ml lysostaphin, and 400ul of 50% ethanol before being loaded onto the GeneJET DNA purification column (ThermoFisher). The columns were washed and eluted in 200 µl of Elution Buffer (ThermoFisher).

4.2.5.2 Illumina Sequencing

gDNA extractions from two starter colonies per *mariner* mutant were analysed by sequencing for presence of the *mariner* transposon and species confirmation. Illumina sequencing library preparation was performed using the Nextera XT DNA library preparation kit (Illumina) according to the manufacturer's instructions. In brief 1 ng of DNA per sample was added to the tagmentation reaction to cleave and tag the DNA for analysis. Tagmented DNA was then amplified and barcoded by PCR prior to pooling and analysis on the NextSeq with single end reading.

4.2.5.3 Bioinformatics

Analysis of the Illumina sequencing data was performed by Lisa Crossman, a senior bioinformatician at UEA. Species identification was performed using MiniKraken (Wood and Salzberg, 2014). Transposon presence was investigated by aligning the reads to the wild-type *mariner* sequence using Burrows-Wheeler Aligner.

4.2.5.4 Colony PCR

Colony PCR was performed to confirm the presence of the transposon within strains where the transposon was not identified by sequencing. A single colony was taken from the same plates used to prepare gDNA extractions from and added to 10 µl of nuclease-free water in a microcentrifuge tube. The tubes were incubated for 10 minutes at 95ºC to lyse the cells. 5 µl of this lysed cell solution was used to prepare colony PCR reactions as described in Table 4.5.

Table 4.5 Colony PCR conditions

Component	**Final Concentration**
PCR master mix (NEBNext High Fidelity 2x Master Mix)	1x
Himar/ME Forward primers	0.25µM
Himar/ME Reverse primers	0.25µM
Colony suspension	5 µl
Molecular grade water	Up to a total volume of 25 µl

The run conditions were an initial denaturation of 2 minutes at 95ºC followed by 25 cycles of: 95ºC for 30 seconds, 53 ºC for 30 seconds, 68 ºC for 1 minute. The final extension period was 10 minutes at 68 ºC. Colony PCR products were analysed by Tapestation as previously described.

4.2.6 Transposon Library Scale-Up

The optimum erythromycin concentration for selection against parent cells within each of the four transposon libraries was determined by plating out each mutant library, alongside each respective parent strain, on a series of TSA plates containing 0 µg/ml, 2 µg/ml, 4 µg/ml, 8 µg/ml, 16 µg/ml, 32 µg/ml, 64 µg/ml, 128 µg/ml to 256 µg/ml of erythromycin. The optimum erythromycin concentration for library scale-up was determined as the first concentration at which the parent strain was unable to grow while facilitating mutant growth.

Plasmid removal for library scale-up was performed by spreading mutants from glycerol stocks on TSA plates containing 12, 16 and 24 µg/ml erythromycin with 10 µg/ml chloramphenicol and incubated over 4 nights at 28ºC to allow for transposition. The plates were harvested by washing the surface with 3 ml of BHI and scraping the colonies into 50 ml centrifuge tubes. The cells were centrifuged at 5,000 g for 4 minutes, the supernatant was removed, and the cells resuspended in 3 ml BHI. A sample of each culture was diluted 1/100 with BHI broth to take an $O.D._{600}$ measurement within quantifiable range. The readings were then used to calculate the volume of starter culture required for a final $O.D._{600}$ of 0.2 in 10 ml of fresh BHI. At this point, two sets of each mutant were prepared to compare the effect of temperature during heat-treatment for the removal of plasmid cells. One set of each erythromycin concentration (12, 16 and 24 µg/ml) was incubated at either 37ºC or 42ºC for two to three generations to reduce the percentage of cells in the culture containing the heat sensitive plasmid. When grown, the cells were centrifuged at 4,000 g for 5 minutes and resuspended in 10% glycerol then frozen at -80ºC.

Following plasmid removal, the cell cultures were titred and plated onto TSA containing either AHT 1.25 µg/ml or AHT 1.25 µg/ml and erythromycin 12 µg/ml and incubated overnight at 37ºC (for the 37ºC set) or 42ºC (for the 42ºC set) to calculate the volume of inoculum required for 20,000 mutants per plate scale-up by colony count. Two sets of 30 plates of TSA with each antibiotic incorporation set (AHT 1.25 µg/ml with 12 µg/ml erythromycin, AHT 1.25 µg/ml with 16 µg/ml erythromycin and AHT 1.25 µg/ml with 24 µg/ml erythromycin) were each inoculated with 20,000 mutants. Each set of plates was incubated overnight at either 37ºC or 42ºC to reach 20,000 mutants per plate.

The scale-up plates were visually inspected for any signs of contamination. Only those plates which showed unity of colony morphology and colour were harvested, any others were discarded. The plates were washed with 3 ml of BHI and colonies from each batch were pooled. The pooled libraries were then centrifuged at 4,000 g for 5 minutes and resuspended in 10% glycerol. Quality control titre plates were made for each library with a set of three antibiotic conditions: TSA with 1.25 µg/ml AHT only, TSA with 1.25 µg/ml and 12/16/24 µg/ml (respective to scale up condition) erythromycin, TSA with 1.25 µg/ml AHT and 10 µg/ml chloramphenicol. The concentrations of AHT and erythromycin for each plate used were the same as the antibiotic concentration used in

the scale up plates from which the library was taken. The results from these quality control plates were used to calculate the composition of each harvested library.

4.3 – Results

4.3.1 Electroporation method development

Previous transformations of NAS attempted by others in the laboratory had yielded low efficiency (CFU/µg of plasmid) results. As such, we set about comparing various conditions for both the preparation of electrocompetent cells, and the post-electroporation recovery of cells, to develop a method to produce higher yields of transformants. A screen of competent cell preparation conditions was performed, investigating both the broth used as a growth medium, and the culture density to which the cells were grown.

Four *Staphylococcus* strains, two *S. aureus* (DSM-26309 and DSM-4910), an *S. epidermidis* (DSM-28319) obtained from the DSMZ collection and an *S. lugdunensis* (16TB0964) obtained from the NRP Biorepository were used to optimise an electroporation protocol based on methods previously reported by Cui *et al.* (2015). The initial optimisation was the growth medium and culture densities used for electrocompetent cell preparation. Electrocompetent cells were prepared by inoculation of a single colony into 10 ml of Tryptic Soy Broth (TSB) (Sigma), Brain Heart Infusion (BHI) broth (Sigma) or Iso-Sensitest broth (ThermoFisher). Cultures were incubated overnight at 37ºC with 180 RPM shaking. Then 100 µl of the overnight culture was used to inoculate three fresh 10 ml aliquots of the same broth type to be grown to different culture densities. These cultures were incubated again at 37ºC with 180 RPM shaking until they had reached an $O.D._{600}$ of 0.3, 0.5 and 0.9 respectively. Optical density was measured by spectrophotometry using 1 ml cuvettes and (ULTROSPEC® 10 Cell Density Meter), cultures that reached the desired density were removed from incubation and placed on ice to prevent further growth. Cells were centrifuged for 5 minutes at 4,000 g and the supernatant was removed. The cells were then resuspended in 10 ml of ice cold, sterile water, and then centrifuged again using the same conditions. The cell pellet was resuspended in 1 ml of ice-cold water and transferred to a microcentrifuge tube and centrifuged again. After this second wash with water, the cells were resuspended in 1 ml of ice cold 10% glycerol and washed once more. The cells were finally resuspended in ice cold 20% glycerol and aliquoted into 100 µl batches and frozen at -80ºC.

Frozen aliquots of electrocompetent cells were defrosted at room temperature for 5 minutes. Once thawed, 5 ng of pT181cop608 plasmid backbone without a transposon (Addgene: Vector Database - pT181), conferring tetracycline resistance (Figure 4.2), was added to each 100 µl of cells and transferred into 1 mm gap electroporation cuvettes (ThermoFisher). Electroporation was performed at 2100 V, 100 Ohms, 25 µF (ECM 630 Electro Cell Manipulator, BTX Harvard Apparatus). Electroporation negative controls were performed by taking an additional aliquot of cells with plasmid but not applying electric shock before recovery. Following electroporation, cells were recovered in 1 ml of Iso-Sensitest broth at 37ºC with 180 RPM shaking for 2 hours and plated on Iso-Sensitest agar containing 10 µg/ml tetracycline, then incubated overnight at 37ºC. The colonies present on agar recovery plates containing tetracycline were counted for each growth condition (Table 4.6).

Table 4.6 Transformation efficiency of electrocompetent cell preparations using different growth conditions

Medium		**Iso-Sensitest**			**TSB**			**BHI**		
O.D.$_{600}$		**0.3**	**0.5**	**0.9**	**0.3**	**0.5**	**0.9**	**0.3**	**0.5**	**0.9**
***S. aureus* DSM-26309**	**[1]Background (CFU)**	250	400	0	50	750	50	25	200	100
	[2]Electroporation (CFU)	150	350	100	3200	750	100	3200	200	10
	[3]Efficiency (CFU/µg)	0	0	$2x10^4$	$6.3x10^5$	0	$1x10^5$	$6.35x10^5$	0	0
***S. aureus* DSM-4910**	**[1]Background (CFU)**	2	10	20	40	-	7	7	4	3
	[2]Electroporation (CFU)	20	2000	500	2400	-	1800	2800	1600	1000
	[3]Efficiency (CFU/µg)	$3.6x10^4$	$3.98x10^5$	$9.6x10^4$	$4.72x10^5$	-	$3.59x10^5$	$5.59x10x10^5$	$3.19x10^5$	$1.99x10^5$
***S. epidermidis* DSM-28319**	**[1]Background (CFU)**	0	0	0	0	0	-	0	0	-
	[2]Electroporation (CFU)	1	45	12	8	40	-	10	0	-
	[3]Efficiency (CFU/µg)	$2x10^2$	$9x10^4$	$2.4x10^4$	$1.6x10^4$	$8x10^4$	-	$2x10^4$	0	-
***S. lugdunensis* 16TB0964**	**[1]Background (CFU)**	0	0	-	0	0	-	0	0	-
	[2]Electroporation (CFU)	1	134	-	1	1	-	1	110	-
	[3]Efficiency (CFU/µg)	$2x10^2$	$2.68x10^4$	-	$2x10^2$	$2x10^2$	-	$2x10^2$	$2.2x10^4$	-

[1]Background count CFUs from a tetracycline loaded agar plate inoculated with parent cells, not electroporated with the transposon plasmid; [2]Number of CFUs present on Iso-Sensitest agar plate containing 10 µg/ml tetracycline, after electroporation with pT181cop608 plasmid; [3]Transformation efficiency calculated as CFUs per µg of plasmid used (5ng used); results marked (-) indicate that the cells did not grow to the target O.D.$_{600}$ within the time constraints of the experiment and as such were not tested with electroporation.

In this experiment, *S. aureus* was more readily transformable than the *S. epidermidis* or *S. lugdunensis* strains tested. The electroporation-negative control plates showed that the *S. aureus* strains either had background resistance to tetracycline or were able to take up the plasmid without the pore opening effect of electric shock. *S. aureus* strain DSM-26309 showed considerably more background growth (mean 61.4% of test plate growth; range 0% - 100%) on negative control plates than the other *S. aureus* strain, DSM-4910, which only showed 2.1% background growth (range 0.25% - 10%). The non-aureus strains however, showed 0 CFU on any negative control plates, indicating that electroporation was necessary for transformation with this plasmid. Results marked '– ' in Table 4.6 did not grow to target optical density within the time constraints of the experiment were not electroporated.

The non-aureus strains transformed with highest efficiency when grown to $O.D._{600}$ 0.5 in every broth, with the exception of the BHI 0.5 transformation of the *S. epidermidis* strain, DSM-28319, which yielded no colonies. Iso-Sensitest was the optimal media for the NAS strains at $O.D._{600}$ 0.5, followed by either TSB or BHI depending on the strain. *S. aureus* transformed optimally after preparation in BHI at $O.D._{600}$ 0.3, closely followed by TSB at the same $O.D._{600}$.

With *S. aureus* transforming at a relatively high efficiency, having used *S. aureus* as a positive control for transformation with the pt181cop608 plasmid, focus shifted onto transforming NAS strains with NAS-specific media. A larger plasmid is likely to transform less efficiently than a smaller one (Hanahan, 1983). As such, the transformation efficiency for NAS needed to be improved before attempting to transform strains with the larger, transposon loaded, pIMAY plasmid (Figure 4.3). Traditionally, two defined media, B broth (Augustin and Götz, 1990) and B2 broth (Schenk and Laddaga, 1992), have been used in the transformation of NAS. Electrocompetent cells were prepared as before using B, B2 and Iso-Sensitest broths (previously the most efficient in our hands), at both 0.3 and 0.5 $O.D._{600}$. and electroporated using the same conditions with the pIMAY plasmid.

This experiment showed that B-broth yielded higher efficiency transformations for the *S. epidermidis* strain, but that Iso-Sensitest was better for the *S. lugdunensis* strain (Table 4.7). B2 broth was a poor growth medium for *S. lugdunensis*, with the cultures not achieving densities of

O.D.$_{600}$ 0.3 within the time frame of the cell preparation. While the *S. epidermidis* strain did grow and was prepared for electroporation, these were unsuccessful. The B broth experiments showed that, consistent with the previous experiment, an O.D.$_{600}$ of 0.5 yielded more transformants (39 CFUs) than O.D.$_{600}$ 0.3 (4 CFUs) for these NAS. The transformation efficiencies for the Iso-Sensitest preparations were much lower than in the previous screen, roughly 10-fold less efficient for *S. epidermidis* and 20-fold less efficient for *S. lugdunensis*. As B broth was only an improvement for the *S. epidermidis* strain (DMS-28319) in this experiment, and less efficient than broths in the previous experiment, it was not taken forward as the optimum growth medium. B2 broth was discounted for being both a poor growth medium and showing no transformants in the cell preparations that did grow. BHI was therefore chosen to be the standard growth medium going forward as it was one of the top two broths for every tested strain, with the exception of *S. epidermidis* DSM-28319.

Table 4.7 Electroporation efficiency with NAS test strains grown in B and B2 broth

		***S. epidermidis* strain DSM-28319**		***S. lugdunensis* strain 16TB0964**	
Medium	**O.D.$_{600}$**	**CFU**	**Transformation efficiency**	**CFU**	**Transformation efficiency**
Iso-Sensitest	**0.5**	4	$8x10^2$	6	$1.2x10^3$
B	**0.3**	4	$8x10^2$	0	0
	0.5	39	$7.8x10^3$	1	$2x10^2$
B2	**0.3**	0	0	-	-
	0.5	0	0	-	-

Transformation negative control plates showed 0 CFU for all conditions; efficiency calculated as CFU per µg of plasmid used (5 ng).

One commonly used method for improving the efficiency of plasmid transformations is heat-shock. As with the shock from electroporation, heat-shock stresses the cell wall in order to open pores for the plasmid to move through (Panja et al., 2008). To assess if heat-shock would be compatible with this electroporation method, two electrocompetent cell preparations made from *S. aureus* (DSM-

26309) were transformed, in parallel, with the pIMAY plasmid (Figure 4.4), by adding an incubation step following addition of 5ng of plasmid to electrocompetent cells at 55ºC for 1 minute prior to electroporation. Heat shock negative controls were processed without additional incubation.

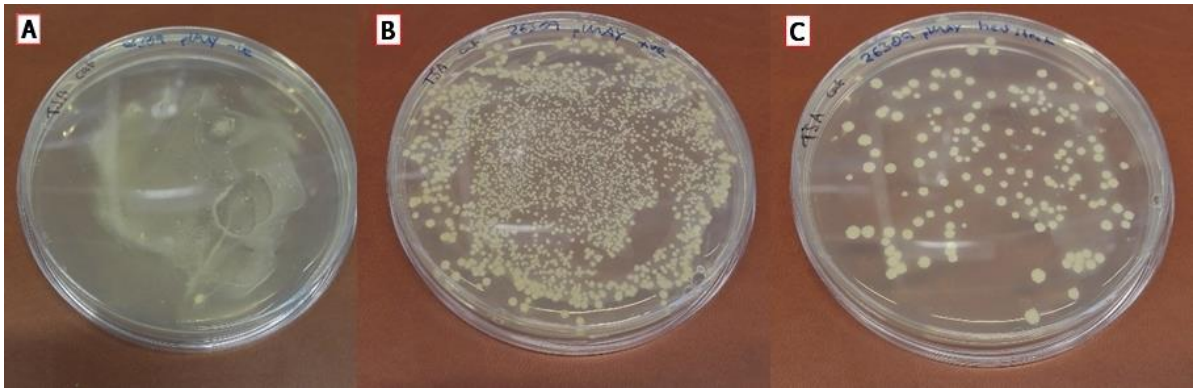

Figure 4.4. Electroporation with heat shock step. *S. aureus* strain DSM-26309 transformed with 5ng of pIMAY plasmid; A – No electroporation negative control; B – electroporation with no heat shock treatment; C – electroporation with heat shock treatment (1 minute at 55ºC).

The heat-shock plate shows visibly fewer colonies than the standard procedure, with 15-fold less efficient transformation (Table 4.8). This showed that any benefit to plasmid uptake by the shock is vastly outweighed by damage caused, killing the majority of the cells. Due to the loss of efficiency conferred by heat-shock, it was not added to the electroporation method. A lower temperature may have been more successful, but this was not investigated further.

Table 4.8 Transformation efficiency of *S. aureus* with heat shock.

Condition	**No electroporation negative control**	**Electroporation**	**Electroporation + Heat shock**
Colony count (CFU)	0	2522	162
Efficiency (colonies per µg plasmid)	0	5.04×10^5	3.24×10^4

S. aureus strain DSM-26309 transformed with 5 ng of pIMAY plasmid.
Heat shock performed at 55ºC for 1 minute.

Finally, the effect of antibiotics in the recovery media was tested. Traditionally, antibiotics are left out of the recovery media to allow time for the cell to transcribe the new DNA and produce the resistance proteins necessary to protect the cell (Augustin and Götz, 1990; Cui et al., 2015; Löfblom et al., 2007) . However, when under stress, cells can eject large unused plasmids to focus on survival (Millan and MacLean, 2019). The shock from electroporation could potentially encourage the cells to reject the resistance plasmid when the relevant antibiotic is not present, as translating the resistance genes would be a waste of energy when recovering from shock. The effect of antibiotics in the electroporation recovery step was tested using *S. aureus* DSM-26309 electroporated with 250 ng of pIMAY plasmid. Following electroporation, one aliquot of cells was recovered as previously described in 1 ml of Iso-Sensitest broth at 28ºC with 180 RPM shaking for 4 hours prior to plating on antibiotic permeated agar, a second aliquot was recovered in 1 ml of Iso-Sensitest broth containing 10 µg/ml chloramphenicol and 10 µg/ml erythromycin.

These initial transformations with the *S. aureus* strain showed that cells were able to be transformed with the pIMAY plasmid. The conferred resistance to chloramphenicol indicated uptake of the plasmid as the resistance gene is located on the plasmid backbone and the resistance to erythromycin confirmed the presence of the transposon construct within the plasmid. While the presence of antibiotics in the recovery media does not prevent the transformants from growing, the number of CFUs on the recovery plates showed that there was a drastic reduction from those electroporations recovered in antibiotic-free media (Table 4.9). As with heat-shock, the potential gain was outweighed by the damage done to the cells and was not pursued further.

Table 4.9 Efficiency of transformations recovered in antibiotic-containing or antibiotic-free media.

		Antibiotic-present recovery	Antibiotic-free recovery
***Mariner* plasmid**	**CFU**	39	1896
	Efficiency	7.8	$3.79x10^2$
Tn5 plasmid	**CFU**	4	448
	Efficiency	0.8	89.6

Colonies counted per after transformation of *S. aureus* DSM-26309 with 250 ng pIMAY plasmid containing either the *mariner* or Tn5 transposon construct; transformants were recovered post-electroporation in BHI or BHI containing 10 µg/ml chloramphenicol and erythromycin.

4.3.2 Transforming non-aureus Staphylococci

With the electroporation developed sufficiently to facilitate the introduction of transposon plasmids into *S. aureus*, the project moved on with the aim of transforming a NAS strain for transposon library generation. A set of 16 NAS were prepared for electroporation by the optimised protocol (Table 4.1) and electroporated with the two transposon mutagenesis plasmids, *mariner* and Tn5 (Figure 4.3).

Of the 16 tested strains, only one was successfully transformed with the tested plasmids, *Staphylococcus cohnii* strain 15TB0993. This strain produced five *mariner* transformation colonies (Figure 4.5a), and 14 colonies on the Tn5 recovery plate (Figure 4.5c). While there were no colonies on the negative control plate for the Tn5 transformation, one colony was present on the *mariner* control (Figure 4.5b). The observed colony did not share the same morphology with the transformed colonies, appearing grey as opposed to white and dull rather than shiny. As such, this colony was more likely to be a result of contamination rather than a spontaneous mutant or resistant parent as a colony of the same strain would be expected to show similar morphology. To confirm plasmid-acquired resistance of all the colonies that grew, they were re-streaked on fresh TSA plates containing chloramphenicol and erythromycin (results not shown). The re-plated colonies from the two positive plates grew well confirming antibiotic resistance, while the re-streaked colony from the *mariner* negative plate did not grow, suggesting it was a contaminant rather than a spontaneous mutant or resistant parent.

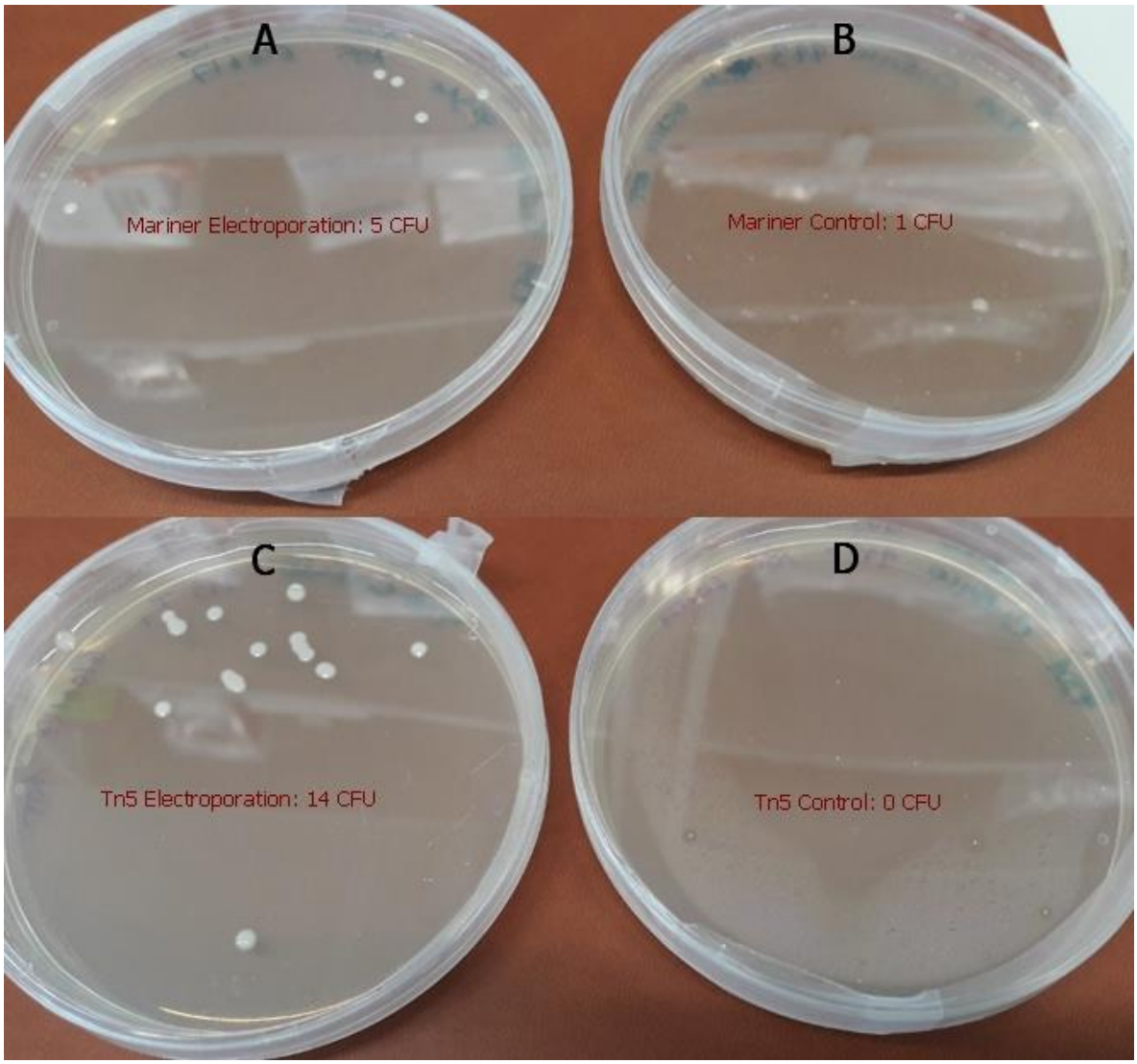

Figure 4.5. *Staphylococcus cohnii* transformations. *Staphylococcus cohnii* strain 15TB0993 electroporations;
A – Electroporated with *mariner* plasmid; B – *Mariner* electroporation control;
C – Electroporated with Tn5 plasmid; D – Tn5 electroporation control.

To ensure that the colonies were true transformants of the expected species, and not contaminants with the expected resistance pattern, colonies from the transformation plates were streaked, alongside the non-transformed parent strain, on a set of chromatic identification plates.

The parent and mutant colonies had the same visible phenotypes on each of the three ID plates (Figure 4.6), suggesting that the mutant colonies were likely the same species as the parent strain, however, the plasmid had to be confirmed as the source of the resistance.

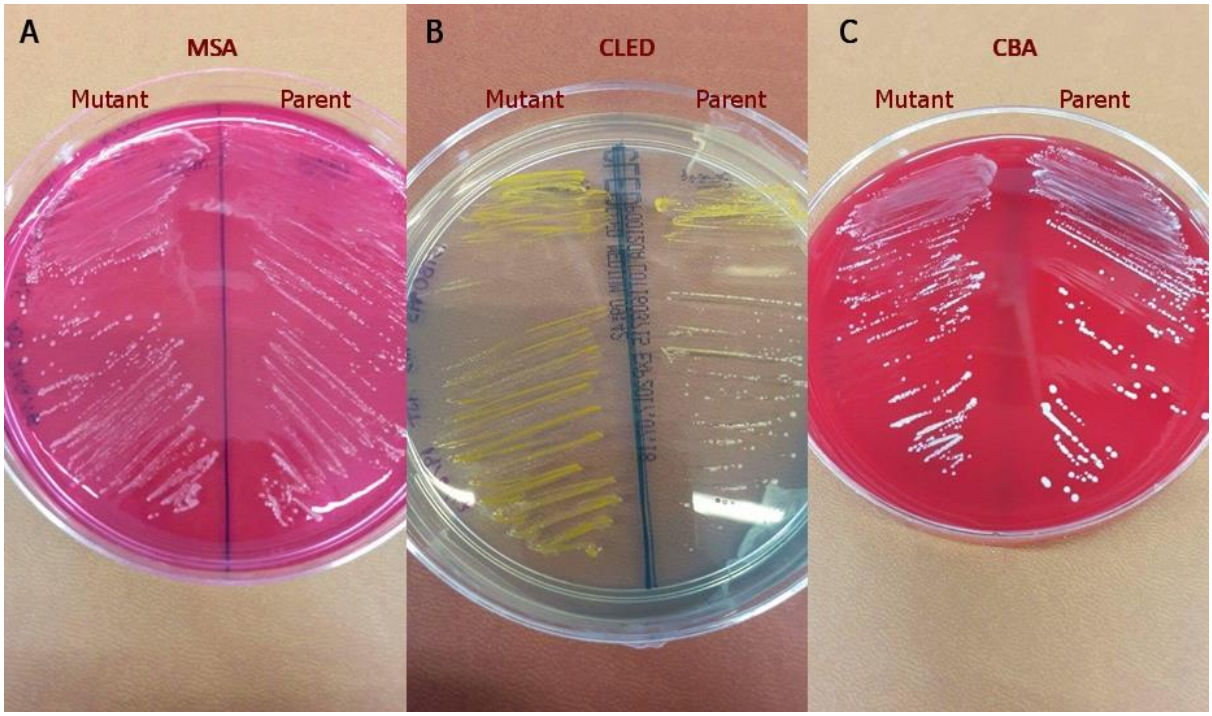

Figure 4.6. 15TB0993 parent and electroporation mutant strains on chromatic ID plates. Tn5 mutant 15TB0993 streaked on the left side of each plate and untransformed parent streaked on the right; A – MSA (Mannitol Salt Agar); B – CLED (Cysteine Lactose Electrolyte Deficient Agar); C – CBA (Columbia Blood Agar)

Plasmid DNA extractions were performed on both mutant strains, along with the parent strain as a control (4.2.3.1) and PCR with primers specific to the transposon constructs was used to confirm the plasmid's presence (Table 4.2). PCR products were analysed using the Tapestation (4.2.3.3) alongside water-negative controls (Figure 4.7). No bands appear in either of the negative controls (B1 and A2). Lanes E1 and F1 contained the positive control, previously transformed *S. aureus* strains containing the Tn5 and *mariner* plasmids. The *S. cohnii* mutants both showed a matching band to their equivalent positive controls. The *mariner* mutant in lane G1 has a clear band around the 1,500 bp mark, while the Tn5 mutant in lane H1 shows a similarly faint band to its positive control at approx. 2000bp. Despite the smearing in the Tn5 PCR lanes, the Tapestation software identified a band. These bands are not found in either of the parent controls confirming the transposon was not already present within the strain and was successfully introduced by electroporation.

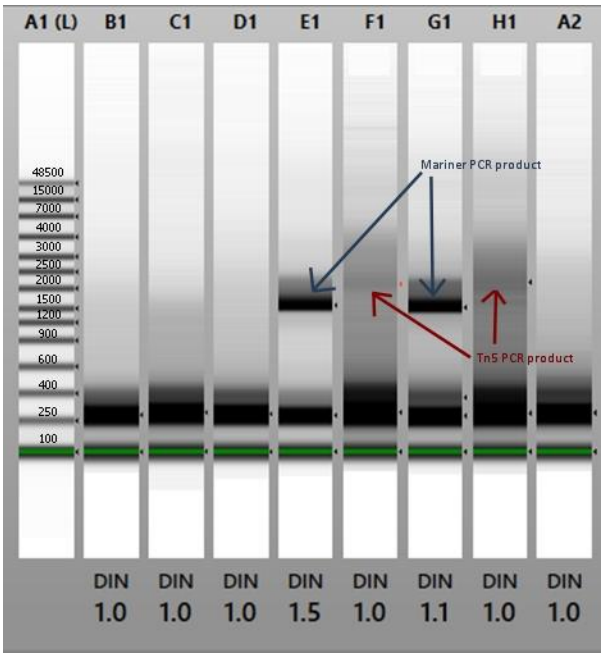

Figure 4.7. Plasmid PCR products extracted from 15TB0993 transformed with *mariner* and Tn5 plasmids. From left to right; (A1) ladder, molecular weight (bp), (B1) water control with Tn5 primers, (C1) 15TB0993 parent strain with *mariner* primers, (D1) 15TB0993 parent strain with Tn5 primers, (E1) DSM-26309 aureus control with *mariner* plasmid and primers, (F1) DSM-26309 aureus control with Tn5 plasmid and primers, (G1) 15TB0993 transformed with ex-*S. aureus mariner* plasmid with *mariner* primers, (H1) 15TB0993 transformed with ex-*S. aureus* Tn5 plasmid with Tn5 primers, (A2) water control with *mariner* primers.

4.3.3 Transformation with a passaged plasmid

As we had no success transforming any of the NAS apart from *S. cohnii* strain 15TB0993 with the S. aureus plasmids, we decided to test whether the plasmids could be successfully transformed into other NAS after passage in *S. cohnii*. The rational for this approach is that bacteria add epigenetic signatures (methylation) to plasmids and when a plasmid has a signature unrecognised by its host, the plasmid can be degraded. We wanted to test whether using the plasmids with the *S. cohnii* methylation pattern (a NAS) rather than the *S. aureus* pattern, would transform more readily into other NAS, as Augustin and Götz succeeded in transforming three NAS strains with a *S. aureus* plasmid isolated from *S. carnosus* (Augustin and Götz, 1990). A set of 18 potential NAS targets, three of which had been unsuccessfully electroporated previously with the *S. aureus* plasmids, were tested (4.2.3.4).

The innate resistance to erythromycin of *S. cohnii* strain 15TB0993 meant that it was not suitable for developing an insertion library as the erythromycin marker on the transposon could not be used

to select for transposon mutants against parent-type cells. This new set of strains was tested for innate resistance to both erythromycin and chloramphenicol so that successfully transformed strains could be taken forward. The five strains with the highest recorded erythromycin MIC (as per our database): 15TB0789, 15TB0951, 15TB0994, 16TB0604 and 16TB0606 all showed growth on the erythromycin plates (Figure 4.8a and c). However, none of the other strains, some of which had recorded MICs above 10 µg/ml, grew. These five strains were discarded. 15TB0726 showed clear growth on the chloramphenicol plate (Figure 4.8d) and was also discarded. The remaining 12 strains were electroporated with both the ex-*S. aureus* plasmids and the new ex-*S. cohnii* plasmids, resulting in five successful transformations (four using the ex-*S. cohnii* plasmid, one using the ex-*S. aureus* plasmid). An increase from 6.3% successfully transforming trains with the first set (4.3.2), using only the ex-*S. aureus* plasmid, to a 41.6% success rate using the combination of both plasmid extractions.

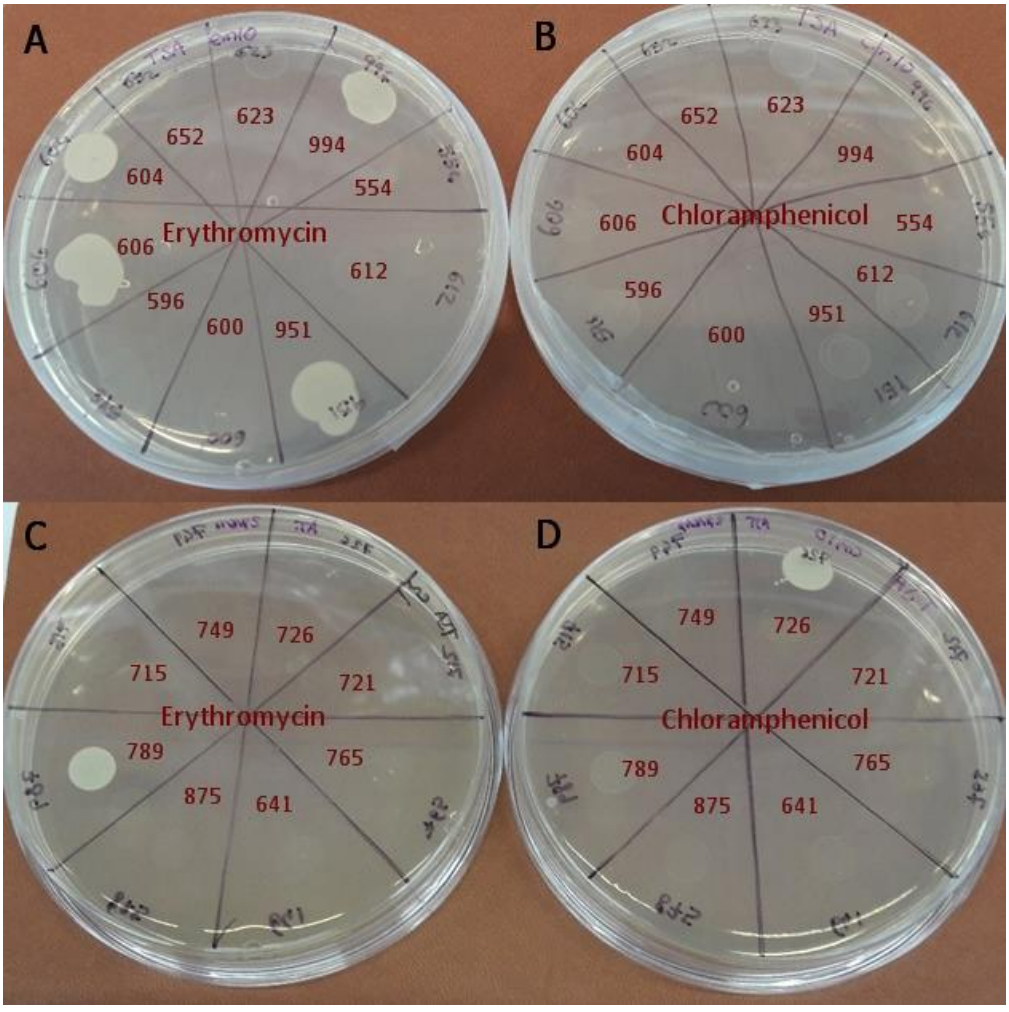

Figure 4.8. Antibiotic resistance of NAS set 2 strains. A and C - Erythromycin 10 µg/ml plates, B and D - chloramphenicol 10 µg/ml plates; plate sections inoculated identified by last three digits of strain ID.

Plates [4.9.a] and [4.9.b] show that 15TB0994 (transformed with the *S. cohnii* 15TB0993 Tn5 and *mariner* plasmids) was the most readily transformed strain tested with these plasmids, as these plates yielded the greatest number of colonies (9 and 5 CFU respectively) (Figure 4.9). This strain (15TB0994) was the only one to be successfully transformed with both a *mariner* and a Tn5 transposon loaded plasmid. The number of CFU recovered following electroporation of 15TB0994 was similar to that of 15TB0993 - nine *mariner* and five Tn5 potential transformants compared to five *mariner* and 14 Tn5 mutants found on the recovery plates, respectively. The other three strains (Figure 4.9c, d and e) did not transform as successfully. Each strain only produced colonies with one of the four plasmids tested (Tn5 ex-*S. cohnii* (extracted from 15TB0993), *mariner* ex-*S. cohnii* (extracted from 15TB0993), Tn5 ex-*S. aureus* (extracted from DSM-26309), *mariner* ex-*S. aureus* (extracted from DSM-26309)), and only 1 CFU was recovered after electroporation (Figure 4.9c, d and e). No colonies were found on any negative control plates, which suggested that even the single colony transformations could have been successful. However, a single colony is far more likely to be due to a spontaneous mutation compared to plates with multiple resistant colonies.

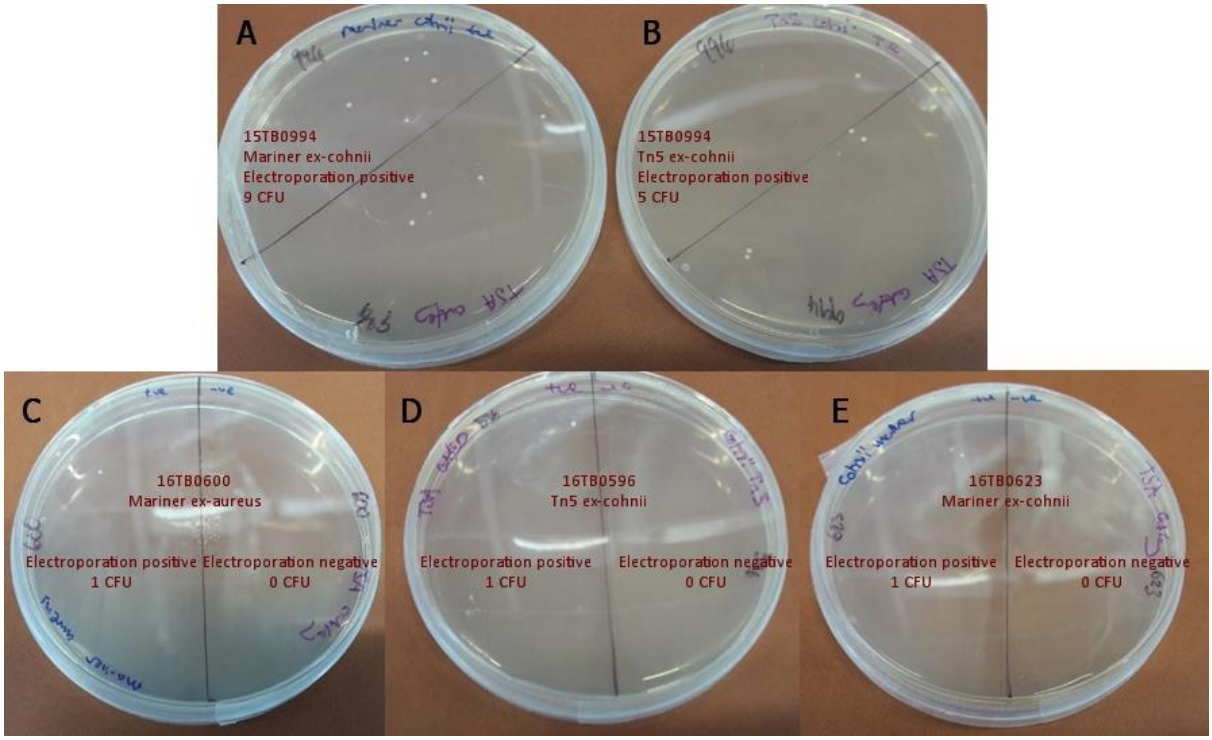

Figure 4.9. Electroporation recovery plates from successful transformations of the NAS set 2.
A - 15TB0994 with ex-*S. cohnii mariner* plasmid, electroporation positive only (negative control plate not shown); B - 15TB0994 with ex-*S. cohnii* Tn5 plasmid, electroporation positive only (negative control plate not shown); C - 16TB0600 with ex-*S. aureus mariner* plasmid, electroporation positive left side of plate, negative control on the right; D - 16TB0596 with ex-*S. cohnii* Tn5 plasmid, electroporation positive left side of plate, negative control on the right; E - 16TB0623 with ex-*S. cohnii mariner* plasmid, electroporation positive left side of plate, negative control on the right.

These potential mutants were re-plated onto fresh antibiotic-containing agar plates to confirm the resistance phenotype, then streaked on the same three identification plates used previously. The potential mutant of 16TB0596 (Figure 4.10a) had a different colony morphology/chromatic change when compared to the parent strain on all three agar plates, indicating contamination.

The other four potential mutants grew with the same morphology and/or chromatic change as their respective parent strains (Figure 4.10). Figure 4.10b, d, e (16TB0600 and the two 15TB0994 mutants) shows these NAS strains had the same phenotypic pattern as each other and the *S. cohnii* strain 15TB0993. Row [c] shows parent and mutant of 16TB0623 matching but with a different phenotypic pattern to *S. cohnii*.

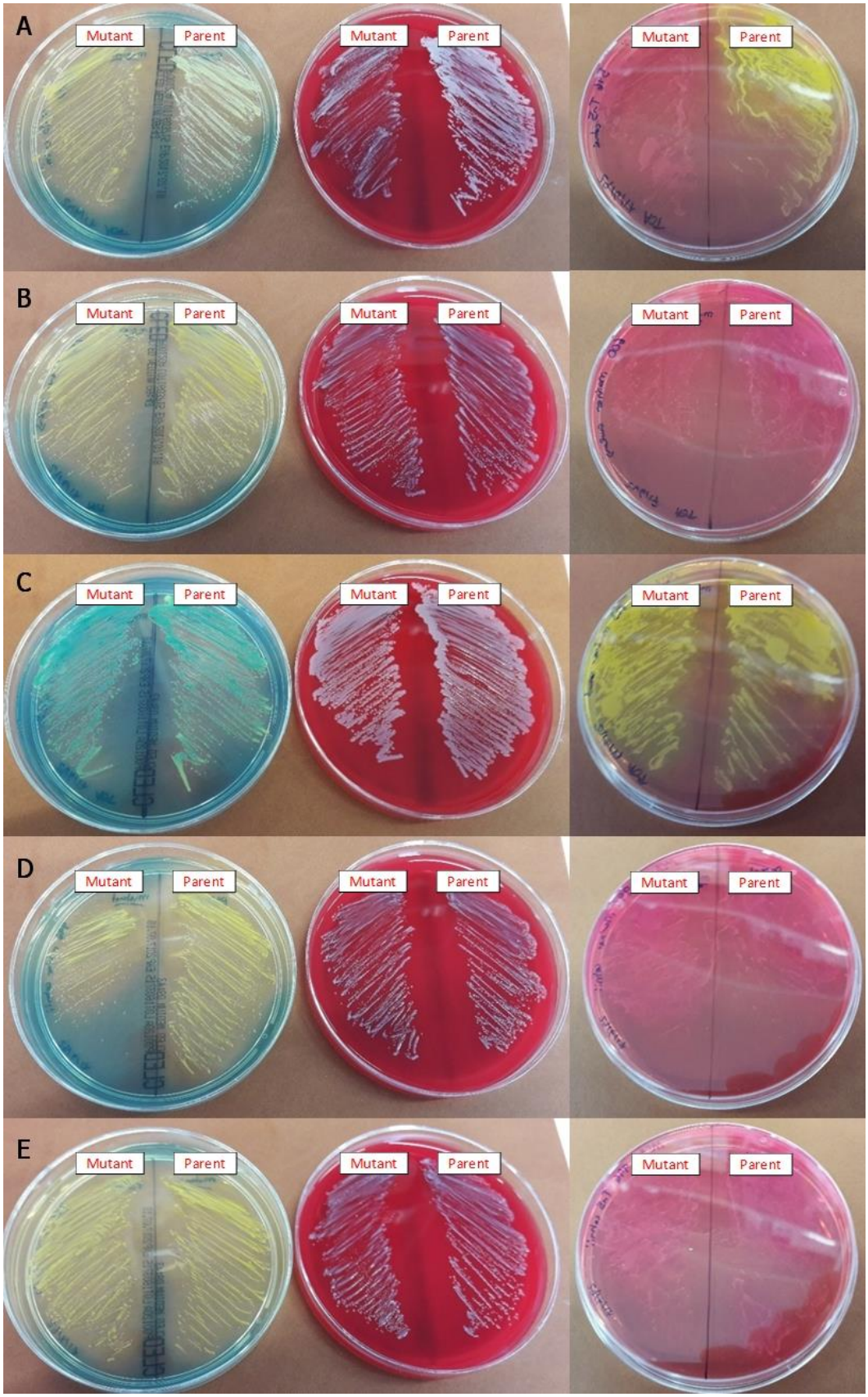

Figure 4.10. Chromatic identification agar plates with potential NAS transformants and parent strains. Mutant strains were streaked on the left side of plates, parent strains on the right; A. 16TB0596 Tn5 ex-*S. cohnii*; B. 16TB0600 *mariner* ex-*S. aureus*; C. 16TB0623 *mariner* ex-*S. cohnii*; D. 15TB0994 *mariner* ex-*S. cohnii*; E**.** 15TB0994 Tn5 ex-*S. cohnii*.

To confirm the observed chloramphenicol and erythromycin resistance was due to the presence of the transposon-plasmid, rather than spontaneous mutagenesis, the plasmid DNA was extracted from mutant strains and analysed by PCR (Figure 4.11). The positive controls of the previously extracted *mariner* plasmids from the DSM-26309 *S. aureus* strain and the 15TB0993 *S. cohnii* showed the PCR product around the expected size (1.4 kb, lanes F1 and A2. A second, much larger band, was also visible on the gel from the 15TB0993 extraction above the 48.5 kB mark at the end of the ladder, which was likely to be plasmid DNA. This band was not present in any of the mutants or parent strains from this screen. With the transposon successfully transformed into a selection of NAS, these transformed strains were taken forward for transposon library production.

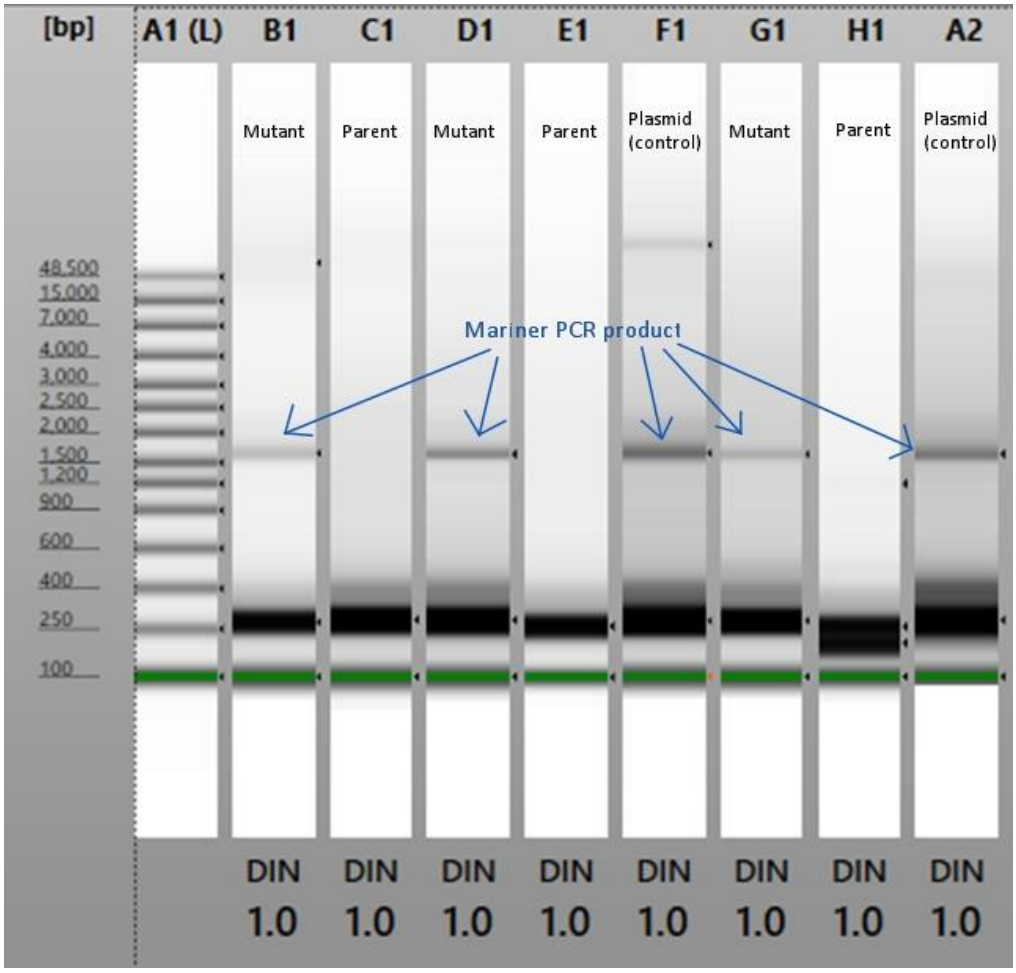

Figure 4.11 Mariner PCR of putative mutants, parents and plasmid control. Plasmid PCR performed using MarSec primers for *mariner* transposon. From left to right; (A1) ladder, (B1) 15TB0994 with *mariner* ex-*S. cohnii* plasmid, (C1) 15TB0994 parent strain colony PCR with *mariner* primers, (D1) 16TB0623 with *mariner* ex-*S. cohnii* plasmid, (E1) 16TB0623 parent strain colony PCR with *mariner* primers, (F1) *mariner* ex-*S. cohnii* plasmid from 15TB0993, (G1) 16TB0600 with *mariner* ex-*S. aureus* plasmid, (H1) 16TB0600 parent strain colony PCR with *mariner* primers, (A2) *mariner* ex-*S. aureus* plasmid from DSM-26309.

4.3.4 Small scale transposon library QC

To test for successful transposon mutagenesis in the transformed strains, small scale transposon mutant libraries were prepared as described in 4.2.4. To determine the proportions of unmutated parent, transposon mutant and residual plasmid, colony counts were taken from a titration series on antibiotic containing agar plates. All cells would be expected to grow on the AHT-only plates. Cells retaining the plasmid backbone, despite high temperature incubation targeting the temperature sensitive repA gene and AHT induced expression of the anti-secY kill gene (Figure 4.3), would be the only cells expected to grow on chloramphenicol containing plates due to the chloramphenicol resistance cassette expressed from the plasmid. Colonies which grow on erythromycin containing plates would be expected to contain the transposon containing the erythromycin resistance cassette. As such, cells which were able to grow on erythromycin but not chloramphenicol were expected to be successful transposon mutants that have integrated the transposon and lost the plasmid.

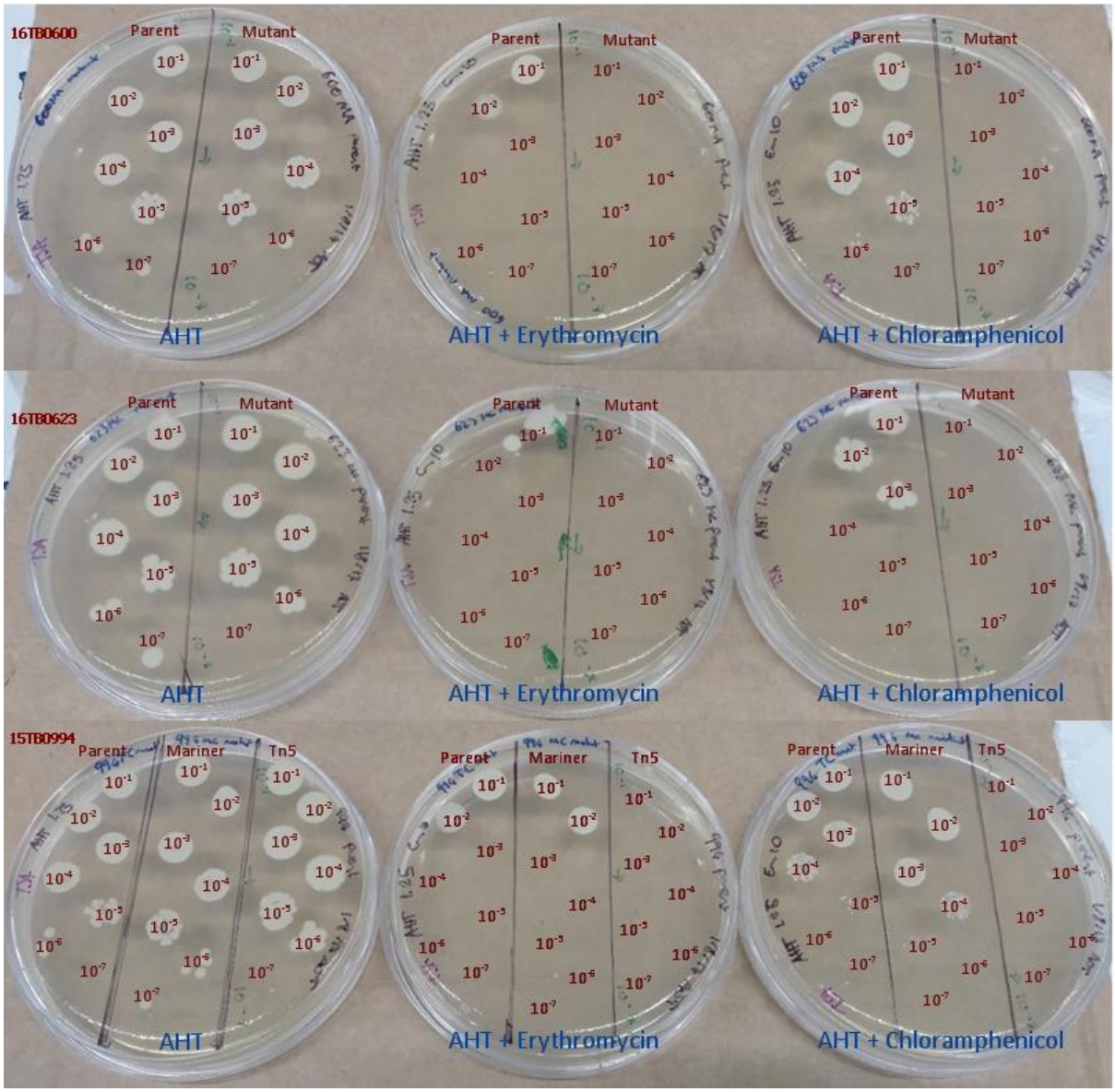

Figure 4.12. AHT titre plates for plasmid removal from successful transformants. All plates contained AHT 1.25 µg/ml; AHT + erythromycin plates also contained 10 µg/ml erythromycin; AHT + chloramphenicol plates also contained 10 µg/ml chloramphenicol. 16TB0600; mutants on left side of plates; parents on right side. 16TB0623; mutants on left side of plates; parents on right side. 15TB0994; Tn5 mutants on left split of plates; *mariner* mutants on middle split and parent on right side. 10 µl Spotted bacteria were titred down from a 10^{-1} dilution down to a 10^{-7} dilution from top to bottom of each agar plate.

From these colony counts each group of cells can be quantified and the relative percentages attributed to each cell type (parent/mutant/plasmid) (Table 4.10). The 16TB0600 *mariner* ex-*S. aureus* mutant strain, henceforth referred to as 16TB0600-*mariner*, shows the greatest proportion of transposon mutants at 100%. The three ex-*S. cohnii* mutants show much lower proportions of transposon mutants ranging from 0.4 to 17.1%. 16TB0600-*mariner* also shows the greatest amount of plasmid clearance with 99.4% of plasmid cells on the chloramphenicol plate but not present on the erythromycin plate. Despite having the lowest transposon mutant population, the 16TB0623

mariner ex-*S. cohnii* mutant strain, henceforth referred to as 16TB0623-*mariner*, showed the greatest proportion of plasmid clearance among the ex-*S. cohnii* mutants at 93.8%. The 15TB0994 Tn5 ex-*S. cohnii* mutant strain, henceforth referred to as 15TB0994-Tn5, had the third greatest plasmid clearance at 85.7% with a calculated mutant population of 2%. Finally, the 15TB0994 *mariner* ex-*S. cohnii* mutant strain, henceforth referred to as 15TB0994-*mariner*, had the lowest plasmid clearance at 77.8% with the second greatest mutant population at 17.1%.

Table 4.10 Transposon population and plasmid clearance of successful transformants

	15TB0994-*mariner*	**15TB0994-Tn5**	**16TB0600-*mariner***	**16TB0623-*mariner***
[1]Transposon mutants (%)	17.1	2.0	100.0	0.4
[2]Plasmid clearance (%)	77.8	85.7	99.4	93.8

[1]Transposon mutant population calculated by the proportion of total colonies counted under no selection pressure (on the AHT only plate) with conferred erythromycin resistance from the transposon (also found in the corresponding erythromycin loaded plate); [2]Plasmid clearance was calculated by the proportion of colonies with erythromycin resistance (those that appeared on the plate containing erythromycin) but lacking the plasmid conferred chloramphenicol resistance (absent on the plate containing chloramphenicol).

4.3.5 Small scale transposon library confirmation

For each strain transformed with the *mariner* plasmid, two gDNA extractions were performed and sequenced by Illumina sequencing (as detailed in methods 4.2.5.2) to determine strain identity and confirm if the transposon was present.

Only the *S. epidermidis* strains (16TB0600 and 15TB0994) could be identified from the sequencing data, with >92% of staphylococcus reads aligning to *S. epidermidis* in all four samples transformed from *S. epidermidis* parents (Table 4.11). The majority of reads generated from the *S. caprae* samples (16TB0623) were unclassified (12.55% and 12.63% classified reads). Reads from these samples that were classified mostly aligned to staphylococcal species, most commonly assigned to *S. epidermidis* (23.77% and 24.14%). Further investigation revealed that *S. caprae* was not in the reference databased used for bioinformatic analysis (Wood and Salzberg, 2014). Conversely, the *mariner* transposon was only confirmed to be present in the mutants transformed from the *S.*

caprae strain (16TB0623) (Table 4.11), suggesting that only this strain had been successfully transformed. Later experiments, however, confirmed that the transposon was present within these mutant strains.

Table 4.11 Illumina sequencing results

Sample	Total reads	Classified reads	Staphylococcus reads	*S. epidermidis* reads	*Mariner* transposon presence
600-1	1,945,267	1,846,933 (94.94%)	1,822,713	1,725,997 (94.69%)	Unconfirmed
600-2	1,476,425	1,398,588 (94.73%)	1,359,385	1,273,673 (93.69%)	Unconfirmed
623-1	2,886,039	362,229 (12.55%)	261,665	62,197 (23.77%)	Confirmed
623-2	1,344,961	169,930 (12.63%)	119,421	28,823 (24.14%)	Confirmed
994-1	1,706,056	1,612,692 (94.53%)	1,578,852	1,464,046 (92.73%)	Unconfirmed
994-2	2,446,230	2,312,956 (94.55%)	2,256,537	2,108,055 (93.42%)	Unconfirmed

Illumina sequencing results from gDNA extractions of potential *mariner* transposon mutants, analysis performed by Lisa Crossman; 600-1/600-2 – 16TB0600-*mariner* extractions 1 and 2 (*S. epidermidis*); 623-1/623-2 – 16TB0623-*mariner* extractions 1 and 2 (*S. caprae*); 994-1/994-2 – 15TB0994-*mariner* extractions 1 and 2 (*S. epidermidis*); Classified reads – reads classified by MiniKraken (percentage of total reads classified); *S. epidermidis* reads – reads classified as *S. epidermidis* species by MiniKraken (percentage of Staphylococcus reads classified as *S. epidermidis*); *Mariner* transposon presence confirmed by alignment to the *E. coli mariner* reference by BWA.

After sequencing, colony PCR was performed on freshly incubated plates of the mutant and parent strains, along with positive controls, to check if the transposon could be found within each strain. Tapestation analysis showed the presence of the *mariner* transposon at the expected amplicon size (~900bp) for two mutant strains tested (16TB0600-*mariner*, Figure 4.13 - D1 and E1) and the Tn5 transposon (~900bp) for the Tn5 mutant (15TB0994-Tn5, Figure 4.13 – E2 and F2). Bands of the expected size were not observed for 16TB0600 parent (C1), 16TB0623 parent (F1) or 15TB0994 parent (A2). The *mariner* mutant was not present in either of the extractions from 16TB0623-

mariner (Figure 4.13 – B2 and C2). Neither of the template free PCR controls had a band around 1000bp (*mariner* primers – B1, Tn5 primers – G2). The Tn5 plasmid positive control showed a single band around 1200bp (H2), slightly smaller than the band seen in the Tn5 mutant extractions. The *mariner* plasmid control, however, did not appear to run successfully. A clear band is seen at 200bp (D2), smaller than the bands seen in the 16TB0600-*mariner* and 16TB0623-*mariner*, the latter of which had been confirmed by Illumina sequencing (Table 4.11). A similar sized band can be seen in one of the 15TB0994-*mariner* extractions (B2, ~200bp) and may represent primer dimers. With transposon confirmed present in 16TB0600-*mariner*, 16TB0623-*mariner* and 15TB0994-Tn5, and the remaining mutant 15TB0994-*mariner* matching the *mariner* plasmid positive control, all four mutants were taken forward for library scale up.

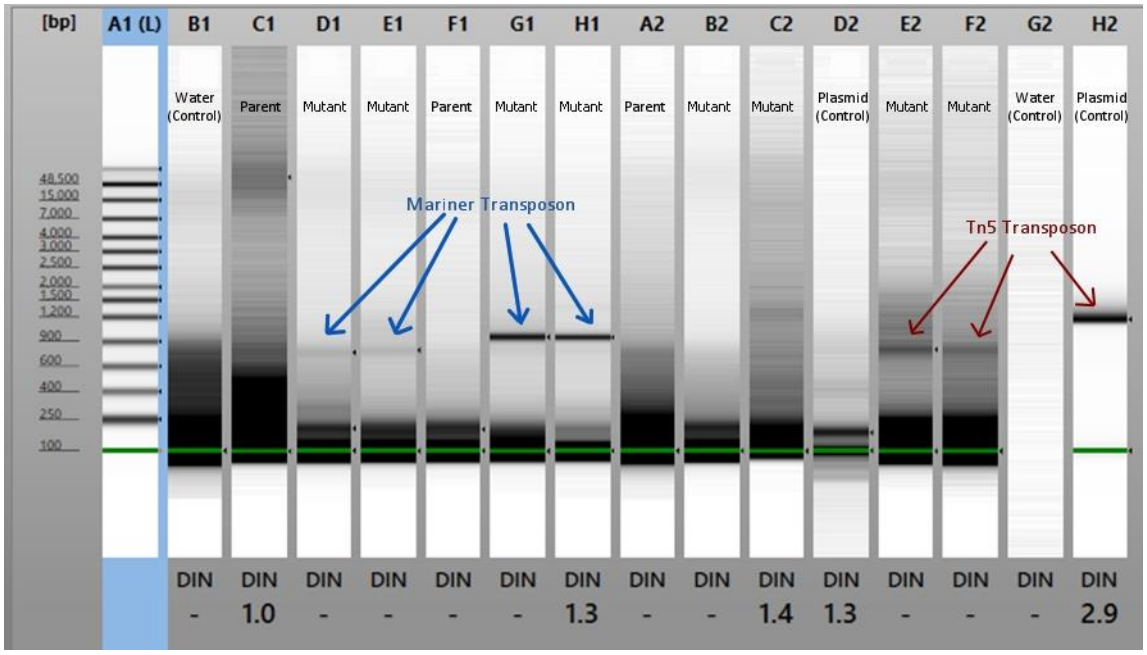

Figure 4.13. Colony PCR products for mariner and Tn5 transposons in putative mutants. Colony PCR performed on lysed single colonies with Himar primers for *mariner* or ME primers for Tn5 transposon; A1 - DNA ladder; B1 - template free PCR control with *mariner* primers; C1 - 16TB0600 parent; D1 - 16TB0600-*mariner* extraction 1 ; E1 - 16TB0600-*mariner* extraction 2 ; F1 - 16TB0632 parent; G1 - 16TB0623-*mariner* extraction 1; H1 - 16TB0623-*mariner* extraction 2 ; A2 - 15TB0994 parent ; B2 - 15TB0994-*mariner* extraction 1 ; C2 - 15TB0994-*mariner* extraction 2 ; D2 - *mariner* plasmid positive control ; E2 - 15TB0994-Tn5 extraction 1; F2 - 15TB0994-Tn5 extraction 2 ; G2 - template free PCR control with Tn5 primers ; H2 - Tn5 plasmid positive control

4.3.6 Transposon library scale-up

The level of erythromycin resistance needed to be determined to enable the optimum selection of transposon mutants versus the parent strain. The erythromycin resistance levels differed between

the innate resistance of the parent strains and the expression level of the erythromycin cassette present on the transposon. The individual resistance concentrations were therefore determined by comparing colony growth of mutant versus parent strain on a series of erythromycin containing agar plates (4.2.6).

There was clear growth of all the tested strains on the antibiotic-free plate which confirmed that absence of growth on the other plates was due to the presence of the antibiotic (Table 4.12). The mutants that had gained the highest resistance were those of 16TB0623-*mariner*, which showed significant growth up to and including highest antibiotic concentration used, 256 µg/ml. The parent strain of 16TB0623 had the lowest resistance to erythromycin, with no growth seen on any of the antibiotic-containing plates. The two 15TB0994 mutants, -Tn5 and -*mariner*, showed significant growth up to 64 and 32 µg/ml erythromycin, respectively, with the parent strain capable of growth on up to 16µg/ml erythromycin. 16TB0600-*mariner* showed the lowest erythromycin tolerance of the mutant strains, with some growth on the 16 µg/ml plate. The parent strain of 16TB0600 showed growth on up to 4 µg/ml erythromycin. All mutant strains had higher erythromycin resistance than their respective parent strains, confirming that erythromycin could be used in library scale-up to select for the transposon mutants.

Table 4.12 Erythromycin resistance of transposon mutants and their respective parent strains

Erythromycin concentration (µg/ml)	Strain						
	16TB0600		16TB0623		15TB0994		
	parent	*mariner*	parent	*mariner*	parent	*mariner*	Tn5
0	✓	✓	✓	✓	✓	✓	✓
2	✓	✓	×	✓	✓	✓	✓
4	✓	✓	×	✓	✓	✓	✓
8	×	✓	×	✓	✓	✓	✓
16	×	✓	×	✓	✓	✓	✓
32	×	×	×	✓	×	✓	✓
64	×	×	×	✓	×	×	✓
128	×	×	×	✓	×	×	×
256	×	×	×	✓	×	×	×

Significant growth of each transposon mutant strain, along with their respective parent strains, plated on TSA containing a range of erythromycin concentrations from 0 to 256 µg/ml;
✓- significant growth observed;
×- no significant growth observed.

The optimum erythromycin concentration for library scale-up was designated as 8 µg/ml for 16TB0600, 16 µg/ml for 16TB0623, 32 µg/ml for *mariner* mutant of 15TB0994 and 64 µg/ml for the Tn5 15TB0994 mutant. As the only mutant confirmed to contain the transposon by sequencing, as well as being the mutant with the highest resistance to erythromycin, 16TB0623-*mariner* was chosen to be the first mutant scaled-up into a high coverage transposon library.

4.4.7 Plasmid removal and heat phenotypes

In total, six library scale-up conditions (4.2.6) were tested with the strain of 16TB0623-*mariner* transformed with a transposon. Three erythromycin concentrations were used at 12, 16 and 24 µg/ml with incubation temperatures of 37ºC and 42ºC for each of the six libraries to be scaled up (1 – 12 µg/ml erythromycin 37ºC, 2 – 16 µg/ml erythromycin 37ºC, 3 – 24 µg/ml erythromycin 37ºC, 4 – 12 µg/ml erythromycin 42ºC, 5 – 16 µg/ml erythromycin 42ºC, 6 – 24 µg/ml erythromycin 42ºC). Similar quality control measures used for the small-scale libraries were also performed i.e.

mutant strains were plated on serial dilutions of erythromycin and chloramphenicol and AHT only, to determine the quantities of transposon mutant, plasmid-containing and parent cells.

All six conditions showed that parent cells had not been fully removed in the collection with between 29% and 75% of cells not containing the transposon (Figure 4.14). The percentage of mutant cells differed greatly across erythromycin concentrations. In both temperature sets, the library grown on plates containing 16 µg/ml erythromycin showed the lowest percentage of parent cells. Increasing or lowering the antibiotic concentration from this level resulted in roughly double the level of parent cells. In both instances, 12 µg/ml of erythromycin resulted in the greatest percentage of parent cells, 73.7% at 37ºC and 7.15% at 42ºC.

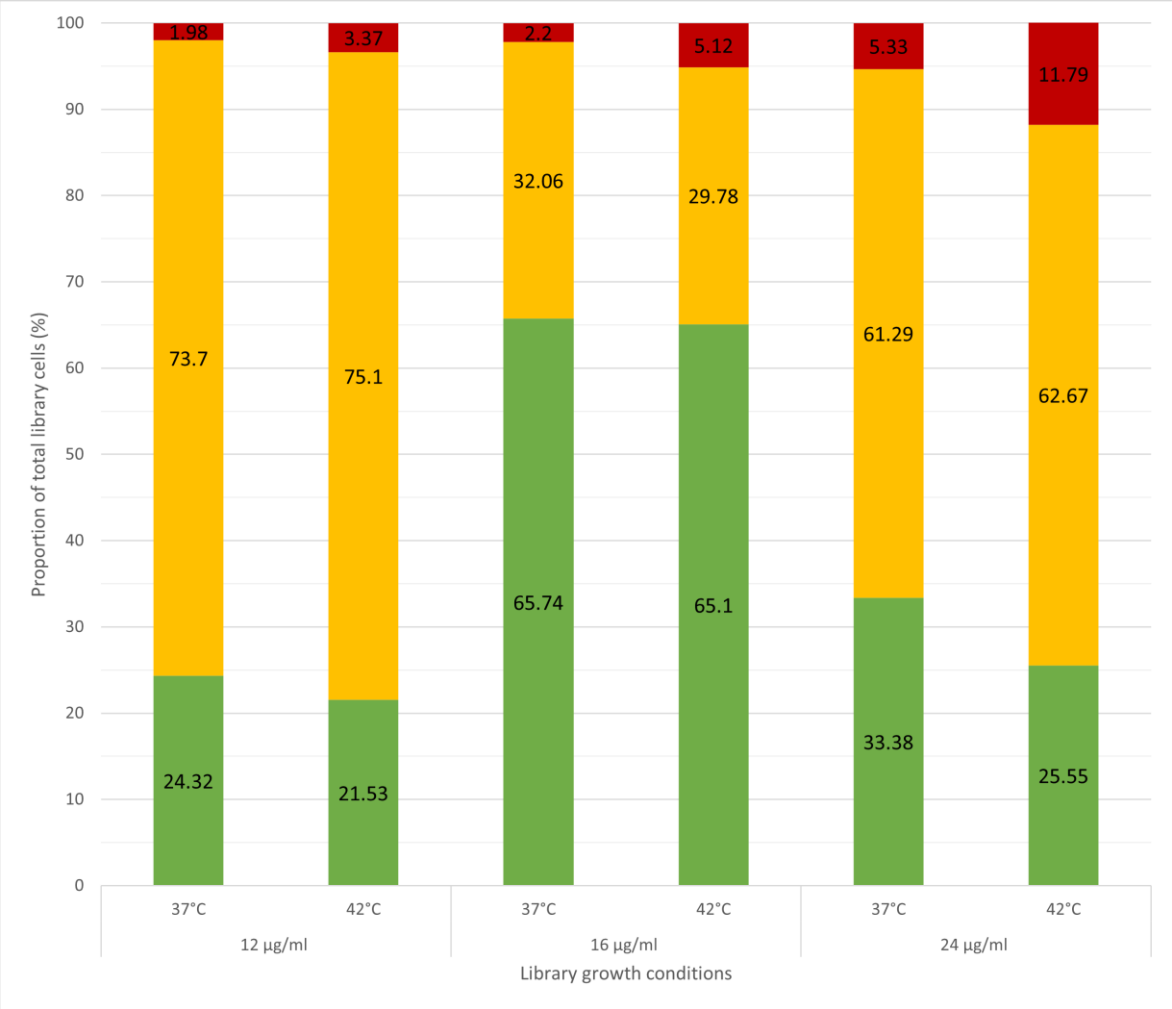

Figure 4.14. Mutant, parent and plasmid composition of scaled up *S. caprae* transposon libraries. Proportions of mutant, parent and plasmid-containing cells within the scaled-up transposon libraries of *S. caprae* 16TB0623-*mariner*. Percentages calculated from titre plates of various antibiotic selection pressures;
■ % mutants = cells containing the transposon integrated to the genome, that had then lost the transposon plasmid (resistant to erythromycin, susceptible to chloramphenicol);
■ % parent = cells not containing the transposon (susceptible to erythromycin);
■ % plasmid = cells containing the plasmid backbone used to deploy the transposon (resistant to chloramphenicol).

The percentage of cells that had retained the plasmid after incubation was also affected by the erythromycin concentration and temperature. The plasmid clearance levels were inversely proportional to the antibiotic concentration, with the most clearance at 12 µg/ml and the least at 24 µg/ml, and were lower at 42 C than 37 C for all three concentrations of erythromycin. The percentage of plasmid cells remaining in a scaled-up library ranged from a low of 2% at 12 µg/ml erythromycin at 37ºC to a high of 12% at 24 µg/ml at 42ºC.

The library with the most mutant cells (65.74%) was the 37ºC, 16 µg/ml library (Table 4.13). The 16 µg/ml library contained 0.22% more plasmid cells than the 12 µg/ml library but had a significantly greater proportion of mutant cells (65.74% compared to 24.30%). While fewer plates were discarded with potential contamination prior to harvesting as erythromycin concentration increased, the higher proportion of mutants to parent cells means that the two 16 µg/ml libraries contained over 80,000 more mutants than their 24 µg/ml counterparts.

Table. 4.13 Mutants per scaled-up *S. caprae* transposon library.

	Incubation temperature (ºC)					
	37			**42**		
	Erythromycin concentration (µg/ml)					
	12	**16**	**24**	**12**	**16**	**24**
Mutants per plate	20,000	20,000	20,000	20,000	20,000	20,000
Plates recovered	15	19	25	10	15	27
% mutants	24.30	65.74	33.38	21.53	65.10	25.55
[1]Total mutants	72,900	249,812	166,900	43,060	195,300	137,970

[1]Total mutants calculated by mutants inoculated per plate, multiplied by plates recovered, divided by the percentage of cells designated as mutants.

4.4 - Discussion

The purpose of this work was to develop a method capable of transforming NAS strains with a transposon loaded plasmid for the generation of transposon mutagenesis libraries. These libraries would be used to build up lists of essential genes for biofilm formation under laboratory conditions which could be used to find novel biomarkers of biofilm formation. These biofilm biomarkers could serve as diagnostic markers to determine if bacteria isolated from a joint sample had come from a biofilm driven infection or was the result of commensal contamination. Discovery of new biomarkers by TIS is a long process. We began by taking plasmids cloned to contain two types of transposons and applied electroporation to transform a collection of NAS strains. We reached the stage of generating a scaled-up library of ~250,000 mutants in a previously untested NAS species (*S. caprae*) which others can now take forward to generate essential gene lists.

4.4.1 Transformation efficiency

The conditions used to prepare electrocompetent cells can have a wide impact on the efficiency at which plasmids will be taken up (Nováková et al., 2014). We tested a range of growth media to find a suitable candidate for use in preparing electrocompetent cells from the collection of NAS species stored within the NRP Biorepository. Large and complex plasmids, such as the transposon loaded plasmids we used in this project, can be challenging to transform into some strains (Szostková and Horáková, 1998). NAS species in particular are challenging to transform due to RM systems preventing the introduction of foreign DNA (Jones et al., 2015).

We found that the optimum conditions for transformation efficiency varied between the tested strains. This was to be expected as different strains will take up certain plasmids more readily due to RM system variance (Monk et al., 2012). However, previous studies report that an O.D. of 0.5 was optimal for preparing electrocompetent cells of *S. aureus* (Jones et al., 2015; Schneewind and Missiakas, 2014) as well as NAS (Cui et al., 2015; Löfblom et al., 2007). While our transformations with *S. aureus* were most efficient at an $O.D._{600}$ of 0.3, the two tested NAS strains transformed most efficiently at 0.5, consistent with the literature.

The two broths that had been previously been used for transforming NAS species, B (Augustin and Götz, 1990) and B2 (Schenk and Laddaga, 1992) broth, performed poorly with NAS species, with neither broth resulting in more efficient transformation than Iso-Sensitest broth in the strains tested. This may be due to the high glucose content of Iso-Sensitest (Oxoid - Product Detail) compared to B (20-fold less) and B2 (4-fold less) as the presence of glucose in rich medium accelerates the synthesis of glycogen, which has been reported to increase the viability of *E. coli* under stressful conditions such as competent cell preparation (Nováková et al., 2014). In our hands, *S. epidermidis* transformation efficiency was 100-fold lower than reported in the literature ($3x10^5$ transformants per μg plasmid DNA) (Augustin and Götz, 1990) and the *S. lugdunensis* transformation efficiency was 1000 fold lower. Differences between NAS strain transformation efficiency could be driven by the growth conditions being better optimised for one strain over the other or because some RM system interference with transformation more than others.

Strain to strain variation highlights the need for optimised conditions for transformation. Schenk *et al.* reported that the transformation efficiency of *S. epidermidis* prepared with B2 broth was 1000-fold lower than in *S. aureus* (Schenk and Laddaga, 1992). Our successful transformations yielded only a few colonies in each instance, even though the approach was optimised and provided good results with smaller plasmids. Ideally, the growth conditions for electrocompetent cell preparation would be optimised for each strain to be tested. However, we were attempting to develop a single broadly applicable method for screening a variety of NAS strains, as it would have been very time consuming to optimise per species.

4.4.2 Mutant selection for library scale-up

Integrated transposon mutants were selected for by antibiotic and high temperature selection. Erythromycin was used to select for cells containing the transposon and the pIMAY plasmid backbone was selected against using AHT to activate the anti-secY kill gene and high incubation temperatures to prevent replication. pIMAY has previously been used in *S. aureus* (Bae and Schneewind, 2006; Schuster et al., 2019) and *Listeria monocytogenes* (Abdelhamed et al., 2015)

transposon mutagenesis as the anti-secY selection for chromosomal plasmid excision enriches the number of mutants with deleted genes.

Removing both parent and plasmid containing cells from a transposon library is important as neither contain the transposon integrated into the chromosome. However, excessive selection pressure could affect the results of gene expression studies (Romero et al., 2012). Previously, our group had been incubating TraDIS libraries at 42ºC to ensure that the heat-sensitive plasmid was selected against during library scale-up. However, this temperature could result in altered gene expression compared to growth at 37ºC, which the bacteria would normally grow inside a host. Prolonged incubation at high temperatures for plasmid curing, which can be harsh conditions for bacterial growth and survival, in turn leading to accumulation of adaptive genetic changes (Naorem et al., 2018). Another concern was the thermostability of erythromycin - high temperature incubations could reduce effectiveness during scale-up (Cruz-Loya et al., 2019; Tuleubaev et al., 2018). We took one transposon library and scaled up using two different temperatures in parallel (42 and 37ºC) and determined that the higher temperature did not significantly reduce plasmid cell population compared to 37ºC. Hence, removal of this plasmid backbone was performed at 37ºC to avoid unnecessarily introducing heat phenotypes into the transposon library. It would, however, be interesting to see if the higher incubation temperature had affected which genes were essential for growth within the cells. This could be confirmed by in a future TraDIS experiment, sequencing libraries prepared under the same antibiotic selection pressure with each of the temperature conditions would confirm if this was necessary. Alternatively, differences in gene expression levels between libraries prepared at each temperature could be assayed by performing RNAseq (Finotello and Di Camillo, 2015).

Until recently, only temperature-sensitive conditional suicide plasmids, such as pIMAY, had previously been used for transposon mutagenesis, as they replicate in a wide range of bacterial species (Meyer, 2009). In 2018, a group in the US designed non-temperature-sensitive IPTG-induced suicide plasmids for transposon mutagenesis In *P. aeruginosa* to avoid enrichment of mutants with adaptive genetic changes and overcome the species-specific nature of some temperature-sensitive plasmids (Naorem, 2018). While our work showed that a high incubation

temperature was not necessary for plasmid removal this approach, which was designed for incubation at 37°C, should be considered as an alternative to pIMAY for future work.

The erythromycin antibiotic selection was unable to completely remove parent cells from the library in scale-up. This may have been a result of overcrowding the plates with colonies, resulting in either parent colonies growing on top of mutant cells or mutant driven breakdown of the antibiotics facilitating parent growth. We grew 20,000 colonies per plate, significantly more than the 500-2,000 colonies per plate recommended by Freed to prevent colonies competing for resources (Freed, 2017), using fewer colonies per plate may have improved antibiotic selection for mutant cells. Erythromycin is bacteriostatic, preventing replication of susceptible cells rather than killing them (Waller and Sampson, 2018); parent cells would not be completely removed from the pool, and if the antibiotic was degraded the cells would be able to replicate again alongside the resistant mutant cells. Future work should either incorporate larger agar plates for growth or prepare more plates with fewer colonies inoculated per plate. During scale-up, plates with any suspicion of contamination were discarded. The number of plates discarded decreased as the erythromycin concentration increased, something that should be considered when scaling up as increasing the antibiotic concentration used would reduce the number of discarded plates, however, increasing the erythromycin concentration above 16 µg/ml resulted in fewer mutants. This may be a result of the increased antibiotic selection pressure driving erythromycin resistant transposon mutants to degrade the antibiotic at a greater rate, as counteraction of antibiotic production and degradation is known to stabilise microbial communities containing susceptible cells (Kelsic et al., 2015; Nicoloff and Andersson, 2016), meaning unnecessarily high concentrations of antibiotic should be avoided.

The best library generated here contained 249,812 mutants, which falls within the range of previously developed transposon libraries (Barquist et al., 2013a). A review of transposon insertion sequencing by Barquist *et al.* compared 15 Tn5 or *mariner* transposon libraries reporting the average total mutants to be 329,294 (Barquist et al., 2013a) (ranging from 4,000 (van Opijnen and Camilli, 2012) to 1.1 million mutants (Langridge et al., 2009; Sassetti et al., 2003)). These libraries showed a range of unique insertions into the host genome ranging between 8,000 (Mann et al., 2012) and 550,000 (Barquist et al., 2013b) (average 162,481). If our *S. caprae* library had the

average proportion of unique insertions/total mutants from this paper (0.65 taken as average unique insertions in 13 Tn5 and *mariner* libraries included in review by Barquist *et al.*(2013a)) then we would expect to see 161,663 unique insertions, however this would need to be confirmed by sequencing. As the average genome size for clinical *S. caprae* strains is 2.6 Mb (George and Kloos, 1994) this number of unique insertions would equate to an insertion frequency of one per 16 base pairs. This would be high coverage library as the average reported in previous Tn5 and *mariner* libraries is one insertion per 108 base pairs (range 8 (Christen et al., 2011) to 610 (Khatiwara et al., 2012)). If the library does indeed have this level of unique insertions spread evenly over the genome it would provide high quality data on genes essential for growth under the selected test conditions (Cain et al., 2020).

4.4.3 Restriction modification systems

The biggest challenge of this project was to successfully transform the transposon loaded plasmids into NAS strains. As discussed in the introduction, RM systems can prevent foreign DNA elements from being introduced, making staphylococcal strains challenging to transform (Ando et al., 2000; Purdy et al., 2002; Vasu and Nagaraja, 2013; Wilson, 1991). To achieve transformation of more staphylococcal strains we initially passaged and re-extracted our plasmids through a *S. cohnii* strain to generate plasmids with an alternative methylation pattern to the ex-*S. aureus* plasmids as first demonstrated with *S. carnosus* by Augustin and Götz (1990). While the strain itself was unsuitable for transposon library preparation (as the parent had innate resistance to erythromycin which was used to select for the transposon in the tested strains), this ex-*S. cohnii* plasmid was successfully transformed into other NAS from the collection. Had this been unsuccessful, the erythromycin resistance cassette on the plasmid could have been replaced with another antibiotic, such as kanamycin, used by Veeranagouda, Husain and Wexler in *B. fragilis* (Veeranagouda et al., 2013) and gentamicin used by Martínez-García *et al.* in *E. coli* (Martínez-García et al., 2014). Further developing a plasmid cocktail from passaging the plasmids through all strains in the collection could result in enough methylation variation to transform any NAS strain in the future.

4.4.4 Future work

The next step in this project would be to sequence the scaled-up transposon library to confirm the number of unique mutants. Assuming the library was of sufficiently high coverage (multiple insertions per locus (Chao et al., 2016)), a library would be grown in a media that promotes biofilm formation, such as Hussain-Hastings-White media (HHW) (Hussain et al., 1991) and incubated on artificial materials used in prosthesis manufacturing such as PMMA and metal. After biofilm maturation, the biofilm would be physically removed from the artificial surface and sequenced. Planktonically growing cells collected from the same media would also be sequenced, with relative insertion site frequency compared between the cells collected from inside and outside of a biofilm environment to identify essential genes for survival in a biofilm (Figure 4.1). Langridge *et al.* previously demonstrated that TraDIS could be used to identify pathogenicity factors by comparing sequenced mutants grown in rich media and a clinically relevant environment, bile (Langridge et al., 2009). Gene lists could then be made from other strains using the same methods with further passage of the transposon loaded plasmids. Our groups initial aim was to generate TraDIS libraries for ~200 strains within the NAS collection to look for conserved biomarkers of biofilm formation. With enough passage of the plasmids through various strains it may be possible to develop a plasmid cocktail capable of successful transformations into all available strains, this would be a big development in the understanding of NAS species as, to our knowledge, only two transposon libraries have been generated in NAS so far, both in *S. epidermidis* (Widhelm et al., 2014; Yajjala et al., 2016). If a series of TraDIS libraries from varying strains could be grown in biofilms and analysed by sequencing, then biofilm biomarkers conserved across many NAS species could be identified. These biomarkers of biofilm formation could be targeted in a reverse transcriptase (RT) RT-qPCR assay, quantifying RNA to measure active gene expression (Riedy et al., 1995; VanGuilder et al., 2008), to determine if isolates cultured from joint tissue had been growing as part of a biofilm or not. There are potentially biomarkers for growth on certain surfaces such as PMMA, if these could be found then it may be possible to develop robust tests for determining if an organism found by routine diagnostic testing has originated from a prosthesis, causing infection.

Chapter 5 – Overall discussion and conclusions

The difficulty with diagnosing PJI is that no one method has suitable sensitivity and specificity (Parvizi et al., 2018; Tande and Patel, 2014). Microbiological culture methods are slow and insensitive, with many patients presenting with symptoms despite a culture-negative report (Parvizi et al., 2014a). Currently, diagnosis of PJI relies on a combination of culture methods and host biomarkers, such as CRP and ESR (Parvizi et al., 2018, 2014b). However, these host biomarkers measure inflammation, which is non-specific for infection and can be triggered by other causes such as aseptic loosening (Parvizi et al., 2011a; Tande and Patel, 2014). Distinguishing low-grade infection from AL can be difficult when presented with conflicting culture and host-marker reports (Li et al., 2020). Diagnosis is further complicated by the risk of culture being contaminated by skin commensals during sampling. The ability to determine if a cultured organism has come from a biofilm could be used to confirm infection, but there is currently a lack of suitable biomarkers for biofilm formation (Khatoon et al., 2018).

In this thesis, we have presented three approaches to PJI diagnosis; host biomarkers for infection, rapid CMg for pathogen identification and we started the process of identifying biofilm biomarkers. We believe that an ideal diagnostic test would use a combination of these three approaches. An ideal pipeline for PJI diagnostics would use preoperatively sampled synovial fluid to detect pathogen and host biomarkers (Figure 5.1). Samples would be split with one half undergoing human DNA depletion and WGA (for pathogen detection) and the other undergoing RNA extraction (for host and pathogen biomarker detection), followed by library preparation for rapid MinION sequencing. DNA free RNA is necessary when identifying mRNA biomarkers to detect expressed genes as contamination with DNA will lead to the detection of the genes themselves (Sharkey et al., 2004). It may be best to target the host and biofilm biomarkers by RT-PCR and combine with WGA pathogen DNA for sequencing. This test would be ideal but would require further work to fully define relevant PJI host biomarkers and identify new biomarkers for biofilm formation.

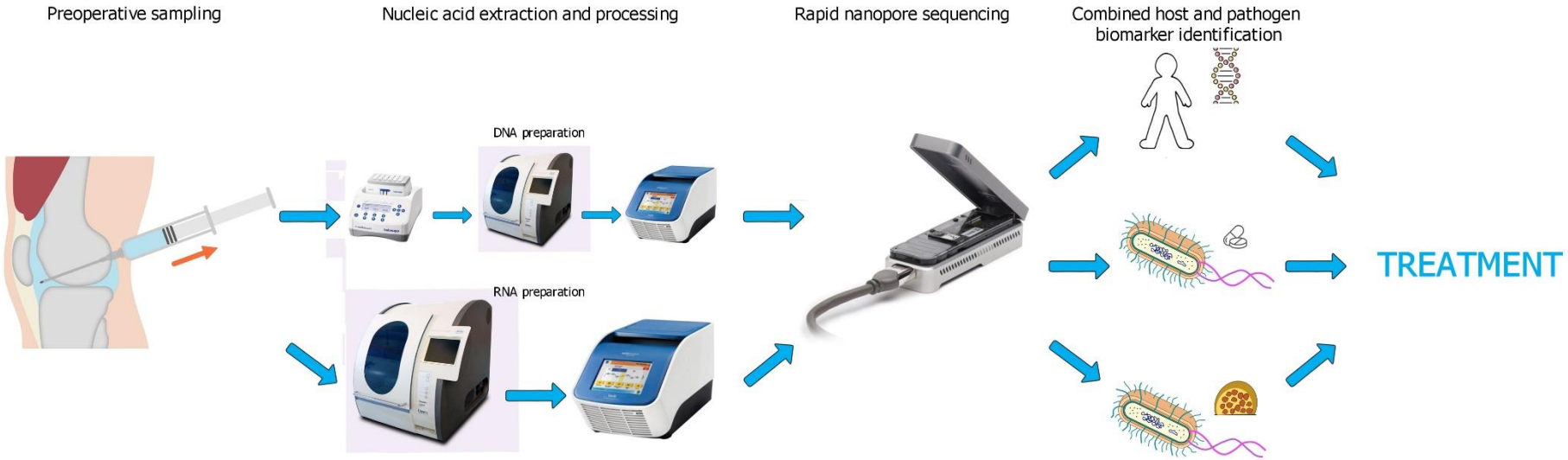

Figure 5.1. Potential future PJI diagnostic pipeline. Preoperative synovial fluid arthroscopies would be split and processed in two ways. RNA would be extracted directly from half of the sample and processed by RT-PCR (to detect host and pathogen biomarkers). The other half would be processed for host cell depletion, DNA extraction and WGA (for pathogen identification). Both would be combined for rapid MinION sequencing. Data would be analysed for host biomarkers of infection, pathogen identification and AMR gene detection, as well as gene expression of pathogen biofilm formation. This information could direct appropriate selection of antibiotic treatment and surgical interventions.

The current cost of sequencing means it is unlikely to be adopted for use on all patients suspected of infection (Chiu and Miller, 2019; Greninger, 2018). Rapid lateral flow tests such as the Lyfstone AS calprotectin test may be used to exclude PJI early, informing treatment plans and selecting patients for a more comprehensive diagnostic workup to identify pathogens and susceptibilities if infected (aseptic patients would not require microbiological investigation). These tests are both cheap and easy to use (Trotter et al., 2020; Warren et al., 2021). The Lyfstone calprotectin POC test showed early promise in our hands as a rule-out test for PJI. The NPV was good when compared to current ICM-based diagnostic criteria, and very high compared to the clinical review of patient outcomes. Consideration needs to be taken when used with patients where metallosis may generate false-positive results. This may be less of a concern in the future as investigations into the potential toxicity of metal on metal implants have advised that they be phased out of implantation (Keegan et al., 2007; Oliveira et al., 2014; Smith et al., 2012).

The use of a mobile phone application to determine results simplifies and standardises analysis avoiding any operator bias (Bastos et al., 2020; Roper et al., 2020). This test shows great promise for use as part of a more comprehensive diagnostic workup as synovial fluid can be taken arthroscopically prior to open surgical intervention (Izakovicova et al., 2019; Tande and Patel, 2014). A study performed at the Cleveland Clinic (Warren et al., 2021) reported specificity and sensitivity of 98.1 and 95.7% respectively. While further studies at multiple sites are required to accurately determine the test's performance, it may be as accurate as the Synovasure α-defensin assay which is one of the tests that can be used in current PJI diagnostic guidelines (Parvizi et al., 2018).

While useful, lateral flow tests are unlikely to ever become a standalone diagnostic for PJI as a single biomarker will never have perfect sensitivity and specificity, especially for a heterogenous disease such as PJI (Parvizi et al., 2018; Tande and Patel, 2014). Inflammation biomarkers are not specific to infection and can be caused by many things, such as metallosis and osteolysis as seen in our study. Likewise, many aseptic conditions can trigger inflammatory responses, such as RA and T2DM; while these conditions did not appear to affect the results in our study, they have been reported to generate false positive results with other inflammatory biomarker assays (Plate et al.,

2018). A combination of host responses that is more specific to PJI, e.g a human mRNA biomarker panel, would be more useful.

CMg could replace current culture based methods for the diagnosis of PJI as it is faster and more comprehensive as several studies have shown high sensitivity and high specificity rates using CMg tests for PJI (Ivy et al., 2018; Ruppé et al., 2017b; Street et al., 2017; Thoendel et al., 2018). When we started this study there were no published reports of this approach, now several independent groups have attempted to apply CMg to PJI diagnosis. We demonstrated that rapid CMg for PJI samples was possible when using effective host cell depletion. Our test performance against routine culture methods was poor (60% sensitivity, 88.89% specificity), however, after investigation into some of the discordant results we can assume that this was partly due to the limitations of culture for the diagnosis of PJI (Parvizi et al., 2014a; Tande and Patel, 2014), rather than a failure of CMg. Many of the additional organisms found by routine culture, but not CMg, were common contaminants or resolved by additional clinical review. Taking into account other clinical findings, our pipeline has a potentially high sensitivity (92%) for genuine infections and may be less prone to skin contamination. Contamination, however, is still a risk and correct application of cut-off values is essential for a reliable CMg pipeline (Charalampous et al., 2019; Escobar-Zepeda et al., 2018). Similar studies removed samples which appeared contaminated from their data sets (Ivy et al., 2018; Street et al., 2017). We did not take this approach, but if we had, our specificity would have been higher (90.91%).

A limitation of this work is that we did not routinely generate enough pathogen genome coverage for the detection of AMR genes, as achieved by Charalampous *et al.* using similar methods (Charalampous et al., 2019). This is because the bacterial load was significantly lower in PJI compared to sputum. Antimicrobial susceptibility is an important part of PJI diagnostics as treatment plans are not always guided by pathogen identification alone. Knowledge of pathogen antimicrobial susceptibilities directs appropriate antimicrobial treatment and occasionally the type of surgery performed, for example, infection caused by vancomycin-resistant *Enterococcus* requires removal of the prosthesis or lifelong antibiotic suppression is necessary (Izakovicova et al., 2019).

The MicroDTTect system, while useful for reducing the risk of contamination, does not represent the best approach to sampling. The bags themselves are expensive but this could be overcome by using sonication or in-house DTT treatment as an inexpensive alternative (Sebastian et al., 2018; Tani et al., 2018). The main issue is that sampling requires explanation of the prosthesis, meaning this could not be performed on patients undergoing a DAIR procedure where the prosthesis is retained, nor can diagnosis be performed before the operation. While metagenomics could advise intravenous or oral antibiotic treatment, surgical strategy and local antibiotic treatment (directly into the joint during surgical intervention in beads or PMMA) will have been decided before sampling (Izakovicova et al., 2019). Ideally, diagnosis would be performed before surgical intervention using arthroscopically sampled synovial fluid.

Synovial fluid was a challenging sample type for the application of CMg in our hands. However future work developing the pipeline could yield success if WGA was applied, as used by Ivy *et al.*, who showed species-level detection of known pathogens in 83% of culture-positive PJI samples (Ivy et al., 2018). Synovial fluid was not routinely collected as part of the MicroDTTect study, a more comprehensive set of samples would be required to properly investigate the potential application of our pipeline to synovial fluid samples.

The ideal diagnostic test for PJI diagnosis would combine the three approaches taken in this thesis – pathogen identification, host biomarker detection and pathogen biofilm biomarker detection - in a single test. In fact, it may be sufficient to only detect the pathogen and the host response, as the host response should be absent if the bacteria detected are skin or lab contaminants. Sequencing RNA instead of DNA using metatranscriptomics rather than metagenomics would make this possible (Langelier et al., 2018). Pathogen RNA and host mRNA could be detected in a single test run in the laboratory on synovial fluid taken from suspected PJI patients to guide surgical and antibiotic treatment options. This would represent a step change in how we diagnose and manage PJI and lead to reduced patient morbidity, improved outcomes and reduced healthcare costs. Lateral flow tests with very high NPV (rule-out tests) could be used to classify aseptic cases so that money could be spent accordingly on only sequencing samples from patients who may be infected (Murray, 2017). If synovial fluid CMg can be improved, then all diagnostics could potentially be performed through a less invasive arthroscopy prior to revision surgery. Sequencing could be used

for pathogen identification, followed by confirmation of biofilm gene expression to support findings of any potential commensals.

The primary issue with a synovial fluid-based approach is that pathogens are challenging to detect in this sample type. Infected synovial fluid contains fewer microbial cells than the surrounding tissue, and has been shown to have poor concordance with intraoperative cultures when sampled preoperatively (Schulz et al., 2021), likely driven by the bactericidal properties of hyaluronic acid in the fluid (Gruber et al., 2008; Inman and Chiu, 1996; Pruzanski et al., 1974). Because we would expect a much lower microbial load than in our whole prosthesis sampling, while some pathogens may be consistently detected, others are likely to be missed on occasion. A standalone diagnostic assay needs very high sensitivity and specificity (Power et al., 2013; Souf, 2016).

Combining host and pathogen biomarkers into a single test could offer comprehensive enough results to achieve near perfect test performance. This has already been attempted by Langelier *et al.* in the lung to diagnose LRTIs. By developing a CMg-based method that integrated both host response markers and unbiased microbe detection the authors were able to differentiate LRTI patients from other critically ill patients with non-infectious acute respiratory illnesses (Langelier et al., 2018). The authors examined differential gene expression between patients with and without LRTI to define a host transcriptional signature of LRTI patients with critical illness. Using a combined metric of pathogen identification and host expression profiling to optimize a rule-out algorithm for LRTI the authors reported both a sensitivity and NPV of 100% in a validation set, where the two approaches are effectively able to cover for each other in the event where infection would be missed by a single approach (Langelier et al., 2018). This would be particularly valuable when using synovial fluid, where pathogens may be difficult to detect due to low bacterial load there will be sufficient human RNA to detect host biomarkers.

Discerning respiratory pathogens from background commensal lung microbiota is a key challenge for LRTI diagnosis (Walter and Wunderink, 2017). By contrast, PJI diagnosis does not have this challenge as bone joints are normally sterile sites (Grif et al., 2012). The challenge for PJI diagnosis is instead to differentiate a pathogen from a commensal contaminant, therefore the additional detection of pathogen gene expression, such as biofilm formation markers, are desirable.

While pathogen detection in the absence of host signatures may suggest contamination, biofilm mediated NAS infections can cause very low levels of inflammation which could potentially cause false-negative host transcriptional signatures, as they do with current host biomarkers (Becker et al., 2014; Rewa et al., 2012; Zimmerli et al., 2004). Pathogen biomarkers of biofilm formation may be necessary to resolve these cases.

One of the greatest challenges to the clinician when diagnosing PJI is differentiating pathogens from contaminating organisms (Boyle et al., 2018; Vaishya et al., 2019). To address this problem, we built transposon libraries in NAS for the generation of biofilm mediating gene lists. We applied previously developed electroporation techniques for the transformation of staphylococci (Augustin and Götz, 1990; Cui et al., 2015) to the process of TIS, building on the previous work of groups such as Langridge *et al.* and Van Opijnen *et al.* who used Tn5 and *mariner* transposons to make essential gene lists in S. Typhi and *S. pneumoniae* respectively (Langridge et al., 2009; van Opijnen et al., 2009).

As expected, transforming staphylococci proved extremely challenging as NAS methylation patterns are notoriously restrictive for the introduction of foreign DNA (Ando et al., 2000; Purdy et al., 2002; Wilson, 1991). Developing a single method for transforming multiple species was very ambitious and progress was slow. However, a transposon library of ~250,000 mutants in *S. caprae* was generated by passaging our plasmids through an *S. cohnii* strain that was compatible. A similar approach was taken by Augustin and Götz (1990) to transform *S. epidermidis* with a plasmid extracted from *S. carnosus*. We suggest that this 'snowball' method - plasmid transformations in compatible species to build a plasmid collection with varying methylation profiles that would then be compatible with new NAS species - could be used to make TIS libraries in any bacterial species. Once generated, these libraries could be used to generate biofilm biomarkers for all common PJI pathogens. Biomarker panels are currently used to differentiate bacterial, viral and fungal infections in the diagnosis of sepsis (Dix et al., 2015; Miller et al., 2018; Tsao et al., 2020; Verboom et al., 2019). However, these tests target human biomarkers rather than pathogen biomarkers. To our knowledge, a biomarker assay measuring pathogen gene expression would be a unique approach.

Pooled CRISPRi screening, which silences targeted genes using single-guide RNAs and catalytically dead Cas proteins (first demonstrated using deactivated Cas9 (Qi et al., 2013)), could be used as an alternative to TIS, and has been successfully applied to many bacterial species since its development, such as *S. pneumoniae* (Liu et al., 2017), *B. subtilis* (Peters et al., 2016) and *E. coli* (Rousset et al., 2018; Wang et al., 2018). CRISPRi does not rely on direct genetic manipulation, and as such offers a more robust method for gene function studies than transformation which can be prevented by RM systems (Lee et al., 2019; Peters et al., 2016). Another advantage of CRISPRi over TIS is that silencing is directly targetable to regions of interest, reducing assay complexity and therefore the amount of sequencing required. However, understanding the impact of off-target effects when designing, synthesising and cloning CRISPRi libraries is technically challenging (Cain et al., 2020). By contrast, TIS studies require no specific prior knowledge of the genetic make-up of the target organism, due to its random nature. As such, TIS can be used to uncover novel genes, assay transcriptionally inactive regions of the genome and investigate specific regions within transcriptional units such as essential protein domains (Page et al., 2020).

The field of TIS is constantly expanding from the four initial studies to identify essential gene lists, to practical applications in the development of new vaccine candidates (Carter et al., 2014; Rowe et al., 2019) and new antibiotics/helper drug targets (Jana et al., 2017). Over the last decade, TIS-like methods have been used in fungal, parasitic, archaeal and mammalian cell types (Cain et al., 2020). For example, phenotypic interrogation by tag sequencing (PhITSeq) has been applied in human cells to assign gene function. Through insertion mutagenesis, Carette *et al.* identified host mutations important for virulence factor interactions with a variety of pathogenic Gram-negative bacteria (Carette et al., 2011), influenza, diptheria and exotoxin A (Carette et al., 2009). These methods could potentially be used to discover host gene expression biomarkers for PJI to accompany pathogen biomarkers in the future.

A combined approach for host and pathogen biomarkers would not have to be based on CMg. RTqPCR can be used for human mRNA (Roy et al., 2020) and pathogen mRNA (Gomes et al., 2018) markers to quantify gene expression. This was initially the intended use of any biofilm biomarkers discovered as part of the TIS work, and has been used to characterise *P. aeruginosa* and

S. aureus dual species biofilms (Magalhães et al., 2019). Studies have previously used RTqPCR to diagnose viral infections using both host and pathogen targets in respiratory samples with high accuracy (Brogaard et al., 2015; Landry and Foxman, 2018). However, we believe that CMg is the future of diagnostics as it is more comprehensive than qPCR and will allow for unbiased detection of rare or even novel pathogens. A CMg assay does not need to be updated when new organisms/targets are identified and can be used to identify novel infections, such as SARS-CoV-2 which was identified in a suspected viral pneumonia patient using metagenomic sequencing (Huang et al., 2020).

Whichever platform is used, PJI diagnostics should be developed to rapidly identify infection (host markers), identify the pathogen, pathogenesis (if biofilm biomarkers are present and expressed) and detect antimicrobial resistance. With this information, tailored treatment plans could be chosen without the need for initial empirical treatment and prophylactic antibiotics could be administered before revision and fastidious organisms could be identified, avoiding the challenge of culture negative PJI. This form of rapid diagnostics could potentially improve patient management, reduce hospital costs and reduce both patient morbidity and mortality.

Appendices

Appendix 1

Alexander J. Trotter, Rachael Dean, Celia E. Whitehouse, Jarle Mikalsen, Claire Hill, Roxanne Brunton-Sim, Gemma L. Kay, Majeed Shakokani, Alexander Z. E. Durst, John Wain, Iain McNamara, Justin O'Grady. Preliminary evaluation of a rapid lateral flow calprotectin test for the diagnosis of prosthetic joint infection. Bone Joint Res. 2020;9(5):202–210.

Follow us @BoneJointRes

freely available online OPEN ACCESS

BJR

INFECTION

Preliminary evaluation of a rapid lateral flow calprotectin test for the diagnosis of prosthetic joint infection

A. J. Trotter,
R. Dean,
C. E. Whitehouse,
J. Mikalsen,
C. Hill,
R. Brunton-Sim,
G. L. Kay,
M. Shakokani,
A. Z. E. Durst,
J. Wain,
I. McNamara,
J. O'Grady

University of East Anglia, Norwich, UK

Aims

This pilot study tested the performance of a rapid assay for diagnosing prosthetic joint infection (PJI), which measures synovial fluid calprotectin from total hip and knee revision patients.

Methods

A convenience series of 69 synovial fluid samples from revision patients at the Norfolk and Norwich University Hospital were collected intraoperatively (52 hips, 17 knees) and frozen. Synovial fluid calprotectin was measured retrospectively using a new commercially available lateral flow assay for PJI diagnosis (Lyfstone AS) and compared to International Consensus Meeting (ICM) 2018 criteria and clinical case review (ICM-CR) gold standards.

Results

According to ICM, 24 patients were defined as PJI positive and the remaining 45 were negative. The overall accuracy of the lateral flow test compared to ICM was 75.36% (52/69, 95% CI 63.51% to 84.95%), sensitivity and specificity were 75.00% (18/24, 95% CI 53.29% to 90.23%) and 75.56% (34/45, 95% CI 60.46% to 87.12%), respectively, positive predictive value (PPV) was 62.07% (18/29, 95% CI 48.23% to 74.19%) and negative predictive value (NPV) was 85.00% (34/40, 95% CI 73.54% to 92.04%), and area under the receiver operating characteristic (ROC) curve (AUC) was 0.78 (95% CI 0.66 to 0.87). Patient data from discordant cases were reviewed by the clinical team to develop the ICM-CR gold standard. The lateral flow test performance improved significantly when compared to ICM-CR, with accuracy increasing to 82.61% (57/69, 95% CI 71.59% to 90.68%), sensitivity increasing to 94.74% (18/19, 95% CI 73.97% to 99.87%), NPV increasing to 97.50% (39/40, 95% CI 85.20% to 99.62%), and AUC increasing to 0.91 (95% CI 0.81 to 0.96). Test performance was better in knees (100.00% accurate (17/17, 95% CI 80.49% to 100.00%)) compared to hips (76.92% accurate (40/52, 95% CI 63.16% to 87.47%)).

Conclusion

This study demonstrates that the calprotectin lateral flow assay could be an effective diagnostic test for PJI, however additional prospective studies testing fresh samples are required.

Cite this article: *Bone Joint Res.* 2020;9(5):202–210.

Keywords: Prosthetic joint infection, Calprotectin, Synovial fluid, Rapid diagnostics

Article focus

- Microbiological diagnosis of prosthetic joint infection (PJI) relies on culture techniques that are slow and insensitive. Inflammation biomarkers such as calprotectin have the potential to rapidly diagnose infection. This pilot study tests the performance of a calprotectin lateral flow assay for the diagnosis of PJI using synovial fluid samples.

Key messages

- The lateral flow test has a high negative predictive value (NPV) compared to International Consensus Meeting (ICM) criteria, useful for ruling out infection. The test is highly accurate for diagnosing PJI when compared to a clinical review-based gold standard (ICM-CR).
- The test may be more accurate for diagnosing PJI in knees than in hips.

Correspondence should be sent to A. J. Trotter; email: a.trotter@uea.ac.uk

doi: 10.1302/2046-3758.95.BJR-2019-0213.R1

Bone Joint Res 2020;9:202–210.

Appendix 2

Alexander J Trotter, Alp Aydin, Michael J Strinden and Justin O'Grady. Recent and emerging technologies for the rapid diagnosis of infection and antimicrobial resistance. Current Opinion in Microbiology 2019, 51:39–45
(https://www.sciencedirect.com/science/article/pii/S1369527418301279)

Available online at www.sciencedirect.com
ScienceDirect
Current Opinion in Microbiology

Recent and emerging technologies for the rapid diagnosis of infection and antimicrobial resistance

Alexander J Trotter[1,2], Alp Aydin[1,2], Michael J Strinden[1,2] and Justin O'Grady[1,2]

The rise in antimicrobial resistance (AMR) is predicted to cause 10 million deaths per year by 2050 unless steps are taken to prevent this looming crisis. Microbiological culture is the gold standard for the diagnosis of bacterial/fungal pathogens and antimicrobial resistance and takes 48 hours or longer. Hence, antibiotic prescriptions are rarely based on a definitive diagnosis and patients often receive inappropriate treatment. Rapid diagnostic tools are urgently required to guide appropriate antimicrobial therapy, thereby improving patient outcomes and slowing AMR development. We discuss new technologies for rapid infection diagnosis including: sample-in-answer-out PCR-based tests, BioFire FilmArray and Curetis Unyvero; rapid susceptibility tests, Accelerate Pheno and microfluidic tests; and sequencing-based approaches, focusing on targeted and clinical metagenomic nanopore sequencing.

Addresses
[1] University of East Anglia, Norwich Research Park, Norwich, Norfolk, NR4 7TJ, UK
[2] Quadram Institute Bioscience, Norwich Research Park, Norwich, Norfolk, NR4 7UQ, UK

Corresponding author: O'Grady, Justin (justin.ogrady@quadram.ac.uk)

Current Opinion in Microbiology 2019, **51**:39–45
This review comes from a themed issue on **Antimicrobials**
Edited by **Mattew I Hutchings, Andrew W Truman and Barrie Wilkinson**
For a complete overview see the Issue and the Editorial
Available online 9th May 2019
https://doi.org/10.1016/j.mib.2019.03.001

Introduction

More than 700 000 people die per year globally due to antimicrobial resistance (AMR) according to an estimate from the UK government-commissioned review on AMR (O'Neill report) [1]. At the current rate, by 2050, AMR is predicted to cause 10 million deaths annually and cost the world economy $100 trillion in total. It is widely recognised that rapid diagnostics are crucial in the fight against AMR, to improve the management of life threatening infections such as sepsis and pneumonia and to enable earlier and more precise targeting of pathogens with appropriate antibiotics (i.e. improved antibiotic stewardship) [2]. The final O'Neill report states that by 2020 all antibiotic prescriptions should be supported by a rapid diagnostic test where available [1].

Current standard methods for diagnosing bacterial infection are based on microbiological culture and have long turn-around times, offer poor clinical sensitivity and are not fit-for-purpose for acute serious infection such as sepsis, pneumonia and meningitis. Acute infections force clinicians into early broad-spectrum treatment, before culture results become available, highlighting the need for rapid diagnostics [3–6]. A paradigm shift in diagnostic microbiology is urgently required, with the ultimate goal of providing pathogen identification and resistance/susceptibility information to clinicians before antibiotics are administered.

In this review, we highlight recent and emerging tests for the rapid diagnosis of pathogens, antimicrobial resistance and antimicrobial susceptibility and their current/future clinical applications. We describe some of the current tests that utilise genotypic methods such as PCR for pathogen identification and antibiotic resistance testing. We also describe technologies and techniques that combine pathogen identification with rapid phenotypic antibiotic susceptibility testing (AST). Finally, we outline key advances in the application of DNA sequencing for the rapid diagnosis of infection and AMR that could be implemented clinically in the near future.

Rapid PCR-based pathogen and antimicrobial resistance detection

Discerning bacterial from viral infections is the simplest level of diagnosis that can be clinically useful to guide antimicrobial therapy, reducing unnecessary antibiotic prescriptions. FebriDx® is a dipstick test measuring c-reactive protein and Myxovirus resistance protein A levels in blood, differentiating bacterial from viral infections using an inflammation biomarker [7]. Polymerase chain reaction (PCR)-based systems such as ID Now and cobas® Liat® have specific tests for specific targets such as influenza A&B [8]. However, an ideal diagnostic test will identify the specific pathogen and provide guidance on appropriate antimicrobial therapy. This is particularly important in clinical syndromes such as urinary tract infections (UTIs), pneumonia and sepsis, which can be caused by many different pathogens (bacteria, fungi or

Appendix 3

This is some of the output of my covid work performed as part of COG-UK during my writeup period:

Erik Volz *et al*. Evaluating the Effects of SARS-CoV-2 Spike Mutation D614G on Transmissibility and Pathogenicity. Cell 2021. https://doi.org/10.1016/j.cell.2020.11.020.

Mark S Graham *et al.* Changes in symptomatology, reinfection, and transmissibility associated with the SARS-CoV-2 variant B.1.1.7: an ecological study. The Lancet Public Health 2021. https://doi.org/10.1016/S2468-2667(21)00055-4.

Dave J. Baker *et al*. CoronaHiT: high-throughput sequencing of SARS-CoV-2 genomes. Genome Medicine 2021. https://doi.org/10.1186/s13073-021-00839-5

Andrew J. Page *et al.* Large scale sequencing of SARS-CoV-2 genomes from one region allows detailed epidemiology and enables local outbreak management. medRxiv 2020. https://doi.org/10.1101/2020.09.28.20201475

Eduan Wilkinson *et al.* A year of genomic surveillance reveals how the SARS-CoV-2 pandemic unfolded in Africa. medRxiv 2021. https://doi.org/10.1101/2021.05.12.21257080

Steven Riley *et al.* REACT-1 round 12 report: resurgence of SARS-CoV-2 infections in England

associated with increased frequency of the Delta variant. medRxiv 2021. https://doi.org/10.1101/2021.06.17.21259103

Oliver Eales *et al.* SARS-CoV-2 lineage dynamics in England from January to March 2021 inferred from representative community samples. medRxiv 2021. https://doi.org/10.1101/2021.05.08.21256867

Muhammad Bilal Sarwar *et al.* SARS-CoV-2 variants of concern dominate in Lahore, Pakistan in April 2021. medRxiv 2021. https://doi.org/10.1101/2021.06.04.21258352

Steven Riley *et al.* REACT-1 round 11 report: low prevalence of SARS-CoV-2 infection in the community prior to the third step of the English roadmap out of lockdown. medRxiv 2021. https://doi.org/10.1101/2021.05.13.21257144

The COVID-19 Genomics UK (COG-UK) consortium. An integrated national scale SARS-CoV-2 genomic surveillance network. The Lancet Microbe 2020. https://doi.org/10.1016/S2666-5247(20)30054-9

List of Definitions

AHT	Anhydrous Tetracycline
AL	Aseptic Loosening
AMR	Antimicrobial Resistance
ARMA	Antimicrobial Resistance Mapping Application
AS	Ankylosing Spondylitis
AUC	Area Under the Receiver Operating Characteristic Curve
BHI	Brain Heart Infusion
BLB	Bacterial Lysis Buffer
BMI	Body Mass Index
BSI	Bloodstream Infection
CLL	Chronic Lymphoid Leukaemia
CMg	Clinical Metagenomics
CRP	C-Reactive Protein
DAIR	Debridement, Antibiotics and Implant Retention
DC	Depletion Cocktail
ddNTPs	Dideoxynucleotide Triphosphates
dNTPs	Deoxyribonucleotide Triphosphates
DTT	Dithiothreitol
ECM	Extracellular Matrix
eDNA	Extracellular DNA
EDTA	Ethylenediaminetetraacetic Acid
ELISA	Enzyme-Linked Immunosorbent Assay
ESR	Erythrocyte Sedimentation Rate
FB	Flush Buffer
FLT	Flush Tether
GUI	Graphical User Interface
HHW	Hussain-Hastings-White Media
HITS	High-throughput Insertion Tracking by deep Sequencing
ICM	International Consensus Meeting
ICM-CR	ICM with Clinical Review
IL-1β	Interleukin 1 Beta
IL-6	Interleukin-6
INSeq	Insertion-sequencing
LB	Loading Beads

LE	Leukocyte Esterase
LRTI	Lower Respiratory Tract Infection
MIC	Minimum Inhibitory Concentration
MoM	Metal-on-Metal
MSCRAMMs	Microbial Surface Components Recognising Adhesive Matrix Molecules
MSIS	Musculoskeletal Infection Society
mtDNA	mitochondrial DNA
NAS	Non-Aureus Staphylococci
NF-κB	Nuclear Factor κB
NGS	Next Generation Sequencing
NNUH	Norfolk and Norwich University Hospital
NPV	Negative Predictive Value
PAMPs	Pathogen-Associated Molecular Patterns
PCR	Polymerase Chain Reaction
PIA	Polysaccharide Intercellular Adhesin
PJI	Prosthetic Joint Infection
PLA_2	Phospholipase A_2
PLA1	Phospholipase A1
PLC	Phospholipase-C
PLD	Phospholipase-D
PMMA	Polymethylmethacrylate
POC	Point-of-Care
PPT	Peri-Prosthetic Tissue
PPV	Positive Predictive Value
PRRs	Pathogen Recognition Receptors
QEH	Queen Elizabeth Hospital
RA	Rheumatoid Arthritis
RANK	Receptor Activator of NF-κB
RANKL	Receptor Activator of NF-κB Ligand
ROC	Receiver Operating Characteristic
RT	Reverse Transcription
SQB	Sequencing Buffer
T2DM	Type-2 Diabetes Mellitus
TIS	Transposon Insertion Sequencing
TJA	Total Joint Arthroplasty
TLRs	Toll-Like Receptors

TNF-α	Tumour Necrosis Factor Alpha
TNFs	Tumour Necrosis Factors
Tn-Seq	Transposon Insertion Sequencing
TraDIS	Transposon Directed Insertion-site Sequencing
TSA	Tryptic Soy Agar
TSB	Tryptic Soy Broth
UC	Ulcerative Colitis
UEA	University of East Anglia
UTI	Urinary Tract Infection
WGA	Whole Genome Amplification
WIMP	What's In My Pot

References

8405-Medical-Single.pdf [WWW Document], 2020. URL https://www.ukas.com/wp-content/uploads/schedule_uploads/00007/8405-Medical-Single.pdf (accessed 6.17.21).

10295-Medical-Single.pdf [WWW Document], 2021. URL https://www.ukas.com/wp-content/uploads/schedule_uploads/00007/10295-Medical-Single.pdf (accessed 6.17.21).

Abbas, S., Clohisy, J.C., Abu-Amer, Y., 2003. Mitogen-activated protein (MAP) kinases mediate PMMA-induction of osteoclasts. J. Orthop. Res. Off. Publ. Orthop. Res. Soc. 21, 1041–1048. https://doi.org/10.1016/S0736-0266(03)00081-0

Abdelhamed, H., Lawrence, M.L., Karsi, A., 2015. A novel suicide plasmid for efficient gene mutation in Listeria monocytogenes. Plasmid 81, 1–8. https://doi.org/10.1016/j.plasmid.2015.05.003

Abildtrup, M., Kingsley, G.H., Scott, D.L., 2015. Calprotectin as a biomarker for rheumatoid arthritis: a systematic review. J. Rheumatol. 42, 760–770. https://doi.org/10.3899/jrheum.140628

Abu-Amer, Y., 2005. Advances in osteoclast differentiation and function. Curr. Drug Targets Immune Endocr. Metab. Disord. 5, 347–355. https://doi.org/10.2174/1568008054863808

Accuracy [WWW Document], 2021. URL https://nanoporetech.com/accuracy (accessed 6.20.21).

Achermann, Y., Vogt, M., Leunig, M., Wüst, J., Trampuz, A., 2010. Improved diagnosis of periprosthetic joint infection by multiplex PCR of sonication fluid from removed implants. J. Clin. Microbiol. 48, 1208–1214. https://doi.org/10.1128/JCM.00006-10

Addgene: Vector Database - pT181 [WWW Document], 2021. URL https://www.addgene.org/vector-database/4302/#? (accessed 6.24.21).

Adewale, B.A., 2020. Will long-read sequencing technologies replace short-read sequencing technologies in the next 10 years? Afr. J. Lab. Med. 9, 1340. https://doi.org/10.4102/ajlm.v9i1.1340

Ahmed, S.S., Haddad, F.S., 2019. Prosthetic joint infection. Bone Jt. Res. 8, 570–572. https://doi.org/10.1302/2046-3758.812.BJR-2019-0340

Al Amir Dache, Z., Otandault, A., Tanos, R., Pastor, B., Meddeb, R., Sanchez, C., Arena, G., Lasorsa, L., Bennett, A., Grange, T., El Messaoudi, S., Mazard, T., Prevostel, C., Thierry, A.R., 2020. Blood contains circulating cell-free respiratory competent mitochondria. FASEB J. Off. Publ. Fed. Am. Soc. Exp. Biol. 34, 3616–3630. https://doi.org/10.1096/fj.201901917RR

Alamanda, V.K., Springer, B.D., 2019. The prevention of infection: 12 modifiable risk factors. Bone Jt. J. 101-B, 3–9. https://doi.org/10.1302/0301-620X.101B1.BJJ-2018-0233.R1

Alamanda, V.K., Springer, B.D., 2018. Perioperative and Modifiable Risk Factors for Periprosthetic Joint Infections (PJI) and Recommended Guidelines. Curr. Rev. Musculoskelet. Med. 11, 325–331. https://doi.org/10.1007/s12178-018-9494-z

Alberts, B., Johnson, A., Lewis, J., Raff, M., Roberts, K., Walter, P., 2002. Molecular Biology of the Cell, 4th ed. Garland Science.

Alijanipour, P., Bakhshi, H., Parvizi, J., 2013. Diagnosis of periprosthetic joint infection: the threshold for serological markers. Clin. Orthop. 471, 3186–3195. https://doi.org/10.1007/s11999-013-3070-z

Allicock, O.M., Guo, C., Uhlemann, A.-C., Whittier, S., Chauhan, L.V., Garcia, J., Price, A., Morse, S.S., Mishra, N., Briese, T., Lipkin, W.I., 2018. BacCapSeq: a Platform for Diagnosis and Characterization of Bacterial Infections. mBio 9, e02007-18. https://doi.org/10.1128/mBio.02007-18

Allignet, J., Galdbart, J.-O., Morvan, A., Dyke, K.G.H., Vaudaux, P., Aubert, S., Desplaces, N., Solh, N.E., 1999. Tracking adhesion factors in Staphylococcus caprae strains responsible for human bone infections following implantation of orthopaedic material. Microbiol. Read. Engl. 145 (Pt 8), 2033–2042. https://doi.org/10.1099/13500872-145-8-2033

Amarasinghe, S.L., Su, S., Dong, X., Zappia, L., Ritchie, M.E., Gouil, Q., 2020. Opportunities and challenges in long-read sequencing data analysis. Genome Biol. 21, 30. https://doi.org/10.1186/s13059-020-1935-5

Ando, T., Xu, Q., Torres, M., Kusugami, K., Israel, D.A., Blaser, M.J., 2000. Restriction-modification system differences in Helicobacter pylori are a barrier to interstrain plasmid transfer. Mol. Microbiol. 37, 1052–1065. https://doi.org/10.1046/j.1365-2958.2000.02049.x

Anscombe, C., Misra, R.V., Gharbia, S., 2018. Whole genome amplification and sequencing of low cell numbers directly from a bacteria spiked blood model. bioRxiv 153965. https://doi.org/10.1101/153965

Antypas, H., Choong, F.X., Libberton, B., Brauner, A., Richter-Dahlfors, A., 2018. Rapid diagnostic assay for detection of cellulose in urine as biomarker for biofilm-related urinary tract infections. NPJ Biofilms Microbiomes 4, 26. https://doi.org/10.1038/s41522-018-0069-y

Ashton, P.M., Nair, S., Dallman, T., Rubino, S., Rabsch, W., Mwaigwisya, S., Wain, J., O'Grady, J., 2015. MinION nanopore sequencing identifies the position and structure of a bacterial antibiotic resistance island. Nat. Biotechnol. 33, 296–300. https://doi.org/10.1038/nbt.3103

Aslam, S., Reitman, C., Darouiche, R.O., 2010. Risk factors for subsequent diagnosis of prosthetic joint infection. Infect. Control Hosp. Epidemiol. 31, 298–301. https://doi.org/10.1086/650756

Atkins, B.L., Athanasou, N., Deeks, J.J., Crook, D.W., Simpson, H., Peto, T.E., McLardy-Smith, P., Berendt, A.R., 1998. Prospective evaluation of criteria for microbiological diagnosis of prosthetic-joint infection at revision arthroplasty. The OSIRIS Collaborative Study Group. J. Clin. Microbiol. 36, 2932–2939. https://doi.org/10.1128/JCM.36.10.2932-2939.1998

Auerbach, C., 1973. History of Research on Chemical Mutagenesis, in: Hollaender, A. (Ed.), Chemical Mutagens: Principles and Methods for Their Detection Volume 3. Springer US, Boston, MA, pp. 1–19. https://doi.org/10.1007/978-1-4615-8972-3_1

Augustin, J., Götz, F., 1990. Transformation of Staphylococcus epidermidis and other staphylococcal species with plasmid DNA by electroporation. FEMS Microbiol. Lett. 66, 203–207. https://doi.org/10.1111/j.1574-6968.1990.tb03997.x

Ayala-Torres, S., Chen, Y., Svoboda, T., Rosenblatt, J., Van Houten, B., 2000. Analysis of Gene-Specific DNA Damage and Repair Using Quantitative Polymerase Chain Reaction. Methods 22, 135–147. https://doi.org/10.1006/meth.2000.1054

Azeredo, J., Azevedo, N.F., Briandet, R., Cerca, N., Coenye, T., Costa, A.R., Desvaux, M., Di Bonaventura, G., Hébraud, M., Jaglic, Z., Kačániová, M., Knøchel, S., Lourenço, A., Mergulhão, F., Meyer, R.L., Nychas, G., Simões, M., Tresse, O., Sternberg, C., 2017. Critical review on biofilm methods. Crit. Rev. Microbiol. 43, 313–351. https://doi.org/10.1080/1040841X.2016.1208146

Bae, T., Schneewind, O., 2006. Allelic replacement in Staphylococcus aureus with inducible counter-selection. Plasmid 55, 58–63. https://doi.org/10.1016/j.plasmid.2005.05.005

Banin, E., Brady, K.M., Greenberg, E.P., 2006. Chelator-induced dispersal and killing of Pseudomonas aeruginosa cells in a biofilm. Appl. Environ. Microbiol. 72, 2064–2069. https://doi.org/10.1128/AEM.72.3.2064-2069.2006

Barquist, L., Boinett, C.J., Cain, A.K., 2013a. Approaches to querying bacterial genomes with transposon-insertion sequencing. RNA Biol. 10, 1161–1169. https://doi.org/10.4161/rna.24765

Barquist, L., Langridge, G.C., Turner, D.J., Phan, M.D., Turner, A.K., Bateman, A., Parkhill, J., Wain, J., Gardner, P.P., 2013b. A comparison of dense transposon insertion libraries in the Salmonella serovars Typhi and Typhimurium. Nucleic Acids Res. 41, 4549–4564. https://doi.org/10.1093/nar/gkt148

Barrack, R.L., Burnett, R.S.J., Sharkey, P., Parvizi, J., 2007. Diagnosing an infection: an unsolved problem. Orthopedics 30, 777–778. https://doi.org/10.3928/01477447-20070901-07

Basnet, H., Massague, J., 2019. Labeling and Isolation of Fluorouracil Tagged RNA by Cytosine Deaminase Expression. Bio-Protoc. 9, e3433. https://doi.org/10.21769/BioProtoc.3433

Bastos, M.L., Tavaziva, G., Abidi, S.K., Campbell, J.R., Haraoui, L.-P., Johnston, J.C., Lan, Z., Law, S., MacLean, E., Trajman, A., Menzies, D., Benedetti, A., Khan, F.A., 2020. Diagnostic accuracy of serological tests for covid-19: systematic review and meta-analysis. BMJ 370, m2516. https://doi.org/10.1136/bmj.m2516

Bäumer, C., Fisch, E., Wedler, H., Reinecke, F., Korfhage, C., 2018. Exploring DNA quality of single cells for genome analysis with simultaneous whole-genome amplification. Sci. Rep. 8, 7476. https://doi.org/10.1038/s41598-018-25895-7

Beceiro, A., Tomás, M., Bou, G., 2013. Antimicrobial resistance and virulence: a successful or deleterious association in the bacterial world? Clin. Microbiol. Rev. 26, 185–230. https://doi.org/10.1128/CMR.00059-12

Becker, K., Heilmann, C., Peters, G., 2014. Coagulase-negative staphylococci. Clin. Microbiol. Rev. 27, 870–926. https://doi.org/10.1128/CMR.00109-13

Bejon, P., Berendt, A., Atkins, B.L., Green, N., Parry, H., Masters, S., McLardy-Smith, P., Gundle, R., Byren, I., 2010. Two-stage revision for prosthetic joint infection: predictors of outcome and the role of reimplantation microbiology. J. Antimicrob. Chemother. 65, 569–575. https://doi.org/10.1093/jac/dkp469

Bengtson, S., Knutson, K., 1991. The infected knee arthroplasty. A 6-year follow-up of 357 cases. Acta Orthop. Scand. 62, 301–311. https://doi.org/10.3109/17453679108994458

Berbari, E.F., Hanssen, A.D., Duffy, M.C., Steckelberg, J.M., Ilstrup, D.M., Harmsen, W.S., Osmon, D.R., 1998. Risk factors for prosthetic joint infection: case-control study. Clin. Infect. Dis. Off. Publ. Infect. Dis. Soc. Am. 27, 1247–1254. https://doi.org/10.1086/514991

Berbari, E.F., Marculescu, C., Sia, I., Lahr, B.D., Hanssen, A.D., Steckelberg, J.M., Gullerud, R., Osmon, D.R., 2007. Culture-negative prosthetic joint infection. Clin. Infect. Dis. Off. Publ. Infect. Dis. Soc. Am. 45, 1113–1119. https://doi.org/10.1086/522184

Berbari, E.F., Osmon, D.R., Carr, A., Hanssen, A.D., Baddour, L.M., Greene, D., Kupp, L.I., Baughan, L.W., Harmsen, W.S., Mandrekar, J.N., Therneau, T.M., Steckelberg, J.M., Virk, A., Wilson, W.R., 2010. Dental procedures as risk factors for prosthetic hip or knee infection: a hospital-based prospective case-control study. Clin. Infect. Dis. Off. Publ. Infect. Dis. Soc. Am. 50, 8–16. https://doi.org/10.1086/648676

Berend, K.R., Lombardi, A.V., Morris, M.J., Bergeson, A.G., Adams, J.B., Sneller, M.A., 2013. Two-stage treatment of hip periprosthetic joint infection is associated with a high rate of infection control but high mortality. Clin. Orthop. 471, 510–518. https://doi.org/10.1007/s11999-012-2595-x

Berg, D.E., Davies, J., Allet, B., Rochaix, J.D., 1975. Transposition of R factor genes to bacteriophage lambda. Proc. Natl. Acad. Sci. U. S. A. 72, 3628–3632. https://doi.org/10.1073/pnas.72.9.3628

Bertelli, C., Greub, G., 2013. Rapid bacterial genome sequencing: methods and applications in clinical microbiology. Clin. Microbiol. Infect. Off. Publ. Eur. Soc. Clin. Microbiol. Infect. Dis. 19, 803–813. https://doi.org/10.1111/1469-0691.12217

Beswick, A.D., Elvers, K.T., Smith, A.J., Gooberman-Hill, R., Lovering, A., Blom, A.W., 2012. What is the evidence base to guide surgical treatment of infected hip prostheses? systematic review of longitudinal studies in unselected patients. BMC Med. 10, 18. https://doi.org/10.1186/1741-7015-10-18

Beutler, B., 2009. Microbe sensing, positive feedback loops, and the pathogenesis of inflammatory diseases. Immunol. Rev. 227, 248–263. https://doi.org/10.1111/j.1600-065X.2008.00733.x

Bingham, J., Clarke, H., Spangehl, M., Schwartz, A., Beauchamp, C., Goldberg, B., 2014. The alpha defensin-1 biomarker assay can be used to evaluate the potentially infected total joint arthroplasty. Clin. Orthop. 472, 4006–4009. https://doi.org/10.1007/s11999-014-3900-7

Biring, G.S., Kostamo, T., Garbuz, D.S., Masri, B.A., Duncan, C.P., 2009. Two-stage revision arthroplasty of the hip for infection using an interim articulated Prostalac hip spacer: a 10- to 15-year follow-up study. J. Bone Joint Surg. Br. 91, 1431–1437. https://doi.org/10.1302/0301-620X.91B11.22026

Bissinger, R., Modicano, P., Alzoubi, K., Honisch, S., Faggio, C., Abed, M., Lang, F., 2014. Effect of saponin on erythrocytes. Int. J. Hematol. 100, 51–59. https://doi.org/10.1007/s12185-014-1605-z

Bjarnsholt, T., Alhede, Maria, Alhede, Morten, Eickhardt-Sørensen, S.R., Moser, C., Kühl, M., Jensen, P.Ø., Høiby, N., 2013. The in vivo biofilm. Trends Microbiol. 21, 466–474. https://doi.org/10.1016/j.tim.2013.06.002

Bonanzinga, T., Ferrari, M.C., Tanzi, G., Vandenbulcke, F., Zahar, A., Marcacci, M., 2019. The role of alpha defensin in prosthetic joint infection (PJI) diagnosis: a literature review. EFORT Open Rev. 4, 10–13. https://doi.org/10.1302/2058-5241.4.180029

Bonanzinga, T., Zahar, A., Dütsch, M., Lausmann, C., Kendoff, D., Gehrke, T., 2017. How Reliable Is the Alpha-defensin Immunoassay Test for Diagnosing Periprosthetic Joint Infection? A Prospective Study. Clin. Orthop. 475, 408–415. https://doi.org/10.1007/s11999-016-4906-0

Bongartz, T., Halligan, C.S., Osmon, D.R., Reinalda, M.S., Bamlet, W.R., Crowson, C.S., Hanssen, A.D., Matteson, E.L., 2008. Incidence and risk factors of prosthetic joint infection after total hip or knee replacement in patients with rheumatoid arthritis. Arthritis Rheum. 59, 1713–1720. https://doi.org/10.1002/art.24060

Both, A., Klatte, T.O., Lübke, A., Büttner, H., Hartel, M.J., Grossterlinden, L.G., Rohde, H., 2018. Growth of Cutibacterium acnes is common on osteosynthesis material of the shoulder in patients without signs of infection. Acta Orthop. 89, 580–584. https://doi.org/10.1080/17453674.2018.1489095

Boyce, B.F., Xiu, Y., Li, J., Xing, L., Yao, Z., 2015. NF-κB-Mediated Regulation of Osteoclastogenesis. Endocrinol. Metab. Seoul Korea 30, 35–44. https://doi.org/10.3803/EnM.2015.30.1.35

Boyle, K.K., Wood, S., Tarity, T.D., 2018. Low-Virulence Organisms and Periprosthetic Joint Infection-Biofilm Considerations of These Organisms. Curr. Rev. Musculoskelet. Med. 11, 409–419. https://doi.org/10.1007/s12178-018-9503-2

Bozic, K.J., Ries, M.D., 2005. The impact of infection after total hip arthroplasty on hospital and surgeon resource utilization. J. Bone Joint Surg. Am. 87, 1746–1751. https://doi.org/10.2106/JBJS.D.02937

Breitwieser, F.P., Lu, J., Salzberg, S.L., 2019. A review of methods and databases for metagenomic classification and assembly. Brief. Bioinform. 20, 1125–1136. https://doi.org/10.1093/bib/bbx120

Brogaard, L., Klitgaard, K., Heegaard, P.M., Hansen, M.S., Jensen, T.K., Skovgaard, K., 2015. Concurrent host-pathogen gene expression in the lungs of pigs challenged with Actinobacillus pleuropneumoniae. BMC Genomics 16, 417. https://doi.org/10.1186/s12864-015-1557-6

Brown, S.D., Nolan, P.M., 1998. Mouse mutagenesis-systematic studies of mammalian gene function. Hum. Mol. Genet. 7, 1627–1633. https://doi.org/10.1093/hmg/7.10.1627

Brown, S.D., Peters, J., 1996. Combining mutagenesis and genomics in the mouse--closing the phenotype gap. Trends Genet. TIG 12, 433–435. https://doi.org/10.1016/0168-9525(96)30094-2

Cai, Y., Fang, X., Zhang, L., Yang, X., Nie, L., Huang, Z., Li, W., Zhang, C., Yang, B., Guan, Z., Zhang, W., 2021. Microbial yield from infectious tissues pretreated by various methods: an invitro study. BMC Musculoskelet. Disord. 22, 209. https://doi.org/10.1186/s12891-021-04071-5

Cain, A.K., Barquist, L., Goodman, A.L., Paulsen, I.T., Parkhill, J., van Opijnen, T., 2020. A decade of advances in transposon-insertion sequencing. Nat. Rev. Genet. 21, 526–540. https://doi.org/10.1038/s41576-020-0244-x

Cappelli, G., Ricardi, M., Ravera, F., Ligabue, G., Ballestri, M., Bonucchi, D., Bondi, M., 2007. Biofilm on artificial surfaces. Contrib. Nephrol. 154, 61–71. https://doi.org/10.1159/000096814

Carette, J.E., Guimaraes, C.P., Varadarajan, M., Park, A.S., Wuethrich, I., Godarova, A., Kotecki, M., Cochran, B.H., Spooner, E., Ploegh, H.L., Brummelkamp, T.R., 2009. Haploid genetic screens in human cells identify host factors used by pathogens. Science 326, 1231–1235. https://doi.org/10.1126/science.1178955

Carette, J.E., Guimaraes, C.P., Wuethrich, I., Blomen, V.A., Varadarajan, M., Sun, C., Bell, G., Yuan, B., Muellner, M.K., Nijman, S.M., Ploegh, H.L., Brummelkamp, T.R., 2011. Global gene

disruption in human cells to assign genes to phenotypes by deep sequencing. Nat. Biotechnol. 29, 542–546. https://doi.org/10.1038/nbt.1857

Carter, R., Wolf, J., van Opijnen, T., Muller, M., Obert, C., Burnham, C., Mann, B., Li, Y., Hayden, R.T., Pestina, T., Persons, D., Camilli, A., Flynn, P.M., Tuomanen, E.I., Rosch, J.W., 2014. Genomic analyses of pneumococci from children with sickle cell disease expose host-specific bacterial adaptations and deficits in current interventions. Cell Host Microbe 15, 587–599. https://doi.org/10.1016/j.chom.2014.04.005

Cazanave, C., Greenwood-Quaintance, K.E., Hanssen, A.D., Karau, M.J., Schmidt, S.M., Gomez Urena, E.O., Mandrekar, J.N., Osmon, D.R., Lough, L.E., Pritt, B.S., Steckelberg, J.M., Patel, R., 2013. Rapid molecular microbiologic diagnosis of prosthetic joint infection. J. Clin. Microbiol. 51, 2280–2287. https://doi.org/10.1128/JCM.00335-13

Cerca, N., Martins, S., Cerca, F., Jefferson, K.K., Pier, G.B., Oliveira, R., Azeredo, J., 2005. Comparative assessment of antibiotic susceptibility of coagulase-negative staphylococci in biofilm versus planktonic culture as assessed by bacterial enumeration or rapid XTT colorimetry. J. Antimicrob. Chemother. 56, 331–336. https://doi.org/10.1093/jac/dki217

Chao, M.C., Abel, S., Davis, B.M., Waldor, M.K., 2016. The design and analysis of transposon insertion sequencing experiments. Nat. Rev. Microbiol. 14, 119–128. https://doi.org/10.1038/nrmicro.2015.7

Charalampous, T., Kay, G.L., Richardson, H., Aydin, A., Baldan, R., Jeanes, C., Rae, D., Grundy, S., Turner, D.J., Wain, J., Leggett, R.M., Livermore, D.M., O'Grady, J., 2019. Nanopore metagenomics enables rapid clinical diagnosis of bacterial lower respiratory infection. Nat. Biotechnol. 37, 783–792. https://doi.org/10.1038/s41587-019-0156-5

Chavakis, E., Choi, E.Y., Chavakis, T., 2009. Novel aspects in the regulation of the leukocyte adhesion cascade. Thromb. Haemost. 102, 191–197. https://doi.org/10.1160/TH08-12-0844

Chavakis, T., Wiechmann, K., Preissner, K.T., Herrmann, M., 2005. Staphylococcus aureus interactions with the endothelium: the role of bacterial "secretable expanded repertoire adhesive molecules" (SERAM) in disturbing host defense systems. Thromb. Haemost. 94, 278–285. https://doi.org/10.1160/TH05-05-0306

Chen, P.-S., Shih, Y.-W., Huang, H.-C., Cheng, H.-W., 2011. Diosgenin, a steroidal saponin, inhibits migration and invasion of human prostate cancer PC-3 cells by reducing matrix metalloproteinases expression. PloS One 6, e20164. https://doi.org/10.1371/journal.pone.0020164

Chernow, B., Zaloga, G.P., Soldano, S., Quinn, A., Lyons, P., McFadden, E., Cook, D., Rainey, T.G., 1984. Measurement of urinary leukocyte esterase activity: a screening test for urinary

tract infections. Ann. Emerg. Med. 13, 150–154. https://doi.org/10.1016/s0196-0644(84)80603-4

Chiu, C.Y., Miller, S.A., 2019. Clinical metagenomics. Nat. Rev. Genet. 20, 341–355. https://doi.org/10.1038/s41576-019-0113-7

Christen, B., Abeliuk, E., Collier, J.M., Kalogeraki, V.S., Passarelli, B., Coller, J.A., Fero, M.J., McAdams, H.H., Shapiro, L., 2011. The essential genome of a bacterium. Mol. Syst. Biol. 7, 528. https://doi.org/10.1038/msb.2011.58

Chua, K.Y.L., Stinear, T.P., Howden, B.P., 2013. Functional genomics of Staphylococcus aureus. Brief. Funct. Genomics 12, 305–315. https://doi.org/10.1093/bfgp/elt006

Clarridge, J.E., 2004. Impact of 16S rRNA gene sequence analysis for identification of bacteria on clinical microbiology and infectious diseases. Clin. Microbiol. Rev. 17, 840–862, table of contents. https://doi.org/10.1128/CMR.17.4.840-862.2004

Clauss, M., Trampuz, A., Borens, O., Bohner, M., Ilchmann, T., 2010. Biofilm formation on bone grafts and bone graft substitutes: comparison of different materials by a standard in vitro test and microcalorimetry. Acta Biomater. 6, 3791–3797. https://doi.org/10.1016/j.actbio.2010.03.011

Clohisy, J.C., Calvert, G., Tull, F., McDonald, D., Maloney, W.J., 2004. Reasons for revision hip surgery: a retrospective review. Clin. Orthop. 188–192. https://doi.org/10.1097/01.blo.0000150126.73024.42

Cobo, J., Miguel, L.G.S., Euba, G., Rodríguez, D., García-Lechuz, J.M., Riera, M., Falgueras, L., Palomino, J., Benito, N., del Toro, M.D., Pigrau, C., Ariza, J., 2011. Early prosthetic joint infection: outcomes with debridement and implant retention followed by antibiotic therapy. Clin. Microbiol. Infect. Off. Publ. Eur. Soc. Clin. Microbiol. Infect. Dis. 17, 1632–1637. https://doi.org/10.1111/j.1469-0691.2010.03333.x

Comfort, N.C., 2001. From controlling elements to transposons: Barbara McClintock and the Nobel Prize. Trends Biochem. Sci. 26, 454–457. https://doi.org/10.1016/s0968-0004(01)01898-9

Conlon, K.M., Humphreys, H., O'Gara, J.P., 2004. Inactivations of rsbU and sarA by IS256 represent novel mechanisms of biofilm phenotypic variation in Staphylococcus epidermidis. J. Bacteriol. 186, 6208–6219. https://doi.org/10.1128/JB.186.18.6208-6219.2004

Costerton, J.W., Stewart, P.S., Greenberg, E.P., 1999. Bacterial biofilms: a common cause of persistent infections. Science 284, 1318–1322. https://doi.org/10.1126/science.284.5418.1318

Couto, N., Schuele, L., Raangs, E.C., Machado, M.P., Mendes, C.I., Jesus, T.F., Chlebowicz, M., Rosema, S., Ramirez, M., Carriço, J.A., Autenrieth, I.B., Friedrich, A.W., Peter, S., Rossen, J.W., 2018. Critical steps in clinical shotgun metagenomics for the concomitant detection

and typing of microbial pathogens. Sci. Rep. 8, 13767. https://doi.org/10.1038/s41598-018-31873-w

COVID-19 Genomics UK (COG-UK) consortium, 2020. An integrated national scale SARS-CoV-2 genomic surveillance network. Lancet Microbe 1, e99–e100. https://doi.org/10.1016/S2666-5247(20)30054-9

Cruz-Loya, M., Kang, T.M., Lozano, N.A., Watanabe, R., Tekin, E., Damoiseaux, R., Savage, V.M., Yeh, P.J., 2019. Stressor interaction networks suggest antibiotic resistance co-opted from stress responses to temperature. ISME J. 13, 12–23. https://doi.org/10.1038/s41396-018-0241-7

Cucarella, C., Solano, C., Valle, J., Amorena, B., Lasa, I., Penadés, J.R., 2001. Bap, a Staphylococcus aureus surface protein involved in biofilm formation. J. Bacteriol. 183, 2888–2896. https://doi.org/10.1128/JB.183.9.2888-2896.2001

Cui, B., Smooker, P.M., Rouch, D.A., Deighton, M.A., 2015. Enhancing DNA electro-transformation efficiency on a clinical Staphylococcus capitis isolate. J. Microbiol. Methods 109, 25–30. https://doi.org/10.1016/j.mimet.2014.11.012

da Fonseca, A.J., Galvão, R.S., Miranda, A.E., Ferreira, L.C. de L., Chen, Z., 2016. Comparison of three human papillomavirus DNA detection methods: Next generation sequencing, multiplex-PCR and nested-PCR followed by Sanger based sequencing. J. Med. Virol. 88, 888–894. https://doi.org/10.1002/jmv.24413

Dale, H., Fenstad, A.M., Hallan, G., Havelin, L.I., Furnes, O., Overgaard, S., Pedersen, A.B., Kärrholm, J., Garellick, G., Pulkkinen, P., Eskelinen, A., Mäkelä, K., Engesæter, L.B., 2012. Increasing risk of prosthetic joint infection after total hip arthroplasty. Acta Orthop. 83, 449–458. https://doi.org/10.3109/17453674.2012.733918

Deamer, D., Akeson, M., Branton, D., 2016. Three decades of nanopore sequencing. Nat. Biotechnol. 34, 518–524. https://doi.org/10.1038/nbt.3423

Deshpande, S.V., Reed, T.M., Sullivan, R.F., Kerkhof, L.J., Beigel, K.M., Wade, M.M., 2019. Offline Next Generation Metagenomics Sequence Analysis Using MinION Detection Software (MINDS). Genes 10, E578. https://doi.org/10.3390/genes10080578

Ding, T., Ledingham, J., Luqmani, R., Westlake, S., Hyrich, K., Lunt, M., Kiely, P., Bukhari, M., Abernethy, R., Bosworth, A., Ostor, A., Gadsby, K., McKenna, F., Finney, D., Dixey, J., Deighton, C., Standards, Audit and Guidelines Working Group of BSR Clinical Affairs Committee, BHPR, 2010. BSR and BHPR rheumatoid arthritis guidelines on safety of anti-TNF therapies. Rheumatol. Oxf. Engl. 49, 2217–2219. https://doi.org/10.1093/rheumatology/keq249a

Dix, A., Hünniger, K., Weber, M., Guthke, R., Kurzai, O., Linde, J., 2015. Biomarker-based classification of bacterial and fungal whole-blood infections in a genome-wide expression study. Front. Microbiol. 6. https://doi.org/10.3389/fmicb.2015.00171

Donlan, R.M., 2002. Biofilms: microbial life on surfaces. Emerg. Infect. Dis. 8, 881–890. https://doi.org/10.3201/eid0809.020063

Donlan, R.M., Costerton, J.W., 2002. Biofilms: survival mechanisms of clinically relevant microorganisms. Clin. Microbiol. Rev. 15, 167–193. https://doi.org/10.1128/CMR.15.2.167-193.2002

Doughty, E.L., Sergeant, M.J., Adetifa, I., Antonio, M., Pallen, M.J., 2014. Culture-independent detection and characterisation of Mycobacterium tuberculosis and M. africanum in sputum samples using shotgun metagenomics on a benchtop sequencer. PeerJ 2, e585. https://doi.org/10.7717/peerj.585

Drago, L., Romanò, C.L., Mattina, R., Signori, V., De Vecchi, E., 2012. Does dithiothreitol improve bacterial detection from infected prostheses? A pilot study. Clin. Orthop. 470, 2915–2925. https://doi.org/10.1007/s11999-012-2415-3

Drake, J.W., 1991. Spontaneous mutation. Annu. Rev. Genet. 25, 125–146. https://doi.org/10.1146/annurev.ge.25.120191.001013

Drummond, J., Tran, P., Fary, C., 2015. Metal-on-Metal Hip Arthroplasty: A Review of Adverse Reactions and Patient Management. J. Funct. Biomater. 6, 486–499. https://doi.org/10.3390/jfb6030486

Duff, G.P., Lachiewicz, P.F., Kelley, S.S., 1996. Aspiration of the knee joint before revision arthroplasty. Clin. Orthop. 132–139. https://doi.org/10.1097/00003086-199610000-00018

Dunkelberger, J.R., Song, W.-C., 2010. Complement and its role in innate and adaptive immune responses. Cell Res. 20, 34–50. https://doi.org/10.1038/cr.2009.139

Eisenstein, M., 2012. Oxford Nanopore announcement sets sequencing sector abuzz. Nat. Biotechnol. 30, 295–296. https://doi.org/10.1038/nbt0412-295

Escobar-Zepeda, A., Godoy-Lozano, E.E., Raggi, L., Segovia, L., Merino, E., Gutiérrez-Rios, R.M., Juarez, K., Licea-Navarro, A.F., Pardo-Lopez, L., Sanchez-Flores, A., 2018. Analysis of sequencing strategies and tools for taxonomic annotation: Defining standards for progressive metagenomics. Sci. Rep. 8, 12034. https://doi.org/10.1038/s41598-018-30515-5

Evangelopoulos, D.S., Stathopoulos, I.P., Morassi, G.P., Koufos, S., Albarni, A., Karampinas, P.K., Stylianakis, A., Kohl, S., Pneumaticos, S., Vlamis, J., 2013. Sonication: a valuable technique for diagnosis and treatment of periprosthetic joint infections. ScientificWorldJournal 2013, 375140. https://doi.org/10.1155/2013/375140

Feehery, G.R., Yigit, E., Oyola, S.O., Langhorst, B.W., Schmidt, V.T., Stewart, F.J., Dimalanta, E.T., Amaral-Zettler, L.A., Davis, T., Quail, M.A., Pradhan, S., 2013. A method for selectively enriching microbial DNA from contaminating vertebrate host DNA. PloS One 8, e76096. https://doi.org/10.1371/journal.pone.0076096

Fernández-Sampedro, M., Fariñas-Alvarez, C., Garces-Zarzalejo, C., Alonso-Aguirre, M.A., Salas-Venero, C., Martínez-Martínez, L., Fariñas, M.C., 2017. Accuracy of different diagnostic tests for early, delayed and late prosthetic joint infection. BMC Infect. Dis. 17, 592. https://doi.org/10.1186/s12879-017-2693-1

Ferrero-Miliani, L., Nielsen, O.H., Andersen, P.S., Girardin, S.E., 2007. Chronic inflammation: importance of NOD2 and NALP3 in interleukin-1beta generation. Clin. Exp. Immunol. 147, 227–235. https://doi.org/10.1111/j.1365-2249.2006.03261.x

Fey, P.D., Olson, M.E., 2010. Current concepts in biofilm formation of Staphylococcus epidermidis. Future Microbiol. 5, 917–933. https://doi.org/10.2217/fmb.10.56

Finotello, F., Di Camillo, B., 2015. Measuring differential gene expression with RNA-seq: challenges and strategies for data analysis. Brief. Funct. Genomics 14, 130–142. https://doi.org/10.1093/bfgp/elu035

Foster, T.J., Geoghegan, J.A., Ganesh, V.K., Höök, M., 2014. Adhesion, invasion and evasion: the many functions of the surface proteins of Staphylococcus aureus. Nat. Rev. Microbiol. 12, 49–62. https://doi.org/10.1038/nrmicro3161

Francis, G., Kerem, Z., Makkar, H.P.S., Becker, K., 2002. The biological action of saponins in animal systems: a review. Br. J. Nutr. 88, 587–605. https://doi.org/10.1079/BJN2002725

Franco-Duarte, R., Černáková, L., Kadam, S., Kaushik, K.S., Salehi, B., Bevilacqua, A., Corbo, M.R., Antolak, H., Dybka-Stępień, K., Leszczewicz, M., Relison Tintino, S., Alexandrino de Souza, V.C., Sharifi-Rad, J., Coutinho, H.D.M., Martins, N., Rodrigues, C.F., 2019. Advances in Chemical and Biological Methods to Identify Microorganisms-From Past to Present. Microorganisms 7, E130. https://doi.org/10.3390/microorganisms7050130

Freed, N.E., 2017. Creation of a Dense Transposon Insertion Library Using Bacterial Conjugation in Enterobacterial Strains Such As Escherichia Coli or Shigella flexneri. J. Vis. Exp. JoVE. https://doi.org/10.3791/56216

Fukumoto, H., Sato, Y., Hasegawa, H., Saeki, H., Katano, H., 2015. Development of a new real-time PCR system for simultaneous detection of bacteria and fungi in pathological samples. Int. J. Clin. Exp. Pathol. 8, 15479–15488.

Gabay, C., Kushner, I., 1999. Acute-phase proteins and other systemic responses to inflammation. N. Engl. J. Med. 340, 448–454. https://doi.org/10.1056/NEJM199902113400607

Gajewska, J., Chajęcka-Wierzchowska, W., 2020. Biofilm Formation Ability and Presence of Adhesion Genes among Coagulase-Negative and Coagulase-Positive Staphylococci Isolates

from Raw Cow's Milk. Pathog. Basel Switz. 9, E654. https://doi.org/10.3390/pathogens9080654

Gallo, J., Kamínek, P., Tichá, V., Riháková, P., Ditmar, R., 2002. Particle disease. A comprehensive theory of periprosthetic osteolysis: a review. Biomed. Pap. Med. Fac. Univ. Palacky Olomouc Czechoslov. 146, 21–28. https://doi.org/10.5507/bp.2002.004

Gawronski, J.D., Wong, S.M.S., Giannoukos, G., Ward, D.V., Akerley, B.J., 2009. Tracking insertion mutants within libraries by deep sequencing and a genome-wide screen for Haemophilus genes required in the lung. Proc. Natl. Acad. Sci. https://doi.org/10.1073/pnas.0906627106

Gelb, H., Schumacher, H.R., Cuckler, J., Ducheyne, P., Baker, D.G., 1994. In vivo inflammatory response to polymethylmethacrylate particulate debris: effect of size, morphology, and surface area. J. Orthop. Res. Off. Publ. Orthop. Res. Soc. 12, 83–92. https://doi.org/10.1002/jor.1100120111

George, C.G., Kloos, W.E., 1994. Comparison of the SmaI-digested chromosomes of Staphylococcus epidermidis and the closely related species Staphylococcus capitis and Staphylococcus caprae. Int. J. Syst. Bacteriol. 44, 404–409. https://doi.org/10.1099/00207713-44-3-404

German Collection of Microorganisms and Cell Cultures GmbH: Details [WWW Document], 2021. URL https://www.dsmz.de/collection/catalogue/details/culture/DSM-4911 (accessed 6.24.21).

Ghosh, S., May, M.J., Kopp, E.B., 1998. NF-kappa B and Rel proteins: evolutionarily conserved mediators of immune responses. Annu. Rev. Immunol. 16, 225–260. https://doi.org/10.1146/annurev.immunol.16.1.225

GISAID - Submission Tracker Global [WWW Document], 2021. URL https://www.gisaid.org (accessed 6.20.21).

Goldring, S.R., 2002. Bone and joint destruction in rheumatoid arthritis: what is really happening? J. Rheumatol. Suppl. 65, 44–48.

Goldring, S.R., Clark, C.R., Wright, T.M., 1993. The problem in total joint arthroplasty: aseptic loosening. J. Bone Joint Surg. Am. 75, 799–801. https://doi.org/10.2106/00004623-199306000-00001

Gomes, A.É.I., Stuchi, L.P., Siqueira, N.M.G., Henrique, J.B., Vicentini, R., Ribeiro, M.L., Darrieux, M., Ferraz, L.F.C., 2018. Selection and validation of reference genes for gene expression studies in Klebsiella pneumoniae using Reverse Transcription Quantitative real-time PCR. Sci. Rep. 8, 9001. https://doi.org/10.1038/s41598-018-27420-2

Goodman, A.L., McNulty, N.P., Zhao, Y., Leip, D., Mitra, R.D., Lozupone, C.A., Knight, R., Gordon, J.I., 2009. Identifying genetic determinants needed to establish a human gut symbiont in its habitat. Cell Host Microbe 6, 279–289. https://doi.org/10.1016/j.chom.2009.08.003

Goswami, K., Parvizi, J., Maxwell Courtney, P., 2018. Current Recommendations for the Diagnosis of Acute and Chronic PJI for Hip and Knee-Cell Counts, Alpha-Defensin, Leukocyte Esterase, Next-generation Sequencing. Curr. Rev. Musculoskelet. Med. 11, 428–438. https://doi.org/10.1007/s12178-018-9513-0

Götz, F., Ahrné, S., Lindberg, M., 1981. Plasmid transfer and genetic recombination by protoplast fusion in staphylococci. J. Bacteriol. 145, 74–81. https://doi.org/10.1128/jb.145.1.74-81.1981

Götz, F., Kreutz, B., Schleifer, K.H., 1983. Protoplast transformation of Staphylococcus carnosus by plasmid DNA. Mol. Gen. Genet. MGG 189, 340–342. https://doi.org/10.1007/BF00337828

Grammatopoulos, G., Bolduc, M.-E., Atkins, B.L., Kendrick, B.J.L., McLardy-Smith, P., Murray, D.W., Gundle, R., Taylor, A.H., 2017. Functional outcome of debridement, antibiotics and implant retention in periprosthetic joint infection involving the hip: a case-control study. Bone Jt. J. 99-B, 614–622. https://doi.org/10.1302/0301-620X.99B5.BJJ-2016-0562.R2

Greninger, A.L., 2018. The challenge of diagnostic metagenomics. Expert Rev. Mol. Diagn. 18, 605–615. https://doi.org/10.1080/14737159.2018.1487292

Greninger, A.L., Naccache, S.N., Federman, S., Yu, G., Mbala, P., Bres, V., Stryke, D., Bouquet, J., Somasekar, S., Linnen, J.M., Dodd, R., Mulembakani, P., Schneider, B.S., Muyembe-Tamfum, J.-J., Stramer, S.L., Chiu, C.Y., 2015. Rapid metagenomic identification of viral pathogens in clinical samples by real-time nanopore sequencing analysis. Genome Med. 7, 99. https://doi.org/10.1186/s13073-015-0220-9

Grif, K., Heller, I., Prodinger, W.M., Lechleitner, K., Lass-Flörl, C., Orth, D., 2012. Improvement of Detection of Bacterial Pathogens in Normally Sterile Body Sites with a Focus on Orthopedic Samples by Use of a Commercial 16S rRNA Broad-Range PCR and Sequence Analysis. J. Clin. Microbiol. 50, 2250–2254. https://doi.org/10.1128/JCM.00362-12

Griffith, F., 1928. The Significance of Pneumococcal Types. J. Hyg. (Lond.) 27, 113–159. https://doi.org/10.1017/s0022172400031879

Griffiths, A.J., Miller, J.H., Suzuki, D.T., Lewontin, R.C., Gelbart, W.M., Griffiths, A.J., Miller, J.H., Suzuki, D.T., Lewontin, R.C., Gelbart, W.M., 2000. An Introduction to Genetic Analysis, 7th ed. W. H. Freeman.

Gross, M., Cramton, S.E., Götz, F., Peschel, A., 2001. Key role of teichoic acid net charge in Staphylococcus aureus colonization of artificial surfaces. Infect. Immun. 69, 3423–3426. https://doi.org/10.1128/IAI.69.5.3423-3426.2001

Gruber, B.F., Miller, B.S., Onnen, J., Welling, R.D., Welling, R., Wojtys, E.M., 2008. Antibacterial properties of synovial fluid in the knee. J. Knee Surg. 21, 180–185. https://doi.org/10.1055/s-0030-1247816

Gunnarsdóttir, R., Müller, K., Jensen, P.E., Jenssen, P.D., Villumsen, A., 2012. Effect of long-term freezing and freeze-thaw cycles on indigenous and inoculated microorganisms in dewatered blackwater. Environ. Sci. Technol. 46, 12408–12416. https://doi.org/10.1021/es3018489

Gupta, S., Mortensen, M.S., Schjørring, S., Trivedi, U., Vestergaard, G., Stokholm, J., Bisgaard, H., Krogfelt, K.A., Sørensen, S.J., 2019. Amplicon sequencing provides more accurate microbiome information in healthy children compared to culturing. Commun. Biol. 2, 291. https://doi.org/10.1038/s42003-019-0540-1

Hanahan, D., 1983. Studies on transformation of Escherichia coli with plasmids. J. Mol. Biol. 166, 557–580. https://doi.org/10.1016/S0022-2836(83)80284-8

Hansford, B.G., Stacy, G.S., 2012. Musculoskeletal aspiration procedures. Semin. Interv. Radiol. 29, 270–285. https://doi.org/10.1055/s-0032-1330061

Harris, L.G., El-Bouri, K., Johnston, S., Rees, E., Frommelt, L., Siemssen, N., Christner, M., Davies, A.P., Rohde, H., Mack, D., 2010. Rapid identification of staphylococci from prosthetic joint infections using MALDI-TOF mass-spectrometry. Int. J. Artif. Organs 33, 568–574. https://doi.org/10.1177/039139881003300902

Hartley, J.C., Harris, K.A., 2014. Molecular techniques for diagnosing prosthetic joint infections. J. Antimicrob. Chemother. 69 Suppl 1, i21-24. https://doi.org/10.1093/jac/dku249

Hayes, F., 2003. Transposon-based strategies for microbial functional genomics and proteomics. Annu. Rev. Genet. 37, 3–29. https://doi.org/10.1146/annurev.genet.37.110801.142807

Heather, J.M., Chain, B., 2016. The sequence of sequencers: The history of sequencing DNA. Genomics 107, 1–8. https://doi.org/10.1016/j.ygeno.2015.11.003

Hensel, M., Shea, J.E., Gleeson, C., Jones, M.D., Dalton, E., Holden, D.W., 1995. Simultaneous identification of bacterial virulence genes by negative selection. Science 269, 400–403. https://doi.org/10.1126/science.7618105

Holinka, J., Bauer, L., Hirschl, A.M., Graninger, W., Windhager, R., Presterl, E., 2011. Sonication cultures of explanted components as an add-on test to routinely conducted microbiological diagnostics improve pathogen detection. J. Orthop. Res. Off. Publ. Orthop. Res. Soc. 29, 617–622. https://doi.org/10.1002/jor.21286

Holland, L.M., Conlon, B., O'Gara, J.P., 2011. Mutation of tagO reveals an essential role for wall teichoic acids in Staphylococcus epidermidis biofilm development. Microbiol. Read. Engl. 157, 408–418. https://doi.org/10.1099/mic.0.042234-0

http://www.microdttect.com/ [WWW Document], 2021. URL http://www.microdttect.com/ (accessed 6.20.21).

Huang, C., Wang, Y., Li, X., Ren, L., Zhao, J., Hu, Y., Zhang, L., Fan, G., Xu, J., Gu, X., Cheng, Z., Yu, T., Xia, J., Wei, Y., Wu, W., Xie, X., Yin, W., Li, H., Liu, M., Xiao, Y., Gao, H., Guo, L., Xie, J., Wang, G., Jiang, R., Gao, Z., Jin, Q., Wang, J., Cao, B., 2020. Clinical features of patients infected with 2019 novel coronavirus in Wuhan, China. The Lancet 395, 497–506. https://doi.org/10.1016/S0140-6736(20)30183-5

Huang, W., Wang, G., Yin, C., Chen, D., Dhand, A., Chanza, M., Dimitrova, N., Fallon, J.T., 2019. Optimizing a Whole-Genome Sequencing Data Processing Pipeline for Precision Surveillance of Health Care-Associated Infections. Microorganisms 7, E388. https://doi.org/10.3390/microorganisms7100388

Hughes, H.C., Newnham, R., Athanasou, N., Atkins, B.L., Bejon, P., Bowler, I.C.J.W., 2011. Microbiological diagnosis of prosthetic joint infections: a prospective evaluation of four bacterial culture media in the routine laboratory. Clin. Microbiol. Infect. Off. Publ. Eur. Soc. Clin. Microbiol. Infect. Dis. 17, 1528–1530. https://doi.org/10.1111/j.1469-0691.2011.03597.x

Hussain, M., Hastings, J.G., White, P.J., 1991. A chemically defined medium for slime production by coagulase-negative staphylococci. J. Med. Microbiol. 34, 143–147. https://doi.org/10.1099/00222615-34-3-143

Inman, R.D., Chiu, B., 1996. Comparative microbicidal activity of synovial fluid on arthritogenic organisms. Clin. Exp. Immunol. 104, 80–85. https://doi.org/10.1046/j.1365-2249.1996.d01-650.x

Innerhofer, P., Klingler, A., Klimmer, C., Fries, D., Nussbaumer, W., 2005. Risk for postoperative infection after transfusion of white blood cell-filtered allogeneic or autologous blood components in orthopedic patients undergoing primary arthroplasty. Transfusion (Paris) 45, 103–110. https://doi.org/10.1111/j.1537-2995.2005.04149.x

Ip, C.L.C., Loose, M., Tyson, J.R., de Cesare, M., Brown, B.L., Jain, M., Leggett, R.M., Eccles, D.A., Zalunin, V., Urban, J.M., Piazza, P., Bowden, R.J., Paten, B., Mwaigwisya, S., Batty, E.M., Simpson, J.T., Snutch, T.P., Birney, E., Buck, D., Goodwin, S., Jansen, H.J., O'Grady, J., Olsen, H.E., MinION Analysis and Reference Consortium, 2015. MinION Analysis and Reference Consortium: Phase 1 data release and analysis. F1000Research 4, 1075. https://doi.org/10.12688/f1000research.7201.1

Ivy, M.I., Thoendel, M.J., Jeraldo, P.R., Greenwood-Quaintance, K.E., Hanssen, A.D., Abdel, M.P., Chia, N., Yao, J.Z., Tande, A.J., Mandrekar, J.N., Patel, R., 2018. Direct Detection and Identification of Prosthetic Joint Infection Pathogens in Synovial Fluid by Metagenomic

Shotgun Sequencing. J. Clin. Microbiol. 56, e00402-18. https://doi.org/10.1128/JCM.00402-18

Izakovicova, P., Borens, O., Trampuz, A., 2019. Periprosthetic joint infection: current concepts and outlook. EFORT Open Rev. 4, 482–494. https://doi.org/10.1302/2058-5241.4.180092

Izano, E.A., Amarante, M.A., Kher, W.B., Kaplan, J.B., 2008. Differential roles of poly-N-acetylglucosamine surface polysaccharide and extracellular DNA in Staphylococcus aureus and Staphylococcus epidermidis biofilms. Appl. Environ. Microbiol. 74, 470–476. https://doi.org/10.1128/AEM.02073-07

Jain, M., Koren, S., Miga, K.H., Quick, J., Rand, A.C., Sasani, T.A., Tyson, J.R., Beggs, A.D., Dilthey, A.T., Fiddes, I.T., Malla, S., Marriott, H., Nieto, T., O'Grady, J., Olsen, H.E., Pedersen, B.S., Rhie, A., Richardson, H., Quinlan, A.R., Snutch, T.P., Tee, L., Paten, B., Phillippy, A.M., Simpson, J.T., Loman, N.J., Loose, M., 2018. Nanopore sequencing and assembly of a human genome with ultra-long reads. Nat. Biotechnol. 36, 338–345. https://doi.org/10.1038/nbt.4060

Jana, B., Cain, A.K., Doerrler, W.T., Boinett, C.J., Fookes, M.C., Parkhill, J., Guardabassi, L., 2017. The secondary resistome of multidrug-resistant Klebsiella pneumoniae. Sci. Rep. 7, 42483. https://doi.org/10.1038/srep42483

Janeway, C.A., 1989. Approaching the asymptote? Evolution and revolution in immunology. Cold Spring Harb. Symp. Quant. Biol. 54 Pt 1, 1–13. https://doi.org/10.1101/sqb.1989.054.01.003

Järvinen, A.-K., Laakso, S., Piiparinen, P., Aittakorpi, A., Lindfors, M., Huopaniemi, L., Piiparinen, H., Mäki, M., 2009. Rapid identification of bacterial pathogens using a PCR- and microarray-based assay. BMC Microbiol. 9, 161. https://doi.org/10.1186/1471-2180-9-161

Johnson, J.S., Spakowicz, D.J., Hong, B.-Y., Petersen, L.M., Demkowicz, P., Chen, L., Leopold, S.R., Hanson, B.M., Agresta, H.O., Gerstein, M., Sodergren, E., Weinstock, G.M., 2019. Evaluation of 16S rRNA gene sequencing for species and strain-level microbiome analysis. Nat. Commun. 10, 5029. https://doi.org/10.1038/s41467-019-13036-1

Jones, M.J., Donegan, N.P., Mikheyeva, I.V., Cheung, A.L., 2015. Improving Transformation of Staphylococcus aureus Belonging to the CC1, CC5 and CC8 Clonal Complexes. PLOS ONE 10, e0119487. https://doi.org/10.1371/journal.pone.0119487

Joshi, H., Jain, V., 2017. Novel method to rapidly and efficiently lyse Escherichia coli for the isolation of recombinant protein. Anal. Biochem. 528, 1–6. https://doi.org/10.1016/j.ab.2017.04.009

Kang, M., Ko, Y.-P., Liang, X., Ross, C.L., Liu, Q., Murray, B.E., Höök, M., 2013. Collagen-binding microbial surface components recognizing adhesive matrix molecule (MSCRAMM) of

Gram-positive bacteria inhibit complement activation via the classical pathway. J. Biol. Chem. 288, 20520–20531. https://doi.org/10.1074/jbc.M113.454462

Karbysheva, S., Di Luca, M., Butini, M.E., Winkler, T., Schütz, M., Trampuz, A., 2020. Comparison of sonication with chemical biofilm dislodgement methods using chelating and reducing agents: Implications for the microbiological diagnosis of implant associated infection. PloS One 15, e0231389. https://doi.org/10.1371/journal.pone.0231389

Karbysheva, S., Grigoricheva, L., Golnik, V., Popov, S., Renz, N., Trampuz, A., 2019. Influence of retrieved hip- and knee-prosthesis biomaterials on microbial detection by sonication. Eur. Cell. Mater. 37, 16–22. https://doi.org/10.22203/eCM.v037a02

Kawai, T., Akira, S., 2007. Signaling to NF-kappaB by Toll-like receptors. Trends Mol. Med. 13, 460–469. https://doi.org/10.1016/j.molmed.2007.09.002

Keegan, G.M., Learmonth, I.D., Case, C.P., 2007. Orthopaedic metals and their potential toxicity in the arthroplasty patient. J. Bone Joint Surg. Br. 89-B, 567–573. https://doi.org/10.1302/0301-620X.89B5.18903

Kelsic, E.D., Zhao, J., Vetsigian, K., Kishony, R., 2015. Counteraction of antibiotic production and degradation stabilizes microbial communities. Nature 521, 516–519. https://doi.org/10.1038/nature14485

Kempthorne, J.T., Ailabouni, R., Raniga, S., Hammer, D., Hooper, G., 2015. Occult Infection in Aseptic Joint Loosening and the Diagnostic Role of Implant Sonication. BioMed Res. Int. 2015, 946215. https://doi.org/10.1155/2015/946215

Kessler, H.H., Mühlbauer, G., Stelzl, E., Daghofer, E., Santner, B.I., Marth, E., 2001. Fully automated nucleic acid extraction: MagNA Pure LC. Clin. Chem. 47, 1124–1126.

Khatiwara, A., Jiang, T., Sung, S.-S., Dawoud, T., Kim, J.N., Bhattacharya, D., Kim, H.-B., Ricke, S.C., Kwon, Y.M., 2012. Genome Scanning for Conditionally Essential Genes in Salmonella enterica Serotype Typhimurium. Appl. Environ. Microbiol. 78, 3098–3107. https://doi.org/10.1128/AEM.06865-11

Khatoon, Z., McTiernan, C.D., Suuronen, E.J., Mah, T.-F., Alarcon, E.I., 2018. Bacterial biofilm formation on implantable devices and approaches to its treatment and prevention. Heliyon 4, e01067. https://doi.org/10.1016/j.heliyon.2018.e01067

Khosla, S., 2001. Minireview: the OPG/RANKL/RANK system. Endocrinology 142, 5050–5055. https://doi.org/10.1210/endo.142.12.8536

Kim, D., Song, L., Breitwieser, F.P., Salzberg, S.L., 2016. Centrifuge: rapid and sensitive classification of metagenomic sequences. Genome Res. 26, 1721–1729. https://doi.org/10.1101/gr.210641.116

Kim, H., Chung, D.-R., Kang, M., 2019. A new point-of-care test for the diagnosis of infectious diseases based on multiplex lateral flow immunoassays. The Analyst 144, 2460–2466. https://doi.org/10.1039/c8an02295j

Kishore, U., Reid, K.B.M., 2007. Collectins and Pentraxins, in: Brown, G.D., Netea, M.G. (Eds.), Immunology of Fungal Infections. Springer Netherlands, Dordrecht, pp. 151–176. https://doi.org/10.1007/1-4020-5492-0_7

Klindworth, A., Pruesse, E., Schweer, T., Peplies, J., Quast, C., Horn, M., Glöckner, F.O., 2013. Evaluation of general 16S ribosomal RNA gene PCR primers for classical and next-generation sequencing-based diversity studies. Nucleic Acids Res. 41, e1–e1. https://doi.org/10.1093/nar/gks808

Klouche, S., Sariali, E., Mamoudy, P., 2010. Total hip arthroplasty revision due to infection: a cost analysis approach. Orthop. Traumatol. Surg. Res. OTSR 96, 124–132. https://doi.org/10.1016/j.rcot.2010.02.005

Kodym, A., Afza, R., 2003. Physical and Chemical Mutagenesis, in: Grotewold, E. (Ed.), Plant Functional Genomics, Methods in Molecular Biology™. Humana Press, Totowa, NJ, pp. 189–203. https://doi.org/10.1385/1-59259-413-1:189

Korber, F., Zeller, I., Grünstäudl, M., Willinger, B., Apfalter, P., Hirschl, A.M., Makristathis, A., 2017. SeptiFast versus blood culture in clinical routine - A report on 3 years experience. Wien. Klin. Wochenschr. 129, 427–434. https://doi.org/10.1007/s00508-017-1181-3

Krismer, B., Nega, M., Thumm, G., Götz, F., Peschel, A., 2012. Highly efficient Staphylococcus carnosus mutant selection system based on suicidal bacteriocin activation. Appl. Environ. Microbiol. 78, 1148–1156. https://doi.org/10.1128/AEM.06290-11

Kunin, V., Copeland, A., Lapidus, A., Mavromatis, K., Hugenholtz, P., 2008. A bioinformatician's guide to metagenomics. Microbiol. Mol. Biol. Rev. MMBR 72, 557–578, Table of Contents. https://doi.org/10.1128/MMBR.00009-08

Kurd, M.F., Ghanem, E., Steinbrecher, J., Parvizi, J., 2010. Two-stage Exchange Knee Arthroplasty: Does Resistance of the Infecting Organism Influence the Outcome? Clin. Orthop. Relat. Res. 468, 2060–2066. https://doi.org/10.1007/s11999-010-1296-6

Kurtz, S., Ong, K., Lau, E., Mowat, F., Halpern, M., 2007. Projections of primary and revision hip and knee arthroplasty in the United States from 2005 to 2030. J. Bone Joint Surg. Am. 89, 780–785. https://doi.org/10.2106/JBJS.F.00222

Kurtz, S.M., Lau, E., Watson, H., Schmier, J.K., Parvizi, J., 2012. Economic burden of periprosthetic joint infection in the United States. J. Arthroplasty 27, 61-65.e1. https://doi.org/10.1016/j.arth.2012.02.022

Lacey, D.L., Timms, E., Tan, H.L., Kelley, M.J., Dunstan, C.R., Burgess, T., Elliott, R., Colombero, A., Elliott, G., Scully, S., Hsu, H., Sullivan, J., Hawkins, N., Davy, E., Capparelli, C., Eli, A., Qian,

Y.X., Kaufman, S., Sarosi, I., Shalhoub, V., Senaldi, G., Guo, J., Delaney, J., Boyle, W.J., 1998. Osteoprotegerin ligand is a cytokine that regulates osteoclast differentiation and activation. Cell 93, 165–176. https://doi.org/10.1016/s0092-8674(00)81569-x

Lafeuille, E., Jauréguiberry, S., Devriese, F., Sadowski, E., Fourniols, E., Aubry, A., CRIOAC Pitié-Salpêtrière, 2021. First evaluation of the automated-multiplex-PCR Unyvero ITI G2 cartridge for rapid diagnosis of osteo-articular infections. Infect. Dis. Now 51, 179–186. https://doi.org/10.1016/j.medmal.2020.09.010

Lam, J., Abu-Amer, Y., Nelson, C.A., Fremont, D.H., Ross, F.P., Teitelbaum, S.L., 2002. Tumour necrosis factor superfamily cytokines and the pathogenesis of inflammatory osteolysis. Ann. Rheum. Dis. 61 Suppl 2, ii82-83. https://doi.org/10.1136/ard.61.suppl_2.ii82

Landry, M.L., Foxman, E.F., 2018. Antiviral Response in the Nasopharynx Identifies Patients With Respiratory Virus Infection. J. Infect. Dis. 217, 897–905. https://doi.org/10.1093/infdis/jix648

Langelier, C., Kalantar, K.L., Moazed, F., Wilson, M.R., Crawford, E.D., Deiss, T., Belzer, A., Bolourchi, S., Caldera, S., Fung, M., Jauregui, A., Malcolm, K., Lyden, A., Khan, L., Vessel, K., Quan, J., Zinter, M., Chiu, C.Y., Chow, E.D., Wilson, J., Miller, S., Matthay, M.A., Pollard, K.S., Christenson, S., Calfee, C.S., DeRisi, J.L., 2018. Integrating host response and unbiased microbe detection for lower respiratory tract infection diagnosis in critically ill adults. Proc. Natl. Acad. Sci. 115, E12353–E12362.

Langridge, G.C., Phan, M.-D., Turner, D.J., Perkins, T.T., Parts, L., Haase, J., Charles, I., Maskell, D.J., Peters, S.E., Dougan, G., Wain, J., Parkhill, J., Turner, A.K., 2009. Simultaneous assay of every Salmonella Typhi gene using one million transposon mutants. Genome Res. 19, 2308–2316. https://doi.org/10.1101/gr.097097.109

Le, K.Y., Park, M.D., Otto, M., 2018. Immune Evasion Mechanisms of Staphylococcus epidermidis Biofilm Infection. Front. Microbiol. 9, 359. https://doi.org/10.3389/fmicb.2018.00359

Lee, H.H., Ostrov, N., Wong, B.G., Gold, M.A., Khalil, A.S., Church, G.M., 2019. Functional genomics of the rapidly replicating bacterium Vibrio natriegens by CRISPRi. Nat. Microbiol. 4, 1105–1113. https://doi.org/10.1038/s41564-019-0423-8

Leggett, R.M., Alcon-Giner, C., Heavens, D., Caim, S., Brook, T.C., Kujawska, M., Martin, S., Peel, N., Acford-Palmer, H., Hoyles, L., Clarke, P., Hall, L.J., Clark, M.D., 2020. Rapid MinION profiling of preterm microbiota and antimicrobial-resistant pathogens. Nat. Microbiol. 5, 430–442. https://doi.org/10.1038/s41564-019-0626-z

Levy, P.Y., Fenollar, F., Stein, A., Borrione, F., Cohen, E., Lebail, B., Raoult, D., 2008. Propionibacterium acnes postoperative shoulder arthritis: an emerging clinical entity. Clin. Infect. Dis. Off. Publ. Infect. Dis. Soc. Am. 46, 1884–1886. https://doi.org/10.1086/588477

Ley, K., Laudanna, C., Cybulsky, M.I., Nourshargh, S., 2007. Getting to the site of inflammation: the leukocyte adhesion cascade updated. Nat. Rev. Immunol. 7, 678–689. https://doi.org/10.1038/nri2156

Li, C., Renz, N., Trampuz, A., 2018. Management of Periprosthetic Joint Infection. Hip Pelvis 30, 138–146. https://doi.org/10.5371/hp.2018.30.3.138

Li, C., Renz, N., Trampuz, A., Ojeda-Thies, C., 2020. Twenty common errors in the diagnosis and treatment of periprosthetic joint infection. Int. Orthop. 44, 3–14. https://doi.org/10.1007/s00264-019-04426-7

Liabaud, B., Patrick, D.A., Geller, J.A., 2013. Higher body mass index leads to longer operative time in total knee arthroplasty. J. Arthroplasty 28, 563–565. https://doi.org/10.1016/j.arth.2012.07.037

Lin, L., Song, H., Ji, Y., He, Z., Pu, Y., Zhou, J., Xu, J., 2010. Ultrasound-mediated DNA transformation in thermophilic gram-positive anaerobes. PloS One 5, e12582. https://doi.org/10.1371/journal.pone.0012582

Lin, M.H., Shu, J.C., Lin, L.P., Chong, K.Y., Cheng, Y.W., Du, J.F., Liu, S.-T., 2015. Elucidating the crucial role of poly N-acetylglucosamine from Staphylococcus aureus in cellular adhesion and pathogenesis. PloS One 10, e0124216. https://doi.org/10.1371/journal.pone.0124216

Liu, C.M., Aziz, M., Kachur, S., Hsueh, P.-R., Huang, Y.-T., Keim, P., Price, L.B., 2012. BactQuant: An enhanced broad-coverage bacterial quantitative real-time PCR assay. BMC Microbiol. 12, 56. https://doi.org/10.1186/1471-2180-12-56

Liu, C.-W., Kuo, C.-L., Chuang, S.-Y., Chang, J.-H., Wu, C.-C., Tsai, T.-Y., Lin, L.-C., 2013. Results of infected total knee arthroplasty treated with arthroscopic debridement and continuous antibiotic irrigation system. Indian J. Orthop. 47, 93–97. https://doi.org/10.4103/0019-5413.106925

Liu, X., Gallay, C., Kjos, M., Domenech, A., Slager, J., van Kessel, S.P., Knoops, K., Sorg, R.A., Zhang, J.-R., Veening, J.-W., 2017. High-throughput CRISPRi phenotyping identifies new essential genes in Streptococcus pneumoniae. Mol. Syst. Biol. 13, 931. https://doi.org/10.15252/msb.20167449

Löfblom, J., Kronqvist, N., Uhlén, M., Ståhl, S., Wernérus, H., 2007. Optimization of electroporation-mediated transformation: Staphylococcus carnosus as model organism. J. Appl. Microbiol. 102, 736–747. https://doi.org/10.1111/j.1365-2672.2006.03127.x

Logsdon, G.A., Vollger, M.R., Hsieh, P., Mao, Y., Liskovykh, M.A., Koren, S., Nurk, S., Mercuri, L., Dishuck, P.C., Rhie, A., de Lima, L.G., Dvorkina, T., Porubsky, D., Harvey, W.T., Mikheenko, A., Bzikadze, A.V., Kremitzki, M., Graves-Lindsay, T.A., Jain, C., Hoekzema, K., Murali, S.C., Munson, K.M., Baker, C., Sorensen, M., Lewis, A.M., Surti, U., Gerton, J.L., Larionov, V., Ventura, M., Miga, K.H., Phillippy, A.M., Eichler, E.E., 2021. The structure, function and

evolution of a complete human chromosome 8. Nature 593, 101–107. https://doi.org/10.1038/s41586-021-03420-7

Loman, N.J., Misra, R.V., Dallman, T.J., Constantinidou, C., Gharbia, S.E., Wain, J., Pallen, M.J., 2012. Performance comparison of benchtop high-throughput sequencing platforms. Nat. Biotechnol. 30, 434–439. https://doi.org/10.1038/nbt.2198

Lorent, J.H., Quetin-Leclercq, J., Mingeot-Leclercq, M.-P., 2014. The amphiphilic nature of saponins and their effects on artificial and biological membranes and potential consequences for red blood and cancer cells. Org. Biomol. Chem. 12, 8803–8822. https://doi.org/10.1039/c4ob01652a

Lu, G., Li, T., Ye, H., Liu, S., Zhang, P., Wang, W., 2020. D-dimer in the diagnosis of periprosthetic joint infection: a systematic review and meta-analysis. J. Orthop. Surg. 15, 265. https://doi.org/10.1186/s13018-020-01761-z

Lyfstone Calprotectin [WWW Document], lyfstone.com/. . lyfstone.com. URL http://localhost:8000/lyfstone-calprotectin/ (accessed 6.17.21).

Magalhães, A.P., França, Â., Pereira, M.O., Cerca, N., 2019. RNA-based qPCR as a tool to quantify and to characterize dual-species biofilms. Sci. Rep. 9, 13639. https://doi.org/10.1038/s41598-019-50094-3

Mahmud, T., Lyons, M.C., Naudie, D.D., Macdonald, S.J., McCalden, R.W., 2012. Assessing the gold standard: a review of 253 two-stage revisions for infected TKA. Clin. Orthop. 470, 2730–2736. https://doi.org/10.1007/s11999-012-2358-8

Malandain, D., Bémer, P., Leroy, A.G., Léger, J., Plouzeau, C., Valentin, A.S., Jolivet-Gougeon, A., Tandé, D., Héry-Arnaud, G., Lemarié, C., Kempf, M., Bret, L., Burucoa, C., Corvec, S., Centre de Référence des Infections Ostéo-articulaires du Grand Ouest (CRIOGO) Study Team, 2018. Assessment of the automated multiplex-PCR Unyvero i60 ITI® cartridge system to diagnose prosthetic joint infection: a multicentre study. Clin. Microbiol. Infect. Off. Publ. Eur. Soc. Clin. Microbiol. Infect. Dis. 24, 83.e1-83.e6. https://doi.org/10.1016/j.cmi.2017.05.017

Malekzadeh, D., Osmon, D.R., Lahr, B.D., Hanssen, A.D., Berbari, E.F., 2010. Prior use of antimicrobial therapy is a risk factor for culture-negative prosthetic joint infection. Clin. Orthop. 468, 2039–2045. https://doi.org/10.1007/s11999-010-1338-0

Malinzak, R.A., Ritter, M.A., Berend, M.E., Meding, J.B., Olberding, E.M., Davis, K.E., 2009. Morbidly obese, diabetic, younger, and unilateral joint arthroplasty patients have elevated total joint arthroplasty infection rates. J. Arthroplasty 24, 84–88. https://doi.org/10.1016/j.arth.2009.05.016

Manekar, S.C., Sathe, S.R., 2018. A benchmark study of k-mer counting methods for high-throughput sequencing. GigaScience 7. https://doi.org/10.1093/gigascience/giy125

Mann, B., van Opijnen, T., Wang, J., Obert, C., Wang, Y.-D., Carter, R., McGoldrick, D.J., Ridout, G., Camilli, A., Tuomanen, E.I., Rosch, J.W., 2012. Control of virulence by small RNAs in Streptococcus pneumoniae. PLoS Pathog. 8, e1002788. https://doi.org/10.1371/journal.ppat.1002788

Marculescu, C.E., Cantey, J.R., 2008. Polymicrobial prosthetic joint infections: risk factors and outcome. Clin. Orthop. 466, 1397–1404. https://doi.org/10.1007/s11999-008-0230-7

Mardis, E.R., 2017. DNA sequencing technologies: 2006-2016. Nat. Protoc. 12, 213–218. https://doi.org/10.1038/nprot.2016.182

Marshak-Rothstein, A., 2006. Toll-like receptors in systemic autoimmune disease. Nat. Rev. Immunol. 6, 823–835. https://doi.org/10.1038/nri1957

Marson, B.A., Deshmukh, S.R., Grindlay, D.J.C., Scammell, B.E., 2018. Alpha-defensin and the Synovasure lateral flow device for the diagnosis of prosthetic joint infection: a systematic review and meta-analysis. Bone Jt. J. 100-B, 703–711. https://doi.org/10.1302/0301-620X.100B6.BJJ-2017-1563.R1

Martínez-García, E., Aparicio, T., de Lorenzo, V., Nikel, P.I., 2014. New transposon tools tailored for metabolic engineering of gram-negative microbial cell factories. Front. Bioeng. Biotechnol. 2, 46. https://doi.org/10.3389/fbioe.2014.00046

Martner, A., Dahlgren, C., Paton, J.C., Wold, A.E., 2008. Pneumolysin released during Streptococcus pneumoniae autolysis is a potent activator of intracellular oxygen radical production in neutrophils. Infect. Immun. 76, 4079–4087. https://doi.org/10.1128/IAI.01747-07

Mathers, K.E., Staples, J.F., 2015. Saponin-permeabilization is not a viable alternative to isolated mitochondria for assessing oxidative metabolism in hibernation. Biol. Open 4, 858–864. https://doi.org/10.1242/bio.011544

Matthews, P.C., Berendt, A.R., McNally, M.A., Byren, I., 2009. Diagnosis and management of prosthetic joint infection. BMJ 338, b1773. https://doi.org/10.1136/bmj.b1773

Matzinger, P., 2002. The danger model: a renewed sense of self. Science 296, 301–305. https://doi.org/10.1126/science.1071059

Mazmanian, S.K., Liu, G., Ton-That, H., Schneewind, O., 1999. Staphylococcus aureus sortase, an enzyme that anchors surface proteins to the cell wall. Science 285, 760–763. https://doi.org/10.1126/science.285.5428.760

MedCalc Statistical Software version 19.2.6 (MedCalc Software Ltd, Ostend, Belgium; https://www.medcalc.org;2020), n.d.

Medzhitov, R., 2007. Recognition of microorganisms and activation of the immune response. Nature 449, 819–826. https://doi.org/10.1038/nature06246

Meehan, A.M., Osmon, D.R., Duffy, M.C.T., Hanssen, A.D., Keating, M.R., 2003. Outcome of penicillin-susceptible streptococcal prosthetic joint infection treated with debridement and retention of the prosthesis. Clin. Infect. Dis. Off. Publ. Infect. Dis. Soc. Am. 36, 845–849. https://doi.org/10.1086/368182

Melendez, J.H., Frankel, Y.M., An, A.T., Williams, L., Price, L.B., Wang, N.-Y., Lazarus, G.S., Zenilman, J.M., 2010. Real-time PCR assays compared to culture-based approaches for identification of aerobic bacteria in chronic wounds. Clin. Microbiol. Infect. Off. Publ. Eur. Soc. Clin. Microbiol. Infect. Dis. 16, 1762–1769. https://doi.org/10.1111/j.1469-0691.2010.03158.x

Meyer, R., 2009. Replication and conjugative mobilization of broad host-range IncQ plasmids. Plasmid 62, 57–70. https://doi.org/10.1016/j.plasmid.2009.05.001

Miga, K.H., Koren, S., Rhie, A., Vollger, M.R., Gershman, A., Bzikadze, A., Brooks, S., Howe, E., Porubsky, D., Logsdon, G.A., Schneider, V.A., Potapova, T., Wood, J., Chow, W., Armstrong, J., Fredrickson, J., Pak, E., Tigyi, K., Kremitzki, M., Markovic, C., Maduro, V., Dutra, A., Bouffard, G.G., Chang, A.M., Hansen, N.F., Wilfert, A.B., Thibaud-Nissen, F., Schmitt, A.D., Belton, J.-M., Selvaraj, S., Dennis, M.Y., Soto, D.C., Sahasrabudhe, R., Kaya, G., Quick, J., Loman, N.J., Holmes, N., Loose, M., Surti, U., Risques, R.A., Graves Lindsay, T.A., Fulton, R., Hall, I., Paten, B., Howe, K., Timp, W., Young, A., Mullikin, J.C., Pevzner, P.A., Gerton, J.L., Sullivan, B.A., Eichler, E.E., Phillippy, A.M., 2020. Telomere-to-telomere assembly of a complete human X chromosome. Nature 585, 79–84. https://doi.org/10.1038/s41586-020-2547-7

Millan, A.S., MacLean, R.C., 2019. Fitness Costs of Plasmids: A Limit to Plasmid Transmission, in: Microbial Transmission. John Wiley & Sons, Ltd, pp. 65–79. https://doi.org/10.1128/9781555819743.ch4

Miller, J.R., Koren, S., Sutton, G., 2010. Assembly algorithms for next-generation sequencing data. Genomics 95, 315–327. https://doi.org/10.1016/j.ygeno.2010.03.001

Miller, R.R., Lopansri, B.K., Burke, J.P., Levy, M., Opal, S., Rothman, R.E., D'Alessio, F.R., Sidhaye, V.K., Aggarwal, N.R., Balk, R., Greenberg, J.A., Yoder, M., Patel, G., Gilbert, E., Afshar, M., Parada, J.P., Martin, G.S., Esper, A.M., Kempker, J.A., Narasimhan, M., Tsegaye, A., Hahn, S., Mayo, P., van der Poll, T., Schultz, M.J., Scicluna, B.P., Klein Klouwenberg, P., Rapisarda, A., Seldon, T.A., McHugh, L.C., Yager, T.D., Cermelli, S., Sampson, D., Rothwell, V., Newman, R., Bhide, S., Fox, B.A., Kirk, J.T., Navalkar, K., Davis, R.F., Brandon, R.A., Brandon, R.B., 2018. Validation of a Host Response Assay, SeptiCyte LAB, for Discriminating Sepsis from Systemic Inflammatory Response Syndrome in the ICU. Am. J. Respir. Crit. Care Med. 198, 903–913. https://doi.org/10.1164/rccm.201712-2472OC

Mitsuhashi, S., Kryukov, K., Nakagawa, S., Takeuchi, J.S., Shiraishi, Y., Asano, K., Imanishi, T., 2017. A portable system for rapid bacterial composition analysis using a nanopore-based sequencer and laptop computer. Sci. Rep. 7, 5657. https://doi.org/10.1038/s41598-017-05772-5

Monastero, R.N., Pentyala, S., 2017. Cytokines as Biomarkers and Their Respective Clinical Cutoff Levels. Int. J. Inflamm. 2017, 4309485. https://doi.org/10.1155/2017/4309485

Mongkolrattanothai, K., Dien Bard, J., 2017. The utility of direct specimen detection by Sanger sequencing in hospitalized pediatric patients. Diagn. Microbiol. Infect. Dis. 87, 100–102. https://doi.org/10.1016/j.diagmicrobio.2016.10.024

Monk, I.R., Casey, P.G., Cronin, M., Gahan, C.G., Hill, C., 2008. Development of multiple strain competitive index assays for Listeria monocytogenes using pIMC; a new site-specific integrative vector. BMC Microbiol. 8, 96. https://doi.org/10.1186/1471-2180-8-96

Monk, I.R., Shah, I.M., Xu, M., Tan, M.-W., Foster, T.J., 2012. Transforming the untransformable: application of direct transformation to manipulate genetically Staphylococcus aureus and Staphylococcus epidermidis. mBio 3, e00277-11. https://doi.org/10.1128/mBio.00277-11

Monroe, D., 2007. Looking for chinks in the armor of bacterial biofilms. PLoS Biol. 5, e307. https://doi.org/10.1371/journal.pbio.0050307

Moon, J., Kim, N., Lee, H.S., Shin, H.-R., Lee, S.-T., Jung, K.-H., Park, K.-I., Lee, S.K., Chu, K., 2017. Campylobacter fetus meningitis confirmed by a 16S rRNA gene analysis using the MinION nanopore sequencer, South Korea, 2016. Emerg. Microbes Infect. 6, e94. https://doi.org/10.1038/emi.2017.81

More than 80% of total knee replacements can last for 25 years [WWW Document], 2021. . NIHR Evid. https://doi.org/10.3310/signal-000776

Morgenstern, C., Cabric, S., Perka, C., Trampuz, A., Renz, N., 2018. Synovial fluid multiplex PCR is superior to culture for detection of low-virulent pathogens causing periprosthetic joint infection. Diagn. Microbiol. Infect. Dis. 90, 115–119. https://doi.org/10.1016/j.diagmicrobio.2017.10.016

Morley, C.R., Trofymow, J.A., Coleman, D.C., Cambardella, C., 1983. Effects of freeze-thaw stress on bacterial populations in soil microcosms. Microb. Ecol. 9, 329–340. https://doi.org/10.1007/BF02019022

Mraovic, B., Suh, D., Jacovides, C., Parvizi, J., 2011. Perioperative hyperglycemia and postoperative infection after lower limb arthroplasty. J. Diabetes Sci. Technol. 5, 412–418. https://doi.org/10.1177/193229681100500231

Müller, A., Klumpp, J., Schmidt, H., Weiss, A., 2016. Complete Genome Sequence of Staphylococcus carnosus LTH 3730. Genome Announc. 4, e01038-16. https://doi.org/10.1128/genomeA.01038-16

Muller, H.J., 1927. ARTIFICIAL TRANSMUTATION OF THE GENE. Science 66, 84–87. https://doi.org/10.1126/science.66.1699.84

Mundy, G.R., 1991. Mechanisms of osteolytic bone destruction. Bone, A new Approach to the Management of Osteolytic Bone Metastases 12, S1–S6. https://doi.org/10.1016/8756-3282(91)90057-P

Murdoch, D.R., Roberts, S.A., Fowler, V.G., Shah, M.A., Taylor, S.L., Morris, A.J., Corey, G.R., 2001. Infection of orthopedic prostheses after Staphylococcus aureus bacteremia. Clin. Infect. Dis. Off. Publ. Infect. Dis. Soc. Am. 32, 647–649. https://doi.org/10.1086/318704

Murray, C., 2017. Point-of-care testing in genomics. Genomics Educ. Programme. URL https://www.genomicseducation.hee.nhs.uk/blog/point-of-care-testing-in-genomics/ (accessed 6.26.21).

Naccache, S.N., Peggs, K.S., Mattes, F.M., Phadke, R., Garson, J.A., Grant, P., Samayoa, E., Federman, S., Miller, S., Lunn, M.P., Gant, V., Chiu, C.Y., 2015. Diagnosis of neuroinvasive astrovirus infection in an immunocompromised adult with encephalitis by unbiased next-generation sequencing. Clin. Infect. Dis. Off. Publ. Infect. Dis. Soc. Am. 60, 919–923. https://doi.org/10.1093/cid/ciu912

Namba, R.S., Inacio, M.C.S., Paxton, E.W., 2013. Risk factors associated with deep surgical site infections after primary total knee arthroplasty: an analysis of 56,216 knees. J. Bone Joint Surg. Am. 95, 775–782. https://doi.org/10.2106/JBJS.L.00211

Namba, R.S., Inacio, M.C.S., Paxton, E.W., 2012. Risk factors associated with surgical site infection in 30,491 primary total hip replacements. J. Bone Joint Surg. Br. 94, 1330–1338. https://doi.org/10.1302/0301-620X.94B10.29184

Naorem, S.S., Han, J., Zhang, S.Y., Zhang, J., Graham, L.B., Song, A., Smith, C.V., Rashid, F., Guo, H., 2018. Efficient transposon mutagenesis mediated by an IPTG-controlled conditional suicide plasmid. BMC Microbiol. 18, 158. https://doi.org/10.1186/s12866-018-1319-0

Nicoloff, H., Andersson, D.I., 2016. Indirect resistance to several classes of antibiotics in cocultures with resistant bacteria expressing antibiotic-modifying or -degrading enzymes. J. Antimicrob. Chemother. 71, 100–110. https://doi.org/10.1093/jac/dkv312

NJR 17th Annual Report 2020.pdf, n.d.

Noé, L., Martin, D.E.K., 2014. A coverage criterion for spaced seeds and its applications to support vector machine string kernels and k-mer distances. J. Comput. Biol. J. Comput. Mol. Cell Biol. 21, 947–963. https://doi.org/10.1089/cmb.2014.0173

Noone, J.C., Helmersen, K., Leegaard, T.M., Skråmm, I., Aamot, H.V., 2021. Rapid Diagnostics of Orthopaedic-Implant-Associated Infections Using Nanopore Shotgun Metagenomic Sequencing on Tissue Biopsies. Microorganisms 9, E97. https://doi.org/10.3390/microorganisms9010097

Nováková, J., Izsáková, A., Grivalský, T., Ottmann, C., Farkašovský, M., 2014. Improved method for high-efficiency electrotransformation of Escherichia coli with the large BAC plasmids. Folia Microbiol. (Praha) 59, 53–61. https://doi.org/10.1007/s12223-013-0267-1

O'Gara, J.P., 2007. ica and beyond: biofilm mechanisms and regulation in Staphylococcus epidermidis and Staphylococcus aureus. FEMS Microbiol. Lett. 270, 179–188. https://doi.org/10.1111/j.1574-6968.2007.00688.x

O'Grady, J.J., Wain, J.R., Mwaigwisya, S., Kay, G.L., 2018. Method for Nucleic Acid Depletion.

Olivares, E., Badel-Berchoux, S., Provot, C., Prévost, G., Bernardi, T., Jehl, F., 2019. Clinical Impact of Antibiotics for the Treatment of Pseudomonas aeruginosa Biofilm Infections. Front. Microbiol. 10, 2894. https://doi.org/10.3389/fmicb.2019.02894

Oliveira, C.A., Candelária, I.S., Oliveira, P.B., Figueiredo, A., Caseiro-Alves, F., 2014. Metallosis: A diagnosis not only in patients with metal-on-metal prostheses. Eur. J. Radiol. Open 2, 3–6. https://doi.org/10.1016/j.ejro.2014.11.001

Olofsson, A.-C., Hermansson, M., Elwing, H., 2003. N-acetyl-L-cysteine affects growth, extracellular polysaccharide production, and bacterial biofilm formation on solid surfaces. Appl. Environ. Microbiol. 69, 4814–4822. https://doi.org/10.1128/AEM.69.8.4814-4822.2003

Osmon, D.R., Berbari, E.F., Berendt, A.R., Lew, D., Zimmerli, W., Steckelberg, J.M., Rao, N., Hanssen, A., Wilson, W.R., Infectious Diseases Society of America, 2013. Diagnosis and management of prosthetic joint infection: clinical practice guidelines by the Infectious Diseases Society of America. Clin. Infect. Dis. Off. Publ. Infect. Dis. Soc. Am. 56, e1–e25. https://doi.org/10.1093/cid/cis803

Oussedik, S., Gould, K., Stockley, I., Haddad, F.S., 2012. Defining peri-prosthetic infection: do we have a workable gold standard? J. Bone Joint Surg. Br. 94, 1455–1456. https://doi.org/10.1302/0301-620X.94B11.30244

Oxoid - Product Detail [WWW Document], n.d. URL http://www.oxoid.com/UK/blue/prod_detail/prod_detail.asp?pr=CM0471 (accessed 6.28.21).

Page, A.J., Bastkowski, S., Yasir, M., Turner, A.K., Viet, T.L., Savva, G.M., Webber, M.A., Charles, I.G., 2020. AlbaTraDIS: Comparative analysis of large datasets from parallel transposon mutagenesis experiments. PLOS Comput. Biol. 16, e1007980. https://doi.org/10.1371/journal.pcbi.1007980

Page, A.J., Langridge, G.C., 2019. Socru: Typing of genome level order and orientation in bacteria. bioRxiv 543702. https://doi.org/10.1101/543702

Palmer, C.K., Gooberman-Hill, R., Blom, A.W., Whitehouse, M.R., Moore, A.J., 2020. Post-surgery and recovery experiences following one- and two-stage revision for prosthetic joint

infection—A qualitative study of patients' experiences. PLOS ONE 15, e0237047. https://doi.org/10.1371/journal.pone.0237047

Panja, S., Aich, P., Jana, B., Basu, T., 2008. How does plasmid DNA penetrate cell membranes in artificial transformation process of Escherichia coli? Mol. Membr. Biol. 25, 411–422. https://doi.org/10.1080/09687680802187765

Paprosky, W.G., Perona, P.G., Lawrence, J.M., 1994. Acetabular defect classification and surgical reconstruction in revision arthroplasty: A 6-year follow-up evaluation. J. Arthroplasty 9, 33–44. https://doi.org/10.1016/0883-5403(94)90135-X

Parikh, M.S., Antony, S., 2016. A comprehensive review of the diagnosis and management of prosthetic joint infections in the absence of positive cultures. J. Infect. Public Health 9, 545–556. https://doi.org/10.1016/j.jiph.2015.12.001

Parisi, T.J., Konopka, J.F., Bedair, H.S., 2017. What is the Long-term Economic Societal Effect of Periprosthetic Infections After THA? A Markov Analysis. Clin. Orthop. 475, 1891–1900. https://doi.org/10.1007/s11999-017-5333-6

Park, M.J., Eun, I.-S., Jung, C.-Y., Ko, Y.-C., Kim, Y.-J., Kim, C.-K., Kang, E.-J., 2012. Streptococcus dysgalactiae subspecies dysgalactiae infection after total knee arthroplasty: a case report. Knee Surg. Relat. Res. 24, 120–123. https://doi.org/10.5792/ksrr.2012.24.2.120

Parvizi, J., Adeli, B., Zmistowski, B., Restrepo, C., Greenwald, A.S., 2012. Management of periprosthetic joint infection: the current knowledge: AAOS exhibit selection. J. Bone Joint Surg. Am. 94, e104. https://doi.org/10.2106/JBJS.K.01417

Parvizi, J., Della Valle, C.J., 2010. AAOS Clinical Practice Guideline: diagnosis and treatment of periprosthetic joint infections of the hip and knee. J. Am. Acad. Orthop. Surg. 18, 771–772. https://doi.org/10.5435/00124635-201012000-00007

Parvizi, J., Erkocak, O.F., Della Valle, C.J., 2014a. Culture-negative periprosthetic joint infection. J. Bone Joint Surg. Am. 96, 430–436. https://doi.org/10.2106/JBJS.L.01793

Parvizi, J., Gehrke, T., Chen, A.F., 2013. Proceedings of the International Consensus on Periprosthetic Joint Infection. Bone Jt. J. 95-B, 1450–1452. https://doi.org/10.1302/0301-620X.95B11.33135

Parvizi, J., Gehrke, T., International Consensus Group on Periprosthetic Joint Infection, 2014b. Definition of periprosthetic joint infection. J. Arthroplasty 29, 1331. https://doi.org/10.1016/j.arth.2014.03.009

Parvizi, J., Suh, D.-H., Jafari, S.M., Mullan, A., Purtill, J.J., 2011a. Aseptic loosening of total hip arthroplasty: infection always should be ruled out. Clin. Orthop. 469, 1401–1405. https://doi.org/10.1007/s11999-011-1822-1

Parvizi, J., Tan, T.L., Goswami, K., Higuera, C., Della Valle, C., Chen, A.F., Shohat, N., 2018. The 2018 Definition of Periprosthetic Hip and Knee Infection: An Evidence-Based and

Validated Criteria. J. Arthroplasty 33, 1309-1314.e2. https://doi.org/10.1016/j.arth.2018.02.078

Parvizi, J., Zmistowski, B., Berbari, E.F., Bauer, T.W., Springer, B.D., Della Valle, C.J., Garvin, K.L., Mont, M.A., Wongworawat, M.D., Zalavras, C.G., 2011b. New definition for periprosthetic joint infection: from the Workgroup of the Musculoskeletal Infection Society. Clin. Orthop. 469, 2992–2994. https://doi.org/10.1007/s11999-011-2102-9

Patel, A., Calfee, R.P., Plante, M., Fischer, S.A., Green, A., 2009. Propionibacterium acnes colonization of the human shoulder. J. Shoulder Elbow Surg. 18, 897–902. https://doi.org/10.1016/j.jse.2009.01.023

Patti, J.M., Allen, B.L., McGavin, M.J., Höök, M., 1994. MSCRAMM-mediated adherence of microorganisms to host tissues. Annu. Rev. Microbiol. 48, 585–617. https://doi.org/10.1146/annurev.mi.48.100194.003101

Peel, Trisha N., Cheng, A.C., Buising, K.L., Choong, P.F.M., 2012. Microbiological aetiology, epidemiology, and clinical profile of prosthetic joint infections: are current antibiotic prophylaxis guidelines effective? Antimicrob. Agents Chemother. 56, 2386–2391. https://doi.org/10.1128/AAC.06246-11

Peel, T. N., Cheng, A.C., Choong, P.F.M., Buising, K.L., 2012. Early onset prosthetic hip and knee joint infection: treatment and outcomes in Victoria, Australia. J. Hosp. Infect. 82, 248–253. https://doi.org/10.1016/j.jhin.2012.09.005

Peel, T.N., Dowsey, M.M., Buising, K.L., Liew, D., Choong, P.F.M., 2013. Cost analysis of debridement and retention for management of prosthetic joint infection. Clin. Microbiol. Infect. Off. Publ. Eur. Soc. Clin. Microbiol. Infect. Dis. 19, 181–186. https://doi.org/10.1111/j.1469-0691.2011.03758.x

Peel, T.N., Dowsey, M.M., Daffy, J.R., Stanley, P.A., Choong, P.F.M., Buising, K.L., 2011. Risk factors for prosthetic hip and knee infections according to arthroplasty site. J. Hosp. Infect. 79, 129–133. https://doi.org/10.1016/j.jhin.2011.06.001

Peel, T.N., Dylla, B.L., Hughes, J.G., Lynch, D.T., Greenwood-Quaintance, K.E., Cheng, A.C., Mandrekar, J.N., Patel, R., 2016. Improved Diagnosis of Prosthetic Joint Infection by Culturing Periprosthetic Tissue Specimens in Blood Culture Bottles. mBio 7, e01776-01715. https://doi.org/10.1128/mBio.01776-15

Pendleton, K.M., Erb-Downward, J.R., Bao, Y., Branton, W.R., Falkowski, N.R., Newton, D.W., Huffnagle, G.B., Dickson, R.P., 2017. Rapid Pathogen Identification in Bacterial Pneumonia Using Real-Time Metagenomics. Am. J. Respir. Crit. Care Med. 196, 1610–1612. https://doi.org/10.1164/rccm.201703-0537LE

Pepys, M.B., Hirschfield, G.M., 2003. C-reactive protein: a critical update. J. Clin. Invest. 111, 1805–1812. https://doi.org/10.1172/JCI18921

Pérez-Prieto, D., Portillo, M.E., Puig-Verdié, L., Alier, A., Martínez, S., Sorlí, L., Horcajada, J.P., Monllau, J.C., 2017. C-reactive protein may misdiagnose prosthetic joint infections, particularly chronic and low-grade infections. Int. Orthop. 41, 1315–1319. https://doi.org/10.1007/s00264-017-3430-5

Perry, M.J., Mortuza, F.Y., Ponsford, F.M., Elson, C.J., Atkins, R.M., 1995. Analysis of cell types and mediator production from tissues around loosening joint implants. Br. J. Rheumatol. 34, 1127–1134. https://doi.org/10.1093/rheumatology/34.12.1127

Peters, J.M., Colavin, A., Shi, H., Czarny, T.L., Larson, M.H., Wong, S., Hawkins, J.S., Lu, C.H.S., Koo, B.-M., Marta, E., Shiver, A.L., Whitehead, E.H., Weissman, J.S., Brown, E.D., Qi, L.S., Huang, K.C., Gross, C.A., 2016. A Comprehensive, CRISPR-based Functional Analysis of Essential Genes in Bacteria. Cell 165, 1493–1506. https://doi.org/10.1016/j.cell.2016.05.003

Phillips, P.L., Schultz, G.S., 2012. Molecular Mechanisms of Biofilm Infection: Biofilm Virulence Factors. Adv. Wound Care 1, 109–114. https://doi.org/10.1089/wound.2011.0301

Piper, K.E., Jacobson, M.J., Cofield, R.H., Sperling, J.W., Sanchez-Sotelo, J., Osmon, D.R., McDowell, A., Patrick, S., Steckelberg, J.M., Mandrekar, J.N., Fernandez Sampedro, M., Patel, R., 2009. Microbiologic diagnosis of prosthetic shoulder infection by use of implant sonication. J. Clin. Microbiol. 47, 1878–1884. https://doi.org/10.1128/JCM.01686-08

Plate, A., Stadler, L., Sutter, R., Anagnostopoulos, A., Frustaci, D., Zbinden, R., Fucentese, S.F., Zinkernagel, A.S., Zingg, P.O., Achermann, Y., 2018. Inflammatory disorders mimicking periprosthetic joint infections may result in false-positive α-defensin. Clin. Microbiol. Infect. Off. Publ. Eur. Soc. Clin. Microbiol. Infect. Dis. 24, 1212.e1-1212.e6. https://doi.org/10.1016/j.cmi.2018.02.019

Pons, M., Pulido, A., v Leal, null, Viladot, R., 1997. Sepsis due to group G Streptococcus after a total hip arthroplasty. A case report. Int. Orthop. 21, 277–278. https://doi.org/10.1007/s002640050167

Poss, R., Thornhill, T.S., Ewald, F.C., Thomas, W.H., Batte, N.J., Sledge, C.B., 1984. Factors influencing the incidence and outcome of infection following total joint arthroplasty. Clin. Orthop. 117–126.

Powell, I.B., Achen, M.G., Hillier, A.J., Davidson, B.E., 1988. A Simple and Rapid Method for Genetic Transformation of Lactic Streptococci by Electroporation. Appl. Environ. Microbiol. 54, 655–660. https://doi.org/10.1128/aem.54.3.655-660.1988

Power, M., Fell, G., Wright, M., 2013. Principles for high-quality, high-value testing. BMJ Evid.-Based Med. 18, 5–10. https://doi.org/10.1136/eb-2012-100645

Premkumar, A., Kolin, D.A., Farley, K.X., Wilson, J.M., McLawhorn, A.S., Cross, M.B., Sculco, P.K., 2021. Projected Economic Burden of Periprosthetic Joint Infection of the Hip and Knee in

the United States. J. Arthroplasty 36, 1484-1489.e3. https://doi.org/10.1016/j.arth.2020.12.005

Pruzanski, W., Leers, W.D., Wardlaw, A.C., 1974. Bacteriolytic and bactericidal activity of sera and synovial fluids in rheumatoid arthritis and in osteoarthritis. Arthritis Rheum. 17, 207–218. https://doi.org/10.1002/art.1780170303

Pulido, L., Ghanem, E., Joshi, A., Purtill, J.J., Parvizi, J., 2008. Periprosthetic joint infection: the incidence, timing, and predisposing factors. Clin. Orthop. 466, 1710–1715. https://doi.org/10.1007/s11999-008-0209-4

Purdue, P.E., Koulouvaris, P., Potter, H.G., Nestor, B.J., Sculco, T.P., 2007. The cellular and molecular biology of periprosthetic osteolysis. Clin. Orthop. 454, 251–261. https://doi.org/10.1097/01.blo.0000238813.95035.1b

Purdy, D., O'Keeffe, T.A.T., Elmore, M., Herbert, M., McLeod, A., Bokori-Brown, M., Ostrowski, A., Minton, N.P., 2002. Conjugative transfer of clostridial shuttle vectors from Escherichia coli to Clostridium difficile through circumvention of the restriction barrier. Mol. Microbiol. 46, 439–452. https://doi.org/10.1046/j.1365-2958.2002.03134.x

Qi, L.S., Larson, M.H., Gilbert, L.A., Doudna, J.A., Weissman, J.S., Arkin, A.P., Lim, W.A., 2013. Repurposing CRISPR as an RNA-guided platform for sequence-specific control of gene expression. Cell 152, 1173–1183. https://doi.org/10.1016/j.cell.2013.02.022

Qin, Z., Ou, Y., Yang, L., Zhu, Y., Tolker-Nielsen, T., Molin, S., Qu, D., 2007. Role of autolysin-mediated DNA release in biofilm formation of Staphylococcus epidermidis. Microbiol. Read. Engl. 153, 2083–2092. https://doi.org/10.1099/mic.0.2007/006031-0

Quince, C., Walker, A.W., Simpson, J.T., Loman, N.J., Segata, N., 2017. Shotgun metagenomics, from sampling to analysis. Nat. Biotechnol. 35, 833–844. https://doi.org/10.1038/nbt.3935

Rang, F.J., Kloosterman, W.P., de Ridder, J., 2018. From squiggle to basepair: computational approaches for improving nanopore sequencing read accuracy. Genome Biol. 19, 90. https://doi.org/10.1186/s13059-018-1462-9

Razonable, R.R., Lewallen, D.G., Patel, R., Osmon, D.R., 2001. Vertebral Osteomyelitis and Prosthetic Joint Infection Due to Staphylococcus simulans. Mayo Clin. Proc. 76, 1067–1070. https://doi.org/10.4065/76.10.1067

Rewa, O., Muscedere, J., Reynolds, S., Jiang, X., Heyland, D.K., 2012. Coagulase-negative Staphylococcus, catheter-related, bloodstream infections and their association with acute phase markers of inflammation in the intensive care unit: An observational study. Can. J. Infect. Dis. Med. Microbiol. J. Can. Mal. Infect. Microbiol. Medicale 23, 204–208. https://doi.org/10.1155/2012/198383

Riedy, M.C., Timm, E.A., Stewart, C.C., 1995. Quantitative RT-PCR for measuring gene expression. BioTechniques 18, 70–74, 76.

Robertson, H.M., 1993. The mariner transposable element is widespread in insects. Nature 362, 241–245. https://doi.org/10.1038/362241a0

Rohde, H., Burdelski, C., Bartscht, K., Hussain, M., Buck, F., Horstkotte, M.A., Knobloch, J.K.-M., Heilmann, C., Herrmann, M., Mack, D., 2005. Induction of Staphylococcus epidermidis biofilm formation via proteolytic processing of the accumulation-associated protein by staphylococcal and host proteases. Mol. Microbiol. 55, 1883–1895. https://doi.org/10.1111/j.1365-2958.2005.04515.x

Romero, I.G., Ruvinsky, I., Gilad, Y., 2012. Comparative studies of gene expression and the evolution of gene regulation. Nat. Rev. Genet. 13, 505–516. https://doi.org/10.1038/nrg3229

Roper, D., Layton, M., Rees, D., Lambert, C., Vulliamy, T., Salle, B.D. la, D'Souza, C., 2020. Laboratory diagnosis of G6PD deficiency. A British Society for Haematology Guideline. Br. J. Haematol. 189, 24–38. https://doi.org/10.1111/bjh.16366

Rosencher, N., Kerkkamp, H.E.M., Macheras, G., Munuera, L.M., Menichella, G., Barton, D.M., Cremers, S., Abraham, I.L., OSTHEO Investigation, 2003. Orthopedic Surgery Transfusion Hemoglobin European Overview (OSTHEO) study: blood management in elective knee and hip arthroplasty in Europe. Transfusion (Paris) 43, 459–469. https://doi.org/10.1046/j.1537-2995.2003.00348.x

Rousset, F., Cui, L., Siouve, E., Becavin, C., Depardieu, F., Bikard, D., 2018. Genome-wide CRISPR-dCas9 screens in E. coli identify essential genes and phage host factors. PLoS Genet. 14, e1007749. https://doi.org/10.1371/journal.pgen.1007749

Rowe, H.M., Karlsson, E., Echlin, H., Chang, T.-C., Wang, L., van Opijnen, T., Pounds, S.B., Schultz-Cherry, S., Rosch, J.W., 2019. Bacterial Factors Required for Transmission of Streptococcus pneumoniae in Mammalian Hosts. Cell Host Microbe 25, 884-891.e6. https://doi.org/10.1016/j.chom.2019.04.012

Roy, J.G., McElhaney, J.E., Verschoor, C.P., 2020. Reliable reference genes for the quantification of mRNA in human T-cells and PBMCs stimulated with live influenza virus. BMC Immunol. 21, 4. https://doi.org/10.1186/s12865-020-0334-8

Roy, S., Hartley, J., Dunn, H., Williams, R., Williams, C.A., Breuer, J., 2019. Whole-genome Sequencing Provides Data for Stratifying Infection Prevention and Control Management of Nosocomial Influenza A. Clin. Infect. Dis. Off. Publ. Infect. Dis. Soc. Am. 69, 1649–1656. https://doi.org/10.1093/cid/ciz020

Ruppé, E., Greub, G., Schrenzel, J., 2017a. Messages from the first International Conference on Clinical Metagenomics (ICCMg). Microbes Infect. 19, 223–228. https://doi.org/10.1016/j.micinf.2017.01.005

Ruppé, E., Lazarevic, V., Girard, M., Mouton, W., Ferry, T., Laurent, F., Schrenzel, J., 2017b. Clinical metagenomics of bone and joint infections: a proof of concept study. Sci. Rep. 7, 7718. https://doi.org/10.1038/s41598-017-07546-5

Ruppé, E., Schrenzel, J., 2018. Messages from the second International Conference on Clinical Metagenomics (ICCMg2). Microbes Infect. 20, 222–227. https://doi.org/10.1016/j.micinf.2018.02.005

Saag, K.G., Teng, G.G., Patkar, N.M., Anuntiyo, J., Finney, C., Curtis, J.R., Paulus, H.E., Mudano, A., Pisu, M., Elkins-Melton, M., Outman, R., Allison, J.J., Suarez Almazor, M., Bridges, S.L., Chatham, W.W., Hochberg, M., MacLean, C., Mikuls, T., Moreland, L.W., O'Dell, J., Turkiewicz, A.M., Furst, D.E., American College of Rheumatology, 2008. American College of Rheumatology 2008 recommendations for the use of nonbiologic and biologic disease-modifying antirheumatic drugs in rheumatoid arthritis. Arthritis Rheum. 59, 762–784. https://doi.org/10.1002/art.23721

Sabokbar, A., Pandey, R., Athanasou, N.A., 2003. The effect of particle size and electrical charge on macrophage-osteoclast differentiation and bone resorption. J. Mater. Sci. Mater. Med. 14, 731–738. https://doi.org/10.1023/a:1025088418878

Sadovskaya, I., Vinogradov, E., Flahaut, S., Kogan, G., Jabbouri, S., 2005. Extracellular carbohydrate-containing polymers of a model biofilm-producing strain, Staphylococcus epidermidis RP62A. Infect. Immun. 73, 3007–3017. https://doi.org/10.1128/IAI.73.5.3007-3017.2005

Sakurai, J., Nagahama, M., Oda, M., 2004. Clostridium perfringens alpha-toxin: characterization and mode of action. J. Biochem. (Tokyo) 136, 569–574. https://doi.org/10.1093/jb/mvh161

Salari, P., Grassi, M., Cinti, B., Onori, N., Gigante, A., 2020. Synovial Fluid Calprotectin for the Preoperative Diagnosis of Chronic Periprosthetic Joint Infection. J. Arthroplasty 35, 534–537. https://doi.org/10.1016/j.arth.2019.08.052

Salter, S.J., Cox, M.J., Turek, E.M., Calus, S.T., Cookson, W.O., Moffatt, M.F., Turner, P., Parkhill, J., Loman, N.J., Walker, A.W., 2014. Reagent and laboratory contamination can critically impact sequence-based microbiome analyses. BMC Biol. 12, 87. https://doi.org/10.1186/s12915-014-0087-z

Sampathkumar, P., Osmon, D.R., Cockerill, F.R., 2000. Prosthetic joint infection due to Staphylococcus lugdunensis. Mayo Clin. Proc. 75, 511–512. https://doi.org/10.4065/75.5.511

Santiago, M., Matano, L.M., Moussa, S.H., Gilmore, M.S., Walker, S., Meredith, T.C., 2015. A new platform for ultra-high density Staphylococcus aureus transposon libraries. BMC Genomics 16, 252. https://doi.org/10.1186/s12864-015-1361-3

Sassetti, C.M., Boyd, D.H., Rubin, E.J., 2003. Genes required for mycobacterial growth defined by high density mutagenesis. Mol. Microbiol. 48, 77–84. https://doi.org/10.1046/j.1365-2958.2003.03425.x

Scallan, E., Hoekstra, R.M., Angulo, F.J., Tauxe, R.V., Widdowson, M.-A., Roy, S.L., Jones, J.L., Griffin, P.M., 2011. Foodborne illness acquired in the United States--major pathogens. Emerg. Infect. Dis. 17, 7–15. https://doi.org/10.3201/eid1701.p11101

Scerbo, M.H., Kaplan, H.B., Dua, A., Litwin, D.B., Ambrose, C.G., Moore, L.J., Murray, C.C.K., Wade, C.E., Holcomb, J.B., 2016. Beyond Blood Culture and Gram Stain Analysis: A Review of Molecular Techniques for the Early Detection of Bacteremia in Surgical Patients. Surg. Infect. 17, 294–302. https://doi.org/10.1089/sur.2015.099

Schatz, D.G., Oettinger, M.A., Schlissel, M.S., 1992. V(D)J recombination: molecular biology and regulation. Annu. Rev. Immunol. 10, 359–383. https://doi.org/10.1146/annurev.iy.10.040192.002043

Schenk, S., Laddaga, R.A., 1992. Improved method for electroporation of Staphylococcus aureus. FEMS Microbiol. Lett. 94, 133–138. https://doi.org/10.1111/j.1574-6968.1992.tb05302.x

Schindler, C.A., Schuhardt, V.T., 1964. LYSOSTAPHIN: A NEW BACTERIOLYTIC AGENT FOR THE STAPHYLOCOCCUS. Proc. Natl. Acad. Sci. U. S. A. 51, 414–421. https://doi.org/10.1073/pnas.51.3.414

Schlaberg, R., Chiu, C.Y., Miller, S., Procop, G.W., Weinstock, G., Professional Practice Committee and Committee on Laboratory Practices of the American Society for Microbiology, Microbiology Resource Committee of the College of American Pathologists, 2017. Validation of Metagenomic Next-Generation Sequencing Tests for Universal Pathogen Detection. Arch. Pathol. Lab. Med. 141, 776–786. https://doi.org/10.5858/arpa.2016-0539-RA

Schmidt, K., Mwaigwisya, S., Crossman, L.C., Doumith, M., Munroe, D., Pires, C., Khan, A.M., Woodford, N., Saunders, N.J., Wain, J., O'Grady, J., Livermore, D.M., 2017. Identification of bacterial pathogens and antimicrobial resistance directly from clinical urines by nanopore-based metagenomic sequencing. J. Antimicrob. Chemother. 72, 104–114. https://doi.org/10.1093/jac/dkw397

Schneewind, O., Mihaylova-Petkov, D., Model, P., 1993. Cell wall sorting signals in surface proteins of gram-positive bacteria. EMBO J. 12, 4803–4811.

Schneewind, O., Missiakas, D., 2014. Genetic manipulation of Staphylococcus aureus. Curr. Protoc. Microbiol. 32, Unit 9C.3. https://doi.org/10.1002/9780471729259.mc09c03s32

Schulz, P., Dlaska, C.E., Perka, C., Trampuz, A., Renz, N., 2021. Preoperative synovial fluid culture poorly predicts the pathogen causing periprosthetic joint infection. Infection 49, 427–436. https://doi.org/10.1007/s15010-020-01540-2

Schuster, C.F., Howard, S.A., Gründling, A., 2019. Use of the counter selectable marker PheS* for genome engineering in Staphylococcus aureus. Microbiol. Read. Engl. 165, 572–584. https://doi.org/10.1099/mic.0.000791

Schwarz, E.M., Lu, A.P., Goater, J.J., Benz, E.B., Kollias, G., Rosier, R.N., Puzas, J.E., O'Keefe, R.J., 2000. Tumor necrosis factor-alpha/nuclear transcription factor-kappaB signaling in periprosthetic osteolysis. J. Orthop. Res. Off. Publ. Orthop. Res. Soc. 18, 472–480. https://doi.org/10.1002/jor.1100180321

Scott, D.L., Wolfe, F., Huizinga, T.W.J., 2010. Rheumatoid arthritis. Lancet Lond. Engl. 376, 1094–1108. https://doi.org/10.1016/S0140-6736(10)60826-4

Sebastian, S., Malhotra, R., Sreenivas, V., Kapil, A., Chaudhry, R., Dhawan, B., 2018. Sonication of orthopaedic implants: A valuable technique for diagnosis of prosthetic joint infections. J. Microbiol. Methods 146, 51–54. https://doi.org/10.1016/j.mimet.2018.01.015

Secor, P.R., Jennings, L.K., James, G.A., Kirker, K.R., Pulcini, E.D., McInnerney, K., Gerlach, R., Livinghouse, T., Hilmer, J.K., Bothner, B., Fleckman, P., Olerud, J.E., Stewart, P.S., 2012. Phevalin (aureusimine B) production by Staphylococcus aureus biofilm and impacts on human keratinocyte gene expression. PloS One 7, e40973. https://doi.org/10.1371/journal.pone.0040973

Self, W.H., Rosen, J., Sharp, S.C., Filbin, M.R., Hou, P.C., Parekh, A.D., Kurz, M.C., Shapiro, N.I., 2017. Diagnostic Accuracy of FebriDx: A Rapid Test to Detect Immune Responses to Viral and Bacterial Upper Respiratory Infections. J. Clin. Med. 6. https://doi.org/10.3390/jcm6100094

Sendi, P., Banderet, F., Graber, P., Zimmerli, W., 2011a. Clinical comparison between exogenous and haematogenous periprosthetic joint infections caused by Staphylococcus aureus. Clin. Microbiol. Infect. Off. Publ. Eur. Soc. Clin. Microbiol. Infect. Dis. 17, 1098–1100. https://doi.org/10.1111/j.1469-0691.2011.03510.x

Sendi, Parham, Banderet, F., Graber, P., Zimmerli, W., 2011. Periprosthetic joint infection following Staphylococcus aureus bacteremia. J. Infect. 63, 17–22. https://doi.org/10.1016/j.jinf.2011.05.005

Sendi, P., Christensson, B., Uçkay, I., Trampuz, A., Achermann, Y., Boggian, K., Svensson, D., Widerström, M., Zimmerli, W., GBS PJI study group, 2011b. Group B streptococcus in prosthetic hip and knee joint-associated infections. J. Hosp. Infect. 79, 64–69. https://doi.org/10.1016/j.jhin.2011.04.022

Shahi, A., Deirmengian, C., Higuera, C., Chen, A., Restrepo, C., Zmistowski, B., Parvizi, J., 2015. Premature Therapeutic Antimicrobial Treatments Can Compromise the Diagnosis of Late Periprosthetic Joint Infection. Clin. Orthop. 473, 2244–2249. https://doi.org/10.1007/s11999-015-4142-z

Shahi, A., Parvizi, J., 2016. The role of biomarkers in the diagnosis of periprosthetic joint infection. EFORT Open Rev. 1, 275–278. https://doi.org/10.1302/2058-5241.1.160019

Shanbhag, A.S., Bailey, H.O., Hwang, D.S., Cha, C.W., Eror, N.G., Rubash, H.E., 2000. Quantitative analysis of ultrahigh molecular weight polyethylene (UHMWPE) wear debris associated with total knee replacements. J. Biomed. Mater. Res. 53, 100–110. https://doi.org/10.1002/(sici)1097-4636(2000)53:1<100::aid-jbm14>3.0.co;2-4

Shanbhag, A.S., Jacobs, J.J., Black, J., Galante, J.O., Glant, T.T., 1995. Cellular mediators secreted by interfacial membranes obtained at revision total hip arthroplasty. J. Arthroplasty 10, 498–506. https://doi.org/10.1016/s0883-5403(05)80152-4

Shanbhag, A.S., Jacobs, J.J., Glant, T.T., Gilbert, J.L., Black, J., Galante, J.O., 1994. Composition and morphology of wear debris in failed uncemented total hip replacement. J. Bone Joint Surg. Br. 76, 60–67.

Sharkey, F.H., Banat, I.M., Marchant, R., 2004. Detection and Quantification of Gene Expression in Environmental Bacteriology. Appl. Environ. Microbiol. 70, 3795–3806. https://doi.org/10.1128/AEM.70.7.3795-3806.2004

Sharma, R.R., Marwaha, N., 2010. Leukoreduced blood components: Advantages and strategies for its implementation in developing countries. Asian J. Transfus. Sci. 4, 3–8. https://doi.org/10.4103/0973-6247.59384

Shehadul Islam, M., Aryasomayajula, A., Selvaganapathy, P.R., 2017. A Review on Macroscale and Microscale Cell Lysis Methods. Micromachines 8, 83. https://doi.org/10.3390/mi8030083

Siljander, M.P., Sobh, A.H., Baker, K.C., Baker, E.A., Kaplan, L.M., 2018. Multidrug-Resistant Organisms in the Setting of Periprosthetic Joint Infection-Diagnosis, Prevention, and Treatment. J. Arthroplasty 33, 185–194. https://doi.org/10.1016/j.arth.2017.07.045

Singh, J.A., Sperling, J.W., Schleck, C., Harmsen, W., Cofield, R.H., 2012. Periprosthetic infections after shoulder hemiarthroplasty. J. Shoulder Elbow Surg. 21, 1304–1309. https://doi.org/10.1016/j.jse.2011.08.067

Singh, J.A., Yu, S., Chen, L., Cleveland, J.D., 2019. Rates of Total Joint Replacement in the United States: Future Projections to 2020–2040 Using the National Inpatient Sample. J. Rheumatol. https://doi.org/10.3899/jrheum.170990

Singhal, D., Foreman, A., Jervis-Bardy, J., Bardy, J.-J., Wormald, P.-J., 2011. Staphylococcus aureus biofilms: Nemesis of endoscopic sinus surgery. The Laryngoscope 121, 1578–1583. https://doi.org/10.1002/lary.21805

Siryaporn, A., Kuchma, S.L., O'Toole, G.A., Gitai, Z., 2014. Surface attachment induces Pseudomonas aeruginosa virulence. Proc. Natl. Acad. Sci. U. S. A. 111, 16860–16865. https://doi.org/10.1073/pnas.1415712111

SMI B 44: investigation of orthopaedic implant associated infections [WWW Document], 2016. . GOV.UK. URL https://www.gov.uk/government/publications/smi-b-44-investigation-of-prosthetic-joint-infection-samples (accessed 6.17.21).

Smith, A.J., Dieppe, P., Vernon, K., Porter, M., Blom, A.W., 2012. Failure rates of stemmed metal-on-metal hip replacements: analysis of data from the National Joint Registry of England and Wales. The Lancet 379, 1199–1204. https://doi.org/10.1016/S0140-6736(12)60353-5

Souf, S., 2016. Recent advances in diagnostic testing for viral infections. Biosci. Horiz. Int. J. Stud. Res. 9. https://doi.org/10.1093/biohorizons/hzw010

Southwood, R.T., Rice, J.L., McDonald, P.J., Hakendorf, P.H., Rozenbilds, M.A., 1985. Infection in experimental hip arthroplasties. J. Bone Joint Surg. Br. 67, 229–231. https://doi.org/10.1302/0301-620X.67B2.3980532

Staphylococcus aureus subsp. aureus NCTC 8325 chromosome, complete genome, 2016.

Stern, A., Sorek, R., 2011. The phage-host arms race: shaping the evolution of microbes. BioEssays News Rev. Mol. Cell. Dev. Biol. 33, 43–51. https://doi.org/10.1002/bies.201000071

Stewart, R.D., Auffret, M.D., Warr, A., Walker, A.W., Roehe, R., Watson, M., 2019. Compendium of 4,941 rumen metagenome-assembled genomes for rumen microbiome biology and enzyme discovery. Nat. Biotechnol. 37, 953–961. https://doi.org/10.1038/s41587-019-0202-3

Stranieri, I., Kanunfre, K.A., Rodrigues, J.C., Yamamoto, L., Nadaf, M.I.V., Palmeira, P., Okay, T.S., 2018. Assessment and comparison of bacterial load levels determined by quantitative amplifications in blood culture-positive and negative neonatal sepsis. Rev. Inst. Med. Trop. São Paulo 60, e61. https://doi.org/10.1590/S1678-9946201860061

Street, T.L., Sanderson, N.D., Atkins, B.L., Brent, A.J., Cole, K., Foster, D., McNally, M.A., Oakley, S., Peto, L., Taylor, A., Peto, T.E.A., Crook, D.W., Eyre, D.W., 2017. Molecular Diagnosis of Orthopedic-Device-Related Infection Directly from Sonication Fluid by Metagenomic Sequencing. J. Clin. Microbiol. 55, 2334–2347. https://doi.org/10.1128/JCM.00462-17

Stríz, I., Trebichavský, I., 2004. Calprotectin - a pleiotropic molecule in acute and chronic inflammation. Physiol. Res. 53, 245–253.

Sudji, I.R., Subburaj, Y., Frenkel, N., García-Sáez, A.J., Wink, M., 2015. Membrane Disintegration Caused by the Steroid Saponin Digitonin Is Related to the Presence of Cholesterol. Mol. Basel Switz. 20, 20146–20160. https://doi.org/10.3390/molecules201119682

Suen, K., Keeka, M., Ailabouni, R., Tran, P., 2018. Synovasure “quick test” is not as accurate as the laboratory-based α-defensin immunoassay: a systematic review and meta-analysis. Bone Jt. J. 100-B, 66–72. https://doi.org/10.1302/0301-620X.100B1.BJJ-2017-0630.R1

Sun, H.-X., Xie, Y., Ye, Y.-P., 2009. Advances in saponin-based adjuvants. Vaccine 27, 1787–1796. https://doi.org/10.1016/j.vaccine.2009.01.091

Suren, C., Feihl, S., Cabric, S., Banke, I.J., Haller, B., Trampuz, A., von Eisenhart-Rothe, R., Prodinger, P.M., 2020. Improved pre-operative diagnostic accuracy for low-grade prosthetic joint infections using second-generation multiplex Polymerase chain reaction on joint fluid aspirate. Int. Orthop. 44, 1629–1637. https://doi.org/10.1007/s00264-020-04552-7

Szostková, M., Horáková, D., 1998. The effect of plasmid DNA sizes and other factors on electrotransformation of Escherichia coli JM109. Bioelectrochem. Bioenerg. 47, 319–323. https://doi.org/10.1016/S0302-4598(98)00203-7

Taha, M., Abdelbary, H., Ross, F.P., Carli, A.V., 2018. New Innovations in the Treatment of PJI and Biofilms-Clinical and Preclinical Topics. Curr. Rev. Musculoskelet. Med. 11, 380–388. https://doi.org/10.1007/s12178-018-9500-5

Tande, A.J., Patel, R., 2014. Prosthetic joint infection. Clin. Microbiol. Rev. 27, 302–345. https://doi.org/10.1128/CMR.00111-13

Tani, S., Lepetsos, P., Stylianakis, A., Vlamis, J., Birbas, K., Kaklamanos, I., 2018. Superiority of the sonication method against conventional periprosthetic tissue cultures for diagnosis of prosthetic joint infections. Eur. J. Orthop. Surg. Traumatol. 28, 51–57. https://doi.org/10.1007/s00590-017-2012-y

Taylor, R.W., Turnbull, D.M., 2005. Mitochondrial DNA mutations in human disease. Nat. Rev. Genet. 6, 389–402. https://doi.org/10.1038/nrg1606

Thoendel, M., Jeraldo, P.R., Greenwood-Quaintance, K.E., Yao, J.Z., Chia, N., Hanssen, A.D., Abdel, M.P., Patel, R., 2016. Comparison of microbial DNA enrichment tools for metagenomic whole genome sequencing. J. Microbiol. Methods 127, 141–145. https://doi.org/10.1016/j.mimet.2016.05.022

Thoendel, M.J., Jeraldo, P.R., Greenwood-Quaintance, K.E., Yao, J.Z., Chia, N., Hanssen, A.D., Abdel, M.P., Patel, R., 2018. Identification of Prosthetic Joint Infection Pathogens Using a Shotgun Metagenomics Approach. Clin. Infect. Dis. Off. Publ. Infect. Dis. Soc. Am. 67, 1333–1338. https://doi.org/10.1093/cid/ciy303

Thomas, T., Gilbert, J., Meyer, F., 2012. Metagenomics - a guide from sampling to data analysis. Microb. Inform. Exp. 2, 3. https://doi.org/10.1186/2042-5783-2-3

Titball, R.W., 1993. Bacterial phospholipases C. Microbiol. Rev. 57, 347–366. https://doi.org/10.1128/mr.57.2.347-366.1993

Tormo, M.Á., Knecht, E., Götz, F., Lasa, I., Penadés, J.R., 2005. Bap-dependent biofilm formation by pathogenic species of Staphylococcus: evidence of horizontal gene transfer? Microbiol. Read. Engl. 151, 2465–2475. https://doi.org/10.1099/mic.0.27865-0

Trampuz, A., Osmon, D.R., Hanssen, A.D., Steckelberg, J.M., Patel, R., 2003. Molecular and antibiofilm approaches to prosthetic joint infection. Clin. Orthop. 69–88. https://doi.org/10.1097/01.blo.0000087324.60612.93

Trampuz, A., Piper, K.E., Hanssen, A.D., Osmon, D.R., Cockerill, F.R., Steckelberg, J.M., Patel, R., 2006. Sonication of explanted prosthetic components in bags for diagnosis of prosthetic joint infection is associated with risk of contamination. J. Clin. Microbiol. 44, 628–631. https://doi.org/10.1128/JCM.44.2.628-631.2006

Trampuz, A., Piper, K.E., Jacobson, M.J., Hanssen, A.D., Unni, K.K., Osmon, D.R., Mandrekar, J.N., Cockerill, F.R., Steckelberg, J.M., Greenleaf, J.F., Patel, R., 2007. Sonication of removed hip and knee prostheses for diagnosis of infection. N. Engl. J. Med. 357, 654–663. https://doi.org/10.1056/NEJMoa061588

Trotter, A.J., Aydin, A., Strinden, M.J., O'Grady, J., 2019. Recent and emerging technologies for the rapid diagnosis of infection and antimicrobial resistance. Curr. Opin. Microbiol. 51, 39–45. https://doi.org/10.1016/j.mib.2019.03.001

Trotter, A.J., Dean, R., Whitehouse, C.E., Mikalsen, J., Hill, C., Brunton-Sim, R., Kay, G.L., Shakokani, M., Durst, A.Z.E., Wain, J., McNamara, I., O'Grady, J., 2020. Preliminary evaluation of a rapid lateral flow calprotectin test for the diagnosis of prosthetic joint infection. Bone Jt. Res. 9, 202–210. https://doi.org/10.1302/2046-3758.95.BJR-2019-0213.R1

Tsang, S.-T.J., Ting, J., Simpson, A.H.R.W., Gaston, P., 2017. Outcomes following debridement, antibiotics and implant retention in the management of periprosthetic infections of the hip: a review of cohort studies. Bone Jt. J. 99-B, 1458–1466. https://doi.org/10.1302/0301-620X.99B11.BJJ-2017-0088.R1

Tsao, Y.-T., Tsai, Y.-H., Liao, W.-T., Shen, C.-J., Shen, C.-F., Cheng, C.-M., 2020. Differential Markers of Bacterial and Viral Infections in Children for Point-of-Care Testing. Trends Mol. Med. 26, 1118–1132. https://doi.org/10.1016/j.molmed.2020.09.004

Tuleubaev, B., Ahmetova, S., Koshanova, A., Rudenko, A., Tashmetov, E., 2018. Heat stability of the antimicrobial activity of antibiotics after high temperature exposure. Orthop. Proc. 100-B, 34–34. https://doi.org/10.1302/1358-992X.2018.16.034

Tunney, M.M., Patrick, S., Gorman, S.P., Nixon, J.R., Anderson, N., Davis, R.I., Hanna, D., Ramage, G., 1998. Improved detection of infection in hip replacements. A currently underestimated problem. J. Bone Joint Surg. Br. 80, 568–572. https://doi.org/10.1302/0301-620x.80b4.8473

Tyson, J.R., O'Neil, N.J., Jain, M., Olsen, H.E., Hieter, P., Snutch, T.P., 2018. MinION-based long-read sequencing and assembly extends the Caenorhabditis elegans reference genome. Genome Res. 28, 266–274. https://doi.org/10.1101/gr.221184.117

Uçkay, I., Lübbeke, A., Emonet, S., Tovmirzaeva, L., Stern, R., Ferry, T., Assal, M., Bernard, L., Lew, D., Hoffmeyer, P., 2009. Low incidence of haematogenous seeding to total hip and knee prostheses in patients with remote infections. J. Infect. 59, 337–345. https://doi.org/10.1016/j.jinf.2009.08.015

Vaishya, R., Sardana, R., Butta, H., Mendiratta, L., 2019. Laboratory diagnosis of Prosthetic Joint Infections: Current concepts and present status. J. Clin. Orthop. Trauma 10, 560–565. https://doi.org/10.1016/j.jcot.2018.10.006

Valle, J., Vergara-Irigaray, M., Merino, N., Penadés, J.R., Lasa, I., 2007. sigmaB regulates IS256-mediated Staphylococcus aureus biofilm phenotypic variation. J. Bacteriol. 189, 2886–2896. https://doi.org/10.1128/JB.01767-06

van Opijnen, T., Bodi, K.L., Camilli, A., 2009. Tn-seq: high-throughput parallel sequencing for fitness and genetic interaction studies in microorganisms. Nat. Methods 6, 767–772. https://doi.org/10.1038/nmeth.1377

van Opijnen, T., Camilli, A., 2012. A fine scale phenotype–genotype virulence map of a bacterial pathogen. Genome Res. 22, 2541–2551. https://doi.org/10.1101/gr.137430.112

van Rheenen, P.F., Van de Vijver, E., Fidler, V., 2010. Faecal calprotectin for screening of patients with suspected inflammatory bowel disease: diagnostic meta-analysis. BMJ 341, c3369. https://doi.org/10.1136/bmj.c3369

Vandeventer, P.E., Weigel, K.M., Salazar, J., Erwin, B., Irvine, B., Doebler, R., Nadim, A., Cangelosi, G.A., Niemz, A., 2011. Mechanical disruption of lysis-resistant bacterial cells by use of a miniature, low-power, disposable device. J. Clin. Microbiol. 49, 2533–2539. https://doi.org/10.1128/JCM.02171-10

VanGuilder, H.D., Vrana, K.E., Freeman, W.M., 2008. Twenty-five years of quantitative PCR for gene expression analysis. BioTechniques 44, 619–626. https://doi.org/10.2144/000112776

Vanhegan, I.S., Malik, A.K., Jayakumar, P., Ul Islam, S., Haddad, F.S., 2012. A financial analysis of revision hip arthroplasty: the economic burden in relation to the national tariff. J. Bone Joint Surg. Br. 94, 619–623. https://doi.org/10.1302/0301-620X.94B5.27073

Vasu, K., Nagaraja, V., 2013. Diverse functions of restriction-modification systems in addition to cellular defense. Microbiol. Mol. Biol. Rev. MMBR 77, 53–72. https://doi.org/10.1128/MMBR.00044-12

Vazquez, V., Liang, X., Horndahl, J.K., Ganesh, V.K., Smeds, E., Foster, T.J., Hook, M., 2011. Fibrinogen is a ligand for the Staphylococcus aureus microbial surface components

recognizing adhesive matrix molecules (MSCRAMM) bone sialoprotein-binding protein (Bbp). J. Biol. Chem. 286, 29797–29805. https://doi.org/10.1074/jbc.M110.214981

Veeranagouda, Y., Husain, F., Wexler, H.M., 2013. Transposon mutagenesis of Bacteroides fragilis using a mariner transposon vector. Anaerobe 22, 126–129. https://doi.org/10.1016/j.anaerobe.2013.04.012

Verboom, D.M., Koster-Brouwer, M.E., Varkila, M.R.J., Bonten, M.J.M., Cremer, O.L., 2019. Profile of the SeptiCyte™ LAB gene expression assay to diagnose infection in critically ill patients. Expert Rev. Mol. Diagn. 19, 95–108. https://doi.org/10.1080/14737159.2019.1567333

Vervier, K., Mahé, P., Tournoud, M., Veyrieras, J.-B., Vert, J.-P., 2016. Large-scale machine learning for metagenomics sequence classification. Bioinforma. Oxf. Engl. 32, 1023–1032. https://doi.org/10.1093/bioinformatics/btv683

Vijay, K., 2018. Toll-like receptors in immunity and inflammatory diseases: Past, present, and future. Int. Immunopharmacol. 59, 391–412. https://doi.org/10.1016/j.intimp.2018.03.002

Vlamakis, H., Chai, Y., Beauregard, P., Losick, R., Kolter, R., 2013. Sticking together: building a biofilm the Bacillus subtilis way. Nat. Rev. Microbiol. 11, 157–168. https://doi.org/10.1038/nrmicro2960

Waheed, A., Barker, J., Barton, S.J., Owen, C.P., Ahmed, S., Carew, M.A., 2012. A novel steroidal saponin glycoside from Fagonia indica induces cell-selective apoptosis or necrosis in cancer cells. Eur. J. Pharm. Sci. Off. J. Eur. Fed. Pharm. Sci. 47, 464–473. https://doi.org/10.1016/j.ejps.2012.07.004

Waller, D.G., Sampson, A.P., 2018. 51 - Chemotherapy of infections, in: Waller, D.G., Sampson, A.P. (Eds.), Medical Pharmacology and Therapeutics (Fifth Edition). Elsevier, pp. 581–629. https://doi.org/10.1016/B978-0-7020-7167-6.00051-8

Walter, J.M., Wunderink, R.G., 2017. Severe Respiratory Viral Infections: New Evidence and Changing Paradigms. Infect. Dis. Clin. North Am., Complex Infectious Disease Issues in the Intensive Care Unit 31, 455–474. https://doi.org/10.1016/j.idc.2017.05.004

Wang, T., Guan, C., Guo, J., Liu, B., Wu, Y., Xie, Z., Zhang, C., Xing, X.-H., 2018. Pooled CRISPR interference screening enables genome-scale functional genomics study in bacteria with superior performance. Nat. Commun. 9, 2475. https://doi.org/10.1038/s41467-018-04899-x

Wang, X., Niu, C., Sun, G., Dong, D., Villaruz, A.E., Li, M., Wang, D., Wang, J., Otto, M., Gao, Q., 2011. ygs is a novel gene that influences biofilm formation and the general stress response of Staphylococcus epidermidis. Infect. Immun. 79, 1007–1015. https://doi.org/10.1128/IAI.00916-10

Warren, J., Anis, H.K., Bowers, K., Pannu, T., Villa, J., Klika, A.K., Colon-Franco, J., Piuzzi, N.S., Higuera, C.A., 2021. Diagnostic Utility of a Novel Point-of-Care Test of Calprotectin for Periprosthetic Joint Infection After Total Knee Arthroplasty: A Prospective Cohort Study. J. Bone Joint Surg. Am. 103, 1009–1015. https://doi.org/10.2106/JBJS.20.01089

Wick, R.R., Judd, L.M., Holt, K.E., 2019. Performance of neural network basecalling tools for Oxford Nanopore sequencing. Genome Biol. 20, 129. https://doi.org/10.1186/s13059-019-1727-y

Widhelm, T.J., Yajjala, V.K., Endres, J.L., Fey, P.D., Bayles, K.W., 2014. Methods to generate a sequence-defined transposon mutant library in Staphylococcus epidermidis strain 1457. Methods Mol. Biol. Clifton NJ 1106, 135–142. https://doi.org/10.1007/978-1-62703-736-5_12

Wilson, G.G., 1991. Organization of restriction-modification systems. Nucleic Acids Res. 19, 2539–2566. https://doi.org/10.1093/nar/19.10.2539

Wood, D.E., Salzberg, S.L., 2014. Kraken: ultrafast metagenomic sequence classification using exact alignments. Genome Biol. 15, R46. https://doi.org/10.1186/gb-2014-15-3-r46

Wooley, J.C., Godzik, A., Friedberg, I., 2010. A primer on metagenomics. PLoS Comput. Biol. 6, e1000667. https://doi.org/10.1371/journal.pcbi.1000667

Wouthuyzen-Bakker, M., Ploegmakers, J.J.W., Kampinga, G.A., Wagenmakers-Huizenga, L., Jutte, P.C., Muller Kobold, A.C., 2017. Synovial calprotectin: a potential biomarker to exclude a prosthetic joint infection. Bone Jt. J. 99-B, 660–665. https://doi.org/10.1302/0301-620X.99B5.BJJ-2016-0913.R2

Wouthuyzen-Bakker, M., Ploegmakers, J.J.W., Ottink, K., Kampinga, G.A., Wagenmakers-Huizenga, L., Jutte, P.C., Kobold, A.C.M., 2018. Synovial Calprotectin: An Inexpensive Biomarker to Exclude a Chronic Prosthetic Joint Infection. J. Arthroplasty 33, 1149–1153. https://doi.org/10.1016/j.arth.2017.11.006

Wu, X., Wang, Y., Tao, L., 2011. Sulfhydryl compounds reduce Staphylococcus aureus biofilm formation by inhibiting PIA biosynthesis. FEMS Microbiol. Lett. 316, 44–50. https://doi.org/10.1111/j.1574-6968.2010.02190.x

Wyatt, M.C., Beswick, A.D., Kunutsor, S.K., Wilson, M.J., Whitehouse, M.R., Blom, A.W., 2016. The Alpha-Defensin Immunoassay and Leukocyte Esterase Colorimetric Strip Test for the Diagnosis of Periprosthetic Infection: A Systematic Review and Meta-Analysis. J. Bone Joint Surg. Am. 98, 992–1000. https://doi.org/10.2106/JBJS.15.01142

Yajjala, V.K., Widhelm, T.J., Endres, J.L., Fey, P.D., Bayles, K.W., 2016. Generation of a Transposon Mutant Library in Staphylococcus aureus and Staphylococcus epidermidis Using bursa aurealis. Methods Mol. Biol. Clifton NJ 1373, 103–110. https://doi.org/10.1007/7651_2014_189

Ye, S.H., Siddle, K.J., Park, D.J., Sabeti, P.C., 2019. Benchmarking Metagenomics Tools for Taxonomic Classification. Cell 178, 779–794. https://doi.org/10.1016/j.cell.2019.07.010

Zaruta, D.A., Qiu, B., Liu, A.Y., Ricciardi, B.F., 2018. Indications and Guidelines for Debridement and Implant Retention for Periprosthetic Hip and Knee Infection. Curr. Rev. Musculoskelet. Med. 11, 347–356. https://doi.org/10.1007/s12178-018-9497-9

Zelenin, S., Hansson, J., Ardabili, S., Ramachandraiah, H., Brismar, H., Russom, A., 2015. Microfluidic-based isolation of bacteria from whole blood for sepsis diagnostics. Biotechnol. Lett. 37, 825–830. https://doi.org/10.1007/s10529-014-1734-8

Zimmer Biomet. Diagnostics C. Synovasure Alpha Defensin Lateral Flow Test Kit: Instructions For Use. https://cddiagnostics.com/instructions/PDF/LF%20Test%20Kit%20IFUs/EN_M40004B_V6_Synovasure_Alpha_Defensin_Lateral_Flow_IFU.pdf (date last accessed 3 February 2020), n.d.

Zimmerli, W., Trampuz, A., Ochsner, P.E., 2004. Prosthetic-joint infections. N. Engl. J. Med. 351, 1645–1654. https://doi.org/10.1056/NEJMra040181

Zmistowski, B., Karam, J.A., Durinka, J.B., Casper, D.S., Parvizi, J., 2013. Periprosthetic joint infection increases the risk of one-year mortality. J. Bone Joint Surg. Am. 95, 2177–2184. https://doi.org/10.2106/JBJS.L.00789